STUDIES ON PHOTOINDUCED PROCESSES IN ROOM TEMPERATURE IONIC LIQUIDS AND FLUORESCENCE BEHAVIOR OF QUANTUM DOTS AND THEIR HYBRIDS WITH THE IONIC LIQUIDS

A Thesis Submitted for the Degree of

DOCTOR OF PHILOSOPHY

by

Kotni Santhosh

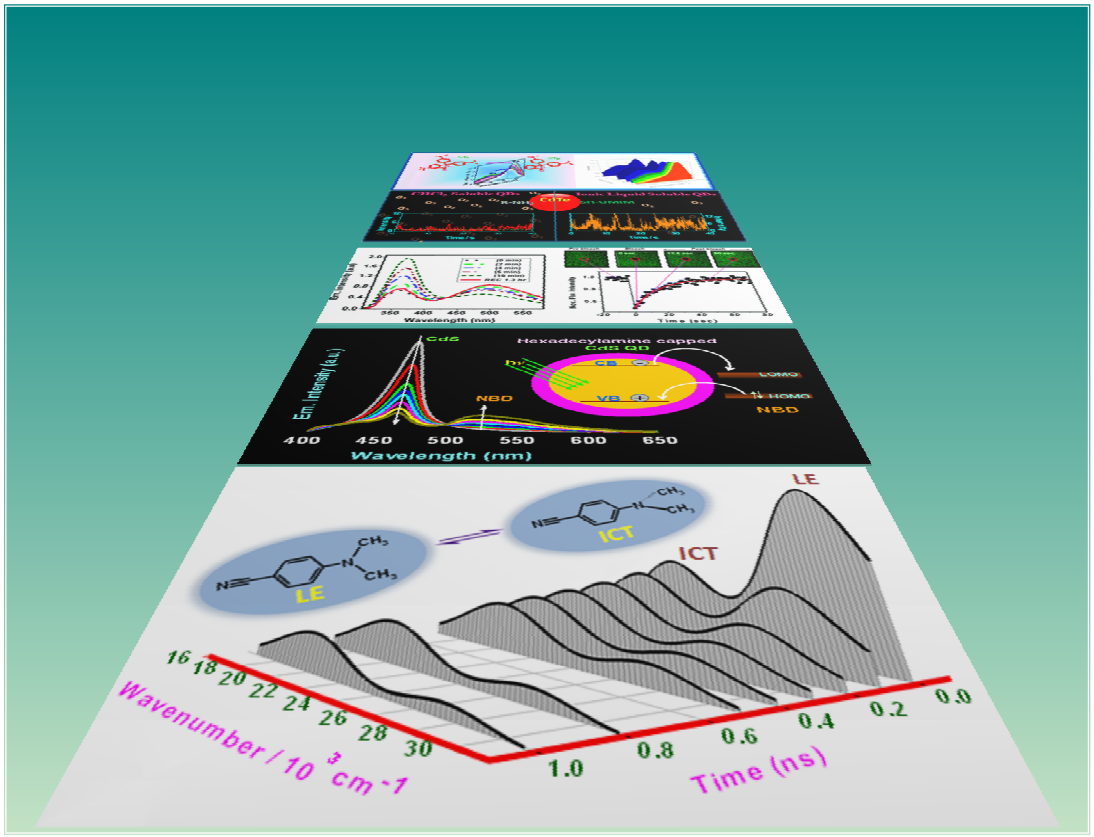

School of Chemistry
University of Hyderabad
Hyderabad-500 046
INDIA

January 2013

STUDIES ON PHOTOINDUCED PROCESSES IN ROOM TEMPERATURE IONIC LIQUIDS AND FLUORESCENCE BEHAVIOR OF QUANTUM DOTS AND THEIR HYBRIDS WITH THE IONIC LIQUIDS

A Thesis

Submitted for the Degree of

DOCTOR OF PHILOSOPHY

by

Kotni Santhosh

School of Chemistry

University of Hyderabad

Hyderabad – 500 046

INDIA

January 2013

Dedicated

To

My Family

STATEMENT

I hereby declare that the matter embodied in the thesis entitled **"*Studies on Photoinduced Processes in Room Temperature Ionic Liquids and Fluorescence Behavior of Quantum Dots and their Hybrids with the Ionic Liquids*"** is the result of investigations carried out by me in the School of Chemistry, University of Hyderabad, India under the supervision of **Prof. Anunay Samanta**.

In keeping with the general practice of reporting scientific investigations, the acknowledgements have been made wherever the work described is based on the findings of other investigators. Any omission or error that might have crept in is regretted.

January 2013 **Kotni Santhosh**

SCHOOL OF CHEMISTRY

UNIVERSITY OF HYDERABAD

HYDERABAD-500 046, INDIA

Phone: +91-40-2313 4813 (O)
+91-40-2313 0715 (R)
Fax: +91-40-2301 1594
Email: assc@uohyd.ernet.in
anunay.samanta@gmail.com

Prof. Anunay Samanta

CERTIFICATE

Certified that the work embodied in the thesis entitled **"*Studies on Photoinduced Processes in Room Temperature Ionic Liquids and Fluorescence Behavior of Quantum Dots and their Hybrids with the Ionic Liquids*"** has been carried out by **Mr. Kotni Santhosh** under my supervision and the same has not been submitted elsewhere for any degree.

Anunay Samanta
(Thesis Supervisor)

Dean
School of Chemistry
University of Hyderabad

Acknowledgement

I express my sincere gratitude to Prof. Anunay Samanta, my research supervisor, for his constant cooperation, encouragement and kind guidance. He has been quite helpful to me in both academic and personal fronts.

I would like to acknowledge Prof. Amitabha Chattopadhyay for the multiphoton confocal fluorescence microscope facility at Centre for Cellular and Molecular Biology (CCMB), Hyderabad.

I am quite thankful to Prof. P. Ramamurthy for the picosecond laser facility at National Centre for UltraFast Processes (NCUFP), Chennai. Special thanks are due to Mr. P. Ashok Kumar for his help during fluorescence decay measurements. I thank Mr. Durga Prasad for Transmission Electron Microscope (TEM) measurements at Centre for Nanotechnology, University of Hyderabad.

I would like to thank the former and present Dean(s), School of Chemistry, for their constant support, inspiration and for the available facilities. I am extremely appreciative individually to all the faculty members of the school for their help, cooperation and encouragement at various stages.

I express my heartfelt appreciation to dedicated teachers I got at different stages of my life. I will never forget Satya Rao sir, who taught me Telugu Aksharaalu (Telugu Alphabets). During school life the teachings of Shankar Rao sir, Sujatha madam, Narasimha Rao sir, Narayana Rao sir and Narayana Murthy sir inspired me and made me to realize the value of education. I still enjoy the happy moments I had with my school mates and friends Aavupaati Melleswara Rao, Ganesh, Nageswara Rao, Gautham, Vishnu Vardhan, Uma, Sravani, Bharathi. During my college days I got extremely good teachers especially Ram Mohan sir for chemistry. Because of his lectures I had turned my interest towards chemistry. I thank Sivakumar sir for his encouragement and help in learning chemistry. For me he is much more than a teacher. I must not forget to mention two important names, my sweet buddies, Subha and Sasidhar. Subha was inspiration to me to aim higher in life. I thank god for the gift he has given me in the form of Sasidhar. I am really lucky to have a friend like Sasidhar, with whom I share everything.

In Andhra University I got very good Professors like Prof. G. Nageswara Rao sir, Prof. A. Satyanarayana Rao sir, Prof. Ramana sir, Prof. Krishna Prasad sir, whose lectures I enjoyed most. In particular I express my sincere gratitude to Prof. Krishna Prasad sir for his encouragement to enter into the research field. I am grateful for the valuable friendship of my M.Sc. class mates Mohan, Bhaskar (Bachi), Lakshminarayana, Laxman, M. Ravi Kumar (Boss), K. Ravi Kumar, Masthan Vali, Phani, Revathi, Swathi, Jaya Laxmi, Nageswara Rao, Suresh, Chiranjeevi, Sudarshan, Rajendra Prasad, Kiran Kumar Varma, Prathap, Veerraju, Jagadeesh, Teja.

I value my association with my former lab-mates: Moloy Sarkar, Aniruddha Paul, Bhaswati, Ravi from whom I have learned many valuable aspects of research. I am extremely thankful to Bhaswati, Ravi and Dinesh for their help in learning instruments. I acknowledge my junior friends Sanghamitra, Satyajit, Soumya, Ashok, Chandrasekhar, Praveen, Navendu for maintaining the friendly and cooperative atmosphere in the lab. I also value my association with Tanmay da. I would also like to thank my project students Murthy, Snigdha and Pawan, who helped me in my research projects and with whom I had spent a wonderful time.

I am really lucky for my close association with "the gang" of HCU, which includes Anand, Balu, Ajay, Bharath, Kishore Ravada, Kishore Pilli, Kalyan, Srinivas (SKD sir's lab), Rambabu, G. Durga Prasad, Srinivas (KCK sir's lab), Arjun, Narayana, Chandrasekhar, Naidu, Ramesh (TPR sir's lab), Gupta, Hari, Raja Gopal, Anji, Rajesh, Murali, Karunakar, Malli (Sahu sir's lab), Ganesh, Malli (Basavaiah sir's lab), Bhanu, Venki, Srinu (Plant science). I am scared whether I have missed some close people.

I thank all the non-teaching staff of the school of chemistry for their time-to-time cooperation. They had all been quite helpful.

Financial assistance from DST and CSIR, New Delhi is greatly acknowledged. Special thanks are due to CSIR for providing me a research fellowship.

I express my sincere gratitude to my uncle (chinnanna) Chandra Sekhar Rao, grandmother Bullemma and grandfather Sri Ramulu for their constant encouragement and support, without which I would not have reached at this stage of life. Chinnanna's support and suggestions for my higher studies are always memorable and valuable. I am really lucky to have Manikyam mamma (grandmother), Neeraja, Ravi, Pavani Pinni, Naidu chinnanna, Jaya pinni, Shyam (annayya), Vamsi, Sonali, Divyamsi as my family members.

Dedication of this thesis is just a small gift for my family members especially for my father (Surya Rao) and mother (Parvathi) for being so selfless and just offering me their love and support. I don't have words to explain the struggle my mother faced to keep me in higher position. Amma, I am very much thankful to you.

I would like to thank all my relatives for their close association with me.

When she is reading this she might be thinking how come I have forgotten her. It's very difficult to forget you Varshini (my sweetest sister). You are so special to me.

Santhosh

List of Publications

1. "Excited State Dynamics of 9,9′-Bianthryl in Room Temperature Ionic Liquids as Revealed by Picosecond Time-Resolved Fluorescence Study." D. C. Khara, A. Paul, **K. Santhosh** and A. Samanta, ***J. Chem. Sci.***, 121 **(2009)** 309-315.

2. "Fluorescence Response of 4-(N,N′-Dimethylamino)benzonitrile in Room Temperature Ionic Liquids: Observation of Photobleaching under Mild Excitation Condition and Multiphoton Confocal Microscopic Study of the Fluorescence Recovery Dynamics." **K. Santhosh**, S. Banerjee, N. Rangaraj and A. Samanta, ***J. Phys. Chem. B***, 114 **(2010)** 1967-1974. **(Chapter 3)**

3. "Spectroscopic and Theoretical Investigations on Effective and Selective Interaction of Fullerenes C_{60} and C_{70} with a Derivatized Zn-phthalocyanine: Stabilization of Charge-Recombined State by Side-On Approach of C_{70}." A. Ray, **K. Santhosh**, S. Chattopadhyay, A. Samanta and S. Bhattacharya, ***J. Phys. Chem. A***, 114 **(2010)** 5544-5550.

4. "Modulation of the Excited State Intramolecular Electron Transfer Reaction and Dual Fluorescence of Crystal Violet Lactone in Room Temperature Ionic Liquids." **K. Santhosh** and A. Samanta, ***J. Phys. Chem. B***, 114 **(2010)** 9195-9200. **(Chapter 4)**

5. "Absorption Spectrophotometric, Fuorescence, Transient Absorption and Quantum Chemical Investigations on Fullerene/Phthalocyanine Supramolecular Complexes." A. Ray, **K. Santhosh** and S. Bhattacharya, ***Spectrochimica Acta Part A: Molecular and Biomolecular Spectroscopy*****,** 78 **(2011)** 1364-1375.

6. "New Photophysical Insights in Noncovalent Interaction between Fulleropyrrolidine and a Series of Zincphthalocyanines." A. Ray, **K. Santhosh** and S. Bhattacharya, ***J. Phys. Chem. A***, 115 **(2011)** 9929-9940.

7. "Fluorescence Quenching of CdS Quantum Dots by 4-Azetidinyl-7-Nitrobenz-2-Oxa-1,3-Diazole: A Mechanistic Study." **K. Santhosh**, S. Patra, S. Soumya, D. C. Khara and A. Samanta, ***ChemPhysChem***, 12 **(2011)** 2735-2741. **(Chapter 6)**

8. "Physicochemical Insights in Noncovalent Interaction of a Newly Designed Triporphyrin with Fullerenes C_{60} and C_{70} in Solution." B. K. Ghosh, **K. Santhosh**, A. K. Bauri and S. Bhattacharya, ***Spectrochimica Acta Part A: Molecular and Biomolecular Spectroscopy,*** 97 **(2012)** 1166-1171.

9. "Diffusion of Organic Dyes in Bovine Serum Albumin Solution Studied by Fluorescence Correlation Spectroscopy." S. Patra, **K. Santhosh**, A. Pabbathi and A. Samanta, ***RSC Advances***, 2 **(2012)** 6079-6086.

10. "What Determines the Rate of Excited-State Intramolecular Electron-Transfer Reaction of 4-(N,N'-dimethylamino)benzonitrile in Room Temperature Ionic Liquids? A Study in [bmim][PF_6]." **K. Santhosh** and A. Samanta, ***ChemPhysChem***, 13 **(2012)** 1956-1961. **(Chapter 3)**

11. "Photophysical and Theoretical Insights on Fullerene/Zincphthalocyanine Supramolecular Interaction in Solution." A. Ray, **K. Santhosh** and S. Bhattacharya, ***J. Phys. Chem. B***, 116 **(2012)** 11979-11998.

12. "Exploring the CdTe Quantum Dots in Ionic Liquids by Employing a Luminescent Hybrid of the Two." **K. Santhosh** and A. Samanta, ***J. Phys. Chem. C***, 116 **(2012)** 20643-20650. **(Chapter 7)**

13. "Specific and Non-Specific Solute-Solvent Interactions of the Aminochalcones in a Room Temperature Ionic Liquid: A Steady-State and Time-Resolved Fluorescence Study." **K. Santhosh**, G. K. Grandhi, S. Ghosh and A. Samanta. (communicated) **(Chapter 5)**

Presentations

Oral Presentations

1. "Fluorescence Spectroscopic Studies of Dual Fluorescent Molecules in Room Temperature Ionic Liquids", **K. V. Rao Scientific Society**, Hyderabad, March 26th, **2011.**

2. "Introduction to Fluorescence and Reactions in Nanocavities/Nanochannels", **Open House**, School of Chemistry, University of Hyderabad, November 5th, **2011.**

3. "What Determines the Rate of Excited State Intramolecular Electron Transfer Reaction of 4-(N,N′-dimethylamino)benzonitrile in Room Temperature Ionic Liquids? A Study in [bmim][PF_6]", **Seminar at Tokyo Institute of Technology**, Tokyo, Japan, December, **2011.**

4. "On the Mechanism of Fluorescence Quenching of the Quantum Dots by Organic Molecular Systems: A Mechanistic Study", **Chemfest-2012**, 9th Annual In-House Symposium of the School of Chemistry, University of Hyderabad, February 25th, **2012.**

Poster Presentations

1. "Fluorescence Response of 4-(N,N′-dimethylamino)benzonitrile in Room Temperature Ionic Liquids: Photoinduced Change and Slow Recovery in the Dark", **Discussion Meeting on Chemical Reactions in Unusual Media,** National Chemical Laboratory (NCL), Pune, Maharashtra, October 8th – 9th, **2009. (Best Poster Presentation Award)**

2. "Modulation of the Excited State Intramolecular Electron Transfer Reaction and Dual Fluorescence of Crystal Violet Lactone in Room Temperature Ionic Liquids", **Trombay Symposium on Radiation and Photochemistry (TSRP)**, Lonavala, Maharashtra, September 16th – 19th, **2010. (Best Poster Presentation Award)**

3. "On the Mechanism of Fluorescence Quenching of the Quantum Dots by Organic Molecular Systems", **National Symposium on Radiation and Photochemistry (NSRP)**, Jay Narain Vyas (JNV) University, Jodhpur, Rajasthan, March 10th – 12th, **2011.**

4. "Specific and Non-Specific Solute-Solvent Interactions of Chalcone Derivatives in Room Temperature Ionic Liquids", **14th National Symposium in Chemistry** at National Institute of Interdisciplinary Science and Technology (NIIST), Trivandrum, Kerala organized by **Chemical Research Society of India (CRSI)**, February 2nd – 5th, **2012.**

5. "Exploring the CdTe Quantum Dots in Ionic Liquids by Employing a Luminescent Hybrid of the Two", **4th Interdisciplinary Symposium on Materials Chemistry (ISMC)** organized by **Bhabha Atomic Research Centre (BARC)**, Mumbai, Maharashtra, December 11th – 15th, **2012.**

Thesis Layout

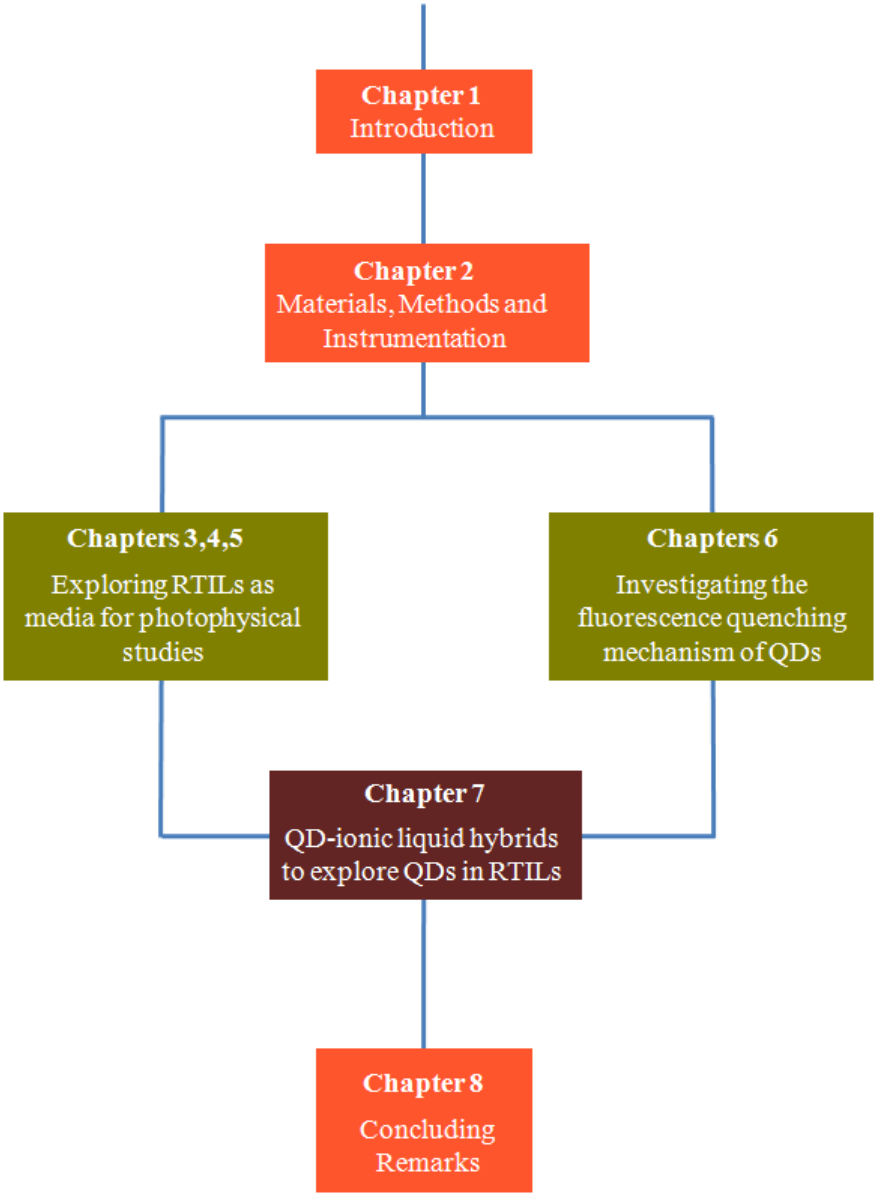

The thesis has been divided into eight chapters. ***Chapter 1*** starts with a brief introduction on room temperature ionic liquids (RTILs), their structural and physical properties and chemical and biological applications. Studies on Photoinduced electron transfer reactions, solvation dynamics, rotational dynamics and fluorescence correlation spectroscopic studies in RTILs have also been included. Introduction is further extended to

give a brief idea on semiconductor quantum dots (QDs), their surface properties, optical properties, applications and photoinduced processes. Motivation behind the thesis and the systems studied are also discussed. ***Chapter 2*** provides the details of the materials, methods of synthesis, methods of purification of the solvents, various methodologies for the sample preparation for different experiments, instrumentation and methods of data analysis. ***Chapter 3*** delineates fluorescence response and excited state intramolecular electron transfer reaction of 4-(N,N′-dimethylamino)benzonitrile (DMABN) in RTILs. ***Chapter 4*** explains modulation of the dual fluorescence of crystal violet lactone (CVL) in RTILs. ***Chapter 5*** deals with the specific and non-specific interactions of the RTILs with aminochalcone solute molecules. ***Chapter 6*** presents possible mechanism of fluorescence quenching of the QDs by organic fluorophores. ***Chapter 7*** deals with QD-ionic liquids hybrids and the influence of the properties of the RTILs on the optical properties of the QDs. ***Chapter 8*** summarizes the findings of the present investigations by touching upon the scope of further studies based on the present work.

Synopsis

of the Thesis entitled

STUDIES ON PHOTOINDUCED PROCESSES IN ROOM TEMPERATURE IONIC LIQUIDS AND FLUORESCENCE BEHAVIOR OF QUANTUM DOTS AND THEIR HYBRIDS WITH THE IONIC LIQUIDS

to be submitted to the

University of Hyderabad

for the degree of

Doctor of Philosophy

by

Kotni Santhosh

School of Chemistry
University of Hyderabad
Hyderabad – 500 046
INDIA

Synopsis

The thesis entitled ***"Studies on Photoinduced Processes in Room Temperature Ionic Liquids and Fluorescence Behavior of Quantum Dots and Their Hybrids With the Ionic Liquids"*** deals with two classes of promising materials, room temperature ionic liquids (RTILs) and nanocrystalline semiconductors or quantum dots (QDs). Though several photophysical studies have been carried out to understand the complex behavior of RTILs, studies on the influence of some novel properties of the RTILs on the photoinduced processes such as excited state electron transfer, proton transfer and energy

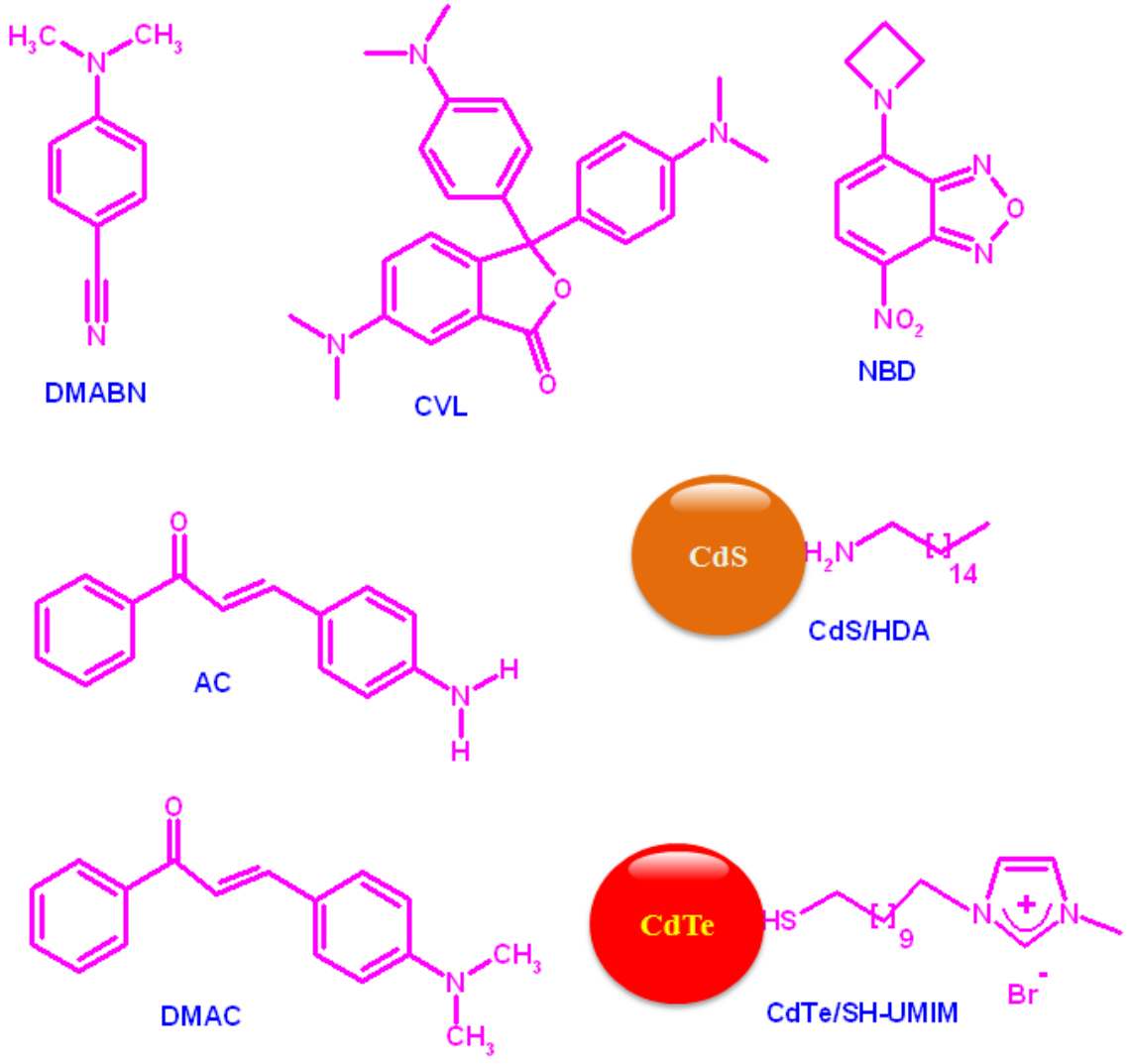

Chart 1. Structures of the fluorescent probes and QDs employed in the present work

transfer are still lacking. Here, we have taken up the case of excited state intramolecular electron transfer reaction of some electron donor acceptor (EDA) molecules (Chart 1) in RTILs. The EDA molecules, whose fluorescence intensities are sensitive to solvent polarity, viscosity and specific solute-solvent interactions, are particularly selected with an intention to comprehend the influence of these properties on the excited state intramolecular electron transfer reactions. QDs are selected with a two dimensional objective, firstly, to investigate the mechanisms of fluorescence quenching as majority of the applications are linked to their quenching mechanism. Secondly, to explore luminescent QDs in RTILs as combining QDs as photosensitizers and RTILs as electrolyte medium can enhance the performance and durability of the QD sensitized solar cells. Several methods and instrumental techniques that include NMR and IR for compound characterization, TEM for QD morphology identification, cone and plate viscometer for RTIL viscosity measurements, UV-vis spectrophotometer, steady-state and time-resolved fluorescence techniques, multiphoton confocal fluorescence microscope for ensemble photophysical studies and time-resolved confocal microscope for the fluorescence measurements at single particle level have been employed for carrying out the work presented here.

A brief chapter-wise content of the thesis is given below

Chapter 1. Introduction

This chapter starts with an introduction on RTILs, including their structural characterization and heterogeneity, wide variety of properties and chemical and biological applications. Several photophysical studies carried out in RTILs, covering experiments at ensemble and single molecule level, are discussed here to understand the heterogeneity of the RTILs and to accentuate the influence of their microscopic properties and specific interactions on solvation dynamics, rotational dynamics and photoinduced electron transfer reactions. This chapter also includes discussion on QDs and their surface properties, solubility, types of core/shell QDs, optical properties including on/off blinking and multiple exciton generation, various photophysical

processes involved and their versatile applications. Finally the motivation behind the thesis and details of the systems studied conclude the chapter.

Chapter 2. Materials, Methods and Instrumentation

This chapter provides a brief description of the materials and methods of purification of the various conventional solvents, RTILs and other reagents used in this work. Synthesis of some of the EDA molecules, quantum dots and RTILs used in the studies is briefly described. Various methodologies like sample preparation for different experiments, which include the sample preparation for confocal fluorescence microscope and transmission electron microscope (TEM) experiments are discussed. Measurements of fluorescence quantum yield and analysis of time-correlated single-photon counting (TCSPC) data, single particle QD blinking experiments have been discussed in detail. All the instrumental setups used in this study are also briefly discussed.

Chapter 3. Fluorescence Response and Excited State Intramolecular Electron Transfer Reaction of 4-(N,N'-Dimethylamino)benzonitrile in RTILs

This chapter deals with fluorescence response and excited state intramolecular electron transfer reaction of 4-(N,N′-dimethylamino)benzonitrile (DMABN) in RTILs. DMABN (Chart 1) is a well known dual fluorescent probe, which undergoes excited state twisted intramolecular charge transfer (TICT) reaction to emit from locally excited (LE) and charge transfer (ICT) states. To control the rate of excited state intramolecular electron transfer reaction, DMABN has been studied in RTILs. Interestingly, it is found that DMABN undergoes photobleaching under mild excitation conditions that leads to a time-dependent change of the fluorescence response of the system. Near reversibility of photobleached emission is observed due to high viscosity of the RTILs, which is not the case in conventional less viscous solvents. Multiphoton confocal fluorescence microscopy study of the fluorescence recovery after photobleaching (FRAP) of DMABN has allowed the estimation of the diffusion coefficient of the molecule in 1-butyl-3-methylhexafuorophosphate, [bmim][PF_6], RTIL. The finding reveals that the microviscosity surrounding DMABN is quite different from the bulk viscosity of the medium. Time-resolved emission behavior of DMABN in [bmim][PF_6] reveals that

excited state LE →ICT transformation is mainly controlled by polarity of the RTIL, though possible influence of the ultrafast component of the solvation dynamics on the electron-transfer process cannot be ruled out.

Chapter 4. Modulation of the Dual Fluorescence of Crystal Violet Lactone in RTILs

Crystal violet lactone (CVL) is a dual fluorescent molecule, which emits from two charge transfer states, CT_A and CT_B. Emission from CT_B state is sensitive to viscosity and hydrogen bonding interactions of surrounding solvent medium. To modulate the excited state intramolecular electron transfer reaction and dual fluorescence of CVL (Chart 1), fluorescence response of CVL has been investigated in six RTILs using steady state and time-resolved emission techniques. It is shown that the excited state CT_A → CT_B transformation and dual fluorescence of CVL can be controlled by appropriate choice of the RTILs. While the second emission from the CT_B state can barely be seen in 1,3-dialkylimidazolium RTILs, dual fluorescence is quite prominent in 1-butyl-2,3-dimethylimidazolium RTIL, [bmMim][Tf_2N]. These contrasting results have been explained taking into account the hydrogen bonding interactions of the 1,3-dialkylimidazolium ions (mediated through the C(2)-hydrogen) with CVL and the viscosity of the RTILs. A comparison of the measured solvation time and excited state reaction time suggests that the CT_A → CT_B reaction rate in moderately viscous ILs is primarily dictated by the dynamics of solvation.

Chapter 5. Specific and Non-Specific Solute-Solvent Interactions of Aminochalcones in RTILs

Unlike most other electron donor-acceptor (EDA) molecules, the aminochalcones exhibit unusual solvent polarity dependent fluorescence behavior. Though the emission is characterized by a single emission maximum, commonly accepted model of aminochalcones consider two fluorescent states to explain the unusual fluorescence behavior of these molecules in conventional less viscous solvents. Photophysical behavior of two aminochalcones (Chart 1), namely 4-aminochalcone (AC) and 4-dimethylaminochalcone (DMAC) has been studied in viscous RTIL, [bmim][PF_6], by steady-state and time-resolved fluorescence techniques to control and to see the emission

from both the excited states. The experiments reveal interesting results that the emitting state in these compounds is different from the commonly accepted model. The studies also reveal an interesting difference of photophysical behavior of the two structurally similar amino chalcone in [bmim][PF_6] RTIL. The differences of fluorescence decay profiles, solvation dynamics and excitation wavelength dependent emission behavior of AC from DMAC are attributed to specific H-bonding interactions of this compound with the RTIL.

Chart 6. On the Mechanism of Fluorescence Quenching of Quantum Dots by Organic Fluorophores

The intense fluorescence of QDs is due to recombination of the bound electron (e) and hole (h) pair, known as exciton, produced on electronic excitation. As majority of the applications of QDs are linked to the exciton quenching dynamics, a clear understanding of the mechanism of fluorescence quenching of the QDs is absolutely essential. For this, we have taken up a case study of Fluorescence quenching of CdS quantum dots (QDs, Chart 1) by 4-aze-tidinyl-7-nitrobenz-2-oxa-1,3-diazole (NBD, Chart 1), where the two quenching partners satisfy the spectral overlap criterion necessary for Förster resonance energy transfer (FRET), is studied by steady-state and time-resolved fluorescence techniques. Even though the two interacting species display quenching behavior, which appears typical of a FRET mechanism, careful investigation reveals that the quenching process is neither dynamic nor does it involve the FRET mechanism. It is shown that the quenching actually proceeds through a static interaction between the quenching partners and is probably mediated by a charge transfer process. The quenching rate constant, which is dependent on the number of NBD molecules adsorbed on the CdS surface, has been evaluated by employing a kinetic model. The present results point to the need for a deeper analysis of the experimental quenching data to avoid erroneous conclusions.

Chapter 7. Exploring the CdTe Quantum Dots in RTILs

Low cost of the materials, size dependent tunability of the luminescence properties and possibility of multiple exciton generation (MEG) allow QDs to produce high-performing and low-cost quantum dot sensitized solar cells (QDSCs). The

sulfide/polysulfide and ferricyanide/ferrocyanide salts in aqueous media or $[Co(o\text{-}phen)_3]^{2+/3+}$ in organic solvents are usually used as electrolytes in quantum dot based liquid junction solar cells. However, practical limitations of leakage and evaporation of the solvent is a major impediment to the commercialization and long-term use of these devices for applications. As RTILs are non volatile and highly thermally stable, they can be a better alternative to the volatile organic solvents. Prior to the employment of the RTILs in QDSCs, it is necessary to study the interaction of the RTILs with the QDs, in particular, their influence on the luminescence properties of the QDs as the efficiency of a solar cell depends on the interactions of the electrolytes with the photosensitizers. To make these studies possible, a task specific ionic liquid (**SH-UMIM**) has been designed and successfully employed to prepare luminescent CdTe**/SH-UMIM** QD-ionic liquid hybrid (Chart 1), which is soluble in both hydrophilic and hydrophobic RTILs. Fluorescence studies based on both ensemble and single-particle blinking measurements reveal that improved emission properties of the QDs in RTILs is due to the protection offered to it by **SH-UMIM** and enhanced stability of the QDs toward O_2 is due to low solubility of O_2 and viscous nature of the RTILs.

Chapter 8. Concluding Remarks

This chapter summarizes the findings of the present investigation. The scope of further studies based on the present work and literature reports has also been outlined.

“Never do anything against conscience even if the state demands it.”

Albert Einstein

“You have to dream before your dreams can come true.”

Abdul Kalam

CONTENTS

STATEMENT i

CERTIFICATE iii

Acknowledgement v

List of Publications vii

Presentations ix

Thesis Layout xi

Chapter 1 Introduction 1

1.1. Room temperature ionic liquids 1

1.1.1. Properties 3

1.1.2. Applications 9

1.1.3. Photophysical studies 10

1.2. Semiconductor quantum dots 16

1.2.1. Surface passivation and solubility 17

1.2.2. Core/Shell quantum dots 19

1.2.3. On/Off blinking 21

1.2.4. Multiple exciton generation 22

1.2.5. Applications 22

1.2.6. Fluorescence quenching 23

1.3. Photoinduced electron transfer reactions 24

1.3.1. Intermolecular process 25

1.3.2. Intramolecular process 27

1.4. Motivation behind the thesis 30

References 34

Chapter 2 Materials, Methods and Instrumentation 43

2.1. Materials 43

2.2. Synthesis of EDA molecules, quantum dots and ionic liquids 45

2.2.1. EDA molecules 45

2.2.2. Quantum dots 45

2.2.3. Ionic liquids 46
2.3. Purification of conventional solvents 49
2.4. Purification of the RTILs 50
2.5. Sample preparation 51
2.5.1. Spectral measurements 51
2.5.2. TEM measurements 51
2.5.3. Single-particle blinking studies 51
2.6. Instrumentation 53
2.6.1. Time-correlated single photon counting setup 54
2.6.2. Time-resolved confocal fluorescence microscope 55
2.7. Measurement of fluorescence quantum yield 57
2.8. Measurement of change in dipole moment on photoexcitation 57
2.9. Data analysis and construction of time-resolved emission spectra 58
2.10. Estimation of solvation time and position of the time-zero spectrum 59
2.11. Estimation of size and concentration of the QDs in solution 59
2.12. Standard error limits 60
References 61
Chapter 3 Fluorescence Response and Excited State Intramolecular Electron Transfer Reaction of 4-(N,N′-Dimethylamino)benzonitrile in RTILs 63
3.1. Introduction 63
3.2. Absorption and fluorescence behavior of DMABN in RTILs 65
3.3. Effect of temperature 69
3.4. Excitation wavelength dependence 72
3.5. Dependence on exposure time 73
3.5.1. Possible explanations 74
3.6. FRAP study 78

3.7. Time-resolved fluorescence behavior of DMABN in [bmim][PF_6] 80
3.8. Conclusion 86
References 88
Chapter 4 Modulation of the Dual Fluorescence of Crystal Violet Lactone in RTILs 91
4.1. Introduction 91
4.2. Absorption and emission behavior in 1,3-dialkylimidazolium RTILs 94
4.3. Absorption and emission behavior in other RTILs 98
4.4. Time-resolved emission spectra (TRES) and time-resolved area normalized emission spectra (TRANES) 99
4.5. Estimation of $CT_A \rightarrow CT_B$ transformation time 100
4.6. Estimation of the solvent relaxation time 102
4.7. Excitation wavelength dependence 102
4.8. Conclusion 103
References 104
Chapter 5 Specific and Non-Specific Solute-Solvent Interactions of Aminochalcones in RTILs 107
5.1. Introduction 107
5.2. Results 110
5.3. Discussion 116
5.3.1. Number and nature of the state 116
5.3.2. Contrasting behavior of AC and DMAC 118
5.4. Conclusion 120
References 121
Chapter 6 On the Mechanism of Fluorescence Quenching of Quantum Dots by Organic Fluorophores 123
6.1. Introduction 123
6.2. Steady state and time-resolved experiments 125
6.3. Possible mechanisms of fluorescence quenching 128

6.3.1. FRET 128
6.3.2. Depassivation of the QD surface 130
6.3.3. Charge transfer 131
6.4. QD fluorescence quenching: The kinetic model 135
6.5. Conclusion 137
References 138
Chapter 7 Exploring the CdTe Quantum Dots in RTILs 141
7.1. Introduction 141
7.2. CdTe/SH-UMIM QD-IL Hybrids 143
7.3. CdSe/SH-UMIM QD-IL Hybrids 151
7.4. Conclusion 152
References 153
Chapter 8 Concluding Remarks 155
8.1. Overview 155
8.2. Future scope and challenges 158

CHAPTER 1

Introduction

This chapter discusses briefly about different types of room temperature ionic liquids (RTILs), their structural and physical properties and chemical and biological applications. Photophysical studies in RTILs are discussed to accentuate the influence of microscopic properties and specific interactions of the RTILs on the solvation dynamics, rotational dynamics and photoinduced electron transfer reactions. This chapter also introduces another promising class of materials, semiconductor quantum dots (QDs), and discusses their surface properties, solubility, single particle blinking behavior, optical properties, various photophysical processes and some of their applications. Finally, the motivation behind this thesis is presented.

1.1. Room temperature ionic liquids

Ionic liquids (ILs) are low-melting salts composed entirely of cations and anions. In general, the cation is a bulk organic structure with low symmetry. Due to weak coulombic interactions between the cations and anions, the ILs exist as fluid at or below 100^{o}C. The term 'ionic liquid' differs from 'molten salt', which represents high melting salts like NaCl with strong electrostatic interactions between cations and anions.[1] Room temperature ionic liquids (RTILs) are the class of ILs, which are liquids at ambient temperature (20 – 30 ^{o}C) and pressure (1 bar). The lowest melting point reported till date is -96 ^{o}C.[2] Low volatility, high thermal stability and the ability to dissolve many inorganic and organic compounds have made the RTILs as possible green alternatives to the traditional solvents, most of which are volatile organic compounds (VOCs), used in chemical reactions, catalysis and separation processes.[3-5]

Though, ethyl ammonium nitrate was identified as the first RTIL as early as in 1914,[6] significant exploration of these materials commenced in early 1980s with the use of salts based on chloroaluminate anions ($AlCl_4^-$ or $Al_2Cl_7^-$) by Wilkes and his co-workers.[7,8] Non-

symmetrical imidazolium (a), pyrrolidinium (b), pyridinium (c), piperidinium (d), ammonium (e) and phosphonium (f) are the commonly used cations of the RTILs (Chart 1.1). In most of the cases, as anions dictate the hydrophilic and hydrophobic behavior and reactivity of the ILs, these are classified into four categories (Chart 1.1) on the basis of the anion.[9] The "first generation ILs" are based on $AlCl_4^-$ or $Al_2Cl_7^-$ anions. However, highly hygroscopic and high reactivity of these salts towards water limited their use in applications. This lead to a "second generation ILs" based on nearly neutral and air stable anions,[10] BF_4^-, PF_6^-, SbF_6^- although they are highly viscous and produce detectable amounts of HF acid on hydrolysis.[11] The other group of ILs based on perfluorinated anions such as $(CF_3SO_2)_2N^-(\equiv Tf_2N^-)$ addresses these problems and are characterized with low melting points, low viscosity and high electrical conductivity. However, ILs based on these anions are expensive, possess stronger binding ability to Lewis acidic metal ions and also the presence of fluorine makes the disposal of

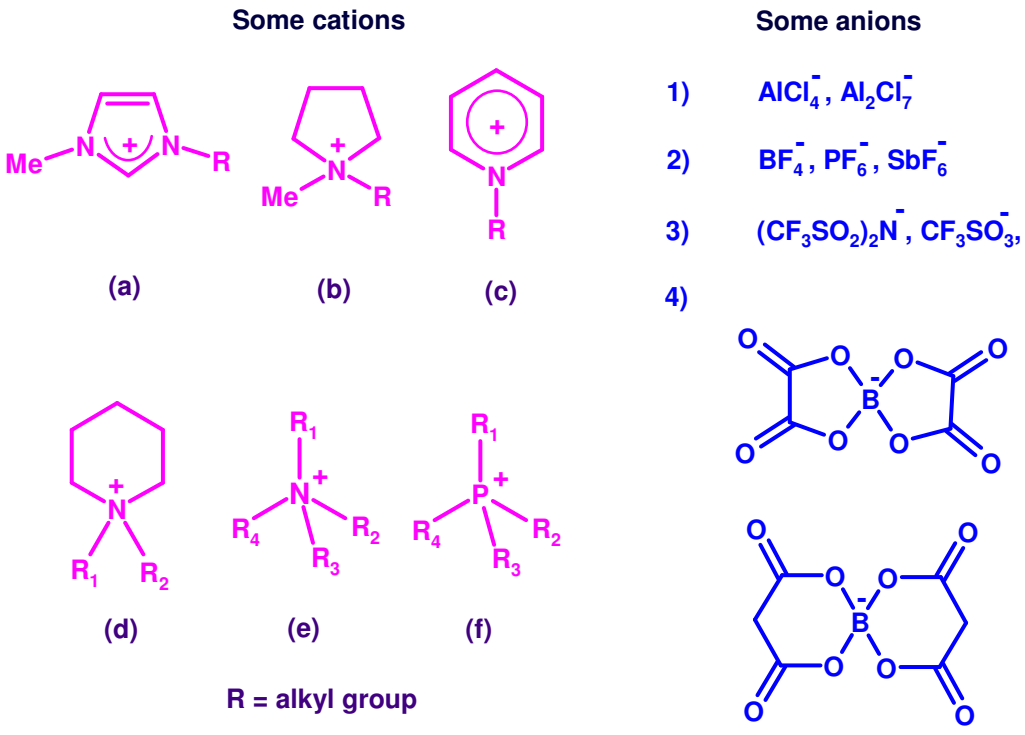

Chart 1.1. Structures of different cations and anions

ILs more complicated.[11-13] This led to the realization of other alternative ILs based on low coordinating, cheaper and non-fluorinated carborane and orthoborate (Chart 1.1) anions.[14,15] In recent years, amino acid based RTILs are being used extensively for biological applications.[16,17] Task specific ILs with specific functional groups can also be prepared for specific applications.[18-20]

1.1.1. Properties

RTILs continue to attract significant attention of the researchers due to their number of useful properties such as negligible vapor pressure, ability to dissolve a large variety of organic and inorganic substances, high thermal and chemical stability, wide liquidous range, wide electrical conductivity, moderate to high polarity, non-toxicity, non-flammable nature and the advantage of recyclability.[3-5,21-23] As the properties of the ILs are dependent on the constituent ions, ILs with desired properties can be synthesized by appropriate choice of the cation and anion, and hence, they are also termed as "designer solvents".[24] Chart 1.2 depicts the structures of some common imidazolium RTILs.

Chart 1.2. Structure and abbreviation of some common imidazolium RTILs

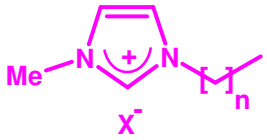

n =	1	3
X = BF_4,	[emim][BF_4]	[bmim][BF_4]
= PF_6,		[bmim][PF_6]
= Tf_2N,	[emim][Tf_2N]	[bmim][Tf_2N]
= $EtSO_4$,	[emim][$EtSO_4$]	[bmim][$EtSO_4$]

Melting point. Most of the melting point values of ILs are uncertain as they undergo supercooling. Temperature of the phase transfer depends on whether the IL is heated or cooled.[9] Since the properties of the ILs depend on the structure, attempts have been made to correlate the melting point of the ILs to the nature of their cation or anion. For most of the ILs it has been observed that the melting point increases with increase in branching of the alkyl chain length, and it decreases with increase in size or asymmetry of the cation.[25,26]

Table 1.1 collects some of the physical properties, which include the melting points of some imidazolium ILs. Though, some correlation has been found in terms of the effect of the cation, particularly in case of salts based on imidazolium cations, anion effect remains uncertain.[9] Although, NMR, crystallographic and IR experiments have clearly shown the existence of H-bonding interactions between cation and anion of the ILs,[9,27-32] this property can not completely explain the influence of anion on the melting point. For instance, even though, [bmim][Cl] has three $C-H\cdots Cl$ interactions per unit compared to two in 1-butyl-2,3-dimethylimidazolium chloride, [bmMim][Cl], the latter has a higher melting point.[32] Low charge density and lack of hydrogen bonding interaction are the main reasons for low melting point of salts based on Tf_2N^- anion, whereas more spherical anions like BF_4^- and PF_6^- with

Table 1.1. Physical properties of some common imidazolium RTILs

RTIL	T_{mp} / °C	T_d / °C	η / cP	ρ / (g/cc)	σ / (ms/cm)	$E_T(30)$
[emim][Cl]	86[a]	-	s	s	-	-
[bmim][Cl]	65[a]	-	s	s	-	-
[emim][BF_4]	6[a]	447[b]	66.5[c]	1.25[c]	13[d]	49.1[e]
[prmim][BF_4]	-17[b]	435[b]	103[b]	1.24[b]	5.9[b]	-
[bmim][BF_4]	-81[f]	435[b]	154[c]	1.2[c]	3.5[b]	48.9[e]
[emim][PF_6]	60[g]	-	s	s	5.2[d]	s
[bmim][PF_6]	-61[f]	-	371[c]	1.37[c]	1.5[d]	52.3[h]
[emim][Tf_2N]	-3[i]	-	34[i]	1.52[i]	8.8[i]	47.7[j]
[bmim][Tf_2N]	-4[i]	>400[b]	52[k]	1.43[k]	3.9[k]	47.2[j]

T_{mp}: melting point, T_d: decomposition temperature,

s: solid, η: viscosity, ρ: density, σ: specific conductivity,

$E_T(30)$: microscopic solvent polarity parameter[33]

(a) ref[34]; (b) ref[35]; (c) at 20°C, ref[3]; (d) at 25°C, ref[36]; (e) ref[37]; (f) ref[38]; (g) ref[39]; (h) ref[33]; (i) at 20°C, ref[40]; (j) ref[41]; (k) ref[42]

potential hydrogen bonding ability lead to higher melting points. Thus, delocalization of charge along with hydrogen bonding interaction can explain the anion effect to some extent.

Thermal stability and volatility. Most of the ILs are found thermally stable with decomposition temperatures > 400 °C (Table 1.1). Though the commencement of thermal decomposition is similar for different cations,[9] the value appears to decrease with increase in anion hydrophilicity.[22] The thermal stability of the ILs comprising different anions decreases as $PF_6^- > Tf_2N^- \sim BF_4^- >$ halide [9,22]

Though, RTILs are found to have negligible vapor pressure and considered as suitable green alternatives to the VOCs in many organic chemical processes, reports have also shown that they have significant vapor pressure and thus, can be distilled under reduced pressure without any thermal decomposition.[43-45] Earle and coworkers were the first to show the vacuum distillation of RTILs, stating that most of the commonly used aprotic ILs can be distilled at 200-300 °C and low pressure.[44] For instance, the vacuum distillation of 1-hexyl-3-methylimidazolium bis(trifluoromethanesulfonyl)imide is reported at 170 °C and 0.07 millibar. Later, attempts have been made to separate the mixture of ILs in pure form, which is also found very useful for the recyclability of spent RTILs. Though, Earle and coworkers could not provide direct proof of ions in the gas phase of their distillation process, recent report by Leone et al. identified intact ion pair of 1-butyl-3-methylimidazolium tricyanomethanide, using tunable vacuum ultraviolet photoionization time-of-flight mass spectrometry (PI-TOFMS).[46]

Viscosity and density. Unlike conventional solvents, RTILs are highly viscous like oils and even the least viscous RTIL is around 30 times more viscous than commonly used solvents like water, acetonitrile or alcohols (Table 1.1). The viscosity (η) of the RTILs decreases with increase in temperature and the trend does not follow Arrhenius behavior, but obeys Vogel-Tammann-Fulcher (VFT) equation (1).[47]

$$ln(\eta) = ln(\eta_0) + \frac{DT_C}{T-T_C} \text{ ---------- (1)}$$

Where, η_0 is the viscosity at infinite temperature, D is the fragility parameter and T_C is the characteristic temperature at which viscosity diverges. The impurities like halides and water

content present in the RTILs affect their η values.[2,48] The viscosity of the ILs is attributed to van der Waals forces among cations and anions.[15] This statement has been further supported by the observation that viscosity of the 1-alkyl-3-methylimidazolium RTILs with Tf_2N^- and BF_4^- anions increase with number of carbons in the alkyl chain (Table 1.1). Branching of the alkyl chain reduces the viscosity of the imidazolium ILs. Symmetry and H-bonding between counter anions are additional parameters responsible for the viscosity of the ILs. Based on these two parameters the decreasing order of viscosity Cl> PF_6^- > BF_4^- > Tf_2N^- can be explained.[25,26] H-bonding is the sole reason for the higher viscosities of alcohol-functionalized RTILs than their alkyl counterparts.[49,50] Interestingly, photophysical measurements have established that the microscopic viscosities of the RTILs are different from the bulk viscosities, where the estimated microscopic viscosities are dependent on the fluorescent probe employed.[51]

Density of the RTILs is also higher compared to most of the commonly used solvents. The molar mass and volume of the counteranion significantly affect the density of the RTILs, in agreement with the fact that for most of the RTILs an increase in density is observed with increase in molar mass and decrease in volume of the anion.[15,25,26,52,53]

Conductivity and ionic diffusion. Transport properties are crucial when RTILs are used as alternative electrolyte media in electrochemical applications such as in lithium ion batteries, double-layer capacitors, fuel cells. Since RTILs are composed entirely of ions, large conductivity values are generally expected. However, RTILs with inorganic electrolytes show values similar to organic solvents.[35,36,40,42] Though, some correlation between chemical structures of the RTILs and conductivities is observed, complete relation between these two could not be drawn yet. For some RTILs, it is observed that the conductivity decreases with decrease in planarity of the cation as evidenced in 1-alkyl-3-methylimidazolium > N,N-dialkylpyrrolidinium > tetraalkylammonium RTILs.[36] Table 1.1 shows conductivity values of some imidazolium RTILs. In general, ionic diffusion (D) in any liquid medium is dependent on its viscosity (η). For RTILs, the value of D follows Stokes-Einstein equation (2),[54]

$$D = \frac{kT}{6\pi\eta r} \text{ ----------(2)}$$

where, k is Boltzmann constant, T is the absolute temperature and r is the effective hydrodynamic or Stokes radius. RTILs are also characterized with high heat conductivities and hence they allow a very rapid dispersal of the heat of reaction.[9]

Polarity. Static dielectric constant (ε) is the common measurement of polarity of any liquid. Dielectric constants of some of the measured RTILs (ε = 9-13 at 25 °C) indicate that these media are much less polar than acetonitrile (ε = 35.9 at 25 °C)[55] and similar to pyridine (ε = 12.3 at 25°C).[56,57] However, these measured bulk polarity values could not explain most of the experimental observations in RTILs.[54] Since, actual polarity of the solvent accounts for the microscopic interactions (coulombic, H-bonding, electron pair donor and acceptor forces etc.) between solute and solvent molecules, microscopic polarity $E_T(30)$ or E_T^N would be more appropriate than ε. Several solvatochromic probes (Chart 1.3) like betaine dye and different polarity parameters like Kamlet-Taft parameters have been employed to appraise the polarity of RTILs.[33,37,58,59] The estimated $E_T(30)$ or E_T^N values (Table 1.1) indicate that the polarity of the most of the RTILs is in between that of acetonitrile and methanol.[33] It is also important to note that purity of the RTILs severely affects their polarity values.[60]

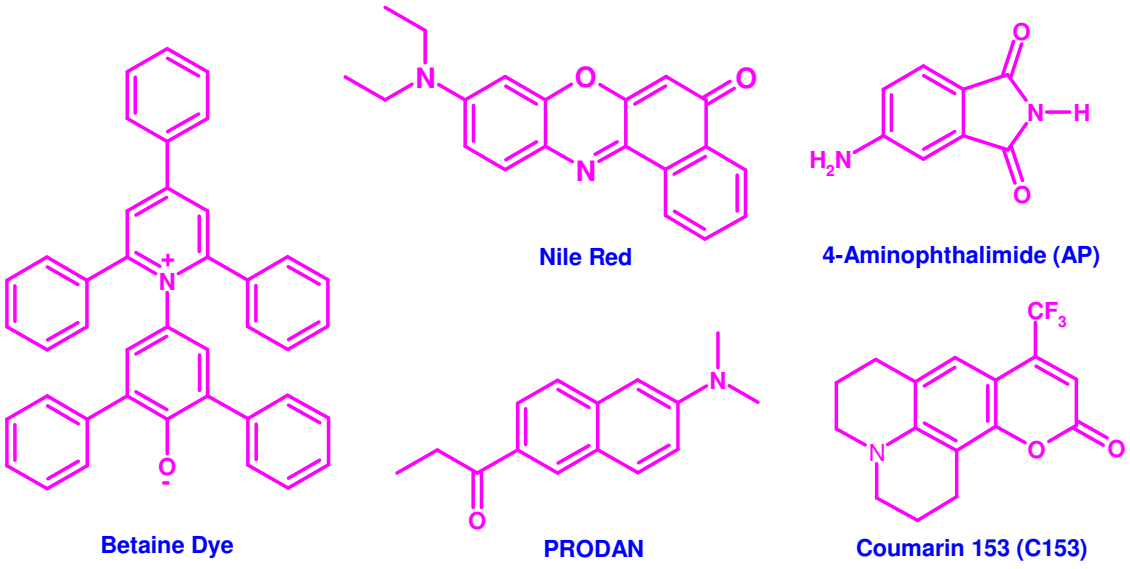

Chart 1.3. Structures of some commonly used solvatochromic probes for the measurements of polarity of RTILs

Structural characterization and heterogeneity. Structural organization is important to understand how ILs affect the chemical reactions and other processes. Many experimental and theoretical studies have been carried out to establish the structure of the ILs in both solid and liquid phases. Though some ILs are glass formers and intricate to crystallize, many ILs could be crystallized with one or more polymorphs.[61-63] It is found that ILs with small, symmetric and rigid anions such as halides, BF_4^-, PF_6^- could be crystallized easily than those with flexible anions like Tf_2N^- and $CF_3SO_3^-$.[30,62,64-67] While the crystallographic data on imidazolium salts reveal cation-anion hydrogen bonding network, the presence of such interactions in liquid salts is not yet clear.[30-32] However, attempts have been made to explore the crystal structures of RTILs by *in situ* crystallization at low temperatures.[68] IR studies on a number of RTILs have shown the existence of C–H---X hydrogen bonding interactions in liquid state too.[27-29] Even the existence of contact ion pair in propionitrile solution of IL, as evidenced by multinuclear NMR experiments, reveal how strong is the H-bonding interaction between halide and hydrogen atoms of the imidazolium ring.[9] Simulation studies on ILs confirm the presence of long range charge ordering of the cation and anion to minimize the coulombic energy of the IL.[69-73] The charge ordering of 1-alkyl-3-methylimidazolium ($[C_nmim]^+$; n = 1, 2, 4, 8) ILs based on I^-, PF_6^-, BF_4^- and $CF_3SO_3^-$ anions is found to be similar to those of molten metal halides.[69,74,75]

Interestingly, neutron scattering experiments,[76] X-ray diffraction,[77] optical Kerr effect,[78,79] Raman scattering,[80] fluorescence spectroscopic studies,[37,47,81-83] molecular simulation studies,[72] sum frequency generation experiments[84] etc. have characterized ILs as heterogeneous media consisting of "local structures". However, the issue of heterogeneity has not yet resolved. Some simulation and experimental results support microheterogeneity and some others favor nanostructural organization of the ILs. For instance, simulation studies by Lopes and Padua described the "local structure" as nano aggregation of alkyl chains of the imidazolium cations in nonpolar domains with ionic channels formed by anions and the imidazolium cations.[85]

Other properties. Other important properties of RTILs are refractive index and their miscibility with water and other organic solvents. Refractive indices of [bmim][X] salts are comparable to those of organic solvents.[52] The miscibility with water classify them as

hydrophilic and hydrophobic ILs. Anion mainly controls their solubility. For example, PF_6^-, Tf_2N^- etc. salts are hydrophobic, whereas the halides, BF_4^-, alkylsulfate based salts are hydrophilic in nature.[9] Though, PF_6^-, Tf_2N^- based ILs are generally water insoluble, additional functional groups such as OH in the alkyl chain of the cation enhances the miscibility of the ILs with water. On the other hand, increase in alkyl chain length of the cation induces hydrophobic regions and decreases the miscibility with water.[25,26,52]

As the addition of conventional solvents fine tune many physical properties of the RTILs, such as polarity,[60,86,87] viscosity,[2,48,88] electrochemical behavior[89,90] and solvation,[60,87,91] their mixtures with conventional solvents broaden their applications. For instance, electrochemical studies on RTIL-conventional solvent mixtures have shown the influence of less viscous solvent on the ionic association/dissociation phenomenon.[89,90] Solvent with high dielectric constant and hydrogen bonding ability favors ionic dissociation, whereas solvent with low dielectric constant promotes ionic association.[89]

1.1.2. Applications

Low volatility, high thermal stability, and the ability to dissolve many inorganic and organic compounds have made the ILs as possible alternatives to the volatile organic solvents in chemical reactions, catalysis, mass spectrometry and separation processes.[3-5,92] Because of high proton conductivity, low reactivity, and wide electrochemical window provided by the ILs, these serve as excellent electrolyte in electrochemical applications such as in lithium ion batteries, double-layer capacitors, fuel cells, and actuators.[21-23,93,94] Synthesis of biocompatible ILs allows them to be solvents for enzyme-based reactions, biocatalysis, protein folding, and unfolding studies.[16,95] In materials chemistry, ILs have been used for the synthesis of inorganic nanomaterials, metal oxide nanorods, and nanowires.[96,97] Transition-metal nanoparticles synthesized in ILs have been found to show high stability and good catalytic activity.[98] RTILs even can be used as stationary phase in gas chromatography.[99] The biphasic acid scavenging utilizing ionic liquids (BASIL) method has been widely used in industrial applications,[100,101] for example, alkoxyphenylphosphines based raw materials for the production of photoinitiators to cure coatings and printing inks by exposure to UV light have been synthesized by this method. The flexibility of functionalization of the anion or cation allows synthesis of task-specific ILs for a particular application.[18,19] Recently, ILs

have been modified with thiol-functional group to cap semiconductor nanocrystalline materials (quantum dots) to explore the properties of the latter in RTILs.[20]

1.1.3. Photophysical studies

RTILs continue to attract significant attention from researchers worldwide for some of their unique properties, where physical chemists have intense interest in characterizing them through both simulation and experimental studies. Various photoinduced processes are being studied in RTILs primarily to obtain insight into their complex nature and also to exploit some of their properties to control the photoprocesses of various systems. Many photophysical studies characterized the RTILs as heterogeneous media in terms of polarity and viscosity. The solvation dynamics, rotational dynamics, electron transfer and proton transfer reactions carried out in these media offered a better understanding of the effect of these microscopic properties on chemical reactions.[37,47,72,81,82,102,103] Some important photophysical studies in RTILs are briefly discussed in the following sections.

Excitation wavelength dependent fluorescence behavior. According to Kasha's rule, irrespective of the excitation energy, fluorescence of molecules originates from lowest vibrational energy level of the lowest excited state of the same multiplicity.[104] Hence, emission spectrum is expected to be independent of excitation wavelength. However, under specific conditions and in specific media the emission spectrum is found dependent on the excitation wavelength. This unusual observation is termed as 'Red Edge Excitation' (REE) and the media are described as heterogeneous in nature.[105,106] Like proteins,[107] polymers,[108] micelles,[109] and phospholipid vesicles,[110] the RTILs are also characterized as heterogeneous medium.[47,51,72,81,82,111-113] REE is also termed as red edge excitation shift (REES), edge excitation shift (EES) or edge excitation red shift (EERS). To observe REE, two important conditions, the presence of ensemble of energetically different molecules in the ground state and the time of excited state relaxation processes such as solvation or energy transfer from the fluorescent state to a low lying energy state of the same fluorescent molecule must be shorter or comparable to the fluorescence lifetime of the species, should be satisfied.[105,106] As the molecules absorbing at the red side of the absorption band have stronger solute-solvent interactions, REE can be identified only when the fluorophore is excited at the red side of the

absorption spectrum (Scheme 1.1).

REE in RTILs can provide information on the photophysical reactions like excited state intramolecular electron transfer, proton transfer reactions etc. For instance, emission intensities from two excited states of dual fluorescent molecule 4-(N,N'-dimethylamino)benzonitrile (DMABN) in RTILs can be controlled by the excitation wavelength.[47] Increase in excitation wavelength on red side increases the emission from more charge transferred species indicating that increase in excitation wavelength selects molecules located in more polar region. REE also provides information on the existence of specific solute-solvent interactions between fluorophore and RTILs. It has been shown that specific H-bonding interactions between 8-anilinonaphthalene-1-sulfonate (ANS) and anion of the RTIL contribute to the REE observed in [bmim][BF_4] and [bmim][PF_6] RTILs.[114]

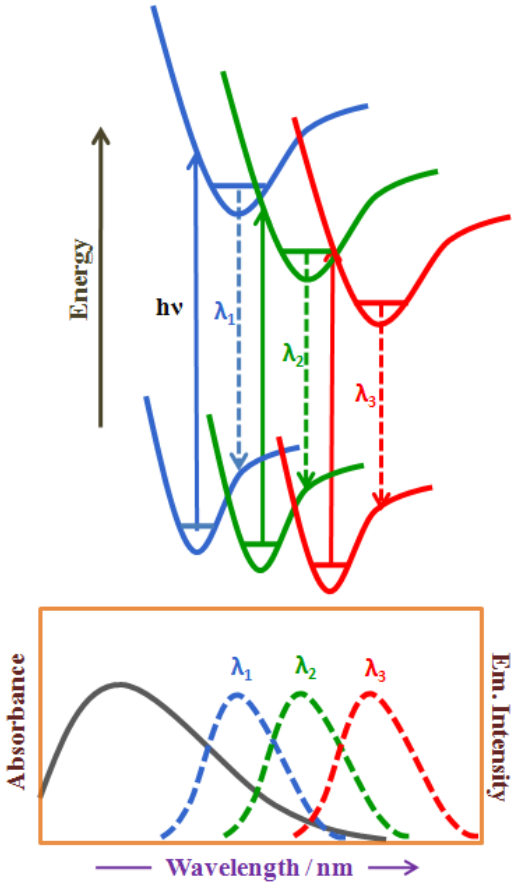

Scheme 1.1. Pictorial illustration of molecular basis of REE

Solvation dynamics. Solvation dynamics is the reorientation of solvent dipoles or charged species around a newly formed solute dipole on photoexcitation and the time required for this solvent rearrangement is called solvent relaxation time.[115] Since RTILs are sufficiently polar, time-resolved fluorescence experiments on dipolar molecules can provide valuable information on the time scale of the reorganization of the ionic constituents of the RTIL around the photogenerated, newly formed charge separated species. The rate of solvation dynamics of any fluorophore depends on the viscosity, molecular structure and temperature of the surrounding solvent medium.[115] As RTILs are highly viscous, the rate of solvation in these media is slow compared to that in commonly used less viscous organic solvents and

water. As the solvation time of less viscous conventional solvents is less than 100 ps and the excited state lifetimes of fluorophores are of the order of few nanoseconds, emission of molecules in conventional less viscous solvents originates from completely solvated/relaxed state.[115] However, in viscous and heterogeneous media like RTILs, proteins and micelles, the solvation process slows down and several stages of solvent relaxation can be monitored leading to a time-dependent shift in the fluorescence spectra, which is schematically illustrated in Scheme 1.2. This phenomenon is called dynamic Stokes shift[116] and solvation dynamics of several probes has been studied using this concept.

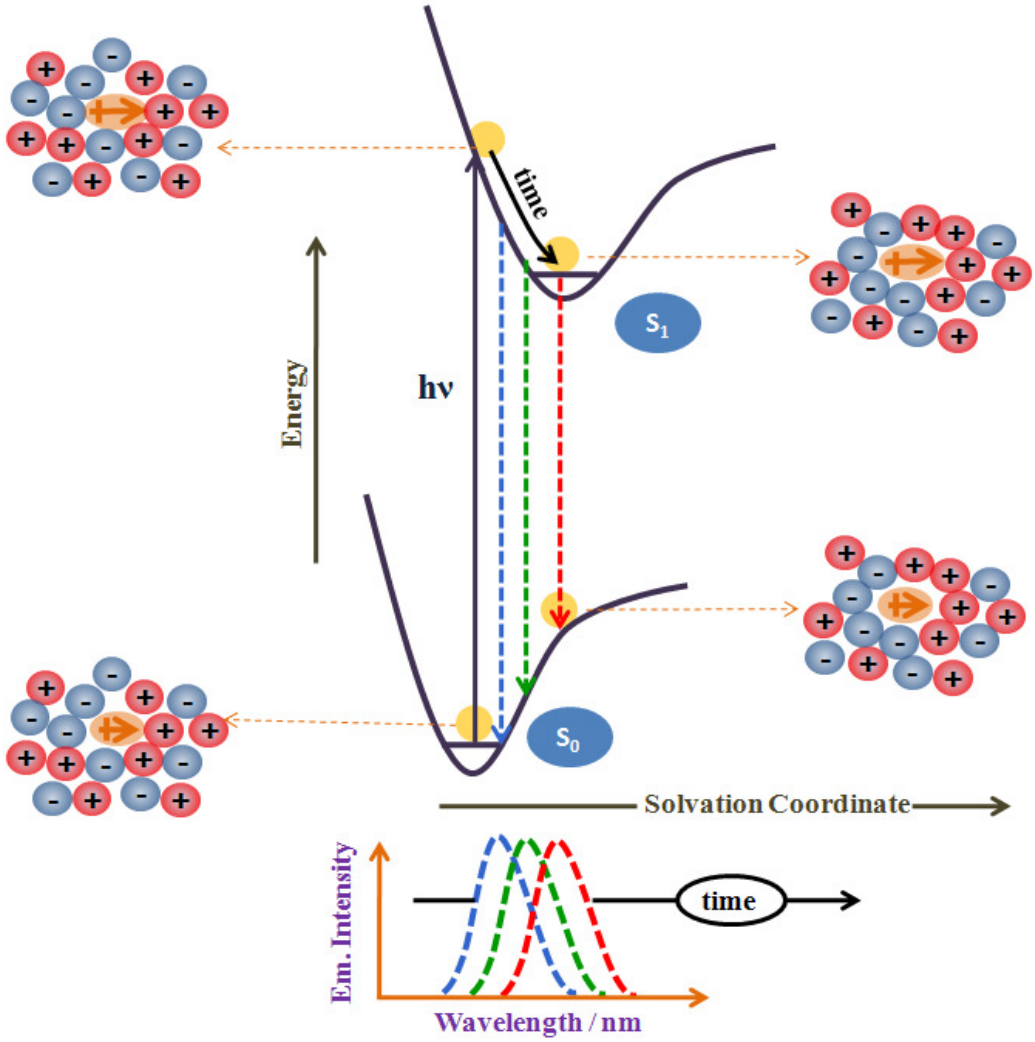

Scheme 1.2. Pictorial illustration of dynamic Stokes shift in RTILs

Under normal conditions, the solvation dynamics in conventional solvents found to be monoexponential. Ever since the work of Karmakar and Samanta, many researchers have contributed to the studies on solvation dynamics in RTILs.[41,117-125] All these results suggest that the solvation of RTILs is much slower compared to that in conventional solvents and biphasic in nature. The slow component is however accompanied by an ultrafast component, termed as missing component as most part of this component is missed due to finite time resolution of the instrumental set up (typically 25 ps). Although the ultrafast or missing component is independent of the viscosity of the RTIL, 30-50 % of the dynamics has been observed to be ultrafast depending upon the nature of the RTIL used.[41,117-119,125] Though no clear conclusion on the origin of the ultrafast component is drawn yet, planar ring system and polarizability of the cation, small amplitude motion of the ions in the first solvation shell, ion mass are considered to be responsible for the ultrafast component of the solvation dynamics.[120,121,126-128] Though there are different opinions on the time scale of ultrafast component, studies based on femtosecond upconversion technique show that only 10-20 % of the dynamics is ultrafast and occurs within 10 ps timescale.[121] While the dynamics is biphasic in nature, some authors have preferred nonexponential description of solvation dynamics to emphasize the collective contribution of both anion and cation to the slow dynamics of the solvation.[119,125-127] However, in both cases, the average solvation time is found to be similar, with better correlations observed in less viscous RTILs (< 100 cP). The solvation dynamics in RTIL is found to be probe dependent.[129-131] Solvation dynamics studies have also been carried out in mixtures of RTILs with conventional solvents and also in micellar solutions of RTILs.[132,133]

Simulation studies have also contributed equally to the better understanding of the results of the solvation dynamics in RTILs. These results, however presented different pictures on the mechanism. For example, studies by Shim et al. ascribed the fast component to the translational motion of the anions,[122] whereas Kobrak and Znamenskiy considered collective cation-anion motion as responsible for the same component. [134,135] Later, Shim et al. attributed the ultrafast dynamics to the local density of the ions near the solvation probe molecule.[136] When the local density is high, few ions close to the probe molecule are responsible for the ultrafast component, whereas, when the local density is low the ions from the further region contribute significantly to the ultrafast component.

Solvation dynamics often controls the rate of the excited state reaction. For instance, the excited state intramolecular electron transfer reaction of dual fluorescent crystal violet lactone (CVL) in viscous RTILs is controlled by complete solvation of the latter and slowed down by several hundreds of picoseconds compared to that in conventional less viscous solvents.[137,138] In contrast to this result, the viscosity of the RTIL shows negligible effect on the excited state intramolecular electron transfer of DMABN.[139] This indicates that the role of solvation dynamics on excited state reactions is completely dependent on the nature of the fluorophore being studied. Solvation-independent excited state reactions are not only restricted to the electron-transfer reaction, but are also observed in the case of excited-state intramolecular proton transfer reactions as well. It has been shown that the excited-state intramolecular proton-transfer reaction of 4'-N,N-diethylamino-3-hydroxyflavone (DEAHF) is partially coupled with the solvation surface of the excited state and the average excited-state intramolecular proton-transfer time is much faster than the full solvation time.[140]

Fluorescence anisotropy – Rotational dynamics. Fluorescence anisotropy is a measure of emission depolarization of a fluorescent molecule that absorbs polarized light. Rotational motion in the excited state is the common cause of emission depolarization.[115] Specific solute-solvent interactions, viscosity and temperature of the surrounding solvent medium are the major parameters, which control the dynamics of solute rotation. Hence, along with solvation dynamics, rotational relaxation of the solute molecules in RTILs through time-resolved fluorescence anisotropy studies can also provide information on the solute-solvent interactions and the solvent properties of the medium. As RTILs constitute of ions, it is obvious to expect influence of those ions on the rotational dynamics of either cationic and/or anionic charged probe molecules. Interestingly, most of the rotational relaxation studies reveal that the rotational times of the charged species in RTILs are just dependent on the viscosity of the medium and the effect of ionic constituents of the RTILs on the rotational dynamics is found negligible.[126,131,141] Stronger interaction of the oppositely charged ions of the RTIL forming ion pairs or larger aggregates is possibly responsible for these observed results. However, when the solute molecule is capable of hydrogen bonding interaction with the anion or cation of the RTIL, the observed rotational times are found to be higher than the expected values based on the viscosity of the medium.[142,143] For example, though van der

Waals radius of coumarin 153 (C153) is higher than that of 4-aminophthalimide (AP), AP shows a slower rotational motion than coumarin C153 in alcoholic functionalized RTIL, 1-(hydroxyethyl)-3-methylimidazolium bis(trifluoromethanesulfonyl)imide due to hydrogen bonding interactions.[142]

Fluorescence correlation spectroscopic studies. Fluorescence correlation spectroscopy (FCS) is an advanced fluorescence technique at the single molecule level for the study of molecular diffusion, singlet-triplet dynamics, chemical reactions, binding studies, conformational changes of organic molecules, protein dynamics etc.[115] This technique is based on correlation of fluorescence intensity fluctuations of a dilute solution of fluorophores (1 nM to pM) in a small excitation volume, approximately 1 fL.

Studies on diffusion of organic fluorophores by FCS technique help in understanding the heterogeneous structure of the RTILs. Baker and co-workers were the first to use this technique to study the translational diffusion of charged and neutral fluorophores in [bmim][PF_6].[144] These experiments highlight the convenience to work with low sample concentration and sensitivity over other existing methods such as triplet-triplet annihilation, excimer luminescence and fluorescence recovery after photobleaching. The research based on FCS technique in RTILs is intensified in recent years. Baker and co-workers reported biphasic diffusion for rhodamine 6G in N-alkyl-N-methylpyrrolidinium bis(trifluoromethanesulfo- nyl)imide, [C_nmPr][Tf_2N], RTILs with n = 3, 4, 6, 8 and 10.[145] Increase in alkyl chain length decreases both the fast and slow diffusion coefficients with increase in relative contribution of the slower diffusion. They attributed the observation to self-aggregation of the nonpolar alkyl chains of the cationic ring. Bhattacharyya and co-workers have studied diffusion of neutral and anionic dyes in two imidazolium ionic liquids with the same cation and different anions and the results have been compared to those in water.[103] A wider distribution of the diffusion coefficients of a dye in RTILs is attributed to the heterogeneity of the media. Diffusion coefficients of anionic and neutral dyes are found similar in water. However, due to electrostatic interactions between RTILs and solute molecules, the anionic dye diffuses 1.7 times slower than the neutral dye indicating that FCS experiments not only provide information on structural heterogeneity but are also useful to understand the electrostatic/specific interactions between ionic liquids and fluorescent probe

molecules.[103] The recent experiments by Patra and Samanta compare the results of FCS and fluorescence lifetime data to explain the heterogeneity and existence of non-polar and polar regions of the RTILs.[83] These are the few studies, where FCS technique has been employed to characterize the RTILs and the observed results are consistent with the studies based on molecular dynamic simulations and neutron scattering experiments.

1.2. Semiconductor quantum dots

Quantum dots (QDs) are semiconductor nanocrystals, which were discovered way back in 1980's. The term "quantum dot" was coined by Mark Reed.[146] QDs exhibit interesting size-dependent optical properties due to three-dimensional quantum confinement of the photo generated electron and holes, known as excitons.[147] The typical size of QD varies from 1-100 nm. The electronic transitions in QDs are discrete in nature suggestive of isolated atoms or molecules and also show useful properties of bulk semiconductor crystals, thus act like a link between small molecules and bulk crystals.[148] Scheme 1.3 illustrates the electronic energy levels corresponding to a semiconductor in transition from molecule to nanocrystal and bulk crystal. Bulk crystalline semiconductor has continuous conduction (CB) and valence band (VB) energies separated by a fixed energy E_g (bulk), whereas the energy levels of nanocrystalline semiconductors are discrete in nature and the energy gap between CB and VB varies with size of the nanoparticles.[147,149,150] Large density of electronic states offers higher extinction coefficients and broader absorption spectral features, which are available only for less number of chromophores. QDs are novel fluorophores and their intense fluorescence is due to recombination of electron (e) and hole (h) produced on electronic excitation.[148] Commonly, QDs constitute atoms from groups II, III, IV, V and VI. CdS, CdSe, CdTe belong to II-VI

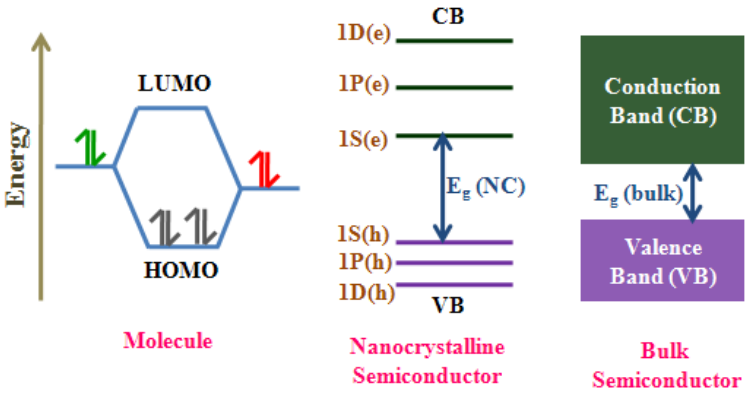

Scheme 1.3. Electronic energy states of a molecule, nanocrystalline and bulk semiconductor

QDs[151] and PbS and PbSe are the examples of IV-VI QDs.[152] The size of the QD can be controlled with reaction temperature or time. For example, QDs of smaller size can be synthesized at lower temperature with longer reaction time or at higher temperature with shorter reaction time. After achieving desired particle size, they need to be protected with capping agents for further stabilization.[153,154] Although other synthesis techniques are available, solution phase technique is more suitable to have control over size, shape and monodispersity of the QDs.[148]

1.2.1. Surface passivation and solubility

The atoms on the surface of the QDs are incompletely bonded with the atoms inside the crystal lattice leaving non bonding (dangling) orbitals on the surface of the QDs. These unpassivated/dangling orbitals form a band structure,[155,156] which acts as a trap for the electron in CB increasing the probability of nonradiative decay pathways.[148] This severely

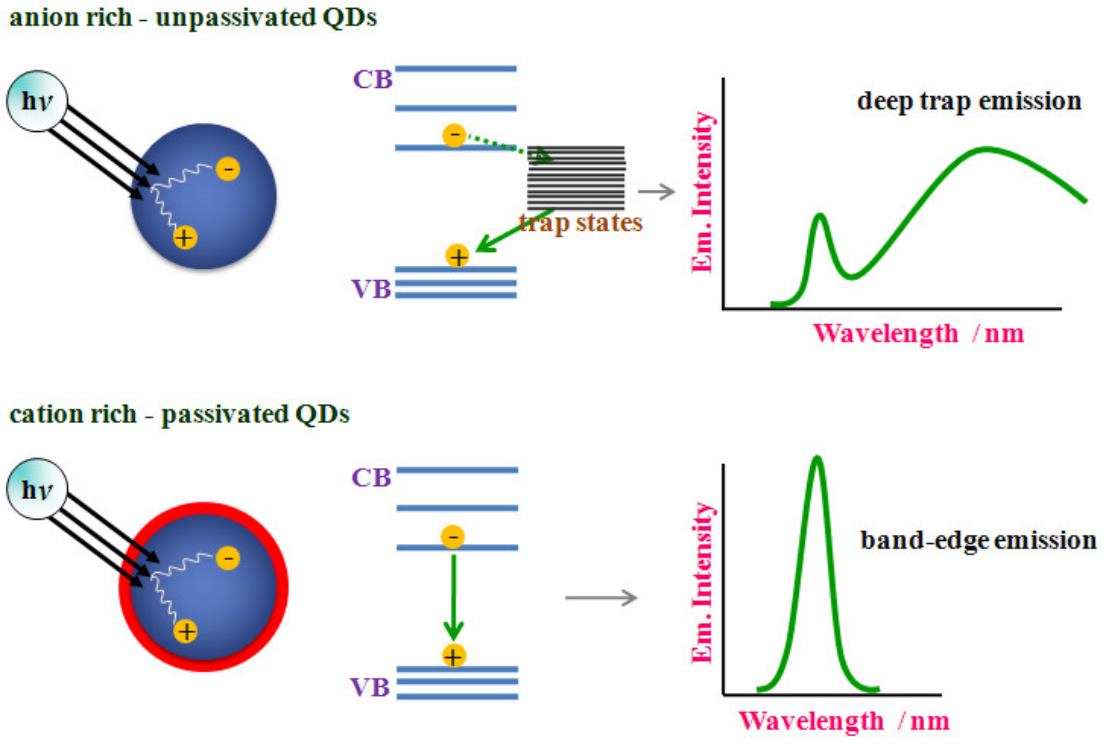

Scheme 1.4. Surface trap states and their influence on QD fluorescence

affects the optical properties of the QDs, with more influence on QDs of smaller sizes as the number of dangling orbitals on the surface increases with decrease in size. QDs with trap states display two emission bands; a narrow one corresponding to band edge emission from CB to VB and a broad deep trap emission at lower energy due to the combination of electron from the dense trap states to the hole in VB (Scheme 1.4). To reduce the contribution of the deep trap emission, QDs surface should be protected with surface capping agents. As shown in Chart 1.4, the capping agents are organic ligands containing basic atoms like S, N, O, P,

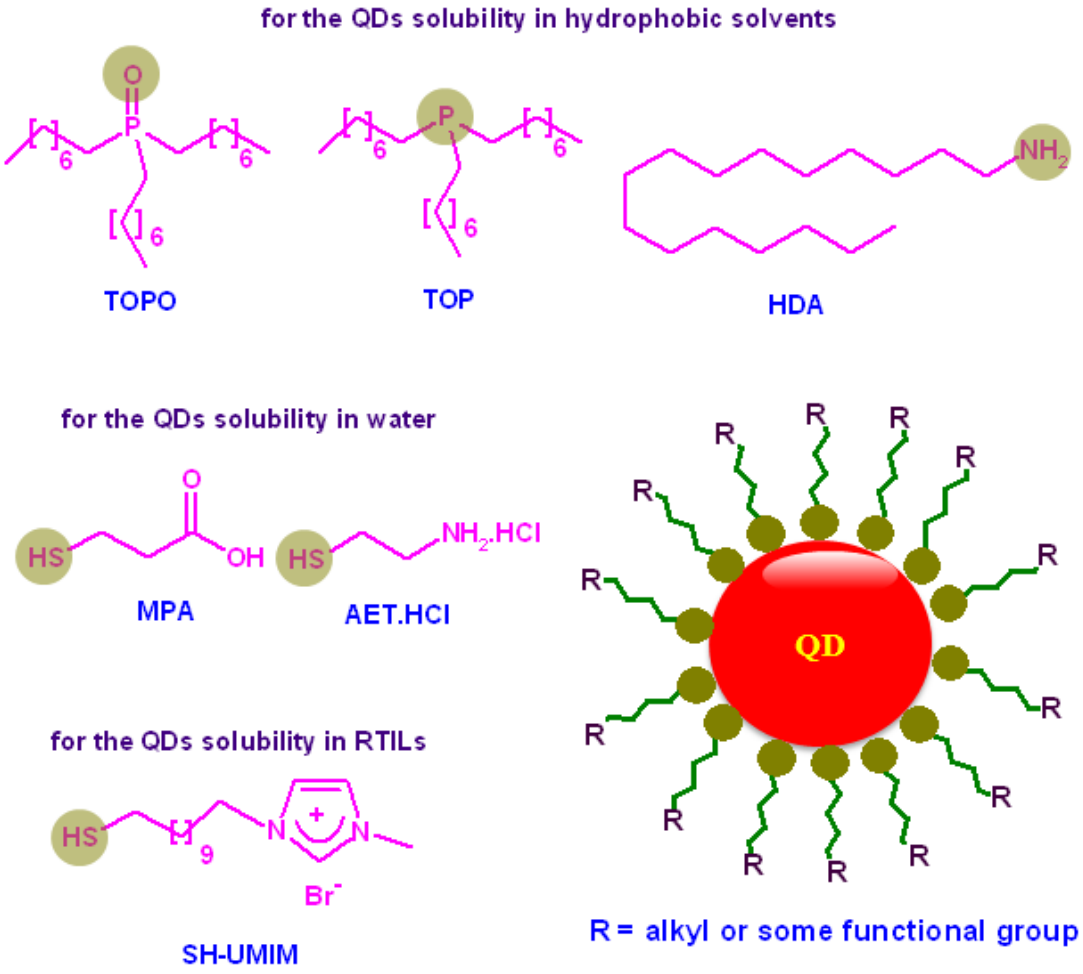

Chart 1.4. Various kinds of capping agents used for QD surface passivation

which can donate electron pair and form ligand-metal coordinate covalent bond with the empty (dangling) orbitals on the surface of the QD, thereby reducing nonradiative events associated with the surface trap states.[148] As chalcongenide ions (e.g. Se^{2-}) on the surface of the QDs don't interact with the basic moieties of the capping agents, QDs with anionic facets are generally responsible for the deep trap emission.[155] However, QDs with cationic facets facilitate the stronger binding between QD surface and the capping agent and enhance the band edge emission by reducing the contribution from deep trap emission (Scheme 1.4).

These capping agents not only protect the QDs but also responsible for their solubility. Trioctylphosphine oxide (TOPO), trioctylphosphine (TOP), hexadecylamine (HDA) are useful for making QDs soluble in nonpolar solvents like toluene, chloroform, whereas 3-mercaptopropionic acid (MPA), aminoethanethiol (AET) hydrochloride are some of the capping agents that are useful for making water soluble nanocrystals (Chart 1.4).[154,157] Hydrophilic polymers and surfactants have also been used to solublize the QDs in polar solvents.[158,159] When it comes to the solubility in RTILs, Nakashima and Kawai managed to transfer the CdTe QDs into a hydrophobic RTIL by extracting an aqueous solution of cationic thiol derivative capped QDs with 1-butyl-3-methylimidazolium bis(trifluoromethanesulfonyl)imide. While this was a first successful attempt to transfer the QDs into an RTIL,[160] one of the major drawbacks, is that the applicability of this method is restricted only to the hydrophobic RTILs.[161] Recently, thiol based task specific imidazolium ionic liquid, 1-methyl-(11-undecanethiol)imidazolium bromide (**SH-UMIM**), has been synthesized and successfully employed to make CdTe QDs soluble in different hydrophilic and hydrophobic RTILs.[20]

1.2.2. Core/Shell quantum dots

For practical applications it is necessary to employ QDs that are stable, highly fluorescent and less sensitive to the environment (surface chemistry and photo oxidation). QDs stability and fluorescence intensity can be enhanced drastically by coating the core of the QDs with an insulating inorganic shell. Thus in core/shell nanocrystals at least two types of inorganic semiconductor nanomaterials are present. The shell provides passivation of the trap states and also tunes the optical properties of the core QD.[162,163] Depending upon the band gaps and energy-level alignment of the semiconductors, core/shell QDs are classified

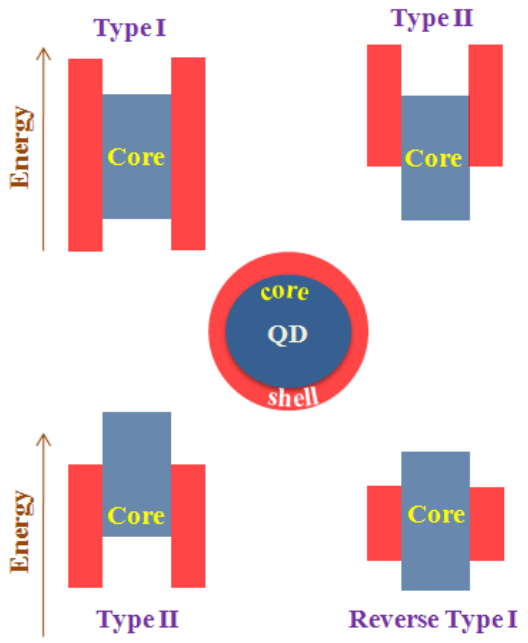

Scheme 1.5. Energy-level alignment in different types of core/shell QDs. Upper and lower edges of the rectangles indicate CB and VB energies respectively

into type-I, type-II and reverse type-I systems (Scheme 1.5).[162]

In type-I, the band gap of shell material is larger than that of core confining photogenerated electrons and holes within the core. CdSe/ZnS was the first type-1 core/shell QD reported. ZnS improves the stability and enhances the fluorescence intensity of the core CdSe QD.[164] Shell growth induces small red shift in the absorption and luminescence spectra indicating partial leakage of exciton into the shell material.[162] In type-II, either valence edge or conduction edge of the shell material is within the band gap of the core and based on the band alignment, either electrons or holes of the core interact with the shell material resulting into spatial separation of electrons and holes. Type-II systems (e.g. CdTe/CdSe and CdSe/ZnTe QDs) are designed particularly for near infrared emission.[165] Unlike in type-I, the fluorescence lifetimes of type-II QDs are very long as the shell grown in this type reduces the overlap of the electron and hole wavefunctions.[148] In reverse type-I, the band gap of the shell is smaller than that of core and depending upon the shell thickness the photogenerated electrons and holes will be confined into the shell material. Significant red shift of the band gap can be achieved with increase in shell thickness.[148] So far, CdS/CdSe, ZnSe/CdSe and CdS/HgS are the extensively studied reverse type-I core/shell QDs.[166-168]

Synthesis and properties of a wide variety of core/shell QDs are described in recent articles.[162,163,169] SILAR (successive ion laser adsorption and reaction) method is being used extensitvely for the synthesis of core/shell nanoparticles, where formation of one monolayer of shell at a time is achieved by alternating injections of the cationic and anionic precursors of the shell material.[170] The number of monolayers can be increased with further additions. UV-vis and fluorescence spectroscopy, powder X-ray, transmission electron microscopy

(TEM), scanning transmission electron microscopy (STEM), X-ray photoelectron spectroscopy (XPS) are some of the commonly used techniques for the characterization of both core and core/shell semiconductor nanocrystals.[162]

1.2.3. On/Off blinking

Fluorescence on-and-off blinking or fluorescence intermittency is a single particle property and it is one of the striking features of the QDs. It is the switching of fluorescence intensity between bright "on" and dark "off" states.[171,172] Trapping of charge carriers can cause QD blinking. Fluorescence "on" state corresponds to the recombination of electron in CB with hole in the VB. Transfer of charge carrier to the trap states is a nonradiative process and responsible for "off" state of the QD.[173] The duration of "off" time is the time spent by charge carrier in the dark trap state. Repeated cycles of "on" and "off" events lead to QD intermittency. Auger ionization is the other way of causing QD intermittency, in which charge carrier gains energy from other exciton and escapes to higher energy levels or out of the core, yielding ionized QD (Scheme 1.6).[174,175] The energy transfer is nonradiative in nature and responsible for the "off" state of the QD. Auger ionization/recombination is very fast, which occurs nearly at 10 ps time scale. Since the fluorescence lifetime of the nanocrystals is in the order of nanoseconds, Auger ionization is considered to be the most probable mechanism for the observed blinking dynamics. QD blinking is found to follow power law or extended power law dynamics.[174,176-178] However, when blinking occurs at longer time scales (say, several milliseconds), then the blinking pattern is explained by diffusion controlled mechanism proposed by Marcus and coworkers.[179]

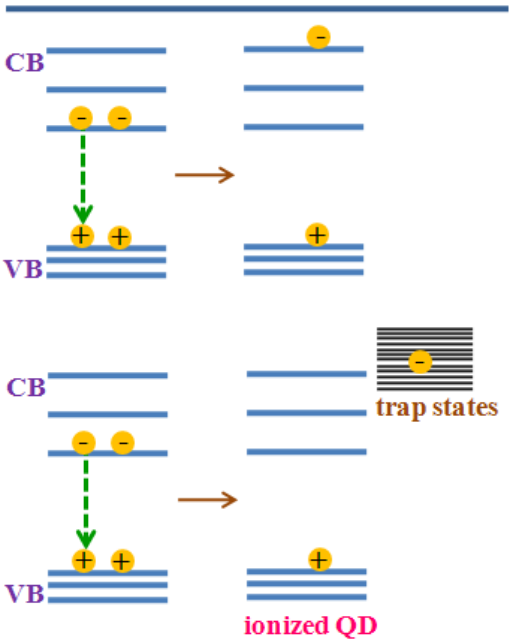

Scheme 1.6. Schematic representation of Auger ionization

Although QD on/off blinking helps understanding the mechanisms and reaction rates of

the charge transfer reactions from QDs to quencher molecules,[177] many applications of QDs are limited by their blinking behavior. For instance, when QDs are used as fluorescent tags for tracking the motion of particles in biological environments, repeated loss of signal due to blinking restricts their use as fluorescent tags.[180,181] Reducing the trap states on the surface of the QD suppresses the blinking pattern. Use of thiol based capping agents, synthesis of polymer coated QDs and core/multishell QDs are some of the ways to improve QD fluorescence and to suppress the on/off intermittency. Dubertret and coworkers have reported non blinking behavior of CdSe QDs coated with thick CdS shell.[182] Suppression of blinking and Auger recombination is achieved for near infrared type-II InP/CdS core/shell nanocrystals[183] and also near suppression of blinking is observed for single CdSe nanoparticles capped with thiol based β-mercaptoethanol.[184]

1.2.4. Multiple exciton generation

Multiple exciton generation (MEG) or carrier multiplication is other important optical property of the semiconductor nanocrystals. MEG is the efficient formation of more than one excitons (bound electron and hole pairs) on photoexcitation with a single photon.[185-187] When QDs are excited with photon energy at least double the band gap, the excess kinetic energy of the excitons produced can be further utilized for the generation of another electron hole pair yielding biexciton. Thus, MEG with quantum efficiency more than 100% is achievable with photon energy multiple times higher than the band gap energy of the QD. MEG is potentially important for the applications in photovoltaic devices like solar cells to increase the conversion efficiency of solar energy to electrical energy.[186] However, here Auger process needs to be discussed. After producing biexciton or multi-exciton, Auger ionization may eliminate the excess charge carriers produced and as this process is normally fast (ps), the excess charge carriers should be transferred to conducting materials before their decay through Auger ionization/recombination.[185,187] The process of MEG and the charge transfer in the semiconductor nanocrystals can be studied using ultrafast transient absorption measurements.[188]

1.2.5. Applications

Due to their high molar extinction coefficient, thermal stability, long luminescence lifet-

imes and photostability, strongly luminescent QDs offer a number of advantages over the commonly used organic dye molecules in several applications, for example as biological reporters, tunable emitters in light emitting diodes (LEDs), photodetector devices.[189-191] In addition, the low cost of these materials, size dependent tunability of the luminescence properties, and possibility of multiple exciton generation (MEG) allow QDs to produce high-performing and low-cost QD-based photovoltaic devices.[185,186,192-195]

1.2.6. Fluorescence quenching

Any process that leads to destruction of the photogenerated electron or hole contributes to fluorescence quenching of the QDs. As majority of the applications of the QDs are linked to the exciton quenching dynamics,[196-200] a clear understanding of the mechanism of fluorescence quenching of the QDs is absolutely essential. Perhaps, this explains why fluorescence quenching studies of the QDs have received significant attention in recent years.[196,198,199,201-210] Charge (electron or hole) and energy transfer are the two most commonly encountered exciton quenching mechanisms.

Charge transfer induced fluorescence quenching is determined by the redox potentials of the donor and acceptor and the rate depends exponentially on the donor-acceptor distance.[211] As the efficiency of solar cell depends on the rate of interfacial charge transfer between heterogeneous interfaces of QDs and nanocrystalline metal oxides, like TiO_2 and ZnO, the rate limiting factors of charge transfer should be optimized and resolved. This led to several studies on charge transfer induced fluorescence quenching of the quantum dots by inorganic and organic molecules. For example, the research groups of Kamat and Lian reported ultrafast electron transfer from QDs to metal oxide nanoparticles and organic molecules.[212,213] Recent picosecond and microsecond transient absorption studies by Weiss and coworkers show that the time scales of charge transfer from PbS QDs to benzoquinone (BQ) molecules adsorbed on the surface of the QD and to the freely diffusing BQ molecules are very different.[214] These experiments and others also reveal that the rate of charge transfer depends on the type of QD and quencher and the size and shape of the QD.[202,207,211,212] Recently it has also been reported how modulation of the interfacial charge transfer improves the efficiency of a solar cell.[192] Though, the quenching of QD emission by charge transfer (electron and/or hole) can proceed through either dynamic or static quenching mechanisms,[176,215,216] there are

some cases where both dynamic and static quenching mechanisms contribute to QD exciton quenching.[217] While, time-resolved fluorescence and ultrafast transient absorption studies provide direct evidence of intermediate ions produced and help estimating the ensemble averaged rate of charge transfer reactions, single particle fluorescence technique based blinking studies are being emerged as efficient means to quantify the distribution of rates of electron transfer reactions at the single particle level.[176,177]

Quenching due to Förster resonance energy transfer (FRET) is governed by the spectral overlap of the donor emission and acceptor absorption, interaction between their transition dipoles and the donor–acceptor distance.[115] Exciton dissociation of QDs by FRET is a dynamic quenching process which decreases the fluorescence intensity and lifetimes of the semiconductor nanocrystals.[203,204,218] QDs are stable and efficient FRET donors, which are being used for sensing intracellular pH, detecting DNA hybridization, for photosensitization reactions, cellular imaging, tracking biological reactions, protein conformational changes etc.[204,219-221]

Some donor-acceptor systems may satisfy essential conditions required for both charge and energy transfer quenching. Though not much studies on these systems are reported, Boulesbaa et al. have shown that rhodamine B quenches 84% of CdSe fluorescence by electron transfer and 16% by energy transfer, indicating that electron transfer is more efficient than energy transfer.[207] Though charge transfer and energy transfer have their own applications, TiO_2/squarainedye/CdSe hybrid system designed with simultaneous FRET and electron transfer mechanisms has been successfully employed for devising a solar cell with efficient photocurrent generation.[222] Here, CdSe QD captures broader spectrum of incident photons and through FRET it excites near IR absorbing squaraine dye linker, which further transfers its electrons to TiO_2 nanoparicles exhibiting good power conversion efficiency and stability towards photoillumination.

1.3. Photoinduced electron transfer reactions

Photoinduced electron transfer (PET) is the basis of the design and development of systems for solar energy conversion,[223-226] luminescent systems for sensing environments,[227] nanometer scale wires and logic gates[228,229] and also used for making components of

molecular electronic devices.[230] Inter and intramolecular electron/charge transfer reactions are discussed briefly in the following sections.

1.3.1. Intermolecular process

The intermolecular PET reactions help understanding the long range electron transfer mechanisms involved in photosynthesis.[231] Primary electron transfer takes place between photoexcited molecule and the molecule in the ground to produce an excited state charge transferred species. Here, the photoexcited molecule can be either donor or acceptor.[232] The initial charge transferred species now undergoes several secondary processes depending upon the surrounding environment.[233,234] Electron transfer in non polar solvents often leads to fluorescent charge transfer complex known as exciplex. On the other hand, polar solvents tend to produce charge separated radical ion pair, usually called as geminate ion pair (GIP) or

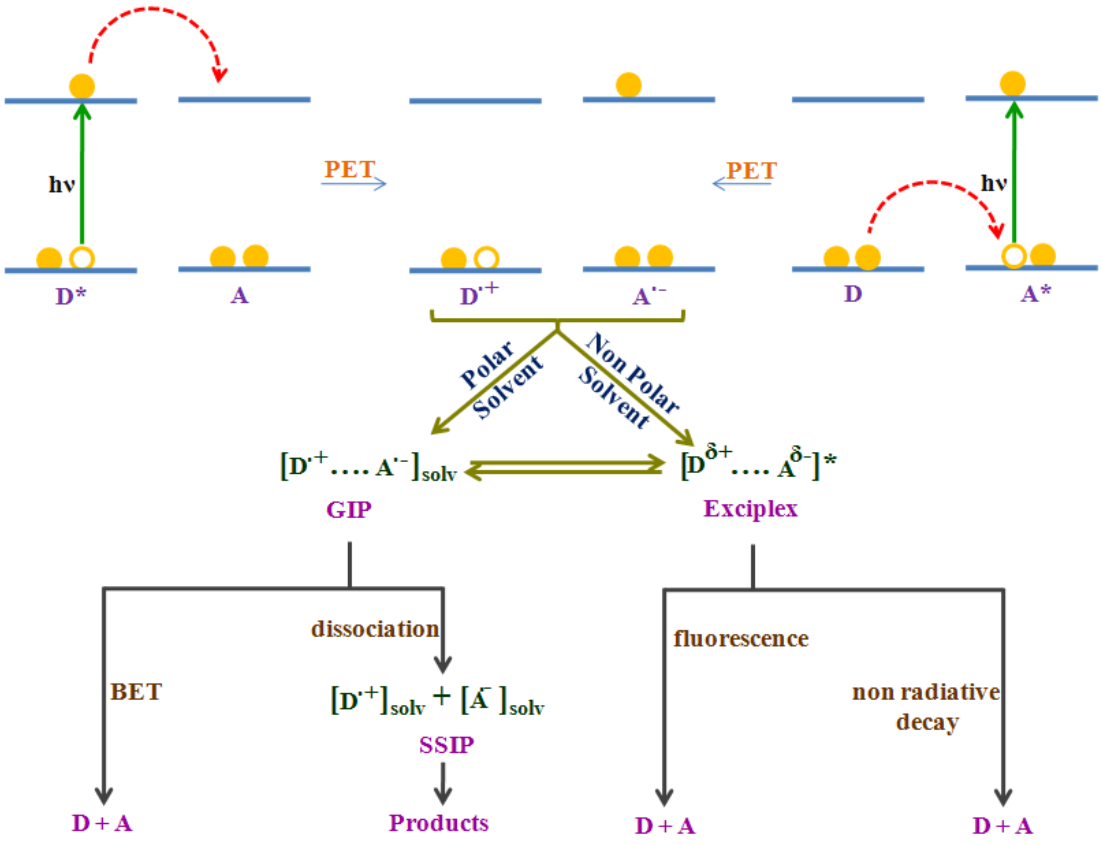

Scheme 1.7. General description of intermolecular PET reaction

contact ion pair. These species later may undergo back electron transfer (BET) to produce molecules in the ground state and/or ionic dissociation to generate solvent-separated ion pairs (SSIP), triplet recombination to produce one species in the ground state and other in the triplet excited state, other charge transfer intermediates, stable products etc.[233-236] Scheme 1.7 illustrates possible processes involved in the intermolecular PET reactions.

The free energy (ΔG) of the electron transfer process depends on the oxidation (E_D^{ox}) and reduction (E_A^{red}) potentials of the donor and acceptor molecules respectively.[236,237]

$$\Delta G = E_D^{ox} - E_A^{red} - E_{0,0} - {e^2}/{\varepsilon r_q} \text{----------(3)}$$

where, $E_{0,0}$ is the energy corresponding to 0-0 transition of either photoexcited donor or acceptor. ${e^2}/{\varepsilon r_q}$ is the coulombic energy of interaction of the ion pair at the effective distance (r_q) of the donor and acceptor. The coulombic energy depends on the solvent polarity and is negligible in highly polar solvents like acetonitrile.

Various experimental techniques like, laser flash photolysis,[234,235,238] ESR or spin trapping,[239] transient photocurrent measurement,[240] scavenging or trapping the intermediates[241] etc. have been employed to monitor the intermolecular PET reactions. Among these techniques, laser flash photolysis technique is popular as it directly identifies the products and intermediates of the electron transfer reactions.

Effect of RTIL. Some of the interesting findings of intermolecular PET reactions in RTILs are summarized below.

The photoinduced electron transfer reaction between pyrene and N,N-dimethylaniline (DMA) studied by Paul and Samanta has revealed that the mechanism of electron transfer depends on the microscopic properties of the ionic liquids but not on their bulk properties.[54] This donor (DMA)-acceptor (pyrene) pair is well known for exciplex emission, which however could not be observed in imidazolium RTILs as these ionic liquids are more polar than acetonitrile. The rate constant of PET induced fluorescence quenching (k_q) is found to be higher than the diffusion controlled rate constant (k_{diff}) suggesting that the microviscosity around the donor-acceptor pair is different from the bulk viscosity of the RTILs. Recently, Maroncelli and co-workers have shown that $k_q > k_{diff}$ is not typical of RTILs but also common in conventional solvents of higher viscosities.[242] Vauthey and co-

workers have studied PET between DMA and 3-cyanoperylene in three RTILs and compared the results with those in conventional solvents of similar viscosity.[243] They have found that the diffusive motion of the solute molecules in both the media is comparable and although the solvation dynamics controls the intrinsic electron transfer in both the cases, the rate of electron transfer in RTILs is slower compared to conventional solvents of similar viscosities. Several other studies help understanding the effect of viscosity, polarity and ionic constituents of the RTILs on the rates of bimolecular electron transfer reactions in these media.[244-249]

1.3.2. Intramolecular process

Intramolecular photoinduced electron transfer takes place from donor end to the acceptor end of an intramolecular system (in the singlet or triplet excited state) to produce charge separated radical ions (Scheme 1.8a).[233] Distance between the donor and acceptor groups and the structure of molecular linker that connects both of them control the efficiency of intramolecular electron transfer.[233] The molecular linker can be (i) short or long flexible chain or (ii) a rigid spacer. Transfer of electron is possible through space or through bond. When spatial overlap between donor and acceptor is not favorable due to limited configurational flexibility, electron transfer takes place through bond interactions of the donor and acceptor. Electron transfer is more favorable when the connecting link is short and depends on viscosity and temperature in case of longer flexible chains. In rigid spacers, the rate of electron transfer is less dependent on the surrounding solvent medium and more dependent on the separation distance and orientation of the donor and acceptor groups.[233]

The concept of intramolecular PET has been widely used in many applications particularly in designing multi-component electron donor-acceptor (EDA) systems containing fluorophore-spacer-receptor architecture (Scheme 1.8b). Due to electron transfer from electron rich receptor to electron deficient fluorophore, these molecular systems are weakly fluorescent and this can be termed as ‘off’ state.[250] The receptor acts as a guest binding site and in the presence of a specific foreign molecule the PET communication between the receptor and fluorophore is disrupted thereby ‘switching on’ of the fluorescence. These molecular systems are employed for fluorescence ‘off-on’ signaling of guests and the sensors designed based on this mechanism are termed as PET sensors.[250] As amines are efficient que-

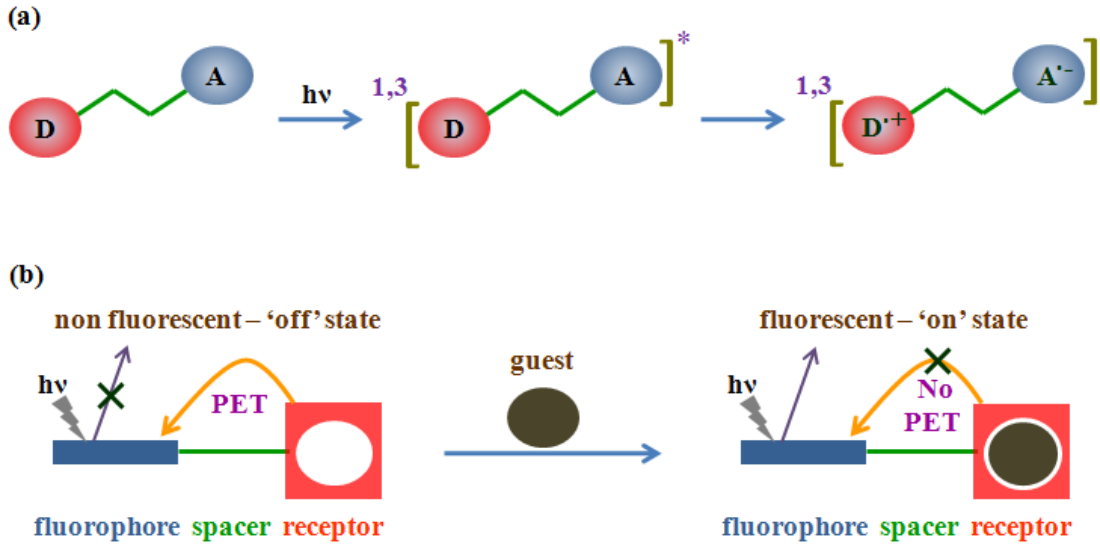

Scheme 1.8. Pictorial illustration of intramolecular PET reaction

nchers of fluorescence and good ligands for various guests, they are popular as receptors and sensors for various guest molecules can be made by just changing the receptor moiety satisfying the redox conditions. Crown ethers are also suitable receptors for specific binding and identification of ionic and neutral guest species.[251]

Characteristics of EDA molecules. EDA molecules commonly emit from an intramolecular charge transfer (ICT) state, which is most often more polar then the ground state. Several families of EDA molecules have been studied extensively and in most cases, a decrease in fluorescence quantum yield and lifetime is observed with increase in solvent polarity.[252,253] However, there are few molecular systems which exhibit a fluorescence behavior uncommon for EDA systems. The fluorescence quantum yield and lifetime of those molecules increase with increase in polarity of the solvent medium. Stilbenes,[254] flavones,[255] aminochalcone,[256,257] thioazoloquinoxalines[258] are few molecular systems of this category and show uncommon behavior. It is necessary to consider more than one exited state to explain the unusual solvent dependence of the fluorescence behavior of such EDA molecules. The number of excited states considered varies from system to system. For example, a three-state model in the case of stilbenes[254] and a two-state model in the case of flavone derivates.[255]

EDA molecules – Dual fluorescence. Dual fluorescent molecule is the one which emits from two structurally different fluorescent states. Cis-trans isomerization,[254] proton transfer,[140] electron transfer [259] are some of the commonly observed mechanisms responsible for the dual fluorescence of many systems reported so far. However, the first dual fluorescent system was based on excited state intramolecular charge transfer reaction. Around five decades ago, Lippert had reported dual fluorescence of 4-(N,N'-dimethylamino)benzonitrile (DMABN) in polar solvent.[260] Several mechanisms such as twisted intramolecular charge transfer (TICT),[261,262] planar intramolecular charge transfer (PICT)[263] and rehybridization by intramolecular charge transfer (RICT)[264] have been proposed to explain the dual fluorescence of DMABN. Among these, TICT mechanism is most acceptable as it explains most of the observed findings of DMABN and other dual fluorescent molecules.[265] The TICT concept was proposed by Grabowski and co-workers.[261,262] According to this mechanism complete decoupling of donor and acceptor orbitals and localization of transferred electron on the acceptor orbital impart highly dipolar character to the TICT state and allow its formation only in polar solvents. As the relative intensities of the two emissions depend on the surrounding solvent environment, dual fluorescent molecules offer an excellent opportunity to study the rate of formation of the TICT state from the locally excited state and its dependence on the structure of the molecule and surrounding environment yielding valuable information related to microscopic properties of the solvent medium. Dual fluorescent molecules also serve as better sensors over single fluorescent systems and critical review by Demchenko highlights the importance of dual fluorescent molecules exhibiting reversible excited state reaction for the microscale applications such as microarrays, microfluidic systems, living cell imaging etc.[266] The TICT state need not be fluorescent. Most of the coumarin molecules,[267] rhodamine dyes,[268] and squaraine dyes[269] are characterized with non-fluorescent TICT state.

EDA molecules in RTILs. EDA molecules, which emit from intramolecular charge transfer state, are often used to determine the microscopic polarity of the RTILs. Dipolar EDA molecules, such as 4-aminophthalimie and 4-dimethylaminophthalimide have been used for the estimation of the $E_T(30)$ values of pyridinium and four imidazolium ionic liquids.[37] These results establish that the polarity of these RTILs is in between that of acetonitrile and methanol. Later, $E_T(30)$ of a large variety of RTILs have been determined by using betaine

dye[33] and the results are consistent with the polarity values estimated using these EDA molecules. A number of articles can be found in literature, where EDA molecules like C153 have been employed to understand the dynamics of solvation in RTILs.[41,118,120,121,123-125,128,270] Further, as stated in a previous section, the rate of excited state intramolecular electron transfer reaction in some dual fluorescent EDA molecules in RTILs is solvation dependent, whereas in some other systems, it is independent of the dynamics of solvation.[138,139]

1.4. Motivation behind the thesis

The main interest in the two promising class of materials, quantum dots (QDs) and room temperature ionic liquids (RTILs), presented in this chapter is to explore the utility of RTILs as medium for photophysical reactions and to understand the photogenerated exciton quenching mechanisms of the semiconductor nanocrystals (QDs). The applications of RTILs as electrolytes[21-23,93,94] and QDs as photosensitizers[192] also inspired us to combine these two materials and to investigate the influence of RTILs on the optical properties of the QDs, for designing efficient and long lasting quantum dot sensitized solar cells.

Though many photophysical studies have been carried out to understand the microscopic properties and red edge excitation (REE) effect of the RTILs, the influence of the RTILs on the excited state intramolecular charge transfer reactions is largely unexplored. As DMABN (Chart 1.5) is a dual fluorescent molecule, whose emission behavior is dependent on the viscosity and polarity of the medium,[265] we thought it might be possible to regulate or tune the fluorescence response of DMABN in RTILs thus yielding information on the influence of RTILs on the excited state intramolecular electron transfer reactions of DMABN.

Apart from polarity and viscosity, specific solute-solvent hydrogen bonding interactions also affect fluorescence properties of the organic molecules. Experimental and simulation studies show that C(2)-hydrogen atom of imidazolium RTILs is acidic in nature and can interact through H-bonding with the solute molecules.[271-273] Crystal violet lactone (CVL) is a dual fluorescent molecule, whose fluorescence is sensitive to H-bonding interactions and its excited state reaction involves electron transfer and solvation of the charge separated states.[259] As RTILs possess a wide range of polarity and viscosity values and it is also possible to control the proton donating ability of these liquids, we have studied the photophysical behavior of CVL (Chart 1.5) in six carefully chosen RTILs of different viscos-

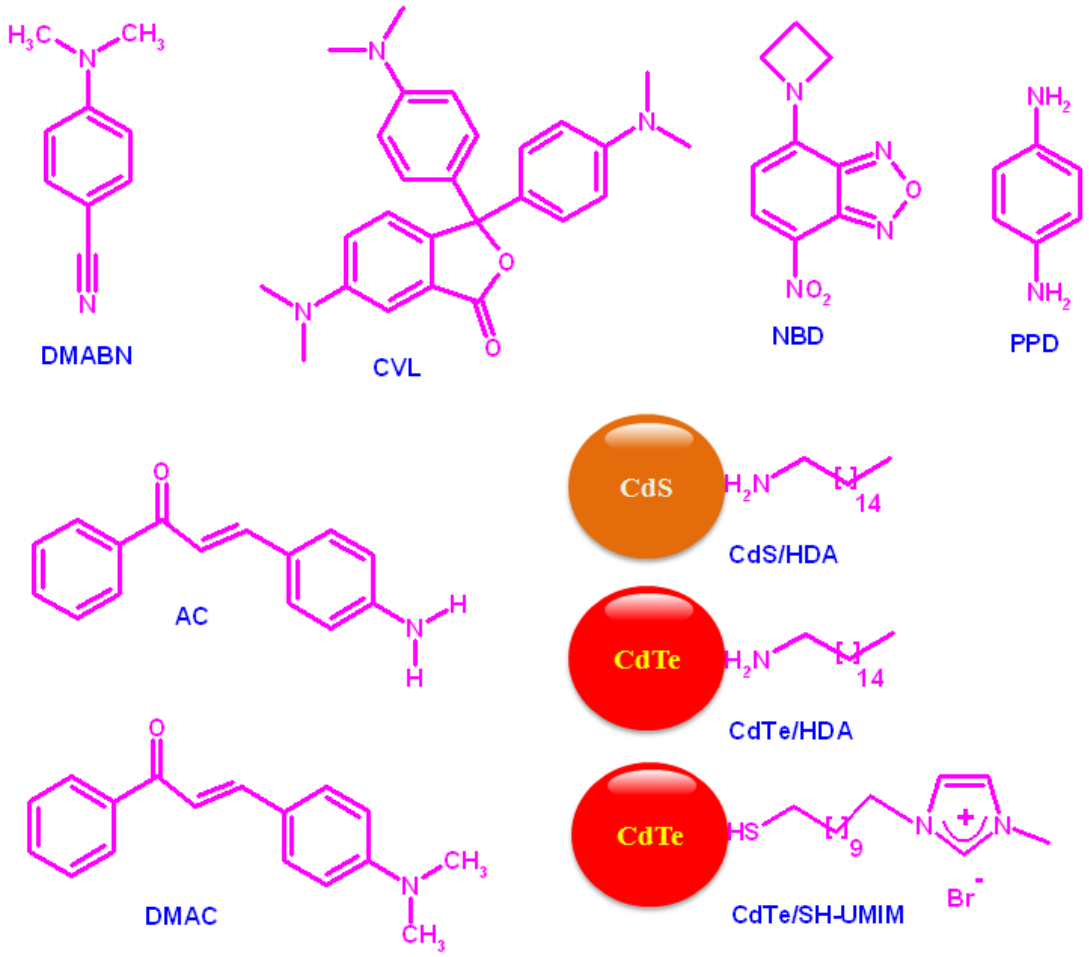

Chart 1.5. Structures of the probe molecules and QDs employed in the present study

ity, polarity and hydrogen bond-donating ability, with a view to exploring the influence of viscosity, polarity and H-bonding interactions on the excited state intramolecular charge transfer reactions

Aminochalcones are a class of EDA systems whose fluorescence quantum yield and lifetime values increase with increase in polarity of the solvent medium.[256,257,274] Though aminochalcones can emit from less polar trans isomer (E*) and a more polar TICT state (A*), the emission spectra in all conventional solvents are characterized with a single emission band.[256,257,274] As, TICT state is highly polar in nature and its formation is accompanied by structural changes,[265] the transformation of E* → A* can be controlled by polarity and

viscosity of the surrounding medium. To modulate the excited state reaction and observe emission from both E* and A* states just by varying the polarity and viscosity of the RTILs, 4-aminochalcone (AC) and 4-dimethylaminochalcone (DMAC) (Chart 1.5) have been studied in [bmim][PF_6] RTIL (Chart 1.6) at different temperatures.

As majority of the applications of QDs are linked to the exciton quenching dynamics, a clear understanding of the fluorescence quenching mechanism of the QDs is absolutely essential.[196-200] Charge (electron or hole) and energy transfer are the two most commonly encountered exciton quenching mechanisms. While quenching due to energy transfer process is governed by the spectral overlap of the donor emission and acceptor absorption and the donor–acceptor distance, charge transfer induced quenching is determined by the redox potentials of the donor and acceptor.[176,202,212,215,275,276] The literature suggests that fluorescence

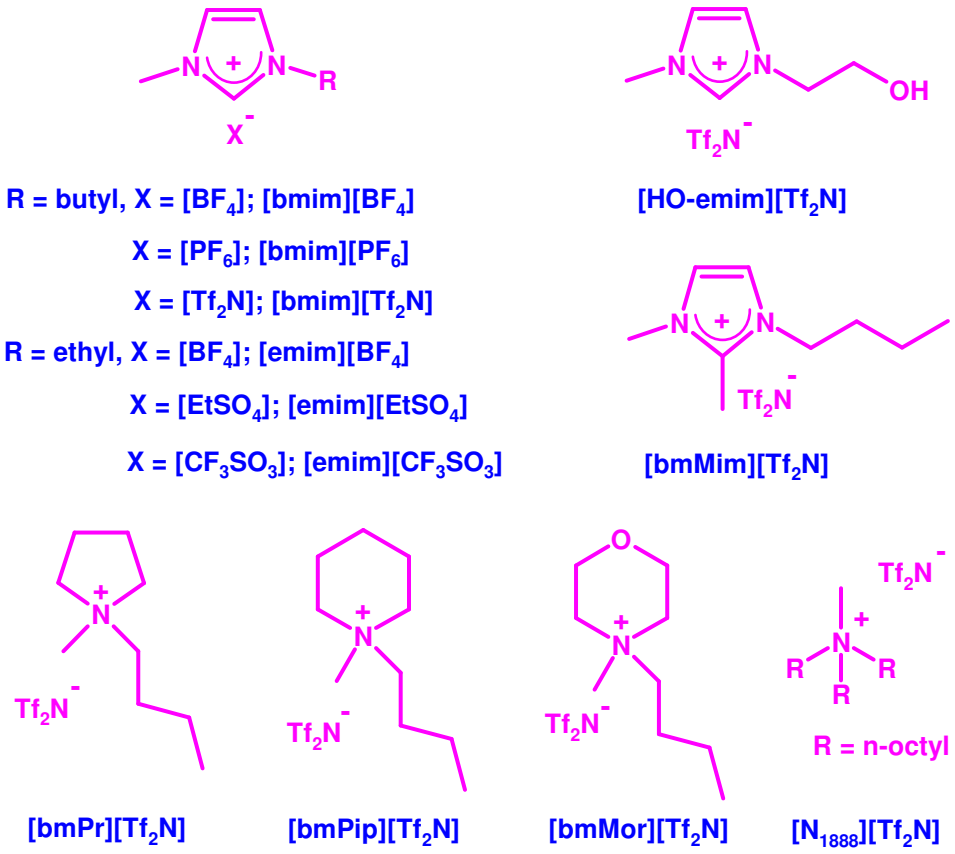

Chart 1.6. Structures and abbreviations of the RTILs involved in this study

quenching of the QDs by organic molecules is most often attributed to the energy transfer mechanism on the basis of the spectral overlap criterion and decrease in average lifetime.[277-281] In order to prove that these parameters are not sufficient to conclude on FRET mechanism and also to go deeply into the quenching mechanisms of the QD fluorescence by organic molecules, we have taken up a case study of CdS/HDA QD (Chart 1.5) fluorescence quenching by 4-azetidinyl-7-nitrobenz-2-oxa-1,3-diazole (NBD) and p-phenylenediamine (PPD) in toluene.

QDs are being employed as photosensitizers in quantum dot sensitized solar cells (QDSCs), where water or organic solvent is used as electrolyte.[282-284] However, practical limitations of leakage and evaporation of the solvent is a major impediment to the commercialization and long-term use of these devices for applications.[285] RTILs are regarded as a viable electrolyte alternative to the electrolyte solutions in aqueous or organic solvents to enhance the durability of the solar cells.[285-287] Prior to the employment of the RTILs in QDSCs, it is necessary to study the interaction of the RTILs with the QDs, in particular, their influence on the luminescence properties of the QDs as the efficiency of a solar cell depends on the interactions of the electrolytes with the photosensitizers.[288] However, lack of these studies is due to the solubility problem of the QDs in RTILs. To overcome this issue we have designed a task-specific ionic liquid, which helps preparing QD-ionic liquid hybrids (CdTe/**SH-UMIM**, Chart 1.5) soluble in different hydrophilic and hydrophobic RTILs and also allows the fluorescence spectroscopic studies at ensemble and single particle level.

REFERENCES

(1) Wasserscheid, P.; Keim, W. *Angew. Chem. Int. Ed.* **2000**, *39*, 3772.
(2) Seddon, K. R.; Stark, A.; Torres, M. J. *Pure Appl. Chem.* **2000**, *72*, 2275.
(3) Seddon, K. R. *Ionic Liquids, Industrial Applications for Green Chemistry, American Chemical Society, Washington DC*, 2002.
(4) Dubreuil, J. F.; Bourahla, K.; Rahmouni, M.; Bazureau, J. P.; Hamelin, J. *Catal. Commun.* **2002**, *3*, 185.
(5) Hallett, J. P.; Welton, T. *Chem. Rev.* **2011**, *111*, 3508.
(6) Walden, P. *Bull. Acad. Imper. Sci.St. Petersberg)* **1914**, 1800.
(7) Wilkes, J. S.; Levinsky, J. A.; Wilson, R. A.; Hussey, C. L. *Inorg. Chem.* **1982**, *21*, 1263.
(8) Boon, J. A.; Levinsky, J. A.; Pflug, J. L.; Wilkes, J. S. *J. Org. Chem.* **1986**, *51*, 480.
(9) Chiappe, C.; Pieraccini, D. *J. Phys. Org. Chem.* **2005**, *18*, 275.
(10) Sheldon, R. *Chem. Commun.* **2001**, 2399.
(11) Wasserscheid, P.; Welton, T. *Ionic Liquids in Synthesis, Wiley-VCH, Weinheim* 2003.
(12) Golding, J. J.; MacFarlane, D. R.; Spiccia, L.; Forsyth, G. B.; Skelton, B. W.; White, A. H. *Chem. Commun.* **1998**, *18*, 1593.
(13) Polyakov, O. G.; Ivanova, S. M.; Gaudinski, C. M.; Miller, S. M.; Anderson, O. P.; Strauss, S. H. *Organometallics* **1999**, *18*, 3769.
(14) Larsen, A. S.; Holbrey, J. D.; Tham, F. S.; Reed, C. A. *J. Am. Chem. Soc.* **2000**, *122*, 7264.
(15) Xu, W.; Wang, L.-M.; Nieman, R. A.; Angell, C. A. *J. Phys. Chem. B* **2003**, *107*, 11749.
(16) Sankaranarayanan, K.; Sathyaraj, G.; Nair, B. U.; Dhathathreyan, A. *J. Phys. Chem. B* **2012**, *116*, 4175.
(17) Ohno, H.; Fukumoto, K. *Acc. Chem. Res.* **2007**, *40*, 1122.
(18) Davis, J. H. *Chem. Lett.* **2004**, *33*, 1072.
(19) Lee, S. *Chem. Commun.* **2006**, 1049.
(20) Santhosh, K.; Samanta, A. *J. Phys. Chem. C* **2012**, *116*, 20643.
(21) Enomoto, T.; Nakamori, Y.; Matsumoto, K.; Hagiwara, R. *J. Phys. Chem. C* **2011**, *115*, 4324.
(22) Ngo, H. L.; LeCompte, K.; Hargens, L.; McEwen, A. *Thermochim. Acta* **2000**, *357*, 97.
(23) Lewandowski, A.; Swiderska-Mocek, A. *J. Power Sources* **2009**, *194*, 601.
(24) Freemantle, M. *Chem. Eng. News* **1998**, *76*, 32.
(25) Dzyuba, S.; Bartsch, R. A. *ChemPhysChem* **2002**, *3*, 161.
(26) Carda-Broch, S.; Berthold, A.; Armstrong, D. W. *Anal. Bioanal. Chem.* **2003**, *375*, 191.
(27) Jeon, Y.; Sung, J.; Seo, C.; Lim, H.; Cheong, H.; Kang, M.; Moon, B.; Ouchi, Y.; Kim, D. *J. Phys. Chem. B* **2008**, *112*, 4735.
(28) Mele, A.; Tran, C. D.; Lacerda, S. H. D. P. *Angew. Chem. Int. Ed.* **2003**, *42*, 4364.
(29) Mele, A.; Romano, G.; Giannone, M.; Ragg, E.; Fronza, G.; Raos, G.; Marcon, V. *Angew. Chem. Int. Ed.* **2006**, *45*, 1123.
(30) Gordon, C. M.; Holbrey, J. D.; Kennedy, A. R.; Seddon, K. R. *J. Mater. Chem.* **1998**, *8*, 2627.
(31) Wilkes, J. S.; Zaworotko, M. J. *Chem. Commun.* **1992**, 965.
(32) Kölle, P.; Dronskowski, R. *Inorg. Chem.* **2004**, *43*, 2803.
(33) Reichardt, C. *Green Chem.* **2005**, *7*, 339.

(34) Dupont, J.; Souza, R. F. D.; Suarez, P. A. Z. *Chem. Rev.* **2002**, *102*, 3667.
(35) Nishida, T.; Tashiro, Y.; Yamamoto, M. *J. Fluorine Chem.* **2003**, *120*, 135.
(36) Buzzeo, M. C.; Evans, R. G.; Compton, R. G. *ChemPhysChem* **2004**, *5*, 1106.
(37) Aki, S. N. V. K.; Brennecke, J. F.; Samanta, A. *Chem. Commun.* **2001**, 413.
(38) Law, G.; Watson, P. R. *Langmuir* **2001**, *17*, 6138.
(39) Fuller, J.; Carlin, R. T.; Long, H. C. D.; Haworth, D. *Chem. Commun.* **1994**, 299.
(40) Bonhote, P.; Dias, A.; Papageorgiou, N.; Kalyanasundaram, K.; Gratzel, M. *Inorg. Chem.* **1996**, *35*, 1168.
(41) Karmakar, R.; Samanta, A. *J. Phys. Chem. A* **2002**, *106*, 6670.
(42) MacFarlane, D. R.; Meakin, P.; Sun, J.; Amini, N.; Forsyth, M. *J. Phys. Chem. B* **1999**, *103*, 4164.
(43) Wasserscheid, P. *Nature* **2006**, *439*, 797.
(44) Earle, M. J.; Esperanca, J. M. S. S.; Gilea, M. A.; Lopes, J. N. C.; Rebelo, L. P. N.; Magee, J. W.; Seddon, K. R.; Widegren, J. A. *Nature* **2006**, *439*, 831.
(45) Taylor, A. W.; Lovelock, K. R. J.; Deyko, A.; Licence, P.; Jones, R. G. *Phys. Chem. Chem. Phys.* **2010**, *12*, 1772.
(46) Chambreau, S. D.; Vaghjiani, G. L.; Koh, C. J.; Golan, A.; Leone, S. R. *J. Phys. Chem. Lett.* **2012**, *3*, 2910.
(47) Santhosh, K.; Banerjee, S.; Rangaraj, N.; Samanta, A. *J. Phys. Chem. B* **2010**, *114*, 1967.
(48) Widegren, J. A.; Laesecke, A.; Magee, J. W. *Chem. Commun.* **2005**, 1610.
(49) Holbrey, J. D.; Turner, M. B.; Reichert, W. M.; Rogers, R. D. *Green Chem.* **2003**, *5*, 731.
(50) Branco, L. C.; Rosa, J. N.; Ramos, J. J. M.; Afonso, C. A. M. *Chem. Eur. J.* **2002**, *8*, 3671.
(51) Paul, A.; Samanta, A. *J. Phys. Chem. B* **2008**, *112*, 16626.
(52) Huddleston, J. G.; Visser, A. E.; Reichert, W. M.; Willauer, H. D.; Broker, G. A.; Rogers, R. D. *Green Chem.* **2001**, *3*, 156.
(53) Pringle, J. M.; Golding, J.; Baranyai, K.; Forsyth, C. M.; Deacon, G. B.; Scott, J. L.; MacFarlane, D. R. *New J. Chem.* **2003**, *27*, 1504.
(54) Paul, A.; Samanta, A. *J. Phys. Chem. B* **2007**, *111*, 1957.
(55) Reichardt, C. *Solvents and Solvent Effects in Organic Chemistry;* VCH: Weinheim, Germany, 1988.
(56) Wakai, C.; Oleinikova, A.; Ott, M.; Weingartner, H. *J. Phys. Chem. B* **2005**, *109*, 17028.
(57) Daguenet, C.; Dyson, P. J.; Krossing, I.; Oleinikova, A.; Slattery, J.; Wakai, C.; Weingartner, H. *J. Phys. Chem. B* **2006**, *110*, 12682.
(58) Crowhurst, L.; Mawdsley, P. R.; Perez-Arlandis, J. M.; Salter, P. A.; Welton, T. *Phys. Chem. Chem. Phys.* **2003**, *5*, 2790.
(59) Anderson, J. L.; Ding, J.; Welton, T.; Armstrong, D. W. *J. Am. Chem. Soc.* **2002**, *124*, 14247.
(60) Mellein, B. R.; Aki, S. N. V. K.; Ladewski, R. L.; Brennecke, J. F. *J. Phys. Chem. B* **2007**, *111*, 6452.
(61) Mudring, A.-V. *Aust. J. Chem.* **2010**, *63*, 544.
(62) Hamaguchi, H.; Saha, S.; Ozawa, R.; Hayashi, S. Raman and X-ray studies on the structure of [bmim]X (X = Cl, Br, I, [BF4], [PF6]): rotational isomerism of the [bmim]+ cation. . In *Ionic Liquids IIIA: Fundamentals, Progress, Challenges, and Opportunities, Properties and Structure,*; Rogers, R. D., Seddon, K. R., Eds.; Am. Chem. Soc.: Washington, 2005; pp 68.
(63) Jayaraman, S.; Maginn, E. J. *J. Chem. Phys.* **2007**, *127*, 214504.

(64) Hardacre, C.; Holbrey, J. D.; Nieuwenhuyzen, M.; Youngs, T. G. A. *Acc. Chem. Res.* **2007**, *40*, 1146.
(65) Triolo, A.; Mandanici, A.; Russina, O.; Rodriguez-Mora, V.; Cutroni, M. *J. Phys. Chem. B* **2006**, *110*, 21357.
(66) Holbrey, J. D.; Reichert, W. M.; Rogers, R. D. *Dalton Trans.* **2004**, 2267.
(67) Hardacre, C.; Holbrey, J. D.; Mullan, C. L.; Nieuwenhuyzen, M.; Youngs, T. G. A.; Bowron, D. T. *J. Phys. Chem. B* **2008**, *112*, 8049.
(68) Choudhury, A. R.; Winterton, N.; Steiner, A.; Cooper, A. I.; Johnson, K. A. *J. Am. Chem. Soc.* **2005**, *127*, 16792.
(69) Urahata, S. M.; Ribeiro, M. C. C. *J. Chem. Phys.* **2004**, *120*, 1855.
(70) Burba, C. M.; Frech, R. *J. Chem. Phys.* **2011**, *134*, 134503.
(71) Pauda, A. A. H.; Gomes, M. F. C.; Lopes, J. N. A. C. *Acc. Chem. Res.* **2007**, *40*, 1087.
(72) Hu, Z.; Margulis, C. J. *Proc. Natl. Acad. Sci. USA* **2006**, *103*, 831.
(73) Bhargava, B. L.; Klein, M. L.; Balasubramanian, S. *ChemPhysChem* **2008**, *9*, 67.
(74) Schroeder, C.; Rudas, T.; Neumayr, G.; Gansterer, W.; Steinhauser, O. *J. Chem. Phys.* **2007**, *127*, 044505.
(75) Schroeder, C.; Rudas, T.; Steinhauser, O. *J. Chem. Phys.* **2006**, *125*, 244506.
(76) Hardacre, C.; Holbrey, J. D.; Mullan, C. L.; Youngs, T. G. A.; Bowron, D. T. *J. Chem. Phys.* **2010**, *133*, 074510.
(77) Triolo, A.; Russina, O.; Bleif, H.-J.; Cola, E. D. *J. Phys. Chem. B* **2007**, *111*, 4641.
(78) Xiao, D.; Rajian, J. R.; Li, S. F.; Bartsch, R. A.; Quitevis, E. L. *J. Phys. Chem. B* **2006**, *110*, 16174.
(79) Xiao, D.; Rajian, J. R.; Cady, A.; Li, S.; Bartsch, R.; Quitevis, E. *J. Phys. Chem. B* **2007**, *111*, 4669.
(80) Iwata, K.; Okazima, H.; Saha, S.; Hamaguchi, H. *Acc. Chem. Res.* **2007**, *40*, 1174.
(81) Samanta, A. *J. Phys. Chem. B* **2006**, *110*, 13704.
(82) Jin, H.; Li, X.; Maroncelli, M. *J. Phys. Chem. B* **2007**, *111*, 13473.
(83) Patra, S.; Samanta, A. *J. Phys. Chem. B* **2012**, *116*, 12275.
(84) Iimori, T.; Iwahashi, T.; Ishii, H.; Seki, K.; Ouchi, Y.; Ozawa, R.; Hamaguchi, H.; Kim, D. *Chem. Phys. Lett.* **2004**, *389*, 321.
(85) Lopes, J. N. A. C.; Pádua, A. A. H. *J. Phys. Chem. B* **2006**, *110*, 3330.
(86) Fletcher, K. A.; Baker, S. N.; Baker, G. A.; Pandey, S. *New J. Chem.* **2003**, *27*, 1706.
(87) Seth, D.; Chakraborty, A.; Setua, P.; Sarkar, N. *J. Phys. Chem. B* **2007**, *111*, 4781.
(88) Rodriguez, H.; Brennecke, J. F. *J. Chem. Engg. Data* **2006**, *51*, 2145.
(89) Li, W.; Zhang, Z.; Han, B.; Hu, S.; Xie, Y.; Yang, G. *J. Phys. Chem. B* **2007**, *111*, 6452.
(90) Tokuda, H.; Baek, S. J.; Watanabe, M. *Electrochemistry* **2005**, *73*, 620.
(91) Chakrabarty, D.; Seth, D.; Chakraborty, A.; Sarkar, N. *J. Phys. Chem. B* **2005**, *109*, 5753.
(92) Armstrong, D. W.; Zhang, L. K.; He, L.; Gross, M. L. *Anal. Chem.* **2001**, *73*, 3679.
(93) Armand, M.; Endres, F.; MacFarlane, D. R.; Ohno, H.; Scrosati, B. *Nat. Mater.* **2009**, *8*, 621.
(94) Ding, J.; Zhou, D.; Spinks, G.; Wallace, G.; Forsyth, S.; Forsyth, M.; MacFarlane, D. *Chem. Mater.* **2003**, *15*, 2392.
(95) Fujita, K.; Ohno, H. *Biopolymers* **2010**, *93*, 1093.
(96) Yang, L. X.; Zhu, Y. J.; Wang, W. W.; Tong, H.; Ruan, M. L. *J. Phys. Chem. B* **2006**, *110*, 6609.
(97) Okazaki, K.-i.; Kiyama, T.; Hirahara, K.; Tanaka, N.; Kuwabata, S.; Torimoto, T. *Chem. Commun.* **2008**, 691.

(98) Migowski, P.; Dupont, J. *Chem. Eur. J.* **2007**, *13*, 32.
(99) Anderson, J. L.; Armstrong, D. W. *Anal. Chem.* **2003**, *75*, 4851.
(100) Seddon, K. R. *Nature Materials* **2003**, *2*, 363.
(101) Rogers, R. D.; Seddon, K. R. *Science* **2003**, *302*, 792.
(102) Pramanik, R.; Sarkar, S.; Ghatak, C.; Rao, V. G.; Mandal, S.; Sarkar, N. *J. Phys. Chem. B* **2011**, *115*, 6957.
(103) Sasmal, D. K.; Mandal, A. K.; Mondal, T.; Bhattacharyya, K. *J. Phys. Chem. B* **2011**, *115*, 7781.
(104) Birks, J. B. *Photophysics of Aromatic Molecules*; Wiley-Inter-Science: London, 1970.
(105) Demchenko, A. P. *Luminescence* **2002**, *17*, 19.
(106) Demchenko, A. P. In *Topics in Fluorescence Spectroscopy*; Lakowicz, J. R., Ed.; Plemum Press: New York, 1991; Vol. 3.
(107) Demchenko, A. P. *Ukr. Biochim. Zh.* **1981**, *53*, 22.
(108) Al-Hassan, K. A.; El-Bayoumi, M. A. *J. Polymer Sci. B* **1987**, *25*, 495.
(109) Rawat, S.; Mukherjee, S.; Chattopadhyay, A. *J. Phys. Chem. B* **1997**, *101*, 1922.
(110) Lakowicz, J. R.; Nakamoto, S. K. *Biochemistry* **1984**, *23*, 3013.
(111) Mandal, P. K.; Sarkar, M.; Samanta, A. *J. Phys. Chem. A* **2004**, *108*, 9048.
(112) Wang, Y.; Voth, G. A. *J. Am. Chem. Soc.* **2005**, *127*, 12192.
(113) Nishiyama, Y.; Fukuda, M.; Terazima, M.; Kimura, Y. *J. Chem. Phys.* **2008**, *128*, 164514.
(114) Mandal, P. K.; Paul, A.; Samanta, A. *J. Photochem. Photobiol. A: Chemistry* **2006**, *182*, 113.
(115) Lakowicz, J. R. *Principles of Fluorescence Spectroscopy, 3rd edition*; Springer: New York, 2006.
(116) Samanta, A. *J. Phys. Chem. Lett.* **2010**, *1*, 1557.
(117) Karmakar, R.; Samanta, A. *J. Phys. Chem. A* **2002**, *106*, 4447.
(118) Karmakar, R.; Samanta, A. *J. Phys. Chem. A* **2003**, *107*, 7340.
(119) Jin, H.; Baker, G. A.; Arzhantsev, S.; Dong, J.; Maroncelli, M. *J. Phys. chem. B* **2007**, *111*, 7291.
(120) Arzhantzev, S.; Jin, H.; Ito, N.; Maroncelli, M. *Chem. Phys. Lett.* **2006**, *417*, 524.
(121) Lang, B.; Angulo, G.; Vauthey, E. *J. Phys. Chem. A* **2006**, *110*, 7028.
(122) Shim, Y.; Duan, J. S.; Choi, M. Y.; Kim, H. J. *J. Chem. Phys.* **2003**, *119*, 6411.
(123) Chowdhury, R.; Mojumdar, S. S.; Chattoraj, S.; Bhattacharyya, K. *J. Chem. Phys.* **2012**, *137*, 055104.
(124) Mukherjee, P.; Crank, J. A.; Halder, M.; Armstrong, D. W.; Petrich, J. W. *J. Phys. Chem. A* **2006**, *110*, 10725.
(125) Ingram, J. A.; Moog, R. S.; Ito, N.; Biswas, R.; Maroncelli, M. *J. Phys. Chem. B* **2003**, *107*, 5926.
(126) Ito, N.; Arzhantsev, S.; Heitz, M.; Maroncelli, M. *J. Phys. Chem. B* **2004**, *108*, 5771.
(127) Headley, L. S.; Mukherjee, P.; Anderson, J. L.; Ding, R.; Halder, M.; Armstrong, D. W.; Song, X.; Petrich, J. W. *J. Phys. Chem. A* **2006**, *110*, 9549.
(128) Zhang, X.-X.; Liang, M.; Ernsting, N. P.; Maroncelli, M. *J. Phys. Chem. B*, DOI: 10.1021/jp305430a.
(129) Mandal, P. K.; Samanta, A. *J. Phys. Chem. B* **2005**, *109*, 15172.
(130) Mandal, P. K.; Paul, A.; Samanta, A. *Res. Chem. Intermed.* **2005**, *31*, 575.
(131) Ito, N.; Arzhantsev, S.; Maroncelli, M. *Chem. Phys. Lett.* **2004**, *396*, 83.
(132) Paul, A.; Samanta, A. *J. Phys. Chem. B* **2008**, *112*, 947.
(133) Adhikari, A.; Dey, S.; Das, D. K.; Mandal, U.; Ghosh, S.; Bhattacharyya, K. *J. Phys. Chem. B* **2008**, *112*, 6350.

(134) Kobrak, M. N.; Znamenskiy, V. *Chem. Phys. Lett.* **2004**, *395*, 127.
(135) Znamenskiy, V.; Kobrak, M. N. *J. Phys. Chem. B* **2004**, *108*, 1072.
(136) Shim, Y.; Choi, M. Y.; Kim, H. J. *J. Chem. Phys.* **2005**, *122*, 044511.
(137) Schmidhammer, U.; Megerle, U.; Lochbrunner, S.; Riedle, E.; Karpiuk, J. *J. Phys. Chem. A* **2008**, *112*, 8487.
(138) Santhosh, K.; Samanta, A. *J. Phys. Chem. B* **2010**, *114*, 9195.
(139) Santhosh, K.; Samanta, A. *ChemPhysChem* **2012**, *12*, 1956.
(140) Kimura, Y.; Fukuda, M.; Suda, K.; Terazima, M. *J. Phys. Chem. B* **2010**, *114*, 11847.
(141) Khara, D. C.; Samanta, A. *Phys. Chem. Chem. Phys.* **2010**, *12*, 7671.
(142) Paul, A.; Samanta, A. *J. Phys. Chem. B* **2007**, *111*, 4724.
(143) Mali, K. S.; Dutt, G. B.; Mukherjee, T. *J. Chem. Phys.* **2005**, *123*, 174504.
(144) Werner, J. H.; Baker, S. N.; Baker, G. A. *Analyst* **2003**, *128*, 786.
(145) Guo, J.; Baker, G. A.; Hillesheim, P. C.; Dai, S.; Shaw, R. W.; Mahurin, S. M. *Phys. Chem. Chem. Phys.* **2011**, *13*, 12395.
(146) Reed, M. A.; Randall, J. N.; Aggarwal, R. J.; Matyi, R. J.; Moore, T. M.; Wetsel, A. E. *Phys. Rev. Lett.* **1988**, *60*, 535.
(147) Brus, L. E. *J. Chem. Phys.* **1984**, *80*, 4403.
(148) Smith, A. M.; Nie, S. *Acc. Chem. Res.* **2010**, *43*, 190.
(149) Bawendi, M. G.; Steigerwald, M. L.; Brus, L. E. *Annu. Rev. Phys. Chem.* **1990**, *41*, 477.
(150) Alivisatos, A. P. *J. Phys. Chem.* **1996**, *100*, 13226.
(151) Chen, Z.; O'Brien, S. *ACS Nano* **2008**, *2*, 1219.
(152) Machol, J. L.; Wise, F. W.; Patel, R.; Tanner, D. B. *Physica A* **1994**, *207*, 427.
(153) Yin, Y.; Alivisatos, A. P. *Nature* **2005**, *437*, 664.
(154) Murray, C. B.; Norris, D. J.; Bawendi, M. G. *J. Am. Chem. Soc.* **1993**, *115*, 8706.
(155) Underwood, D. F.; Kippeny, T.; Rosenthal, S. J. *J. Phys. Chem. B* **2001**, *105*, 436.
(156) Pokrant, S.; Whaley, K. B. *Eur. Phys. J. D* **1999**, *6*, 255.
(157) Wuister, S. F.; Swart, I.; Driel, F. V.; Hickey, S. G.; Donega, D. D. M. *Nano Lett.* **2003**, *3*, 503.
(158) Kim, S.-W.; Kim, S.; Tracy, J. B.; Jasanoff, A.; Bawendi, M. G. *J. Am. Chem. Soc.* **2005**, *127*, 4556.
(159) Fan, H.; Leve, E. W.; Scullin, C.; Gabaldon, J.; Tallant, D.; Bunge, S.; Boyle, T.; Wilson, M. C.; Brinker, C. J. *Nano Lett.* **2005**, *5*, 645.
(160) Nakashima, T.; Kawai, T. *Chem. Commun.* **2005**, 1643.
(161) Nakashima, T.; Nonoguchi, Y.; Kawai, T. *Polym. Adv. Technol.* **2008**, *19*, 1401.
(162) Reiss, P.; Protiere, M.; Li, L. *Small* **2009**, *5*, 154.
(163) Chaudhuri, R. G.; Paria, S. *Chem. Rev.* **2012**, *112*, 2373.
(164) Hines, M. A.; Guyot-Sionnest, P. *J. Phys. Chem.* **1996**, *100*, 468.
(165) Kim, S.; Fisher, B.; Eisler, H. J.; Bawendi, M. *J. Am. Chem. Soc.* **2003**, *125*, 11466.
(166) Battaglia, D.; Li, J. J.; Wang, Y. J.; Peng, X. G. *Angew. Chem. Int. Ed.* **2003**, *42*, 5035.
(167) Zhong, X. H.; Xie, R. G.; Zhang, Y.; Basche, T.; Knoll, W. *Chem. Mater.* **2005**, *17*, 4038.
(168) Mews, A.; Eychmüller, A.; Giersig, M.; Schooss, D.; Weller, H. *J. Phys. Chem.* **1994**, *98*, 934.
(169) Dabbousi, B. O.; Rodriguez-Viejo, J.; Mikulec, F. V.; Heine, J. R.; Mattoussi, H.; Ober, R.; Jensen, K. F.; Bawendi, M. G. *J. Phys. Chem. B* **1997**, *101*, 9463.
(170) Li, J. J.; Wang, Y. A.; Guo, W. Z.; Keay, J. C.; Mishima, T. D.; Johnson, M. B.; Peng, X. G. *J. Am. Chem. Soc.* **2003**, *125*, 12567.

(171) Nirmal, M.; Dabboussi, B. O.; Bawendi, M.; Macklin, J. J.; Trautman, J. K.; Harris, T. D.; Brus, L. E. *Nature* **1996**, *383*, 802.
(172) Empedocles, S. A.; Bawendi, M. *Acc. Chem. Res.* **1999**, *32*, 389.
(173) Tang, J.; Marcus, R. A. *J. Chem. Phys.* **2005**, *123*, 054704.
(174) Kuno, M.; Fromm, D. P.; Hamann, H. F.; Gallagher, A.; Nesbitt, D. J. *J. Chem. Phys.* **2001**, *115*, 1028.
(175) Cragg, G. E.; Efros, A. L. *Nano Lett.* **2010**, *10*, 313.
(176) Cui, S.-C.; Tachikawa, T.; Fujitsuka, M.; Majima, T. *J. Phys. Chem. C* **2008**, *112*, 19625.
(177) Jin, S.; Hsiang, J.-C.; Zhu, H.; Song, N.; Dickson, R. M.; Lian, T. *Chem. Sci.* **2010**, *1*, 519.
(178) Peterson, J. J.; Nesbitt, D. J. *Nano Lett.* **2009**, *9*, 338.
(179) Pelton, M.; Smith, G.; Scherer, N. F.; Marcus, R. A. *Proc. Natl. Acad. Sci. USA* **2007**, *104*, 14249.
(180) Weiss, S. *Nat. Struct. Biol.* **2000**, *7*, 724.
(181) Kapanidis, A. N.; Weiss, S. *J. Chem. Phys.* **2002**, *117*, 10953.
(182) Mahler, B.; Spinicelli, P.; Buil, S.; Quelin, X.; Hermier, J.-P.; Dubertret, B. *Nature Materials* **2008**, *7*, 659.
(183) Dennis, A. M.; Mangum, B. D.; Piryatinski, A.; Park, Y.-S.; Hannah, D. C.; Casson, J. L.; Williams, D. J.; Schaller, R. D.; Htoon, H.; Hollingsworth, J. A. *Nano Lett.*, DOI: 10.1021/nl302453x.
(184) Hohng, S.; Ha, T. *J. Am. Chem. Soc.* **2004**, *126*, 1324.
(185) Nozik, A. J. *Chem. Phys. Lett.* **2008**, *457*, 3.
(186) Schaller, R. D.; Klimov, V. I. *Phys. Rev. Lett.* **2004**, *92*, 186601/1.
(187) Klimov, V. I. *Annu. Rev. Phys. Chem.* **2007**, *58*, 635.
(188) Yang, Y.; Rodríguez-Córdoba, W.; Lian, T. *Nano Lett.* **2012**, *12*, 4235.
(189) Bakalova, R.; Zhelev, Z.; Ohba, H.; Baba, Y. *J. Am. Chem. Soc.* **2005**, *127*, 11328.
(190) Hoshino, K.; Gopal, A.; Glaz, M. S.; Bout, D. A. V.; Zhang, X. *Appl. Phys. Lett.* **2012**, *101*, 043118.
(191) Vaillancourt, J.; Vasinajindakaw, P.; Lu, X. *Optics and Photonics Lett.* **2011**, *4*, 57.
(192) Kamat, P. V. *Acc. Chem. Res.*, DOI: 10.1021/ar200315d.
(193) Robel, I.; Subramanian, V.; Kuno, M.; Kamat, P. V. *J. Am. Chem. Soc.* **2006**, *128*, 2385.
(194) Etgar, L.; Zhang, W.; Gabriel, S.; Hickey, S. G.; Nazeeruddin, M. K.; Eychmüller, A.; Liu, B.; Grätzel, M. *Adv. Mater.* **2012**, *24*, 2202.
(195) Yang, Z.; Chen, C.-Y.; Roy, P.; Chang, H.-T. *Chem. Commun.* **2011**, *47*, 9561.
(196) Medintz, I. L.; Konnert, J. H.; Clapp, A. R.; Stanish, I.; Twigg, M. E.; Mattoussi, H.; Mauro, J. M.; Deschamps, J. R. *Proc. Natl. Acad. Sci. USA* **2004**, *101*, 9612.
(197) Shim, M.; Wang, C.; Guyot-Sionnest, P. *J. Phys. Chem. B* **2001**, *105*, 2369.
(198) Huang, J.; Stockwell, D.; Huang, Z.; Mohler, D. L.; Lian, T. *J. Am. Chem. Soc.* **2008**, *130*, 5632.
(199) Sykora, M.; Petruska, M. A.; Alstrum-Acevedo, J.; Bezel, I.; meyer, T. J.; Klimov, V. I. *J. Am. Chem. Soc.* **2006**, *128*, 9984.
(200) Schaller, R. D.; Sykora, M.; Jeong, S.; Klimov, V. I. *J. Phys. Chem. B* **2006**, *110*, 25332.
(201) Baker, D. R.; Kamat, P. V. *Langmuir* **2010**, *26*, 11272.
(202) Sharma, S. N.; Pillai, Z. S.; Kamat, P. V. *J. Phys. Chem. B* **2003**, *107*, 10088.
(203) Funston, A. M.; Jasieniak, J. J.; Mulvaney, P. *Adv. Mater.* **2008**, *20*, 4274.
(204) Medintz, I. L.; Pons, T.; Susumu, K.; Boeneman, K.; Dennis, A. M.; Farrell, D.; Deschamps, J. R.; Melinger, J. S.; Bao, G.; Mattoussi, H. *J. Phys. Chem. C* **2009**, *113*, 18552.

(205) Lutich, A. A.; Jiang, G.; Susha, A. S.; Rogach, A. L.; Stefani, F. D.; Feldmann, J. *Nano Lett.* **2009**, *9*, 2636.
(206) Noone, K. M.; Anderson, N. C.; Horwitz, N. E.; Munro, A. M.; Kulkarni, A. P.; Ginger, D. S. *ACS Nano* **2009**, *3*, 1345.
(207) Boulesbaa, A.; Huang, Z.; Wu, D.; Lian, T. *J. Phys. Chem. C* **2010**, *114*, 962.
(208) Rawalekar, S.; Kaniyankandy, S.; Verma, S.; Ghosh, H. N. *ChemPhysChem* **2011**, *12*, 1729.
(209) Verma, S.; Gupta, A.; Sainis, J. K.; Ghosh, H. N. *J. Phys. Chem. Lett.* **2011**, *2*, 858.
(210) Rawalekar, S.; Kaniyankandy, S.; Verma, S.; Ghosh, H. N. *J. Phys. Chem. C* **2010**, *114*, 1460.
(211) Santhosh, K.; Patra, S.; Soumya, S.; Khara, D. C.; Samanta, A. *ChemPhysChem* **2011**, *12*, 2735.
(212) Tvrdy, K.; Frantsuzov, P. A.; Kamat, P. V. *Proc. Natl. Acad. Sci. USA* **2011**, *108*, 29.
(213) Yang, Y.; Rodríguez-Córdoba, W.; Xiang, X.; Lian, T. *Nano Lett.* **2012**, *12*, 303.
(214) Knowles, K. E.; Malicki, M.; Weiss, E. A. *J. Am. Chem. Soc.* **2012**, *134*, 12470.
(215) Vinayakan, R.; Shanmugapriya, T.; Nair, P. V.; Ramamurthy, P.; Thomas, K. G. *J. Phys. Chem. C* **2007**, *111*, 10146.
(216) Huang, J.; Huang, Z.; Jin, S.; Lian, T. *J. Phys. Chem. C* **2008**, *112*, 19734.
(217) Jin, W. J.; Fernandez-Arguelles, M. T.; Costa-Fernandez, J. M.; Pereiro, R.; Sanz-Medel, A. *Chem. Commun.* **2005**, 883.
(218) Soujon, D.; Becker, K.; Rogach, A. L.; Feldmann, J.; Weller, H.; Talapin, D. V.; Lupton, J. M. *J. Phys. Chem. C* **2007**, *111*, 11511.
(219) Dennis, A. M.; Rhee, W. J.; Sotto, D.; Dublin, S. N.; Bao, G. *ACS Nano* **2012**, *6*, 2917.
(220) Jiang, G.; Susha, A. S.; Lutich, A. A.; Stefani, F. D.; Feldmann, J.; Rogach, A. L. *ACS Nano* **2009**, *3*, 4127.
(221) Burks, P. T.; Ostrowski, A. D.; Mikhailovsky, A. A.; Chan, E. M.; Wagenknecht, P. S.; Ford, P. C. *J. Am. Chem. Soc.* **2012**, *134*, 13266.
(222) Choi, H.; Santra, P. K.; Kamat, P. V. *ACS Nano* **2012**, *6*, 5718.
(223) Julliard, M.; Chanon, M. *Chem. Rev.* **1983**, *83*, 425.
(224) Whitten, D. G. *Acc. Chem. Res.* **1980**, *84*, 981.
(225) Bi, D.; Wu, F.; Qu, Q.; Yue, W.; Cui, Q.; Shen, W.; Chen, R.; Liu, C.; Qiu, Z.; Wang, M. *J. Phys. Chem. C* **2011**, *115*, 3745.
(226) Kawatsu, T.; Coropceanu, V.; Ye, A.; Bredas, J.-L. *J. Phys. Chem. C* **2008**, *112*, 3429.
(227) Huang, J.-H.; Wen-Hsien; Sun, Y.-Y.; Chou, P.-T.; Fang, J.-M. *J. Org. Chem.* **2005**, *70*, 5827.
(228) Silva, A. P. D.; Leydet, Y.; Lincheneau, C.; McClenagham, N. D. *J. Physics: Condensed Matter* **2006**, *18*, S1847.
(229) Andersson, M.; Sinks, L. E.; Hayes, R. T.; Zhao, Y.; Wasielewski, M. R. *Angew. Chem. Int. Ed.* **2003**, *42*, 3139.
(230) Kondratenko, M.; Moiseev, A. G.; Perepichka, D. F. *J. Mater. Chem.* **2011**, *21*, 1470.
(231) Nocera, D. G. *Acc. Chem. Res.* **2012**, *45*, 767.
(232) Kavarnos, G. J. *Fundamentals of Photoinduced Electron Trasnfer*; VCH Publishers: New York, 1993.
(233) Kavarnos, G. J.; Turro, N. J. *Chem. Rev.* **1986**, *86*, 401.
(234) In *The Exciplex*; Gordon, M., Ware, W. R., Eds.; Academic Press: New York, 1974.
(235) Mataga, N. *Pure and Appl. Chem.* **1984**, *56*, 1255.

(236) Rehm, D.; Weller, A. *Ber. Bunsen-Ges. Phys. Chem.* **1969**, *73*, 834.
(237) Rehm, D.; Weller, A. *Isr. J. Chem.* **1970**, *8*, 259.
(238) Mataga, N.; Okada, T.; Kanda, Y.; Shioyama, H. *Tetrahedron* **1986**, *42*, 6143.
(239) Schaap, A. P.; Zaklika, K. A.; Kaskar, B.; Fung, L. V.-M. *J. Am. Chem. Soc.* **1980**, *102*, 389.
(240) Jarnigan, R. C. *Acc. Chem. Res.* **1971**, *4*, 420.
(241) Gassman, P. G.; Olson, K. D. *J. Am. Chem. Soc.* **1982**, *104*, 3740.
(242) Liang, M.; Kaintz, A.; Baker, G. A.; Maroncelli, M. *J. Phys. Chem. B* **2012**, *116*, 1370.
(243) Koch, M.; Rosspeintner, A.; Angulo, G.; Vauthey, E. *J. Am. Chem. Soc.* **2012**, *134*, 3729.
(244) Gordon, C. M.; McLean, A. J. *Chem. Commun.* **2000**, 1395.
(245) Skrzypczak, A.; Neta, P. *J. Phys. chem. A* **2003**, *107*, 7800.
(246) Takahashi, K.; Sakai, S.; Tezuka, H.; Hiejima, Y.; Katsumura, Y.; Watanabe, M. *J. Phys. Chem. B* **2007**, *111*, 4807.
(247) Sarkar, S.; Pramanik, R.; Seth, D.; Setua, P.; Sarkar, N. *Chem. Phys. Lett.* **2009**, *477*, 102.
(248) Das, A. K.; Mondal, T.; Sen, M. S.; Bhattacharyya, K. *J. Phys. Chem. B* **2011**, *115*, 4680.
(249) Castner, E. W.; Margulis, C. J.; Maroncelli, M.; Wishart, J. F. *Annu. Rev. Phys. Chem.* **2011**, *62*, 85.
(250) Silva, A. P. D.; Gunaratne, H. Q. N.; Gunnlaugsson, T.; Huxley, A. J. M.; McCoy, C. P.; Rademacher, J. T.; Rice, T. E. *Chem. Rev.* **1997**, *97*, 1515.
(251) Pedersen, C. J. *J. Am. Chem. Soc.* **1967**, *89*, 7017.
(252) Soujanya, T.; Fessenden, R. W.; Samanta, A. *J. Phys. Chem.* **1996**, *100*, 3507.
(253) Saha, S.; Samanta, A. *J. Phys. Chem. A* **2002**, *106*, 4763.
(254) Lapouyade, R.; Czeschka, K.; Majenz, W.; Rettig, W.; Gilabert, E.; Rulliere, C. *J. Phys. Chem.* **1992**, *96*, 9643.
(255) Sarkar, M.; Kanaparthi, R. K.; Bhattacharya, B.; Samanta, A. *J. Phys. Chem. A* **2008**, *112*, 3302.
(256) Jiang, Y.-B.; Wang, X.-J. *J. Photochem. Photobiol. A: Chemistry* **1994**, *81*, 205.
(257) Rurack, K.; Dekhtyar, M. L.; Bricks, J. L.; Resch-Genger, T.; Rettig, W. *J. Phys. Chem. A* **1999**, *103*, 9626.
(258) Shaikh, M.; Mohanty, J.; Singh, P. K.; Bhasikuttan, A. C.; Rajule, R. N.; Satam, V. S.; Bendre, S. R.; Kanetkar, V. R.; Pal, H. *J. Phys. Chem. A* **2010**, *114*, 4507.
(259) Karpiuk, J. *J. Phys. Chem. A* **2004**, *108*, 11183.
(260) Lippert, E.; Luder, W.; Moll, F.; Nagele, W.; Boss, H.; Prigge, H.; Blankenstein, I. S. *Angew. Chem.* **1961**, *73*, 695.
(261) Rotkiewicz, K.; Grellmann, K. H.; Grabowski, Z. R. *Chem. Phys. Lett.* **1973**, *19*, 315.
(262) Rotkiewicz, K.; Grabowski, Z. R.; Krowczynski, A.; Kühnle, W. *J. Lumin.* **1976**, *12-13*, 877.
(263) Zachariasse, K. A.; Haar, T. V. D.; Hebecker, A.; Leinhos, U.; Kühnle, W. *Pure Appl. Chem.* **1993**, *65*, 1745.
(264) Sobolewski, A. L.; Domcke, W. *Chem. Phys. Lett.* **1996**, *250*, 428.
(265) Grabowski, Z. R.; Rotkiewicz, K.; Rettig, W. *Chem. Rev.* **2003**, *103*, 3899.
(266) Demchenko, A. P. *Lab Chip* **2005**, *5*, 1210.
(267) Jones-II, G.; Jackson, W. R.; Choi, C.-Y.; Bergmark, W. R. *J. Phys. Chem.* **1985**, *89*, 294.

(268) Vogel, M.; Rettig, W.; Fiedeldei, U.; Baumgaertel, H. *Chem. Phys. Lett.* **1988**, *148*, 347.

(269) Das, S.; Kamat, P. V.; Barre, B. D. L.; Thomas, K. G.; Ajayghosh, A.; George, M. V. *J. Phys. Chem.* **1992**, *96*, 10327.

(270) Khara, D. C.; Samanta, A. *J. Phys. Chem. B*, DOI: 10.1021/jp3054058.

(271) Chang, H. C.; Jiang, J. C.; Tsai, W. C.; Chen, G. C.; Lin, S. H. *J. Phys. Chem. B* **2006**, *110*, 3302.

(272) Tsuzuki, S.; Tokuda, H.; Mikami, M. *Phys. Chem. Phys. Chem.* **2007**, *9*, 4780.

(273) Thar, J.; Brehm, M.; Seitsonen, A. P.; Kirchner, B. *J. Phys. Chem. B* **2009**, *113*, 15129.

(274) Wang, P.; Wu, S. *J. Photochem. Photobiol. A: Chemistry* **1995**, *86*, 109.

(275) Boulesbaa, A.; Issac, A.; Stockwell, D.; Huang, Z.; Huang, J.; Guo, J.; Lian, T. *J. Am. Chem. Soc.* **2007**, *129*, 15132.

(276) Zhang, Y.; Jing, P.; Zeng, Q.; Sun, Y.; Su, H.; Wang, Y. A.; Kong, X.; Zhao, J.; Zhang, H. *J. Phys. Chem. C* **2009**, *113*, 1886.

(277) Goldman, E. R.; Medintz, I. L.; Whitley, J. L.; Hayhurst, A.; Clapp, A. R.; Uyeda, H. T.; Deschamps, J. R.; Lassman, M. E.; Mattoussi, H. *J. Am. Chem. Soc.* **2005**, *127*, 6744.

(278) Zhou, D.; Piper, J. D.; Abell, C.; Klenerman, D.; Kang, D.-J.; Ying, L. *Chem. Commun.* **2005**, 4807.

(279) Nikiforov, T. T.; Beechem, J. M. *Analytical Biochemistry* **2006**, *357*, 68.

(280) Sadhu, S.; Patra, A. *ChemPhysChem* **2008**, *9*, 2052.

(281) Sadhu, S.; Tachiya, M.; Patra, A. *J. Phys. Chem. C* **2009**, *113*, 19488.

(282) Tena-Zaera, R.; Katty, A.; Bastide, S.; Levy-Clement, C. *Chem. Mater.* **2007**, *19*, 1626.

(283) Lee, H. J.; Yum, J.-H.; Leventis, H. C.; Zakeeruddin, S. M.; Haque, S. A.; Chen, P.; Seok, S. I.; Grätzel, M.; Nazeeruddin, M. K. *J. Phys. Chem. C* **2008**, *112*, 11600.

(284) Kamat, P. V. *J. Phys. Chem. C* **2008**, *112*, 18737.

(285) Zakeeruddin, S. M.; Grätzel, M. *Adv. Funct. Mater.* **2009**, *19*, 2187.

(286) Jovanovski, V.; Gonzalez-Pedro, V.; Gimenez, S.; Azaceta, E.; Cabanero, G.; Grande, H.; Tena-Zaera, R.; Mora-Sero, I.; Bisquert, J. *J. Am. Chem. Soc.* **2011**, *133*, 20156.

(287) Bai, Y.; Cao, Y.; Zhang, J.; Wang, M.; Li, R.; Wang, P.; Zakeeruddin, S. M.; Grätzel, M. *Nat. Mater.* **2008**, *7*, 626.

(288) Licht, S.; Peramunage, D. *Nature* **1990**, *345*, 330.

CHAPTER 2

Materials, Methods and Instrumentation

This chapter starts with a short description on the materials used in this study and their procurement sources. Methods of synthesis of some of the EDA molecules, quantum dots (QDs) and RTILs used in these studies have also been described and this is followed by purification methods of conventional solvents and the RTILs. Methods of sample preparation for spectral measurements and microscopic experiments have been explained. The instrumentation details, especially the time-correlated single photon counting (TCSPC) based picosecond setup and time-resolved confocal fluorescence microscope, are discussed in detail. Various methodologies employed in the present study, such as measurement of fluorescence quantum yield and dipole moment change on photoexcitation, data analysis procedure for construction of the time-resolved emission spectra from the decay curves, estimation of the solvation times and position of the time-zero spectrum and the calculation of size and concentration of the QDs in solution have also been discussed.

2.1. Materials

4-(N,N′-Dimethylamino)benzonitrile (DMABN) was purchased from Sigma-Aldrich and was recrystallized from a mixture of n-hexane and diethyl ether. Spectroscopic grade 9-(dicyanovinyl)julolidine (DCVJ), which was used for estimating the microviscosity of the RTIL, was procured from Molecular Probes and used without further purification. 4-Aminophthalimide was obtained from TCI and recrystallized twice from ethanol in the presence of activated charcoal. Crystal violet lactone (CVL) was purchased from Sigma-Aldrich and recrystallized from acetone. Laser grade coumarin 153 (C153) was procured from Eastman Kodak and used as received. Acetophenone, 4-dimethylaminobenzaldehyde, 4-bromobenzaldehyde, N-methyl pyrrolidinone (NMP), cuprous oxide (Cu_2O) and aqueous solution of ammonia used for the synthesis of aminochalcones were purchased from local companies. Azetidine and 4-chloro-7-nitrobenz-2-oxa-1,3-diazole (NBD-Cl) for the synthesis

of 4-azetidinyl-7-nitrobenz-2-oxa-1,3-diazole (NBD) were purchased from Sigma-Aldrich. Hexadecylamine (HDA), trioctylphosphine (TOP), trioctylphosphineoxide (TOPO), oleic acid from Sigma-Aldrich and cadmium acetate, cadmium oxide (CdO), sulfur, tellurium, selenium powders from Loba company were employed for the synthesis of QDs. p-Phenylenediamine (PPD) for the QD fluorescence quenching studies was procured from Sigma-Aldrich. Sulfuric acid (H_2SO_4) from Merck, (3-aminopropyl)triethoxysilane and 3-mercaptopropionic acid (MPA) from Sigma-Aldrich were used for the sample preparation of QD single particle blinking studies. 1-methylimidazole and 11-bromoundecanethiol for the synthesis of a task-specific ionic liquid was purchased from Sigma-Aldrich. The RTILs, [bmim][PF_6], [bmim][BF_4], [emim][BF_4], [bmim][Tf_2N] and [emim][CF_3SO_3] were of "Advanced Materials Research" grade from Kanto Chemicals (Japan). While [N_{1888}][Tf_2N] was obtained from Merck, C(2)-methylated imidazolium RTIL, [bmMim][Tf_2N] and pyrrolidinium RTIL, [bmPr][[Tf_2N] were synthesized following reported procedure.[1] 1,2-dimethylimidazole, 1-methylpyrrolidine, 1-chlorobutane, 1-bromobutane and lithium bis(trifluoromethanesulfonyl)imide ($LiTf_2N$) for the synthesis of these RTILs were obtained from Sigma-Aldrich. The RTIL, [emim][$EtSO_4$] was obtained as free sample from Wako Chemicals (Japan) and was rigorously dried under high vacuum before use. Charcoal for the color treatment of RTILs was purchased from Acros Organics.

The purity of the compounds were checked by single spot in thin layer chromatography (TLC), nuclear magnetic resonance (NMR) as well as by matching the absorption and emission spectra with literature. Deuterated solvent, chloroform-D, for NMR spectral measurements was obtained from Merck. GR and synthesis grade solvents for synthesis and spectroscopic grade solvents for spectral measurements were obtained from Merck. Various drying agents such as benzophenone, calcium chloride ($CaCl_2$), calcium hydride (CaH_2), phosphorous pentoxide (P_2O_5), iodine, magnesium (Mg) turnings and sodium metal used at different stages of solvent purification, hydrochloric acid (HCl) for cleaning Mg turnings and molecular sieves for the storage of dried solvents were purchased from local companies.

2.2. Synthesis of EDA molecules, quantum dots and ionic liquids

2.2.1. EDA molecules

4-Aminochalcone (AC). This compound was synthesized by following a known method reported by Xu et al.[2] 4-Bromochalcone required for the synthesis of AC was synthesized from simple aldol condensation of acetophenone with 4-bromobenzaldehyde. Briefly, 2.0 mmol of 4-bromochalcone was treated with 20.0 mmol of aqueous ammonia in the presence of 5.0 mol% Cu_2O along with H_2O- NMP (1:1). The reaction was carried out at 80°C for 15 hours and the crude product was purified by column chromatography using a mixture of hexane and ethyl acetate as the eluent.

4-Dimethylaminochalcone (DMAC). Synthesis of DMAC was carried out by following a reported procedure,[3] where 0.02 mol of acetophenone and 20 mL of 10% aqueous NaOH were added to 40 mL of ethanol with stirring to form a uniform solution. Subsequently 2.9 g of 4-dimethylaminobenzaldehyde was added slowly into the above solution. Then the mixture was stirred for 2 hrs at room temperature until a precipitate was formed. The product was purified by recrystallization from acetone.

4-azetidinyl-7-nitrobenz-2-oxa-1,3-diazole (NBD). NBD was synthesized following a standard procedure,[4] in which 1 mmol of 4-chloro-7-nitrobenz-2-oxa-1,3-diazole (NBD-Cl) was dissolved in 3 mL ethylacetate. 2.0 mL ethylacetate solution of 1.2 mmol azetidine was added dropwise to NBD-Cl solution at 0°C with stirring. After stirring for 30 min at this temperature, the reaction mixture was further stirred for another 2 hrs at room temperature. The product, a red precipitate, was filtered out and purified by column chromatography using a silica gel column. Hexane and ethylacetate were used as eluent for the purification of the compound. The purified compound was recrystallized from absolute ethanol.

2.2.2. Quantum dots

CdS/HDA QDs. Hexadecylamine (HDA) capped CdS QDs of size 4.5 nm were synthesized by following a standard procedure with slight modification in the capping agent.[5] A mixture of 0.133 g (0.5 mM) cadmium acetate and 4 g of hexadecylamine was heated to 150°C under argon atmosphere for 20 min to form a clear solution. Separately, a solution of 0.016 g (0.5

mM) of sulfur powder in 2 g of hexadecylamine was prepared at 55°C and quickly injected into the above hot reaction mixture under stirring. The reaction was kept at 150°C for 8 hrs. The QDs from the yellow precipitate was washed with ethanol and separated by adding toluene and centrifugation. For optical studies, excess starting materials were removed by repeated precipitation and centrifugation. Transmission electron microscope (TEM) images provided morphological and size information of the QDs.

CdTe/HDA QDs. CdTe/HDA QDs were synthesized following a reported procedure.[6] Briefly, HDA (5 g) and TOP (3 mL) were mixed in a two-necked round-bottom (RB) flask and heated at 80°C for some time. Meanwhile, a separate solution of 0.16 g of Te powder and 0.41 g of $Cd(CH_3COO)_2$ in TOP (3 mL) was prepared in a reagent bottle and sonicated for some time to obtain an almost clear solution, which was then injected into the capping agents in the RB flask, and the temperature was slowly raised to 165°C. The reaction was stopped when the QDs with desired sizes (checked by monitoring the emission band) were obtained. All the reactions were carried out under argon atmosphere. For spectral measurements, the QDs were purified by washing with methanol, repeated precipitation, and centrifugation. Washed precipitate was added to $CHCl_3$ to obtain a clear and fluorescent solution of the CdTe/HDA QDs in $CHCl_3$.

CdSe/HDA QDs. CdSe/HDA QDs were also synthesized following a reported procedure with slight modifications.[7] Briefly, a mixture of CdO (0.067 g, 0.52 mmol), oleic acid (1.4 mmol), HDA (5 g), and TOPO (2.5 g) was heated to 100°C under an inert atmosphere. Then the temperature of the reaction was raised to 300°C and maintained until CdO was completely dissolved. A separate solution of Se dissolved in TOP (5 mL) was prepared and injected into the RB containing Cd precursors. The temperature was set according to the desired size and growth of the nanoparticles. Finally the reaction was stopped when particles with desired emission was achieved.

2.2.3. Ionic liquids

[bmMim][Tf_2N]. The chloride salt, [bmMim]Cl, for the synthesis of [bmMim][Tf_2N] was first prepared by treating a mixture of 1,2-dimethylimidazole and 1-chlorobutane (distilled from P_2O_5), taken in 1:2 mole ratio at 65°C for 48-72 hrs under nitrogen atmosphere.[1] As the

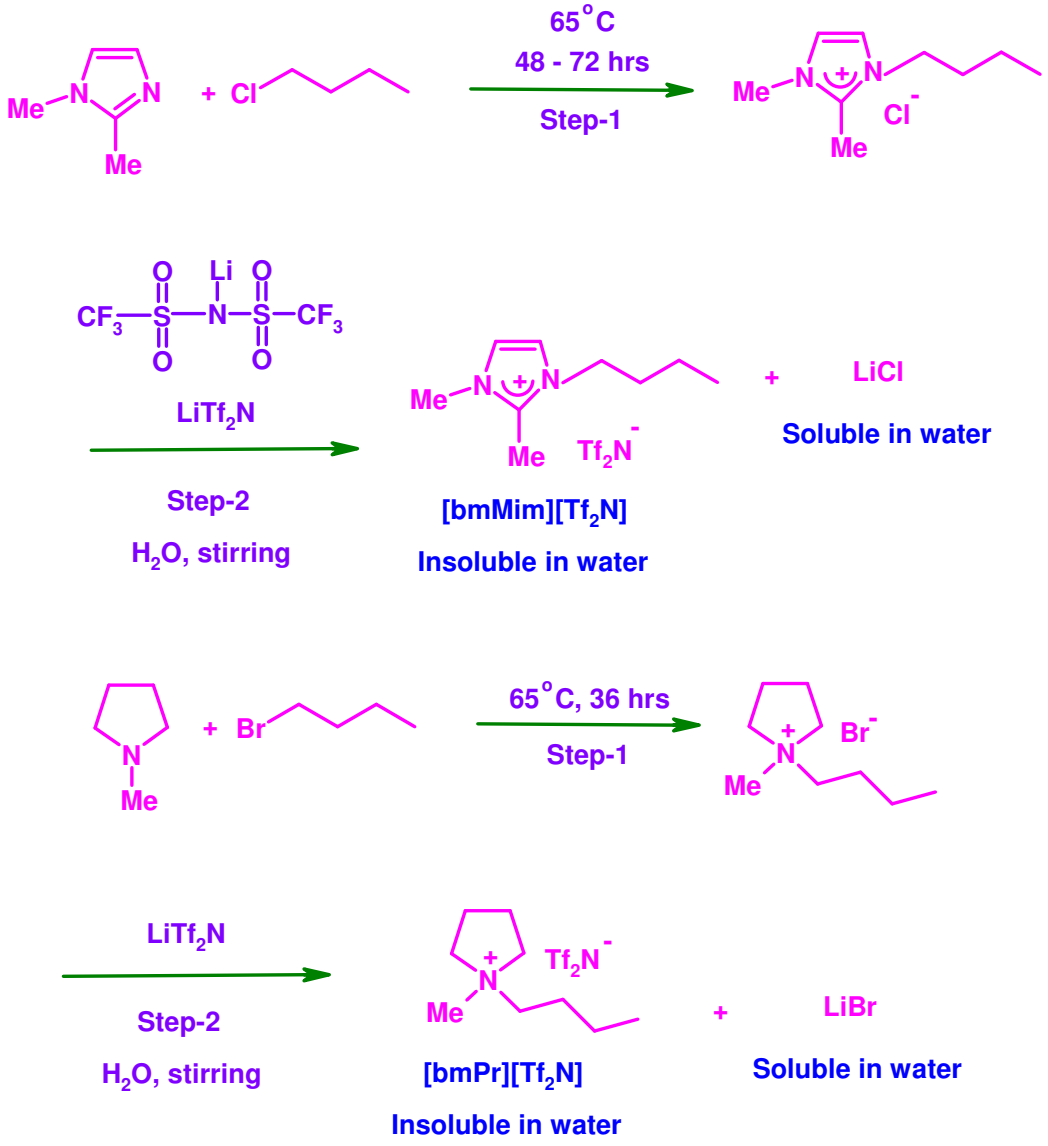

Scheme 2.1. Synthesis of [bmMim][Tf_2N] and [bmPr][Tf_2N] RTILs

reaction was exothermic, addition of 1-chlorobutane was very slow under cooling condition. After the reaction, the reaction mixture was cooled down to room temperature (298 K) and kept overnight in an ice-acetone bath in tightly sealed condition. The white/pale yellow solid so obtained was washed several times with dry and warm ethyl acetate to remove unreacted starting materials. Before proceeding to the next step the chloride salt was dried under high

vacuum for several hours.

The [bmMim][Tf_2N] RTIL was then prepared by dissolving equimolar amounts of [bmMim]Cl and $LiTf_2N$ in double distilled de-ionized water and then stirring the mixture for 12-24 hrs under nitrogen atmosphere. After ion exchange through stirring, the resultant viscous [bmMim][Tf_2N] RTIL was separated out and washed with double distilled de-ionized water for several times, until no trace of halide was detected in the wash-liquid by $AgNO_3$ test. Scheme 2.1 illustrates the steps involved in the synthesis of the RTIL.

[bmPr][Tf_2N]. The synthesis of [bmPr][Tf_2N] also involved two steps.[1] In the first step 1-bromobutane was slowly added to 1-methylpyrrolidine drop wise under cooling condition. After the addition, the mixture was brought to room temperature and refluxed for 36 hrs under inert atmosphere at 65°C. After the reaction, the unreacted starting materials were decanted and the solid bromide salt, [bmPr]Br, obtained was washed several times with dry and warm ethyl acetate.

In the second step, the bromide salt was mixed with equimolar amount of $LiTf_2N$ in double distilled de-ionized water and then stirred the mixture for 12-24 hrs under nitrogen atmosphere, similar to the procedure adopted in the case of [bmMim][Tf_2N] RTIL.[1] Finally, the viscous [bmPr][Tf_2N] RTIL obtained was washed several times with double distilled water until the RTIL was free from bromide impurities (confirmed by $AgNO_3$ test). Scheme 2.1 delineates the synthesis scheme of the ionic liquid.

Synthesis of SH-UMIM. Task-specific thiol functionalized imidazolium ionic liquid (IL), 1-methyl-(11-undecanethiol)imidazolium bromide (**SH-UMIM**) for the preparation of QD-IL hybrids was synthesized as shown in Scheme 2.2. 1-methylimidazole, which was distilled from KOH under reduced pressure prior to use, and 11-bromoundecanethiol were taken in 1:1.5 mol ratio.[8] The latter was slowly added to 1-methylimidazole under cooling conditions, and then the reaction was carried out at room temperature (298 K) for 24 hrs under N_2 atmosphere. Light yellow colored salt, **SH-UMIM**, obtained after the reaction was washed several times with ethylacetate to remove the unreacted starting materials then dried under high vacuum for several hours.

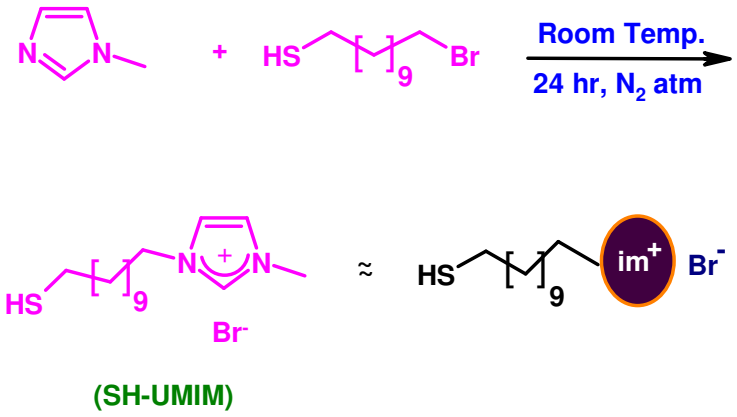

Scheme 2.2. Synthesis of SH-UMIM

2.3. Purification of conventional solvents

Conventional solvents used at different stages of the experiments were purified by following the procedures available in the literature.[9] After drying, molecular sieves were added to protect the solvents from the moisture.

Hexane, toluene, diethyl ether and 1,4-dioxane: The solvents were refluxed over metallic sodium for 3-4 hrs and then benzophenone was added after cooling. The dark solution was refluxed for another hour and distilled under dry condition. The purified solvents were optically transparent in the spectral region of the compounds of interest.

Chloroform: The solvent was stirred overnight with $CaCl_2$ and then distilled under moisture free conditions.

Dichloromethane: The solvent was stirred with CaH_2 for 5-6 hrs and then after distillation the solvent was stored under dry conditions.

Ethyl acetate: After stirring with P_2O_5 for 3-4 hours, the solvent was distilled out under dry atmosphere

Acetone and acetonitrile: Initially the solvents were refluxed for 3-4 hrs with anhydrous P_2O_5 and then distilled under dry conditions.

Dimethylsulfoxide (DMSO): The solvent was stored with dry molecular sieves for overnight and distilled under high vacuum and dry atmosphere.

Methanol and ethanol: The protic polar solvents were refluxed initially with Mg turnings and iodine for 3-4 hrs and then distilled under moisture free atmospheric conditions.

Water: Milli-Q water produced from Millipore, Synergy Pack was used for all the experiments.

2.4. Purification of the RTILs

As RTILs in the present studies were used for spectroscopic experiments, care was taken to ensure that these liquids were free from impurities, particularly those which impart color to the RTILs and contribute to the absorption and emission spectral regions of the fluorophores of interest. Though, most of the "Advanced Materials Research" grade RTILs from Kanto Chemicals (Japan) were optically transparent in the absorption regions of the fluorophores, the contribution of RTIL emission towards the emission of fluorophores was non negligible.[10] This necessitated several purification steps, out of which the charcoal treatment of the acetonitrile solutions of the RTILs at room temperature (298 K) or at 333 K showed best results. Figure 2.1 shows the absorption spectra and photographs of the $[N_{1888}][Tf_2N]$ ionic liquid before and after the charcoal treatment. This method was applied to the colored RTILs. However, a different procedure was employed for the purification of [bmMim][Tf_2N] and

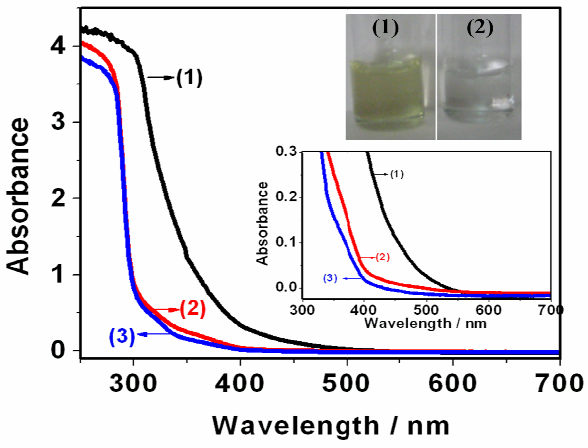

Figure 2.1. Absorption spectra of neat $[N_{1888}][Tf_2N]$ (1), after charcoal treatment at 298 K (2) and at 333 K (3)

[bmPr][Tf_2N] RTILs. The charcoal treatment was carried out with the halide salts obtained in step-1 itself. Aqueous solutions were prepared with the colored halide salts, [bmMim]Cl and [bmPr]Br, obtained in step-1 and mixed with activated charcoal and then refluxed overnight at 120°C. After reflux, charcoal was separated out through filtration to get colorless solutions of the [bmMim]Cl and [bmPr]Br. During the second step, these salts yielded colorless and optically transparent RTILs [bmMim][Tf_2N] and [bmPr][Tf_2N]. Thus purified RTILs were stored in a vacuum desiccator under nitrogen atmosphere. Prior to use, all the RTILs were dried under high vacuum (pressure 10^{-2} – 10^{-3} mbar), sometimes with heating at 50-60°C, for at least 8-10 hrs to minimize the water content.

2.5. Sample preparation

2.5.1. Spectral measurements

For the steady-state and time-resolved spectral measurements of the organic fluorophores in conventional solvents and RTILs, the absorbance of the 1 cm path length solution at the excitation wavelength was maintained around 0.05 – 0.25, to avoid problems due to inner filter effects. Since RTILs are hygroscopic, care was taken to tightly seal the samples with septum and parafilm. For the energy transfer and charge transfer reactions from QDs and for fluorescence studies on QD-IL hybrids, the optical density (OD) values of the QDs at the excitation wavelength were maintained between 0.1 and 0.7.

2.5.2. TEM measurements

Samples for TEM measurements were prepared by placing a drop of clear solution of the QDs (in toluene) on carbon-coated copper grids and the dried samples were used for the experiments. However, in the case of CdTe QDs in RTILs, a drop of clear solution of CdTe/**SH-UMIM** QDs in [bmim][PF_6] was placed on carbon-coated copper grids and used for the measurements.

2.5.3. Single-particle blinking studies

Reported procedure[11] with slight modifications was adopted for the sample preparation of single-particle blinking studies (Scheme 2.3).[8] Initially, cover glasses (2x2 cm) were immersed in a 1 wt % of H_2SO_4 solution for 1 hr and then washed with Milli-Q water. The

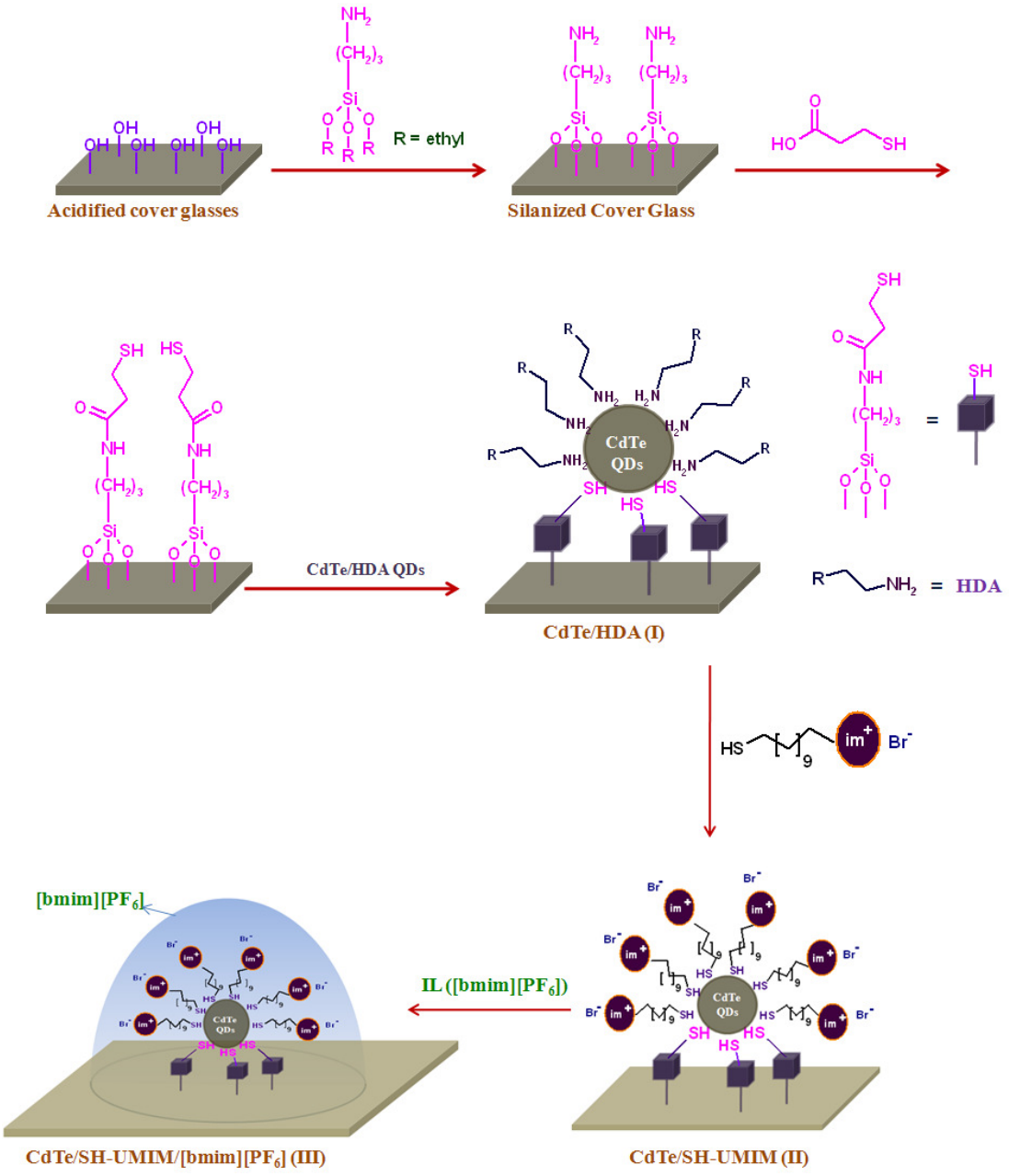

Scheme 2.3. Sample preparation for single particle blinking studies

washed cover glasses were soaked in 50 mM aqueous solution of (3-aminopropyl)triethoxysilane for 1 hr to obtain silanized cover glasses, which were then washed with Milli-Q water several times and then placed in a 50 mM 3-

mercaptopropionicacid (MPA) solution in water for 1 hr. The silanized cover glasses end up with the thiol functional groups were used to attach to the surface of the QDs. These cover glasses were further dipped in a 10 nM solution of the CdTe/HDA QDs in $CHCl_3$ for 1 hr to allow the QDs to be tethered on the silanized cover glasses, and the samples were washed with $CHCl_3$ for several times to remove unadsorbed QDs. This is the sample I used for the blinking studies. Sample II (Scheme 2.3) for further studies was prepared by exchanging the HDA capping agents by **SH-UMIM** by keeping I in 1 μM **SH-UMIM** solution in $CHCl_3$ for 1 hr. Stronger binding ability of the thiol helped replacement of HDA to form CdTe/**SH-UMIM QDs** bound to the silanized cover glass (II). To carry out the blinking studies in RTILs, sample III (CdTe/**SH-UMIM**/[bmim][PF_6]) was prepared by adding [bmim][PF_6] RTIL to II. [bmim][PF_6] was chosen because of its optical purity, which is essential in single-particle blinking studies. Prior to the experiments, all the samples were stored under dark and vacuum conditions.

2.6. Instrumentation

For characterization of the compounds, NMR spectra were recorded using Bruker AVACE 400 MHz NMR spectrometer. The viscosities of the RTILs were measured by a LVDV-III Ultra Brookfield Cone and Plate viscometer (accuracy: 1% and repeatability: 0.2%). For temperature dependent viscosity measurements a Julabo water circulator bath was used. The absorption and steady-state fluorescence spectra were recorded on a UV-visible spectrophotometer (Cary100, Varian) and a spectrofluorimeter (FluoroLog-3, Horiba Jobin Yvon), respectively. Peltier temperature controller (Wavelength electronics) was used with the spectrofluorimeter for steady-state fluorescence measurements at different temperatures. The fluorescence spectra were corrected for the instrument response function.

Fluorescence images for fluorescence recovery after photobleaching (FRAP) experiment were acquired on an inverted Zeiss LSM 510 Meta multiphoton laser scanning confocal fluorescence microscope with a 100×, 1.4 NA oil-immersion objective using 730 nm line of Ti:Saphire laser at 22°C. Fluorescence emission was collected using 505 – 570 nm band-pass filter. All images were acquired at a 512 pixel × 512 pixel resolution. FRAP experiments were carried out by scanning a square region of interest (ROI) of length 43.0 μm and

bleaching a circular region of interest of radius, ω = 4.30 µm. Circular bleach ROI was obtained using the drawing tool of the software provided with the instrument.

The size and shape of the QDs were examined by using Tecnai G2 FE1 F12 transmission electron microscope at an accelerating voltage of 200 kV. The size of the QDs from the TEM images were compared with the values estimated from the methods suggested by Yu et al. (Section 2.11).[12]

Working principles and details of other instrumental setups which were employed in these studies are explained in the following sections.

2.6.1. Time-correlated single photon counting setup

Time-resolved fluorescence measurements were carried out using a time correlated single-photon counting (TCSPC) spectrometer (Horiba Jobin Yvon IBH). The block diagram of the setup is shown in scheme 2.4. Nano LEDs and PicoBrite diode lasers were used as excitation sources, while a micro-channel plate (MCP) photomultiplier tube (Hamamatsu R3809U-50, 160-850 nm range) was used as the detector. Two Nano LEDS having output at 281 nm (FWHM = 960 ps), 439 nm (FWHM = 150 ps) and two PicoBrite lasers with output at 375 nm (FWHM = 55 ps), 405 nm (FWHM = 50 ps) were employed in the present study. While Nano LEDs were operated at a maximum pulse repetition rate of 1 MHz, PicoBrite laser sources were operated at 10 MHz repletion rate. Whenever it was needed, neutral density (ND) filters were used to reduce the excitation intensity. The experiment starts with simultaneous excitation of the sample and sending a signal to the electronics (Scheme 2.4).[13] Constant fraction discriminator (CFD) receives the excitation signal and accurately measures the arrival time of the photon and then diverts the signal towards the time to amplitude convertor (TAC) to start the voltage ramp. The second channel (CFD) which accurately measures the arrival time of the emitted photon makes TAC to stop the voltage ramp. The voltage ramp developed by TAC is proportional to the delay time between the excitation and emission signals. Programmable gain amplifier (PGA) amplifies the resultant voltage, which later be converted to a numerical value by analog-to-digital convertor (ADC). The numerical value with the measured time delay will be stored as a single event and by repeating the process several times with a pulsed excitation source, histogram of the fluorescence intensity decay with time can be constructed.

Different excitation source was used for collecting fluorescence decay profiles of DMABN, which absorbs in the UV region. Diode-pumped millenia CW laser (Spectra Physics) 532 nm was used to pump the Ti:sapphire rod in Tsunami picosecond mode-locked laser system (Spectra Physics). The 840 nm (82 MHz) output of the Ti:sapphire laser was passed through the pulse picker (Spectra Physics) to generate 4 MHz pulses. Using a flexible harmonic generator (FHG) a laser output of 280 nm could be generated with a pulse width (FWHM) of 52 ps, which was used to excite the sample.

The lamp profile was recorded by placing a scatterer (dilute solution of Ludox in water) in place of the sample. For temperature dependent fluorescence decay profiles, a Julabo water circulator bath was used. The analysis of the decay curves and construction of time-resolved emission spectra are covered in the later section.

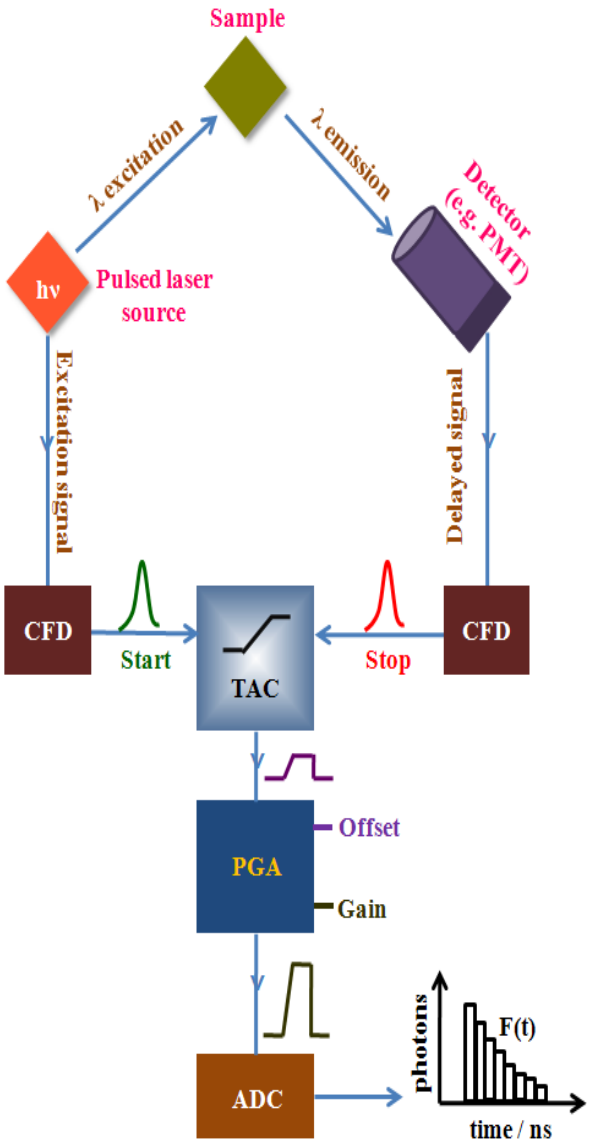

Scheme 2.4. Schematic diagram of the TCSPC setup

2.6.2. Time-resolved confocal fluorescence microscope

Single-particle blinking studies were carried out at 296 K using Micro-Time 200, PicoQuant time-resolved confocal fluorescence microscope.[8] The block diagram of the instrument is shown in Scheme 2.5. Olympus IX71 inverted microscope equipped with Olympus UPlansApo water immersion objective (1.2 NA, 60×) served as microscope body.

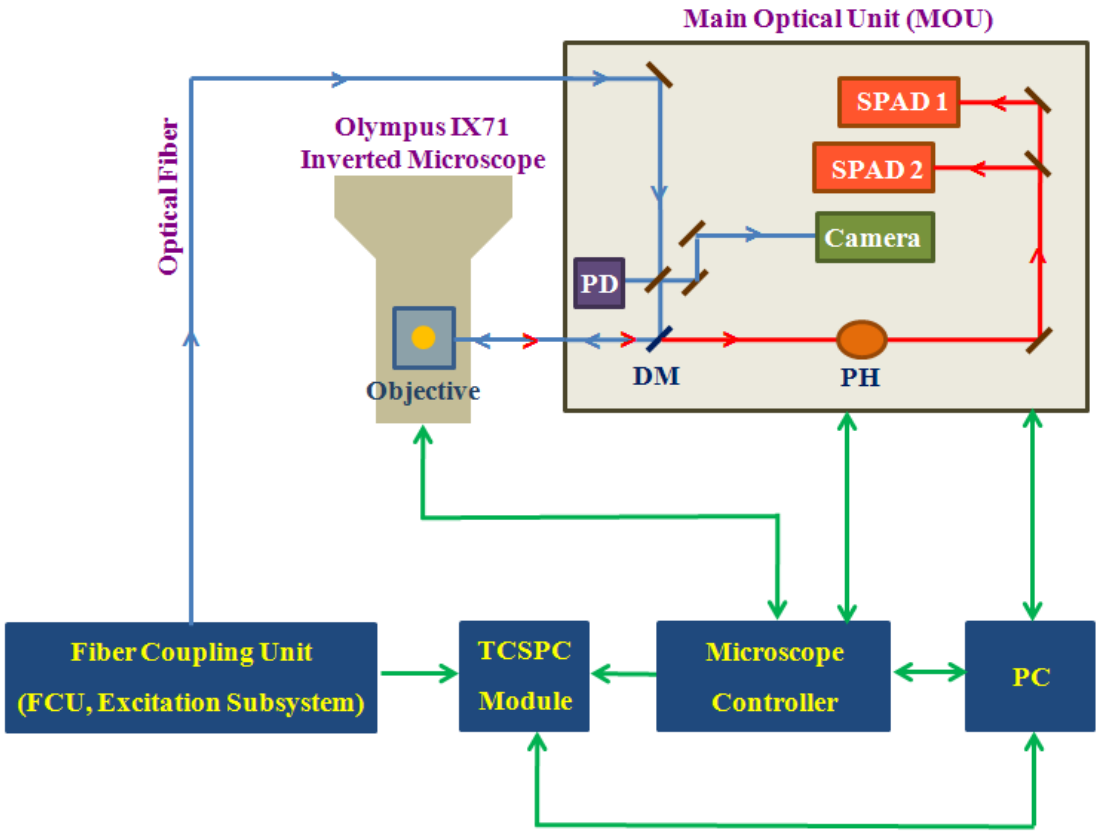

Scheme 2.5. Schematic diagram of the time-resolved confocal fluorescence microscope setup (Source: PicoQuant MicroTime 200 user manual)

A 405 nm picosecond pulsed diode laser (fwhm of 176 ps) with a power of 1 μW was used as the excitation source, whose output was coupled into the main optical unit using polarization maintaining single mode optical fiber. After the reflection at the dichroic mirror, the collimated excitation beam enters into the entrance port of the inverted microscope. Water immersion objective focuses the excitation laser beam on to the CdTe QD sample placed on the cover glass. Emission from the sample was collected by the same objective lens and directed back to the dichroic mirror, from where the fluorescence signal passed through a 430 nm long pass filter and entered into 50 μm diameter pinhole to cut off the out of focus light. Then the recollimated fluorescence signal was detected by single photon avalanche

photodiode (SPAD). The data acquisition was performed with PicoHarp 300 TCSPC module in time-tagged time-resolved (TTTR) mode.

2.7. Measurement of fluorescence quantum yield

For fluorescence quantum yield (Φ) measurements, optically matched solutions (or solutions with very similar optical density values) of the sample and the standard at a given absorbing/excitation wavelength were prepared. The value of Φ was calculated by measuring the integrated area under the emission spectra and by using the following equation,[14]

$$\emptyset_{sample} = \frac{A_{sample} \times OD_{std} \times n^2_{sample}}{A_{std} \times OD_{sample} \times n^2_{std}} \times \emptyset_{std} \qquad (1)$$

where, A is the integrated area under the emission spectrum, OD is the optical density at the excitation wavelength and n is the refractive index of the solvent. The subscripts 'sample' and 'std' refer to the sample of unknown Φ and reference sample of known Φ respectively.

4-Aminophthalimide in methanol (Φ = 0.1)[15] and coumarin 153 in acetonitrile (Φ = 0.56)[16] were used as reference compounds for the Φ measurements of organic fluorophores and QDs employed in the present studies.

2.8. Measurement of change in dipole moment on photoexcitation

The change in the dipole moment (Δμ) of the molecules on electronic excitation was estimated by following the Stokes shift ($\Delta\bar{\nu} = \bar{\nu}_a - \bar{\nu}_f$) of the fluorophore as a function of polarity (E_T^N) of the medium,[17]

$$\left(\bar{\nu}_a - \bar{\nu}_f\right) = 11307.6\{(\Delta\mu/\Delta\mu_D)^2 (a_D/a)^3\} E_T^N + \text{constant} \qquad (2)$$

where, $\bar{\nu}_a$ and $\bar{\nu}_f$ represent peak frequencies of absorption and emission maxima. $\Delta\mu$ and a denote dipole moment change and Onsager cavity radius, respectively, of the fluorophore. The Onsager cavity radii, measured using DFT calculations are 5.70 and 5.08 $\AA$ for DMAC and AC, respectively. $\Delta\mu_D$ and a_D represent the dipole moment change and the Onsager cavity radius of the betaine dye respectively.

2.9. Data analysis and construction of time-resolved emission spectra

For the fluorescence lifetime measurements, emission decay curves were analyzed by nonlinear least-squares iteration procedure using IBH DAS6 (Version 2.2) decay analysis software. This program uses a reconvolution method for the analysis of the experimental data.[18] The quality of the fit was assessed by the χ^2 values and the distribution of the residuals.

The time-resolved emission spectra (TRES) were constructed following the reported procedure.[13] The time-resolved emission decay profiles were collected at 5/10 nm intervals across the steady state emission spectrum. The wavelength selection was made by a monochromator with a band-pass of 1/4 nm. Depending upon the fluorophore, the total number of measurements was in between 30 and 46. Each decay curve was then fitted to a biexponential/triexponential decay function with an iterative reconvolution program provided by the IBH, to achieve best fits with χ^2 around 1.0 – 1.3. This fitting procedure deconvolutes the measured decay from the instrumental response to achieve effective time resolution of the experiments to ~40 ps. For the construction of TRES, the impulse response function, I(λ,t) was then calculated from the best fitted curve at each monitoring emission wavelength. To equate time-integrated intensity at each wavelength to the steady state intensity at the same wavelength, a normalization factor, H(λ), of the following form[13]

$$H(\lambda) = \frac{I_{SS}(\lambda)}{\sum_i \alpha_i(\lambda)\tau_i(\lambda)} \qquad (3)$$

was constructed, where, $I_{ss}(\lambda)$ is the steady-state fluorescence intensity, $\alpha_i(\lambda)$ and $\tau_i(\lambda)$ are the preexponential factor and fluorescence lifetime respectively, at a particular wavelength with $\sum \alpha_i(\lambda) = 1$. The TRES were constructed from the normalized intensity decay functions, I′(λ,t) for the given set of wavelengths and different times, where I′(λ,t) = H(λ) x I(λ,t). The frequencies corresponding to the emission maxima were obtained by fitting the emission profiles to a log-normal function given by the following equation,[19,20]

$$F(\bar{\nu}, t) = h \exp\{-\ln(2)[\ln(1+\alpha)/\gamma]^2\}, \quad \text{for } \alpha > -1$$

$$= 0 \quad \text{for } \alpha \leq -1$$

$$\alpha = 2\gamma\left[\bar{\nu} - \bar{\nu}_p\right]/\Delta \quad (4)$$

where, h is the peak height, $\bar{\nu}_p$ is the peak frequency, γ is the asymmetry parameter and Δ is the width of the curve. Nonlinear least squares fitting was used to obtain the best fitted curves until successive iterations gave identical χ^2 value.

2.10. Estimation of solvation time and position of the time-zero spectrum

Solvation time $(\bar{\tau}_{solv})$ was estimated by fitting the frequency of the time dependent emission maximum, $\bar{\nu}(t)$, against *t* using the following stretched exponential equation[21-23]

$$\bar{\nu}(t) = \bar{\nu}(\infty) + \Delta\bar{\nu}\exp\left(-\left(\frac{t}{\tau_0}\right)^{\beta}\right) \quad (5)$$

where, $0 < \beta \leq 1$, and

$$\bar{\tau}_{solv} = \frac{\tau_0}{\beta}\Gamma(\beta^{-1}) \quad (6)$$

where, Γ is the gamma function.

The actual time-zero spectrum was calculated following a reported procedure,[24]

$$\bar{\nu}(0)_{calc} = (\bar{\nu}_{abs}^{max})_P - \left[(\bar{\nu}_{abs}^{max})_{np} - (\bar{\nu}_{em}^{max})_{np}\right] \quad (7)$$

where, $(\bar{\nu}_{abs}^{max})_P$ represents absorption maximum of the fluorophore in polar solvent, $(\bar{\nu}_{abs}^{max})_{np}$ and $(\bar{\nu}_{em}^{max})_{np}$ represent absorption and emission maxima of the same fluorophore in non-polar solvent. In the present experiments, [bmim][PF_6] was the polar solvent and hexane was the non-polar solvent.

2.11. Estimation of size and concentration of the QDs in solution

The concentrations of the QDs in the solution were estimated following the method suggested by Yu et al.[12] Size (diameter, D nm) of the QD was estimated following the equation, which varies from QD to QD.

$$D_{CdS} = (-6.6521 \times 10^{-8})\lambda^3 + (1.9557 \times 10^{-4})\lambda^2 - (9.2352 \times 10^{-2})\lambda + (13.29)$$

$$D_{CdTe} = (9.8127 \times 10^{-7})\lambda^3 - (1.7147 \times 10^{-3})\lambda^2 + (1.0064)\lambda - (194.84)$$

$$D_{CdSe} = (1.6122 \times 10^{-9})\lambda^4 - (2.6575 \times 10^{-6})\lambda^3 + (1.6242 \times 10^{-3})\lambda^2 - (0.4277)\lambda + (41.57) \quad (8)$$

The calculated D values were well correlated with the experimental values obtained from the TEM measurements.[8,25] The D values were used to find out the molar extinction coefficients (ε) using the following relations[12]

$$\varepsilon_{CdS} = 21536(D)^{2.3}$$

$$\varepsilon_{CdTe} = 10043(D)^{2.12}$$

$$\varepsilon_{CdSe} = 5857(D)^{2.65} \quad (9)$$

The concentration (C) of the QDs in solution was then estimated using the relation,

$$C = \frac{A}{\varepsilon t} \quad (10)$$

where, A is the optical density and t is the optical path length of the solution.

2.12. Standard error limits

Standard error limits involved in the experimental results were

λ_{max} (abs./flu.)	± 1 nm
Φf	± 10%
τ_f (> 1ns)	± 5%
τ_f (< 1ns)	± 5-8% (depending on the excitation source used)
Relaxation time	± 5 – 10%
Viscosity	± 2%
QD size (D / nm)	± 5 – 10%

REFERENCES

(1) Burrell, A. K.; Sesto, R. E. D.; Baker, S. N.; McCleskey, T. M.; Baker, G. A. *Green Chem.* **2007**, *9*, 449.
(2) Xu, H.; Wolf, C. *Chem. Commun.* **2009**, 3035.
(3) Tao, X. T.; Watanabe, T.; Kono, K.; Deguchi, T.; Nakayama, M.; Miyata, S. *Chem. Mater.* **1996**, *8*, 1326.
(4) Saha, S.; Samanta, A. *J. Phys. Chem. A* **1998**, *102*, 7903.
(5) Sadhu, S.; Patra, A. *ChemPhysChem* **2008**, *9*, 2052.
(6) Wuister, S. F.; Swart, I.; Driel, F. V.; Hickey, S. G.; Donega, D. D. M. *Nano Lett.* **2003**, *3*, 503.
(7) Chen, H.-S.; Kumar, R. V. *J. Phys. Chem. C* **2009**, *113*, 12236.
(8) Santhosh, K.; Samanta, A. *J. Phys. Chem. C* **2012**, *116*, 20643.
(9) Perrin, D. D.; Armerego, W. L. F.; Perrin, D. R. *Purification of Laboratoty Cheimicals; Pergamon Press: New York*, 1980.
(10) Santhosh, K.; Banerjee, S.; Rangaraj, N.; Samanta, A. *J. Phys. Chem. B* **2010**, *114*, 1967.
(11) Cui, S.-C.; Tachikawa, T.; Fujitsuka, M.; Majima, T. *J. Phys. Chem. C* **2008**, *112*, 19625.
(12) Yu, W. W.; Qu, L.; Guo, W.; Peng, X. *Chem. Mater.* **2003**, *15*, 2854.
(13) Lakowicz, J. R. *Principles of Fluorescence Spectroscopy, 3rd edition*; Springer: New York, 2006.
(14) Austin, E.; Gouterman, M. *Bioinorg. Chem.* **1978**, *9*, 281.
(15) Soujanya, T.; Krishna, T. S. R.; Samanta, A. *J. Phys. Chem.* **1992**, *96*, 8544.
(16) Jones-II, G.; Jackson, W. R.; Choi, C.-Y.; Bergmark, W. R. *J. Phys. Chem.* **1985**, *89*, 294.
(17) Ravi, M.; Samanta, A.; Radhakrishnan, T. P. *J. Phys. Chem.* **1994**, *98*, 9133.
(18) Bevington, P. R. *Data Reduction and Analysis for the Physical Sciences*; McGraw-Hill: New York, 1969.
(19) Fraser, R. D. B.; Suzuki, E. In *Spectral Analysis*; Blackburn, J. A., Ed.; Marcel Dekker: New York, 1970.
(20) Horng, M. L.; Gardecki, J. A.; Papazyan, A.; Maroncelli, M. *J. Phys. Chem.* **1995**, *99*, 17311.
(21) Ito, N.; Arzhantsev, S.; Maroncelli, M. *Chem. Phys. Lett.* **2004**, *396*, 83.
(22) Arzhantsev, S.; Jin, H.; Baker, G. A.; Maroncelli, M. *J. Phys. Chem. B* **2007**, *111*, 4978.
(23) Jin, H.; Baker, G. A.; Arzhantsev, S.; Dong, J.; Maroncelli, M. *J. Phys. chem. B* **2007**, *111*, 7291.
(24) Fee, R. S.; Maroncelli, M. *Chem. Phys.* **1994**, *183*, 235.
(25) Santhosh, K.; Patra, S.; Soumya, S.; Khara, D. C.; Samanta, A. *ChemPhysChem* **2011**, *12*, 2735.

CHAPTER 3

Fluorescence Response and Excited State Intramolecular Electron Transfer Reaction of 4-(N,N′-Dimethylamino)benzonitrile in RTILs

Dual fluorescence of 4-(N,N′-dimethylamino)benzonitrile (DMABN) is studied in RTILs by steady state and time-resolved fluorescence techniques. Relative intensities and spectral position of the emission from locally excited (LE) and intramolecular charge transfer (ICT) states are consistent with the polarity and viscosity of the RTILs. Interestingly, exposure of the solution to the exciting radiation under very mild condition is found to influence the relative intensities of the two emission bands; an enhancement of the LE emission accompanied by a slight decrease of the ICT emission is observed. The emission intensities, however, return almost to their original values when the exposed solution is kept in the dark. The observation has been attributed to photoreaction of the exposed molecules and the recovery to replenishment of phototransformed molecules by the surrounding unexposed molecules. Fluorescence recovery after photobleaching has been studied by multiphoton confocal fluorescence microscopic technique to obtain insight into the recovery dynamics. Time-resolved emission behavior of DMABN in 1-butyl-3-methylimidazloium hexafluorophosphate, [bmim][PF_6], shows that the LE → ICT transformation rate is determined not by the slow dynamics of solvation in ionic liquid, but is controlled mainly by the rate of structural reorganization of the molecule, which accompanies the electron-transfer process in this polar viscous medium.

3.1. Introduction

RTILs, which attracted the attention of researchers worldwide for some of their unique properties, continue to generate keen interest even today for a variety of reasons.[1-7] One of the motivating factors behind this drive has been to understand some of the physical characteristics of these novel substances. Various photoinduced processes are being studied in RTILs primarily to obtain insight into the complex nature of these media and also to exploit some of their properties to control the photoprocesses of various systems.[8-23] Chapter

1 delineates the structural characterization, heterogeneity and microscopic properties of the RTILs and also covers the photoinduced processes in RTILs that have thrown insight into how the solvation, molecular rotation, diffusion etc. are influenced by the ionic constituents, polarity, viscosity and/or microheterogeneous nature of these substances.[8-14,17,21-30] These studies have also indicated that the viscous RTILs can be very different from the conventional molecular solvents. Slow solvent relaxation in RTIL and its microheterogeneous nature give rise to effects, such as the appearance of emission from unrelaxed states, usually termed as red-edge effect (REE),[9,23-25,31-33] which are not commonly observed in less viscous conventional molecular solvents.

Though many photophysical studies have been carried out to understand the microscopic properties and red edge excitation (REE) effect of the RTILs, their influence on the excited state intramolecular charge transfer reactions is remained largely unexplored. To gain knowledge over such reactions, photophysical study of DMABN (Chart 3.1) is considered in RTILs. As far as photophysical studies are concerned, DMABN is one of the most extensively studied systems, which continues to receive attention from the photophysicists for more than four decades.[34-47] The interest is generated mainly by the dual emission that this system exhibits; in particular, the nature of its second emitting state. It is generally believed that DMABN, which has a near planar geometry in the ground state,[42] on photoexcitation undergoes intramolecular charge transfer (ICT) from the dimethylamino moiety to the cyanophenyl moiety and this charge transfer process is accompanied by some structural

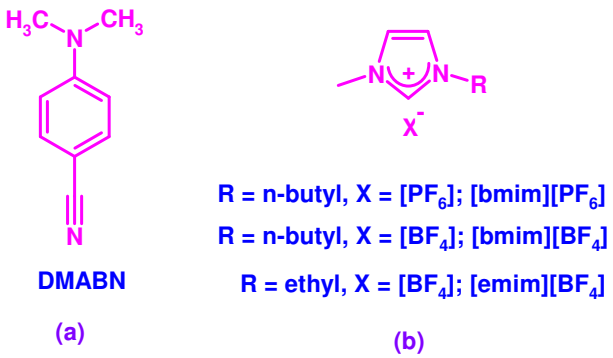

Chart 3.1. (a) Structure/Abbreviation of 4-(N,N′-dimethylamino)benzonitrile (DMABN) and (b) the RTILs employed in the present study

change around the amino nitrogen. The emission originates from the locally excited (LE) state and the ICT state of the molecule.[44,48] The nature of the structural change that accompanies the intramolecular charge transfer process in DMABN and related molecules has been a topic of intense debate,[45-47,49] but twisting around the bond connecting the -$N(Me)_2$ and cyanophenyl moieties and planarization of the amino nitrogen atom are considered as the two main possibilities.[34,44,47-49] Because of the sensitivity of the barrier to LE → ICT transformation on the polarity and viscosity of the medium,[34] we thought it might be possible to regulate or tune the fluorescence response of DMABN in RTILs by exploiting the solvent properties of these liquids. It is primarily with this intention we have taken up this work employing three RTILs of different viscosity, polarity and at different temperatures. While the expected influence of the polarity and viscosity of the RTILs was indeed observed, we could also observe interesting changes in the fluorescence behavior of DMABN with time, which is attributed to the photobleaching of DMABN under very mild condition. The fluorescence recovery after photobleaching (FRAP) of the system has been studied by multiphoton confocal fluorescence microscopic technique to obtain quantitative information on the microviscosity around the photobleached region. Though the steady-state fluorescence intensity distribution of the two emission bands of DMABN represented the combined influence of the polarity and viscosity of the medium on the excited state electron transfer reaction of DMABN, to separate the individual contributions we report picosecond time-resolved fluorescence measurements of DMABN in [bmim][PF_6] (Chart 3.1) and attempts have been made to distinguish the effects of polarity and viscosity of the medium. The results indicate that the rate of excited-state intramolecular electron-transfer reaction of DMABN in RTIL is not governed by the slow solvent-reorganization dynamics, but by the rate of structural relaxation of the molecule.

3.2. Absorption and fluorescence behavior of DMABN in RTILs

It is well-known that the imidazolium ionic liquids are not fully transparent over the entire UV region and that they also exhibit fluorescence.[50,51] This is one of the major limitations to the photophysical studies in RTILs involving molecular systems that absorb at wavelengths below 300 nm. Since the low energy absorption maximum of DMABN appears

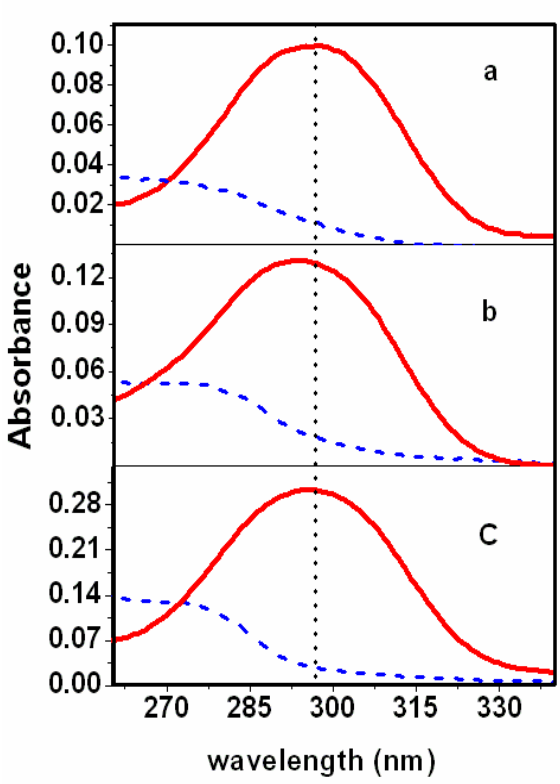

Figure 3.1. Absorption spectra of DMABN (solid line) and the RTILs (dashed line) in [bmim][PF_6] (a), [bmim][BF_4] (b) and [emim][BF_4] (c). All the spectra were recorded with air as reference.

around 295 nm, one needs to be very careful to make sure that the absorption due to the RTILs does not interfere with the measurements. For this study, we have employed "Advanced Material Research" grade RTILs from Kanto Chemicals. Even though these RTILs were not free from the problems stated above, as can be seen from the absorption spectra of the neat RTILs and freshly prepared solutions of DMABN shown in Figure 3.1, the absorbance due to these RTILs is small compared to DMABN at 295 nm, which has been used as the excitation wavelength in most of our measurements.

The top panel of Figure 3.2 compares the fluorescence of three RTILs, while the bottom panel compares the fluorescence intensities of DMABN and [bmim][PF_6] under identical experimental conditions. It is evident from this data that among the three RTILs, [bmim][PF_6] is least fluorescent and its fluorescence signal is negligible compared to the LE emission of

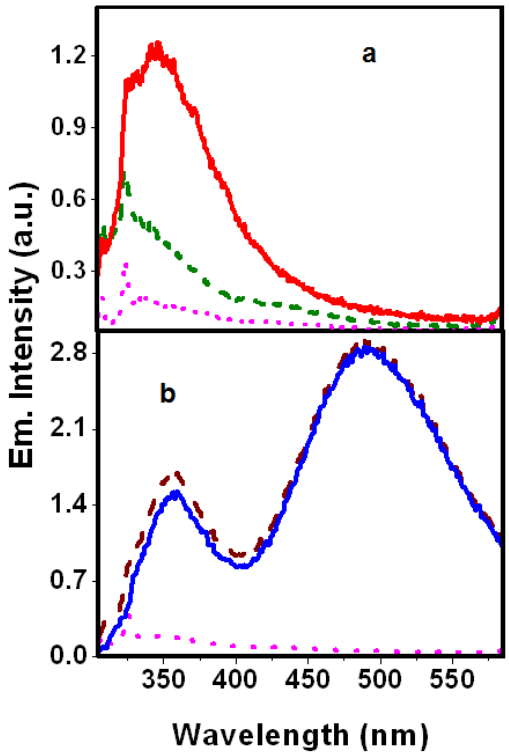

Figure 3.2. (a) Fluorescence spectra (λ_{exc} = 295 nm) of three RTILs. [bmim][PF_6] (dotted line), [bmim][BF_4] (dashed line) and [emim][BF_4] (solid line). (b) Fluorescence spectra of DMABN in [bmim][PF_6]. RTIL-fluorescence uncorrected DMABN (dashed line), RTIL-fluorescence corrected DMABN (solid line) and neat [bmim][PF_6] emission (dotted line). The spectra have been recorded with an excitation slit width of 1 nm and emission slit width of 4 nm.

DMABN. In the case of [bmim][BF_4] and [emim][BF_4], the RTIL emission is non-negligible compared to the LE emission of DMABN, and hence, it may not be possible to obtain quantitative information on the emission contribution of DMABN precisely by subtracting the emission due to RTIL. This is why we have restricted most our measurements, particularly those involving the intensity measurements, to [bmim][PF_6]. Under the present circumstances, the influence of viscosity of the RTIL on the fluorescence response of DMABN has been obtained by varying the temperature of [bmim][PF_6] instead of varying the RTILs.

Figure 3.1 shows that the wavelength corresponding to the absorption maximum does not vary significantly with change of the RTILs and the maximum is observed around 295 nm. This insensitivity of the peak position is consistent with low ground-state dipole moment (6.6 D)[45] of DMABN and small variation of the polarity ($E_T(30)$ = 52.3 – 53.7)[52] among the RTILs (Table 3.1). The emission behavior of DMABN in [bmim][PF_6] is characterized by two well-separated fluorescence bands commonly attributed to the LE and ICT states (Figure 3.2b). As stated earlier, the nature of the long-wavelength emission band of DMABN has been a matter of intense debate and various models in terms of different possible geometries of the molecule in the ICT state have been proposed.[45-48] As the precise geometry of DMABN in the ICT state is not an important consideration in the present study, we refrain from commenting on the structure of the molecule in this state and instead, refer to it simply as ICT state keeping in mind that this state is characterized by a high dipole moment (16 D)[45,53] and a molecular geometry that is substantially different from that in the ground or LE state. Since the dipole moment associated with the ICT state is much larger than that of the LE state, the ICT emission peak shows a wider variation (compared to the absorption or LE emission) even though the three RTILs provide a rather narrow range of polarity (Table 3.1). The ICT emission peak positions indicated in Table 3.1 are found to be consistent with the microscopic polarity parameter $E_T(30)$[52] of the RTILs. As far as the intensity distribution of the two emission bands is concerned, a higher intensity of the ICT emission compared to the LE emission is also in accordance with the polar nature of the RTILs.

Table 3.1. Viscosity and polarity of the RTILs and observed wavenumbers ($\bar{\nu}_{max}$) corresponding to the ICT emission peak

RTIL	Viscosity η (cP) [a]	$E_T(30)$ (kcal mol^{-1}) [b]	$\bar{\nu}_{max}$(cm^{-1})
[bmim][PF_6]	260	52.3	20410
[bmim][BF_4]	98	52.5	20000
[emim][BF_4]	34	53.7	19415

(a) Measured at 25°C. (b) Reference[52].

Table 3.2. Measured viscosities of [bmim][PF_6] and various fluorescence parameters of DMABN at different temperatures

Temperature (K)	Viscosity (η / cp)	Peak Position		I_{LE}/I_{ICT} [a]
		LE (λ_{max} / nm)	ICT (λ_{max} / nm)	
333	38	358	493	0.46
323	58	358	493	0.54
313	93	358	493	0.60
303	160	357	491	0.65
293	300	357	490	0.72
288	431	355	488	0.76
283	615	355	485	0.83
278	928	355	483	0.86
273	-	355	480	0.89
265	-	355	475	1.05

(a) I_{LE} and I_{ICT} refer to the peak emission intensities of the LE and ICT emission bands of DMABN, respectively.

3.3. Effect of temperature

The influence of viscosity (η) of the RTIL on the fluorescence behavior of DMABN has been studied by varying the temperature (T) of the system in [bmim][PF_6]. A temperature range of 278 – 333 K has been probed. This allowed investigation of the fluorescence behavior over a viscosity range of 928 – 38 cP (Table 3.2). The experimentally measured viscosities of [bmim][PF_6] at different temperatures are found to follow the Vogel Tammann Fulcher (VTF) equation (Figure 3.3)

$$ln\eta = ln\eta_0 + \frac{DT_c}{T-T_c} \quad (1)$$

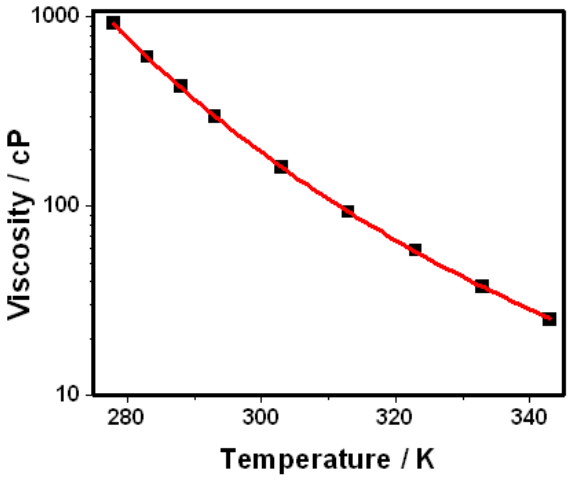

Figure 3.3. Temperature dependence of the experimentally measured viscosity values of [bmim][PF_6].

where, η is the shear viscosity at temperature T, η_0 is the reference viscosity at which the exponential term is zero, D is the fragility parameter, and T_c is a characteristic temperature for which η diverges (the fitting parameters are: D = 8.53, T_c = 153 K and ln η_0 = -3.68).

As temperature not only changes the viscosity, but can also change the polarity of the medium, we have monitored the polarity of [bmim][PF_6] at different temperatures employing a polarity sensitive probe, 4-aminophthalimide (AP), whose peak position is known to be highly sensitive to the polarity of the surrounding medium.[54] However, the fluorescence peak position of AP remains almost unchanged in the temperature range studied indicating that no significant change of the polarity of [bmim][PF_6] occurs in the temperature range of 5 – 60°C.

Figure 3.4 depicts the fluorescence behavior of DMABN in [bmim[PF_6] at different temperatures. With decrease in temperature the following changes are observed: (i) increase in the overall emission intensity, (ii) increase of the ratio of the LE/ICT emission, and (iii) blue shift of the ICT emission peak position. Quantitative information in this regard has been provided in Table 3.2. The first observation is obviously a reflection of a decrease of the nonradiative deactivation rate at lower temperatures. The second observation, that is, an increase in the relative intensity of the LE emission at lower temperature, can be explained considering the temperature dependence of the viscosity of the RTIL. As LE → ICT transformation of DMABN requires a change of its molecular structure, a higher viscosity of the RTIL at low temperature is expected to retard this transformation and hence, one can expect an enhancement of the LE emission. The third observation, that is, a blue shift of the ICT emission peak with decrease of temperature, was unexpected. As peak position of the ICT emission of DMABN is dependent on the polarity of the medium, a shift of the peak

position is expected if there is a temperature-induced change of the polarity of the medium. However, as lowering of temperature can only increase the polarity of the medium, it should have resulted in a red shift of the fluorescence maximum of DMABN whose excited state is more polar than the ground state, had there indeed been a change of the polarity of the medium. It is therefore evident that spectral shift is not due to any changed polarity of the medium.

It is to be noted that lowering of temperature increases the viscosity of the RTIL drastically (vide Table 3.2). In the present case, the viscosity of [bmim][PF_6] varies between

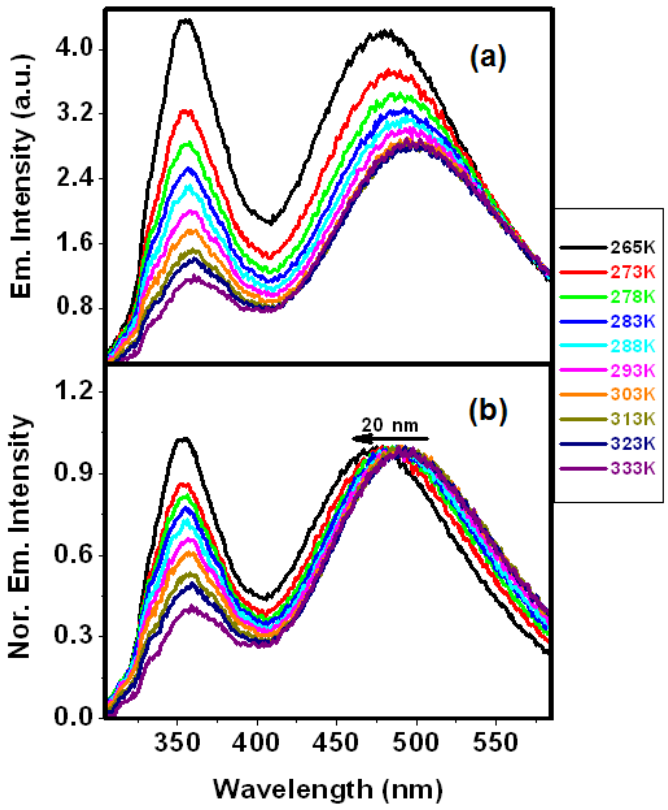

Figure 3.4. (a) Dual fluorescence of DMABN in [bmim][PF_6] (λ_{exc} = 295 nm) at different temperatures. (b) Fluorescence spectra normalized at the ICT emission peak are shown to highlight the shift of the ICT maximum. All the spectra recorded with an excitation slit width of 1 nm to ensure negligible phototransformation of the sample under the experimental condition.

38 and 928 cP when the temperature is changed from 60 to 5 °C. Therefore, the solvation time (τ_{Sol}), which is linearly related to the viscosity of the medium,[9,12] also increases appreciably at lower temperature. When the solvation time becomes higher than the fluorescence lifetime (τ_{Flu}) of the emitting state, one can expect less number of molecules to emit from the fully relaxed state and this can contribute to a gradual blue shift of the ICT emission peak with lowering of temperature. Thus, the blue shift of the ICT emission peak at lower temperature can be the result of incomplete solvation of the ICT state. We have earlier shown that the condition, $\tau_{Sol} >> \tau_{Flu}$ is realized even at room temperature in viscous RTIL for some molecules having short fluorescence lifetime.[9,12,32] In a recent work, Nagasawa et al. has observed a blue shift of the ICT emission of bianthryl with lowering of temperature,[55] which is similar to what we have observed here with DMABN. Since the solvation time in [bmim][PF_6] at different temperatures is available in this work, we can verify whether the $\tau_{Sol} >> \tau_{Flu}$ condition is indeed met with at lower temperatures. While the fluorescence lifetime of the ICT state of DMABN remains almost constant at around 2.5 – 2.6 ns in the temperature range studied, the solvation times in [bmim][PF_6] at 333, 313, 293, 273, and 253 K are reported to be 1.29, 1.45, 2.83, 7.96, and 22.5 ns, respectively.[55] It is thus evident that the ICT state of DMABN is fully solvated at around room temperature, but at lower temperature complete solvation of the emitting state is not possible. Hence, the blue shift of the ICT emission peak of DMABN on lowering of temperature is indeed a consequence of incomplete solvation in viscous solution.

3.4. Excitation wavelength dependence

In conventional molecular solvents, the emission behavior of DMABN is not dependent on the excitation wavelength. However, as the RTILs are microheterogeneous media comprising both hydrophobic and hydrophilic domains,[24,31,33] it is possible for DMABN molecules to experience multiple molecular environments and to exhibit an excitation wavelength behavior. With this idea, we have studied the excitation wavelength dependence of the emission behavior of DMABN in RTILs and the results obtained in [bmim][PF_6], are shown in Figure 3.5. It can be seen with increase in the excitation wavelength from 280 to 310 nm that the ICT emission intensity increases relative to the LE emission. Assuming that the molecular geometry of DMABN in RTILs is not very different from that in conventional

molecular solvents, the excitation wavelength dependence can be explained taking into account the microheterogeneous nature of the RTILs, wherein the DMABN molecules are distributed in several possible environments having different polarities. With increase in the excitation wavelength, DMABN molecules, which lie in more polar environment are preferentially excited. Since for molecules that lie in a more polar environment, the barrier to LE → ICT transformation is lower, an increase of the excitation wavelength results in an enhancement of the ICT emission.

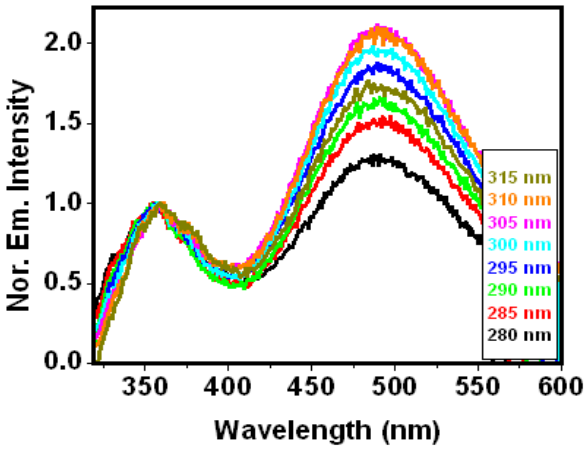

Figure 3.5. Fluorescence spectra of DMABN in [bmim][PF_6] for excitation wavelengths of 280 to 315 nm. The spectra have been normalized at LE peak position and corrected for the fluorescence of [bmim][PF_6]. Excitation slit width of 1 nm was employed to avoid any decomposition of the sample during the measurements.

3.5. Dependence on exposure time

Interestingly, during the course of this study we found that when a freshly prepared DMABN solution is unknowingly exposed to the exciting light in the sample compartment, there occurs a change in the relative intensities of the LE and CT emission. The LE emission is found to gain in intensity at the expense of the ICT emission. The time-dependent change of the intensities of the two emission bands is illustrated in Figure 3.6. That these changes are induced by the exciting photons in the sample compartment is evident from the fact that an increase of the excitation slit width leads to a faster change of the emission profiles and helps quicker attainment of the steady state intensities. We have also observed that when the exposed solution is kept in the dark for a long period (ranging from several minutes to hours depending on the viscosity of the RTIL), the fluorescence profile almost returns to that recorded for a freshly prepared solution (Figure 3.6).

3.5.1. Possible explanations

The fluorescence behavior of DMABN is being studied for over four decades and as stated already, the focus of these studies has been dual fluorescence, geometry of the molecule in the ICT state and factors that influence the LE → ICT transformation.[40,56-58] Photoreactivity of DMABN has rarely been a subject matter of investigation, and apart from a very recent study[59] one can hardly find literature on this topic. Since photodegradation of DMABN is not a matter of concern under normal irradiation conditions, we thought that RTILs could be responsible for the observation.

As the emission due to [bmim][PF_6], which overlaps with the LE emission of DMABN, is negligible (Figure 3.2b) and exposure to light leads to a slight decrease of this intensity, it is evident that weak fluorescence of RTIL is not responsible for the variation of the fluorescence intensities of the two bands.

That the observed changes also are not due to photoinduced heating and consequent change in the viscosity of the RTILs is evident from the fact that heating would have decreased the viscosity and facilitated the LE → ICT transformation. This would have led to

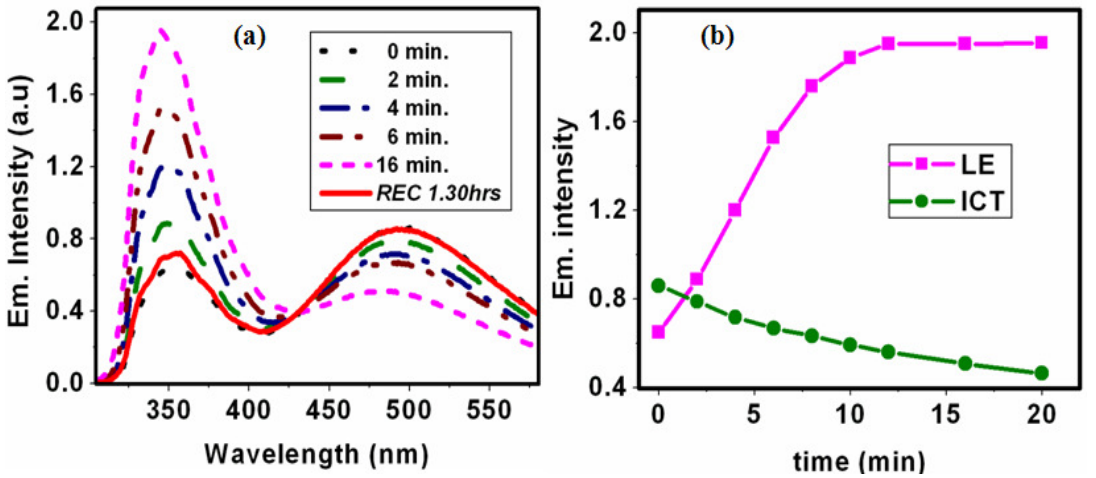

Figure 3.6. (a) Change of the fluorescence spectra of DMABN in [bmim][PF_6] with increasing exposure time to 295 nm radiation in the fluorimeter. An excitation slit-width of 5 nm was employed. The recovered fluorescence spectrum recorded after keeping the sample in the dark for 1.30 hrs is also indicated with an "REC" label. Panel (b) shows the time profiles at two selected regions.

a decrease of the LE emission intensity. Moreover, the possibility of viscosity change is ruled out as the fluorescence response of well-known microviscosity probe, 9-(dicyanovinyl)julolidine (DCVJ),[11] whose fluorescence efficiency is sensitive to the viscosity of the medium, remained unchanged under our experimental conditions.

As RTIL is not responsible for the variation of the emission intensities, the observation has to be attributed to phototransformation of DMABN even though the exposure of the solution to the exciting light was minimal. We note in this context that even though DMABN has been studied very intensely for more than four decades and photoproduct formation of DMABN in polar solvents was reported long ago,[36] there is hardly any literature addressing this issue until very recently.[59] In this recent work, Druzhinin et al. have shown that photoexcitation of DMABN in polar solvents leads to the formation of 4-(methylamino)benzonitrile (MABN). The yield of this reaction varies between 0.0018 and 0.0023 depending on the solvent. They showed that the emission due to the photoproduct, MABN, overlaps with the LE emission of DMABN. As MABN fluorescence is much stronger than the LE emission of DMABN, formation of even a very small amount of the photoproduct leads to fluorescence enhancement in this region.[59] On the basis of this literature, we attribute the change in the fluorescence behavior of DMABN in RTILs to the formation of trace amount of MABN. The signature of photoreaction of DMABN is also evident from the absorption spectra of irradiated solutions of DMABN (Figure 3.7). Even though these changes are small, the observation of an isosbestic point around 280 nm unambiguously establishes that even under very mild conditions DMABN undergoes photor-

Figure 3.7. Absorption spectra of DMABN in [bmim][PF_6] measured at different times following its irradiation (λ_{exc} = 295 nm) inside the fluorimeter.

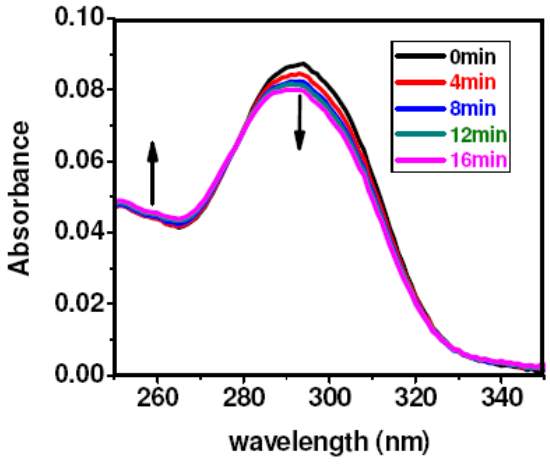

eaction. An increase of lifetime of the LE emission (from 0.24 to 1.12 ns) on irradiation is also consistent with the photoreaction of DMABN.[59]

Interestingly, unlike Druzhinin et al. who observed a steady emission enhancement near the LE region on photoirradiation of DMABN,[59] Figure 3.6 shows that in RTILs the emission intensities not only reach a steady state, but they also return almost to their original values when the exposed solution is kept in the dark for some time (which depends on the viscosity of the RTILs). As phototransformation is commonly an irreversible process, the return to the original state is unexpected.

These apparent inconsistencies can be resolved by considering highly viscous nature of the RTILs and the fact that fluorescence recovery is not strictly 100%. When a very small volume of the DMABN sample is exposed to light, only few molecules from this region are photobleached and the surrounding region comprises the unbleached molecules. In less viscous conventional solvents, because of rapid molecular motion the photobleached molecules are continuously replaced by the unbleached molecules and the photoreaction continues. In other words, even though a small volume of the solution is exposed to light and the photochemical reaction is only restricted to this region, the composition of the entire solution becomes uniform very quickly due to rapid molecular diffusion. Moreover, as the photobleached region is rapidly supplemented by unreacted molecules, photobleaching continues until all the molecules in the entire solution are depleted, a state not easily reached under mild photoirradiation conditions. This is why the fluorescence intensities keep on changing with photoirradiation in conventional solvents such as acetonitrile.[59] Since it takes much longer time in RTILs for the photobleached molecules of the exposed region to be replaced by the unbleached molecules because of slow molecular diffusion in these media, one soon attains a steady state when further irradiation becomes ineffective. This explains why a steady state is reached quickly in RTILs, a situation not easily attained in less viscous solvents. Since the exposure is highly localized to a small region in RTILs and only a few molecules from this region are photobleached leaving a large majority of molecules intact, when kept under dark for some time most of the photobleached molecules are replaced by unbleached molecules making the system appear as if it has returned to the original state. This concept is commonly termed as “Fluorescence Recovery After Photobleaching (FRAP)”

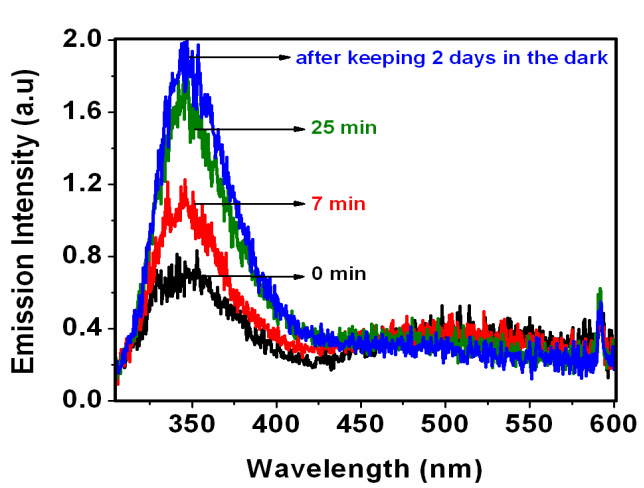

Figure 3.8. Fluorescence spectra of a tetraethylene glycol solution of DMABN following its exposure to short ultraviolet radiation (254 nm) for different times (0 – 25 min). The fluorescence spectra are measured using an exc. slit width of 0.5 nm to avoid any photodecomposition while recording the spectra.

and is found to be quite useful in biological studies of cell membrane diffusion, protein binding, and so forth.[60-62]

To ensure that it is the high viscosity of the medium and not the ionic constituents of the RTILs responsible for the effect, we have also studied the controlled photoirradiation experiment in two conventional viscous solvents, tetraethylene glycol (η = 48 cP) and glycerol (η = 950 cP). A very similar photoinduced change of the emission intensities and fluorescence recovery in the dark in these two media confirm that the ionic constituents of the RTILs play no role in the photoproduct formation.

Additional support in favor of the interpretation for the recovery of the fluorescence intensity of DMABN in terms of the FRAP concept is obtained by the following experiment. When the entire tetraethylene glycol solution (3 mL, taken in a quartz cuvette) is exposed to short-wave ultraviolet radiation (254 nm) of a SPECTROLINE lamp (model ENF-280C/FE), the LE region intensity increases at the cost of the ICT emission continuously with increasing exposure time. However, as the entire solution has been exposed to the short wave ultraviolet radiation this time, no recovery of the original fluorescence intensity could be observed even after keeping two days in the dark (Figure 3.8).

3.6. FRAP study

The most convincing evidence of FRAP is obtained from studies based on multiphoton confocal fluoresnce microscopy technique. These studies also enabled us to follow the diffusion of DMABN molecules with time and to determine the diffusion coefficient. A few microlitres (typically, 5 μL) of a micromolar solution of DMABN in [bmim][PF_6] was sandwiched between a clean glass slide and a coverslip and used for photobleaching and

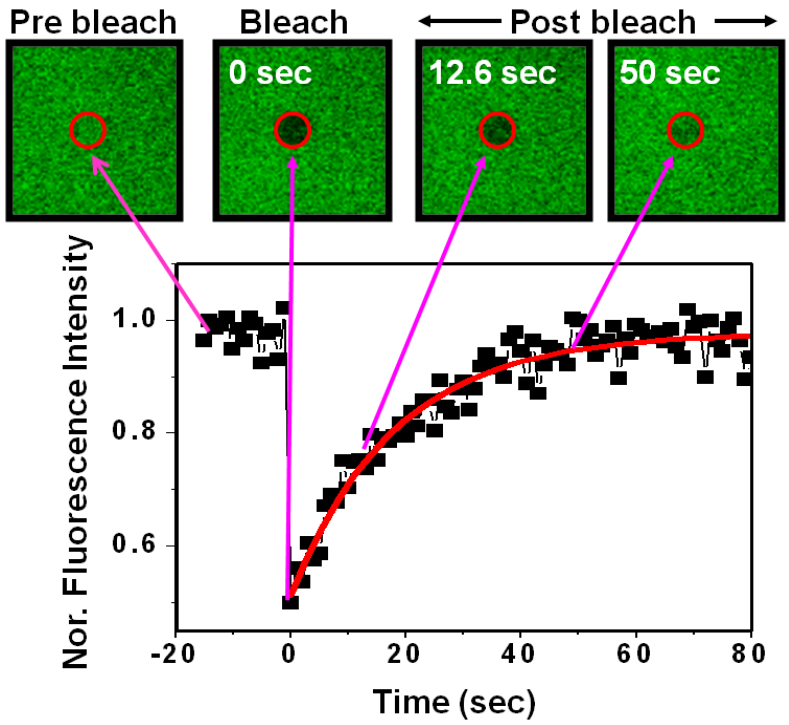

Figure 3.9. Top panel shows the fluorescence images of DMABN in [bmim][PF_6], collected using a multiphoton confocal microscope (λ_{exc} = 730 nm, λ_{em} = 505 – 570 nm). Images were acquired before bleach (pre bleach), immediately after bleach (bleach), and after fluorescence recovery (post bleach). The bottom panel represents the recovery of the normalized fluorescence within the circular ROI as a function of time. Solid line represents the exponential fit to the recovery data. In the top panel, the circular region represents the bleached spot. The mean fluorescence intensity in the circular region, as depicted in the plot of the bottom panel, is normalized to the prebleach intensity outside this region.

FRAP analysis.

As described in the experimental section (chapter 2), FRAP experiment was performed by scanning a square region of interest (ROI) of length 43.0 µm and bleaching a circular region of interest (ROI) of radius 4.30 µm. After photobleaching, the diffusion characteristics of DMABN in [bmim][PF_6] was monitored by acquiring sequence of images by probing the fluorescence signal using a 505 – 570 nm band-pass filter. Figure 3.9 represents the fluorescence recovery plot of DMABN in [bmim][PF_6] after bleaching. Prebleach, bleach, and postbleach images are also shown.

Data representing the mean fluorescence intensity recovered in the bleached circular ROI with time was analyzed by fitting to the following equation

$$I(t) = I_0 - I_1 \exp(-t/\tau_D) \qquad (2)$$

where *I(t)* is the normalized mean fluorescence intensity at time "t" in the bleached ROI, I_0 is the recovered fluorescence at infinite time (t=∞), I_1 is the mobile fraction and τ_D is the average diffusion time of DMABN in [bmim][PF_6]. The time-dependence of the recovery of fluorescence and the fit to the data are shown in Figure 3.9. The τ_D value estimated from the fit is 18.2 s.

The diffusion coefficient is calculated using the relation[61,63]

$$D = \omega^2/4\tau_D \qquad (3)$$

where ω is the radius of the bleached circular ROI (ω = 4.30 µm). The diffusion coefficient, *D*, is calculated to be 2.5×10^{-13} m^2 /s.

The diffusion coefficient as given by the Stokes-Einstein relation is

$$D = kT/6\pi\eta r \qquad (4)$$

where, *k* is the Boltzmann constant, *T* is the temperature, η is the viscosity of the medium, and *r* is the radius of the molecule assuming it to be spherical. Using an η value of 285 cP for [bmim][PF_6] at 295 K and *r* as 4.34 A°,[64] the diffusion coefficient predicted by this equation is 1.75×10^{-12} m^2/s. This value is higher than that obtained from the FRAP experiment by a factor of 7. This difference can only be explained when the microviscosity around the probe

molecule is different from the bulk viscosity of the medium. Therefore, the FRAP study, in addition to providing a quantitative estimate of the viscosity around DMABN, reconfirms the microheterogeneous nature of the RTILs, which is already indicated in several other theoretical and experimental studies.[9,23,24,31-33,65-68]

3.7. Time-resolved fluorescence behavior of DMABN in [bmim][PF_6]

Interestingly, although the steady-state fluorescence measurements including temperature dependent and excitation wavelength fluorescence spectra show the influence of both polarity and viscosity of the RTILs on the excited state intramolecular electron transfer reaction of DMABN, these results do not provide information about the effect of solvation on the rate of LE → ICT transformation. As solvation dynamics in RTILs is a slow process, the electron-transfer reaction of DMABN in these media can occur from the LE state prior to its solvation or during/after the solvation. The former is a distinct possibility when the inherent electron-transfer rate is high. In this situation, the solvation in the RTIL, a large part of which is governed by its viscosity, will not influence the rate of excited state LE → ICT transformation. However, if the ICT state is formed during/after the solvation of the LE state, the viscosity of the medium will influence the rate of the reaction as the transformation involves solvation and the dynamics of solvation in the RTIL is dependent on the viscosity. Hence, a study of the LE → ICT dynamics, in particular, a comparison of the time scales of

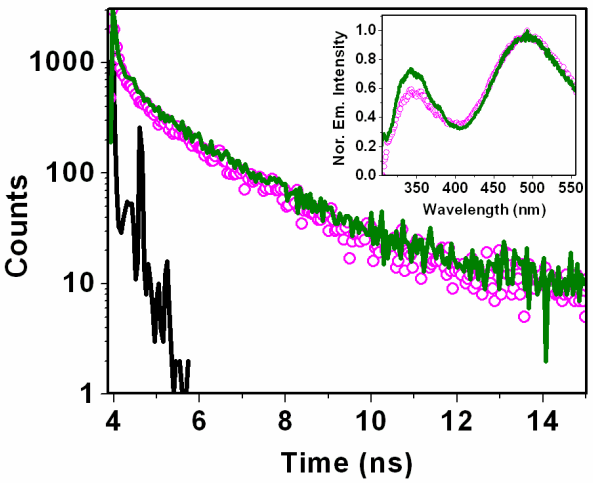

Figure 3.10. Fluorescence decay profiles and emission spectra of DMABN in [bmim][PF_6] RTIL before (circles) and after (solid line) the time-resolved fluorescence experiments.

the solvation of the LE state and excited-state reaction should give an insight into the mechanism of the ICT process of DMABN in RTILs. Therefore, we studied the time-dependence of LE and ICT emission bands of DMABN in [bmim][PF_6] by measuring the fluorescence-decay profiles at every 5/10 nm interval across the entire steady-state emission spectrum as explained in the chapter 2. In this context it is important to note that the excitation intensity used for the time-resolved fluorescence experiments is very less that did not cause any phototransformation of DMAN, which is also evident from the unaffected emission spectrum and intensity decay profile before and after the experiment (Figure 3.10, both steady state and time-resolved emission measurements were carried out at λ_{exc} = 280 nm and slit width of 1 nm was employed for the steady state emission spectral measurements and emission was monitored at LE emission maximum, 350 nm, for fluorescence decay profiles).

The fluorescence decay profiles collected at different emission wavelengths are shown in Figure 3.11. The time profiles at shorter emission wavelengths show faster decay and the decay time increases with the increase in monitoring wavelength. For emission wavelengths corresponding to the ICT emission (i.e. λ_{em}>500 nm), the time profiles are characterized by a rise followed by the decay. The rise at longer emitting wavelengths is indicative of a slow excited-state process, which in this case, can be representative of slow dynamics of solvation or structural change associated with LE → ICT transformation. It can also be due to both processes. If the latter is indeed the case, then it is hard to separate the time scales of the excited-state electron-transfer reaction and the process of solvation. The time-resolved emiss-

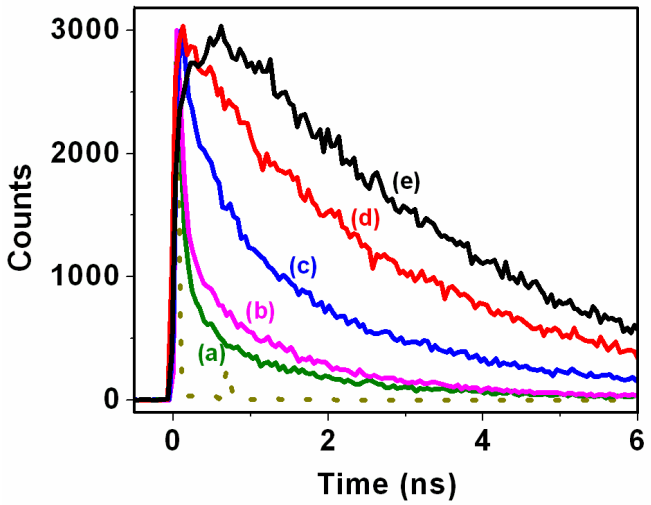

Figure 3.11. Emission wavelength dependent fluorescence decay profiles of DMABN in [bmim][PF_6]. The monitoring wavelengths are (a) 350, (b) 380, (c) 450, (d) 500 and (e) 560 nm. λ_{exc} = 280 nm. Lamp profile is shown as dotted line.

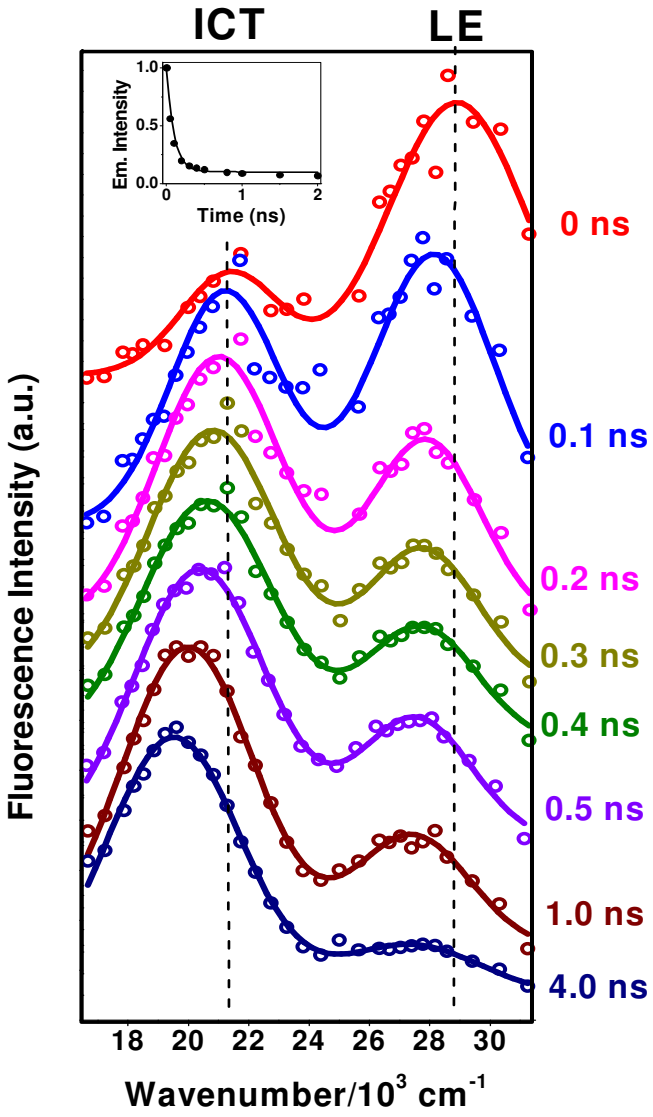

Scheme 3.12. TRES of DMABN in [bmim][PF_6] measured at different time delays. The vertical lines are used to indicate the shift of the emission maxima of LE and ICT states due to solvation. The inset shows the intensity monitored at 30,250 cm^{-1} as a function of time. λ_{exc} = 280 nm.

ion spectra (TRES) of DMABN, constructed from the fluorescence-decay profiles, in which the time evolution of the ICT emission is following the photo-excitation of DMABN, are

depicted in Figure 3.12. The emission intensity of the ICT state gradually builds up and that of the LE state decreases with time. A time-dependent Stokes shift of both the LE and ICT emission maxima, which is suggestive of slow solvation of the two states, is also observable. The fact that the ICT state exhibits a more pronounced Stokes shift compared to the LE state is due to the larger dipole moment of the ICT state.[45,53,69] Though slow solvation of the LE state is evident from the time-dependent shift of the spectral maximum, the solvation time of this state in [bmim][PF_6] could not be precisely estimated from the data, due to the short fluorescence lifetime of the LE state and its parallel participation in the excited state electron transfer reaction. However, as shown in Figure 3.13a, the frequencies corresponding to the ICT emission maxima, which were used for the estimation of solvation time, were obtained by fitting the emission profiles to a log-normal function[70] (see chapter 2 for the details). The time constant of solvation time, which can be described by the normalized spectral-shift correlation function, C(t), is estimated from the peak frequencies of the time-resolved ICT emission spectra using the following equation,

$$C(t) = [\bar{\nu}(t) - \bar{\nu}(\infty)]/[\bar{\nu}(0) - \bar{\nu}(\infty)] \qquad (5)$$

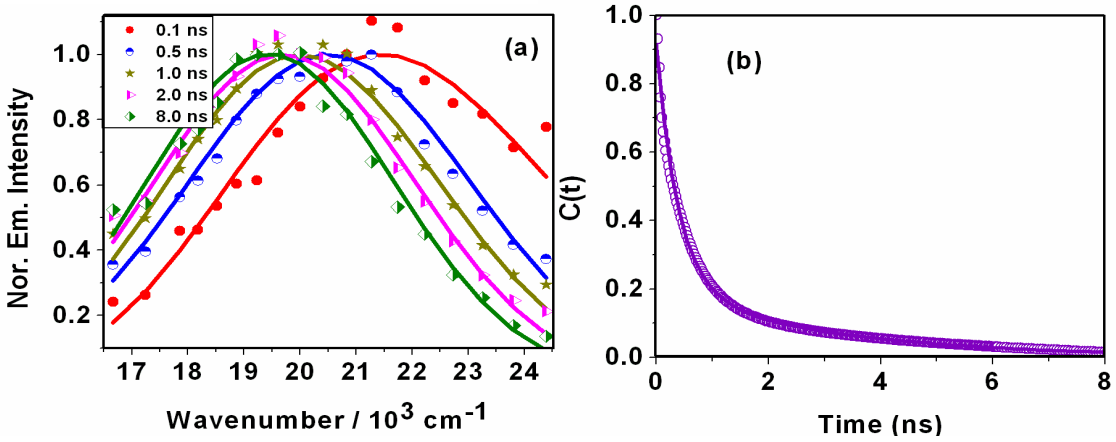

Figure 3.13. (a) TRES of the ICT state of DMABN in [bmim][PF_6] measured at different time delays. The data points are shown along with the lognormal fits. All spectra are normalized at the corresponding peak maximum. λ_{exc} = 280 nm. (b) Decay of the spectral shift correlation function, C(t), of the ICT emission of DMABN in [bmim][PF_6]. The solid line denotes the biexponential fit to the data.

where, $\bar{\nu}(t), \bar{\nu}(\infty)$ and $\bar{\nu}(0)$ are the peak frequencies of ICT emission maxima at times *t*, ∞ and 0, respectively. A biexponential fit (Figure 3.13b) to the time dependence of C(t) provides a solvation time of 980 ps. It is interesting to note that even though DMABN is not the right probe molecule for the measurement of the solvation time (due to multiple excited-state processes contributing to its fluorescence behavior), the dynamic-fluorescence Stokes shift of the ICT emission of this molecule yields a number that is not very different from the solvation time estimated using other probes (1 to 1.8 ns) in [bmim][PF_6].[71]

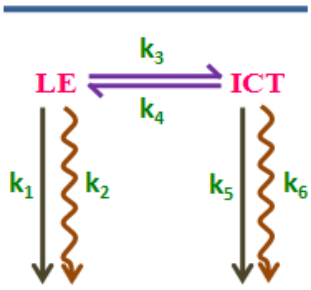

Scheme 3.1.

In conventional less viscous molecular solvents, the excited-state kinetics of DMABN is described by the model depicted in Scheme 3.1,[38,59,72] which assumes attainment of equilibrium in the excited state.

According to this model, the time profiles of the two states, which are given by Equations (6) and (7), show that the two decay times associated with both LE and ICT states are identical

$$[LE] = a_1 \exp\left(-t/\tau_1\right) + a_2 \exp\left(-t/\tau_2\right) \quad (6)$$

$$[ICT] = a_3 \exp\left(-t/\tau_1\right) - a_3 \exp\left(-t/\tau_2\right) \quad (7)$$

Using this reaction scheme, the LE → ICT reaction time of DMABN, which can be determined from one of the decay times of the LE state or from the rise time of the ICT state (both being identical), is estimated to be 4 ps in acetonitrile.[38] As this reaction time is much slower than the solvation time in acetonitrile (200 fs), the effect of solvation on the reaction rate of DMABN is negligible in conventional solvents. However, as solvation is a much slower process in viscous RTILs, the rise time of the ICT state from which the reaction time in conventional solvents is commonly estimated, may actually represent the dynamics of solvation rather than the intrinsic rate of the excited state reaction. It may also indicate the combined influence of both the solvation and reaction times. Moreover, in less viscous conventional solvents, the fluorescence time profiles, in particular, the rise time corresponding to the ICT emission is constant and independent of the monitoring wavelength. However, in [bmim][PF_6] , due to the slow nature of the solvation, the rise time

varies continuously with the monitoring wavelength, thus making it impossible to determine the reaction time from it.

For this reason, we estimated the reaction time from the decay of the LE emission intensity at ~30,250 cm^{-1}. A fitting of this data to $I(t) = I_0 + I_1 \exp(-t/\tau_r)$, where I(t) and I_0 are the intensities at times t and ∞, I_1 is the fraction of the excited-state reaction and τ_r represents the excited-state LE → ICT transformation time, yielded an approximate excited-state reaction time of 100 ps (inset of Figure 3.12). It is evident from the TRES in Figure 3.12 that even at time zero, the ICT emission intensity is non-zero, implying that there is a component of the reaction which is fast. The TRES also suggest that the reaction is almost completed within ~300 ps, beyond which no significant build up of the ICT emission intensity is observable (Figure 3.12). It is interesting to note that even the slow component of the reaction is much faster than the average solvation time (≈ 1 ns) in [bmim][PF_6] . Hence, as in conventional solvents, the rate of LE → ICT transformation of DMABN in RTIL is not governed by the dynamics of solvation.

Similar to that in acetonitrile, one would expect an equally fast (≈ 4 ps) electron-transfer of DMABN in [bmim][PF_6] , if only the polarity of the RTIL influences the excited state reaction. Emission spectra at different time delays (Figure 3.12) show that the evolution of the ICT state from the LE state takes much longer time than in acetonitrile, reflecting the viscosity effect of [bmim][PF_6] on the rate of the excited-state reaction.

It is well known that even though the solvation dynamics in RTILs is a slow process, the solvation has an ultrafast component as well, which can be as large as 50% of the total solvent relaxation.[8,9,12,73,74] It is believed that the slow component of the solvent reorganization is due to the long-range collective anion–cation diffusive motion, whereas the fast component of the dynamics, which is in the sub-picosecond time scale, is due to motions in the close proximity of the probe molecule. There are systems in which the rate of electron transfer reaction is mainly determined by the fast component of the solvation process. The excited-state electron transfer-reaction of 9,9'-bianthryl in RTILs proceeds with different rates and the average rate of the electron-transfer reaction is reported to be much faster than the average solvation time of the RTILs.[17] Theoretical calculations of Shim and Kim, which support this suggestion, indicate that for the adiabatic electron-transfer reactions in RTILs,

the dynamical friction acting on the barrier crossing is not affected by the slow solvation dynamics, but is mostly determined by the fast solvation dynamics.[75] Solvation independent excited state reactions are not restricted to the electron-transfer reactions, but are observed in the case of excited state intramolecular proton-transfer reactions as well. It has been shown recently that the excited state intramolecular proton-transfer reaction of 4'-N,N-diethylamino-3-hydroxyflavone (DEAHF) is partially coupled with the solvation surface of the excited state and the average excited state intramolecular proton-transfer time is much faster than the full solvation time.[76]

In the case of DMABN, as the average solvation time in [bmim][PF_6] is much larger than the measured reaction time, it can be said confidently that the slow component of the solvation dynamics in RTIL does not play any role in the LE → ICT transformation. However, the influence of the fast component of the dynamics, if any, cannot be ignored. The slowness of the excited-state reaction time of DMABN in [bmim][PF_6] compared to less viscous molecular solvents is thus mainly due to slow structural rearrangement of the molecule in this viscous medium that accompanies the LE → ICT transformation.

3.8. Conclusion

Fluorescence behavior of DMABN is studied in RTILs. At lower temperature, when the solvation time is comparable or higher than the fluorescence lifetime of the ICT state of DMABN, unrelaxed emission from the incompletely solvated state of the molecule is observed. The microheterogeneity of the media also gives rise to an excitation wavelength dependent fluorescence response of the system. We have found that photobleaching of DMABN under mild excitation conditions leads to a time-dependent change of the fluorescence response of the system. Interesting difference of the consequence of the photolysis of DMABN in conventional solvents and highly viscous RTILs is revealed in this study. The observation of a photoirradiated stationary state and near-reversibility of the process are shown to be two most interesting consequences of the high viscosity of the RTILs. The results indicate how a seemingly unimportant process can become highly important in RTILs simply because of the localization (confinement) effect due to the high viscosity of these liquids. Multiphoton confocal fluorescence microscopy study of the

photobleaching and recovery dynamics of DMABN have allowed the estimation of the diffusion coefficient of the molecule in [bmim][PF_6] RTIL. The finding, which indicates that the microviscosity around DMABN in [bmim][PF_6] be quite different from the bulk viscosity of the medium, is the first of its kind obtained from a FRAP experiment in RTILs.

Time-resolved emission behavior of DMABN in [bmim][PF_6] is studied with a view to obtain insight into the nature of the excited state intramolecular electron transfer reaction in viscous ionic liquids. It is found that the rate of LE → ICT transformation of DMABN in [bmim][PF_6] is much slower than in isopolar, but less viscous conventional solvents. It is shown that this slowness of the reaction in highly viscous medium does not arise from the slow dynamics of the solvent reorganization in the RTIL, but is due to the viscosity dependence of the intramolecular structural rearrangement process that accompanies the transformation. Even though no influence of the viscosity dependent component of the solvation dynamics is observed, one cannot completely rule out possible influence of the ultrafast component of the solvation dynamics on the electron transfer process.

REFERENCES

(1) Seddon, K. R. *Ionic Liquids, Industrial Applications for Green Chemistry*; American Chemical Society: Washington DC, 2002.

(2) Ohno, H.; Fukumoto, K. *Acc. Chem. Res.* **2007**, *40*, 1122.

(3) Wasserscheid, P.; Welton, T. *Ionic Liquids in Synthesis*; Wiley-VCH: Weinheim, 2003.

(4) Brinchi, L.; Germani, R.; Savelli, G. *Tetrahedron Lett.* **2003**, *44*, 2027.

(5) Pringle, J. M.; Golding, J.; Baranyai, K.; Forsyth, C. M.; Deacon, G. B.; Scott, J. L.; McFarlane, D. R. *New J. Chem.* **2003**, *27*, 1504.

(6) Yuanyuan, Z.; Xiang, C.; Jingbo, L.; Jingsong, Y.; Lijuan, C. *Chem. Biol. and Drug Design* **2009**, *74*, 282.

(7) Zhen, Y.; Wubin, P. *Enzyme and microbiol. tech.* **2005**, *37*, 19.

(8) Samanta, A. *J. Phys. Chem. Lett.* **2010**, *1*, 1557.

(9) Samanta, A. *J. Phys. Chem. B* **2006**, *110*, 13704.

(10) Bhattacharya, B.; Samanta, A. *J. Phys. Chem. B* **2008**, *112*, 10101.

(11) Paul, A.; Samanta, A. *J. Phys. Chem. B* **2008**, *112*, 16626.

(12) Mandal, P. K.; Saha, S.; Karmakar, R.; Samanta, A. *Current Science* **2006**, *90*, 301.

(13) Karmakar, R.; Samanta, A. *J. Phys. Chem. A* **2002**, *106*, 4447.

(14) Karmakar, R.; Samanta, A. *Chem. Phys. Lett.* **2003**, *376*, 638.

(15) Mandal, P. K.; Samanta, A. *J. Phys. Chem. B* **2005**, *109*, 15172.

(16) Aki, S. N. V. K.; Brennecke, J. F.; Samanta, A. *Chem. Commun.* **2001**, 413.

(17) Nagasawa, Y.; Itoh, T.; Yasuda, M.; Ishibashi, Y.; Ito, S.; Miyasaka, H. *J. Phys. Chem. B* **2008**, *112*, 15758.

(18) Chakrabarty, D.; Hazra, P.; Chakraborty, A.; Seth, D.; Sarkar, N. *Che. Phys. Lett.* **2003**, *381*, 697.

(19) Adhikari, A.; Sahu, K.; Dey, S.; Ghosh, S.; Mandal, U.; Bhattacharyya, K. *J. Phys. Chem. B* **2007**, *111*, 12809.

(20) Fukuda, M.; Terazima, M.; Kimura, Y. *Chem. Phys. Lett.* **2008**, *463*, 364.

(21) Iwata, K.; Kakita, M.; Hamaguchi, H.-o. *J. Phys. Chem. B* **2007**, *111*, 4914.

(22) Jin, H.; Baker, G. A.; Arzhantsev, S.; Dong, J.; Maroncelli, M. *J. Phys. Chem. B* **2007**, *111*, 7291.

(23) Jin, H.; Li, X.; Maroncelli, M. *J. Phys. Chem. B* **2007**, *111*, 13473.

(24) Lopes, J. N. C.; Pauda, A. A. H. *J. Phys. Chem. B* **2006**, *110*, 3330.

(25) Hu, Z.; Margulis, C. J. *Proc. Natl. Acad. Sci. U. S. A* **2006**, *103*, 831.

(26) Sarkar, S.; Pramanik, R.; Ghatak, C.; Rao, V. G.; Sarkar, N. *Chem. Phys. Lett.* **2011**, *506*, 211.

(27) Guo, J.; Baker, G. A.; Hillesheim, P. C.; Dai, S.; Shaw, R. W.; Mahurin, S. M. *Phys. Chem. Chem. Phys.* **2011**, *13*, 12395.

(28) Sasmal, D. K.; Mandal, A. K.; Mondal, T.; Bhattacharyya, K. *J. Phys. Chem. B* **2011**, *115*, 7781.

(29) Mali, K. S.; Dutt, G. B.; Mukherjee, T. *J. Chem. Phys.* **2008**, *128*, 124515.

(30) Wu, H.; Wang, H.; Xue, L.; Shi, Y.; Li, X. *J. Phys. Chem. B* **2010**, *114*, 14420.

(31) Mandal, P. K.; Sarkar, M.; Samanta, A. *J. Phys. Chem. A* **2004**, *108*, 9048.

(32) Mandal, P. K.; Paul, A.; Samanta, A. *Journal of Photochemistry and Photobiology A: Chemistry* **2006**, *182*, 113.

(33) Wang, Y.; Voth, G. A. *J. Am. Chem. Soc.* **2005**, *127*, 12192.

(34) Grabowski, Z. R.; Rotkiewicz, K.; Rettig, W. *Chem. Rev.* **2003**, *103*, 3899.

(35) Bhattacharyya, K.; Chowdhury, M. *Chem. Rev.* **1993**, *93*, 507.

(36) Lippert, E.; Luder, W.; Moll, F.; Nagele, W.; Boss, H.; Prigge, H.; Blankenstein, I. S. *Angew. Chem.* **1961**, *73*, 695.
(37) Dahl, K.; Biswas, R.; Ito, N.; Maroncelli, M. *J. Phys. Chem. B* **2005**, *109*, 1563.
(38) Druzhinin, S. I.; Ernsting, N. P.; Kovalenko, S. A.; Lustres, L. P.; Senyushkina, T. A.; Zachariasse, K. A. *J. Phys. Chem. A* **2006**, *110*, 2955.
(39) Gomez, I.; Reguero, M.; Boggio-Pasqua, M.; Robb, M. A. *J. Am. Chem. Soc.* **2005**, *127*, 7119.
(40) Samanta, A. *Resonance* **2007**, *12*, 79.
(41) Silvia, C.; Antonino, P.; Camilla, F.; Caterina, B.; Vincenzo, B. *J. Phys. Chem. B* **2008**, *112*, 8106.
(42) Kuhnle, W.; Zachariasse, K. A. *Acta Crystallographica, sec B:structural science* **1994**, *B50*, 363.
(43) Minezawa, N.; Kato, S. *J. Phys. Chem. A* **2005**, *109*, 5445.
(44) Rotkiewicz, K.; Grellmann, K. H.; Grabowski, Z. R. *Chem. Phys. Lett.* **1973**, *19*, 315.
(45) Schuddeboom, W.; Jonker, S. A.; Warman, J. M.; Leinhos, U.; Kuhnle, W.; Zachariasse, K. A. *J. Phys. Chem.* **1992**, *96*, 10809.
(46) Sobolewski, A. L.; Domcke, W. *Chem. Phys. Lett.* **1996**, *250*, 428.
(47) Zachariasse, K. A.; Grobys, M.; haar, T. d.; Hebecker, A.; Il'ichev, Y. V.; Morawski, O.; Ruckert, I.; Kuhnle. *J. Photochemistry and Photobiology A: Chemistry* **1997**, *105*, 373.
(48) Siemiarczuk, A.; Grabowski, A. R.; Krowczynski, A.; Asher, M.; Ottolenghi, M. *Chem. Phys. Lett.* **1977**, *151*, 315.
(49) Zachariasse, K. A. *Chem. Phys. Lett.* **2000**, *320*, 8.
(50) Paul, A.; Mandal, P. K.; Samanta, A. *Chem. Phys. Lett.* **2005**, *402*, 373.
(51) Paul, A.; Mandal, P. K.; Samanta, A. *J. Phys. Chem. B* **2005**, *109*, 9148.
(52) Reichardt, C. *Green. Chem.* **2005**, *7*, 339.
(53) Rappoport, D.; Furche, F. *J. Am. Chem. Soc.* **2004**, *126*, 1277.
(54) Saroja, G.; Soujanya, T.; Ramachandram, B.; Samanta, A. *Journal of Fluorescence* **1998**, *8*, 405.
(55) Nagasawa, Y.; Oishi, A.; Ttoh, T.; Yasuda, M.; Muramatsu, M.; Ishibashi, Y.; Ito, S.; Miyasaka, H. *J. Phys. Chem. C* **2009**, *113*, 11868.
(56) Hicks, J.; Vandersall, M.; Babarogic, A.; Eisenthal, K. B. *Chem. Phys. Lett.* **1985**, *116*, 18.
(57) Wang, Y.; Eisenthal, K. B. *J. Chem. Phys.* **1982**, *77*.
(58) Wang, Y.; McAuliffe, M.; Novak, F.; Eisenthal, K. B. *J. Phys. Chem.* **1981**, *85*, 3736.
(59) Druzhinin, S. I.; Galievsky, V. A.; Zachariasse, K. A. *J. Phys. Chem. A* **2005**, *109*, 11213.
(60) Drogen, F. V.; Peter, M. *Methods in molecular biology* **2004**, *284*, 287.
(61) Pucadyil, T. J.; Chattopadhyay, A. *Journal of Fluorescence* **2006**, *16*, 87.
(62) Pucadyil, T. J.; Mukherjee, S.; Chattopadhyay, A. *J. Phys. Chem. B* **2007**, *111*, 1975.
(63) Lopez, A.; Dupou, L.; Altibelli, A.; Trotard, J.; Tocanne, J. F. *Biophysical Journal* **1988**, *53*, 963.
(64) Purkayastha, P.; Bhattacharyya, P. K.; Bera, S. C.; Chattopadhyay, N. *Phys. Chem. Chem. Phys.* **1999**, *1*, 3253.
(65) Paul, A.; Samanta, A. *J. Phys. Chem. B* **2007**, *111*, 1957.
(66) Skrzypczak, A.; Neta, P. *J. Phys. Chem. A* **2003**, *107*, 7800.
(67) McLean, A. J.; Muldoon, M. J.; Gordon, C. M.; Dunkin, I. R. *Chem. Commun.* **2002**, 1880.

(68) Nishiyama, Y.; Fukuda, M.; Terazima, M.; Kimura, Y. *J. Chem. Phys.* **2008**, *128*, 164514.
(69) Soujanya, T.; Saroja, G.; Samanta, A. *Chem. Phys. Lett.* **1995**, *236*, 503.
(70) Horng, M. L.; Gardecki, J. A.; Papazyan, A.; Maroncelli, M. *J. Phys. Chem.* **1995**, *99*, 17311.
(71) Ito, N.; Arzhantsev, S.; Maroncelli, M. *Chem. Phys. Lett.* **2004**, *396*, 83.
(72) Swinney, T. C.; Kelley, D. F. *J. Chem. Phys.* **1993**, *99*, 211.
(73) Ingram, J. A.; Moog, R. S.; Ito, N.; Biswas, R.; Maroncelli, M. *J. Phys. Chem. B* **2003**, *107*, 5926.
(74) Arzhantsev, S.; Jin, H.; Baker, G. A.; Maroncelli, M. *J. Phys. Chem. B* **2007**, *111*, 4978.
(75) Shim, Y.; Kim, H. J. *J. Phys. Chem. B* **2009**, *113*, 12964.
(76) Kimura, Y.; Fukuda, M.; Suda, K.; Terazima, M. *J. Phys. chem. B* **2010**, *114*, 11847.

CHAPTER 4

Modulation of the Dual Fluorescence of Crystal Violet Lactone in RTILs

The influence of polarity, viscosity and hydrogen bond donating ability of the medium on the fluorescence behavior of crystal violet lactone (CVL), which undergoes excited state intramolecular electron transfer reaction and exhibits dual fluorescence from two different electronic states, termed as CT_A and CT_B, has been studied in six different room temperature ionic liquids (RTILs) using steady state and time-resolved emission techniques. It is shown that the excited state $CT_A \rightarrow CT_B$ transformation and dual fluorescence of CVL can be controlled by appropriate choice of the RTILs. While the second emission from the CT_B state can barely be seen in 1,3-dialkylimidazolium RTILs, dual fluorescence is quite prominent in 1-butyl-2,3-dimethylimidazolium RTIL, [bmMim][Tf_2N]. These contrasting results have been explained taking into account the hydrogen bonding interactions of the 1,3-dialkylimidazolium ions (mediated through the C(2)-hydrogen) with CVL and the viscosity of the RTILs. A comparison of the measured solvation time and excited state reaction time suggests that the $CT_A \rightarrow CT_B$ reaction rate in moderately viscous RTILs is primarily dictated by the dynamics of solvation.

4.1. Introduction

Photophysical studies of several systems have been carried out in RTILs primarily for two reasons.[1-27] The first objective is to obtain an understanding of these complex media from the photophysical studies. The second objective is to exploit some of the novel properties of the RTILs to regulate the photo-responses of various systems. These studies have not only improved the understanding of these substances, but also shown how the viscosity, polarity and the ionic constituents of the RTILs can influence the molecular rotation, electron and proton transfer reaction, molecular diffusion, solvent relaxation dynamics, and so forth.

As part of the studies on photo-responses of molecular systems in RTILs, we have taken up the study of crystal violet lactone (CVL) in several RTILs. CVL, (Chart 4.1), introduced

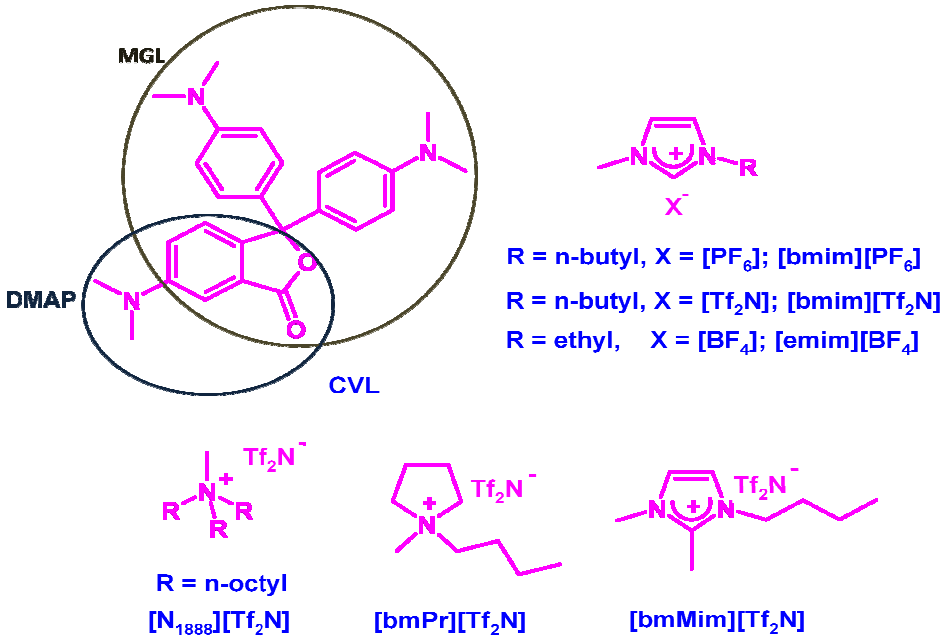

Chart 4.1. Structure/Abbreviation of the crystal violet lactone (CVL) and the RTILs employed in this study

by Karpiuk, is an electron donor-acceptor (EDA) molecule, which exhibits dual emission.[28,29] The photophysical behavior of this molecule can be considered as additive response of the two of its subunits, 6-dimethylaminophthalide (DMAP) and malachite green lactone (MGL), both consisting of a dimethylanilino group as electron donor and a 5-membered lactone ring system as electron acceptor (Chart 4.1). Because of the presence of electron donor and acceptor groups in both the subunits of CVL, the charge transfer in the excited state can be localized in the DMAP or MGL subunit (Chart 4.1). In nonpolar media, the first excited sate (CT_A, μ = 10.7 D),[28] which is charge transfer in nature and localized in the DMAP moiety, is lower in energy compared to the corresponding charge transfer state (CT_B, μ = 25.2 D)[28] localized in the MGL moiety, and the molecule exhibits fluorescence that is typical of the DMAP subunit (Scheme 4.1). However, in polar medium, because of the difference in the dipolar character of the two states, there occurs a state reversal (i.e. CT_B level becomes lower than the CT_A state) and the molecule emits from both the states showing a dual fluorescence behavior. The transformation of the molecule from the CT_A to CT_B state involves the transfer of an electron from the dimethylanilino group to 5-membered lactone ring system and

subsequent solvent stabilization of the final state. The effect of solvation dynamics on the kinetics of $CT_A \rightarrow CT_B$ process has also been studied by Karpiuk and coworkers using femtosecond time-resolved pump-probe technique.[29] In conventional less viscous aprotic solvents, the electron transfer process is believed to be extremely fast (occurs within a few femtoseconds) and the overall rate of the $CT_A \rightarrow CT_B$ process is dictated mostly by the solvation dynamics.[29]

Interestingly, even though CVL exhibits dual fluorescence in acetonitrile, it displays a single fluorescence (CT_A) in alcoholic solvents,[28] which are of comparable/more polar than acetonitrile. The lack of CT_B emission in protic solvents is attributed to the H-bonding interaction between CVL and the solvent (with the latter serving as H-bond donor) leading to the quenching of this fluorescence.[28] This property allows CVL to act as a probe of proticity of the environments.

As the $CT_A \rightarrow CT_B$ transformation of CVL involves both electron transfer and solvation of the charge separated state, the polarity of the medium and dynamics of solvation play important roles in determining the rate and efficiency of the overall process in conventional less viscous solvents. The viscosity of solvent has negligible or no influence provided the medium is not highly viscous (like most of the conventional solvents). However, in highly viscous RTILs, where the dynamics of solvent is governed largely by the viscosity of the media,[1] one can as well expect strong influence of the viscosity on the $CT_A \rightarrow CT_B$ transformation of CVL. Recently, the dynamic heterogeneity of the RTILs has been investigated by monitoring the dual fluorescence of CVL.[20] The fluorescence behavior and

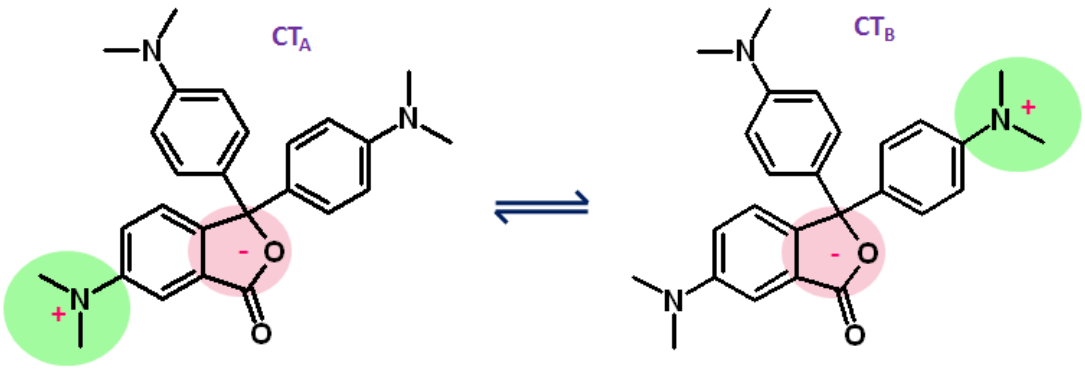

Scheme 4.1. Excited state intramolecular electron transfer reaction of CVL

electron transfer reaction of CVL has also been studied theoretically in one of the RTILs.[30] As the RTILs possess a wide range of polarity and viscosity values and it is also possible to control the proton donating ability of these liquids, we thought it should be possible to modulate the excited state reaction and hence, the fluorescence response of this molecular system. It is with this intention we have taken up this study in which we have investigated the photophysical behavior of CVL in six carefully chosen RTILs (Chart 4.1) of different viscosities and hydrogen bond donating abilities. We have been able to establish the formation of the CT_B state from the CT_A state using the time-resolved emission spectra (TRES) and time-resolved area normalized emission spectra (TRANES) studies to follow the time evolution of the CT_B state, demonstrate the influence of hydrogen bond donating ability of the RTILs and investigate the effect of excitation wavelength on the fluorescence response of CVL.

4.2. Absorption and emission behavior in 1,3-dialkylimidazolium RTILs

To understand the effect of RTILs on the excited state intramolecular charge transfer reaction and dual fluorescence of CVL, three 1,3-dialkylimidazolium RTILs (Chart 4.1), [emim][BF_4], [bmim][PF_6] and [bmim][Tf_2N], whose polarities in the E_T^N scale are 0.710, 0.676 and 0.645 (Table 4.1),[31] respectively and viscosities are 34, 285 and 50 cP, respectively, have been chosen. The long wavelength absorption peak of CVL is found to be insensitive to small difference of the polarity of these RTILs and the absorption maximum (λ_{max}^{abs}) is observed around 362 ± 2 nm (Figure 4.1). On the other hand, significant difference in the emission behavior of CVL is observed with variation of the RTILs (Figure 4.2). In [emim][BF_4], the emission spectrum consists of a single fluorescence band ($\bar{\nu}$ = 22100 cm^{-1}), which is typical of the CT_A emission of CVL. In [bmim][PF_6] and [bmim][Tf_2N], the fluorescence spectra resembled the CT_A emission of the system, but with an additional shoulder in the long wavelength region, which can perhaps be attributed to the CT_B emission of the molecule. Even though λ_{max}^{abs} of CVL is insensitive to small difference in the polarity of the RTILs, presumably due to its small ground state dipole moment (5.5 D),[28] the CT_A emission maximum shows a higher sensitivity and displays a red shift with increase in polarity of the RTILs clearly due to the higher excited state dipole moment (10.7 D) of

Table 4.1. Polarity and viscosity of the RTILs and the observed photophysical parameters of CVL in the six RTILs[a]

RTIL	E_T^N [b]	η / cP [d]	$\bar{\nu}_{max}^{em}$ / 10^3 cm^{-1}	
			CT_A	CT_B
[emim][BF_4]	0.710	34	22.1	
[bmim][PF_6]	0.676	285	22.3	
[bmim][Tf_2N]	0.645	50	22.4	
[bmPr][Tf_2N]	0.598	73	22.5	17.5
[bmMim][Tf_2N]	0.546	90	22.6	17.8
[N_{1888}][Tf_2N]	- [c]	615	23.6	

RTIL	avg. lifetime / ns		Φ_{fl}	$k_{nr}/10^7$ s^{-1}
	$\tau_A/(CT_A)$	$\tau_B/(CT_B)$		
[emim][BF_4]	0.460		0.0002	217
[bmim][PF_6]	0.780		0.0050	127
[bmim][Tf_2N]	0.310		0.0046	321
[bmPr][Tf_2N]	0.750	1.0		
[bmMim][Tf_2N]	1.2	1.5		
[N_{1888}][Tf_2N]	5.8		0.0580	16

(a) Absorption maximum of CVL in these RTILS is observed around 362 ± 2 nm. (b) Reference[31]. (c) Unavailable in the literature and is assumed to be the lowest among the six RTILs based on the absorption and fluorescence properties of CVL in this and other RTILs. (d) Measured viscosities at 23°C.

CVL.[28]

A single fluorescence band of CVL in 1,3-dialkylimidazolium RTILs was unexpected for two reasons. Firstly, these liquids are more polar than acetonitrile, wherein CVL exhibits dual emission (with the CT_B emission stronger than the CT_A emission)[28] and secondly, the molecule exhibits dual fluorescence in pyrrolidinium ionic liquid,[20] a solvent whose viscosity (54 cP) and polarity are very similar to the respective quantities of the RTILs, which we have

used here. It is thus evident that a weak or no CT_B emission in these imidazolium RTILs is not due to the prevention of the $CT_A \rightarrow CT_B$ transformation due to the unfavorable viscosity or polarity of these liquids. In fact, that the excited state reaction does take place in these RTILs is evident from the short fluorescence lifetimes (τ_f), low fluorescence quantum yields (ϕ_f) and high nonradiative rate constants (k_{nr}) of CVL (Table 4.1). A close look at this table suggests that the τ_f, ϕ_f and k_{nr} values and hence, the efficiency of the $CT_A \rightarrow CT_B$ process, is influenced by both the polarity and viscosity of the RTILs. As long as the viscosity of the medium is not too large, the polarity of the RTIL dictates $CT_A \rightarrow CT_B$ rates and hence, the k_{nr} values. As the polarities of these RTILs are very similar, one can hardly expect much difference in the $CT_A \rightarrow CT_B$ rate due to the polarity effect. However, when the medium is too viscous, as in the case of [bmim][PF_6], the $CT_A \rightarrow CT_B$ reaction is hindered thereby making the k_{nr} value the lowest.

The emission behavior of CVL in RTILs can be understood by noting that even though the molecule exhibits dual fluorescence in polar aprotic solvents, it displays a single emission (CT_A) in conventional protic solvents, which are more polar than acetonitrile or the RTILs. It is reported that CT_B emission of the molecule is quenched by the hydrogen bonding interaction with the protic solvent.[28] As the C(2)-hydrogen atom of the imidazolium cation of 1,3-dialkylimidazolium RTILs serve as H-bond donor,[32-34] the emission behavior of CVL in these liquids is expected to be similar to that in protic solvents, in which the molecule does not exhibit the CT_B emission.

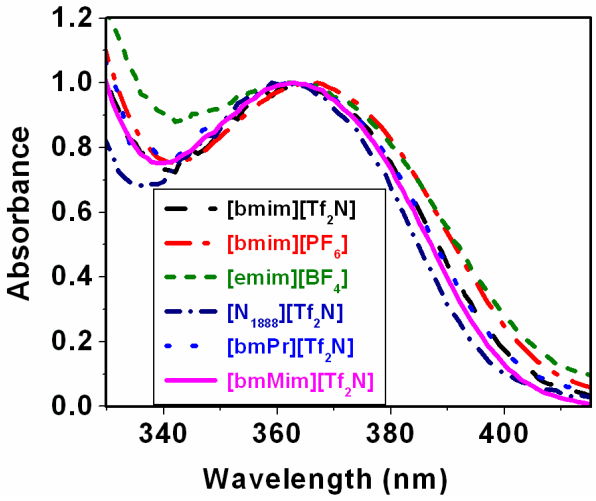

Figure 4.1. Absorption spectra of CVL (normalized at the low energy maximum) in [bmim][Tf_2N] (dash), [bmim][PF_6] (dash dot), [emim][BF_4] (short dash), [N_{1888}][Tf_2N] (short dash dot), [bmPr][Tf_2N] (dot) and [bmMim][Tf_2N] (solid line).

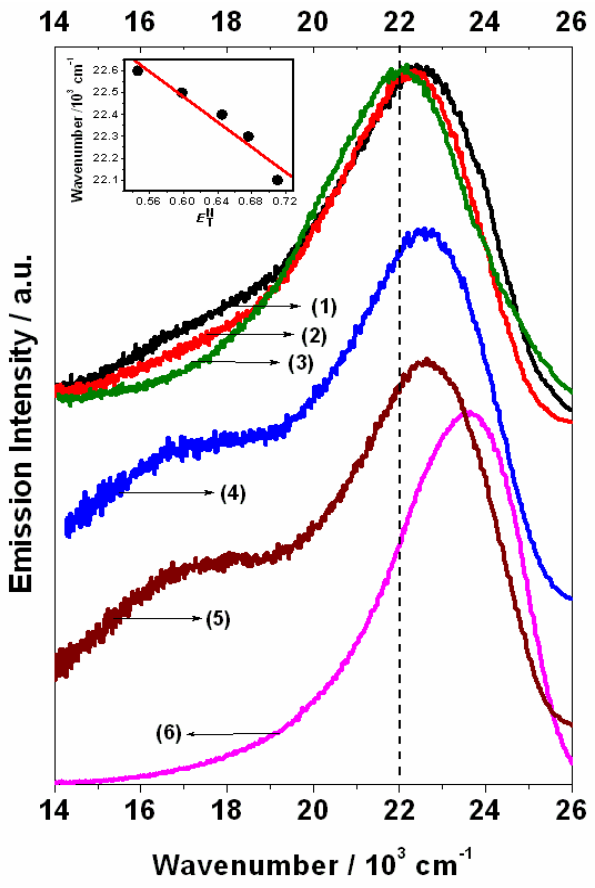

Figure 4.2. Fluorescence spectra of CVL in [bmim][Tf_2N] (1), [bmim][PF_6] (2), [emim][BF_4] (3), [bmPr][Tf_2N] (4), [bmMim][Tf_2N] (5) and [N_{1888}][Tf_2N] (6). Insert shows the linear dependence of the CT_A band maximum on the polarity of the ionic liquid. The vertical line indicates the shift of the spectral maximum.

The two factors that determine the intensity of the weak CT_B emission are the quenching interaction of this state with the proton donors and the rate of formation of this state from the CT_A state. As the polarities of the RTILs are not very different, one should not expect much difference in the $CT_A \rightarrow CT_B$ rate due to the polarity of the medium. However, a much higher viscosity of [bmim][PF_6] compared to two other RTILs can slow down the $CT_A \rightarrow CT_B$ reaction, thereby making the CT_B emission the weakest. Interestingly, the CT_B emission is found to be the weakest in most polar and less viscous [emim][BF_4]. This somewhat surprising behavior can be understood if the hydrophilic nature of [emim][BF_4] is taken into consideration.[35] Since the CT_B emission is highly sensitive to moisture, trace quantity of water present in this RTIL can quench the weak emission. Even though the $CT_A \rightarrow CT_B$ transformation does not involve any major structural change, the viscosity of the medium can

still influence the rate of the process by slowing down the solvation process, as demonstrated later.

4.3. Absorption and emission behavior in other RTILs

To establish unambiguously that the H-bonding interaction is responsible for single emission of CVL in 1,3-dialkylimidazolium RTILs, the photophysics has been studied in two other moderately viscous RTILs, which do not possess the H-bond donating ability. The ionic liquids that belong to this category are [bmPr][Tf_2N] and [bmMim][Tf_2N] (Chart 4.1). While the former is a pyrrolidinium RTIL, the later is an imidazolium RTIL but with its C(2)-H atom methylated. The polarities of the two RTILs are 0.598 and 0.546[31] and the viscosities are 73 and 90 cP respectively. The absorption maximum in [bmPr][Tf_2N] and [bmMim][Tf_2N] appear at around 362 ± 2 nm (Figure 4.1). As expected, CVL exhibits dual fluorescence (Figure 4.2) both in [bmPr][Tf_2N] and [bmMim][Tf_2N] with the CT_A emission maximum at 22,500 cm^{-1} in [bmPr][Tf_2N] and 22,670 cm^{-1} in [bmMim][Tf_2N]. It is evident from the insert to Figure 4.2 that the wavenumbers corresponding to the fluorescence maximum follow a linear relationship with the polarity of the different RTILs.

The strong influence of the viscosity of the medium is also evident from the fact that even though [bmPr][Tf_2N] and [bmMim][Tf_2N] are more polar than conventional solvent, acetonitrile (wherein CVL exhibits dual emission with more intense CT_B emission), the CT_A fluorescence is more pronounced in these RTILs. In order to further establish the role of viscosity on the $CT_A \rightarrow CT_B$ transformation of CVL, we have chosen another RTIL, an ammonium RTIL, [N_{1888}][Tf_2N], which does not possess any H-bond donating centre and has a very high viscosity of 615 cP. The idea is that if the viscosity of the medium has no influence on the $CT_A \rightarrow CT_B$ transformation, the molecule should exhibit dual fluorescence, but if the transformation is viscosity dependent, then one should expect only the CT_A fluorescence of CVL in this RTIL. The observation of single fluorescence band for the system (Figure 4.2) is a clear reflection of the retardation of the excited state reaction. The long fluorescence lifetime of CVL in this medium (5.8 ns) is also a consequence of the absence of excited state reaction.

4.4. Time-resolved emission spectra (TRES) and time-resolved area normalized emission spectra (TRANES)

TRES of CVL in [bmMim][Tf_2N] have been constructed by measuring the fluorescence decay profiles at every 5/10 nm interval across the steady state emission spectrum at 23°C following a standard procedure.[36] The time profiles in the short wavelength region of the emission spectrum were consisted of only decay; whereas, at longer wavelengths, the profiles were characterized by a rise followed by the decay (Figure 4.3). The TRES obtained at different times from the decay profiles are shown in Figure 4.4. The emission spectrum at time, t = 0 represents a single emission band with a little hump on the red side. With increase in time, the hump gradually grows into a new emission band and after t = 2 ns, the spectrum clearly consists of two components, as expected from a dual fluorescent system. The emission spectra at different times reveal the kinetics of the $CT_A \rightarrow CT_B$ reaction of CVL in RTIL. It is interesting to note that along with the excited state reaction, a progressive shift of the CT_A emission maximum, which is an indication of slow solvation of the fluorescent state of the molecule in RTIL, is also observed.

The excited state transformation, i.e. the formation of CT_B state from CT_A, is also evident from the presence of an isoemissive point (observed at ~21670 cm^{-1}) in the TRANES (Figure 4.5) constructed following a reported procedure.[37,38] The excitation spectra corresponding to the CT_A and CT_B emission maxima (Figure 4.6), which resemble the absor-

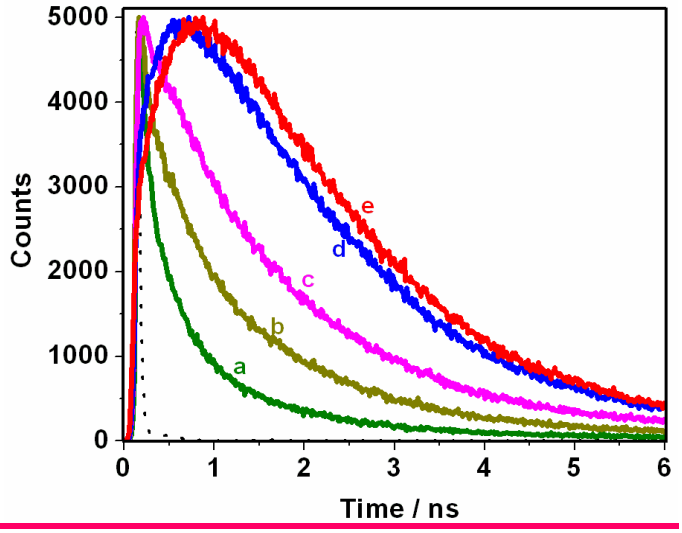

Figure 4.3. Wavelength dependent fluorescence decay profiles of CVL in [bmMim][Tf_2N] at 23°C. The monitoring wavelengths are (a) 405, (b) 440, (c) 505, (d) 585 and (e) 650 nm. Lamp profile is shown as dotted line.

ption spectrum of CVL is also an evidence of the excited state formation of CT_B state from CT_A.

4.5. Estimation of the $CT_A \rightarrow CT_B$ transformation time

The excited state reaction time is estimated from the rise time of the emission intensity at ~17400 cm^{-1}. A fit to the emission intensity data according to

$$I(t) = I_0 - I_1 \exp(-t/\tau_r) \quad (1)$$

where, *I(t)* is the fluorescence intensity at time 't' and I_0 is the intensity at infinite time. I_1 is the fraction of the excited state reaction observed, τ_r represents the excited state reaction time, which yielded an excited state reaction time of 985 ps (Figure 4.4). Considering the fact

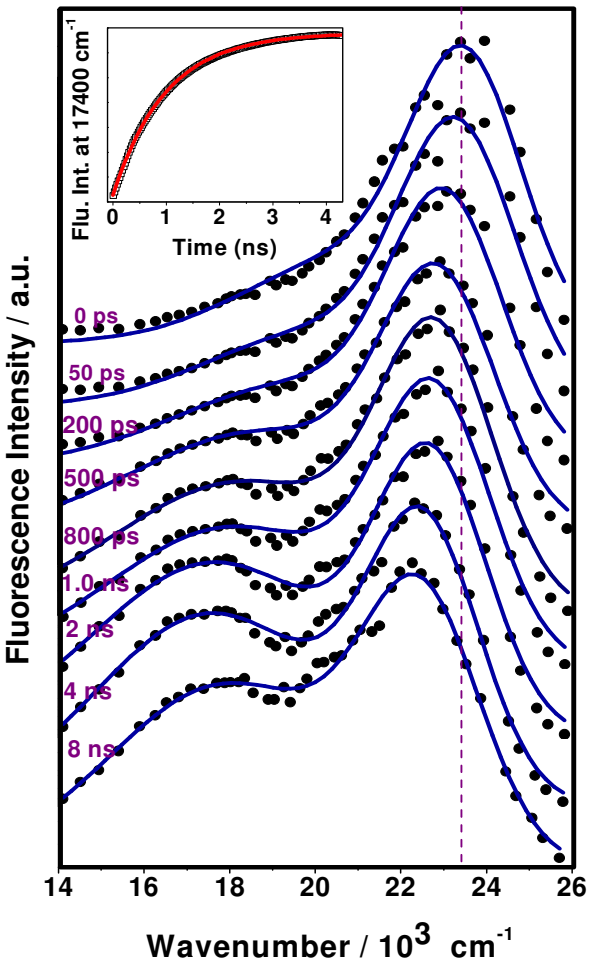

Figure 4.4. Time-resolved emission spectra (TRES) of CVL in [bmMim][Tf_2N] at 23°C measured at different time delays. The vertical line is used to highlight the time-dependent shift of the CT_A emission maximum due to solvation. Insert shows the fluorescence intensity monitored at 17,400 cm^{-1} as a function of time.

that the CT_B state of CVL is characterized by a short fluorescence lifetime (~ 1.5 ns), the measured value should not be considered as very accurate. One should also note that as the $CT_A \rightarrow CT_B$ transformation of CVL involves both electron transfer and solvation of the CT_B state, the measured time obtained by following the time evolution of the solvated CT_B state represents the slower of the two processes. As can be seen from the next section, the time measured here is a reflection of slow solvation dynamics in the RTIL.

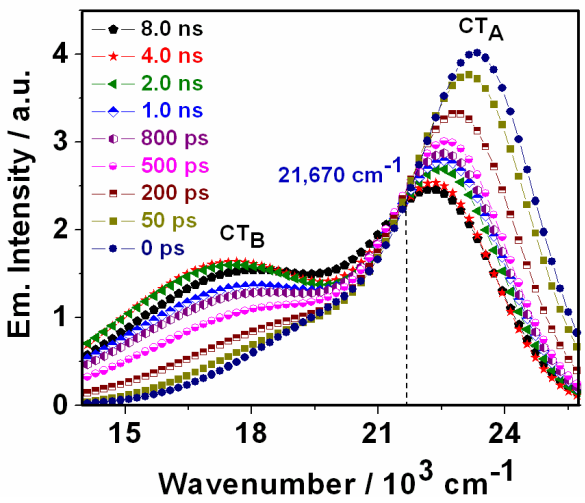

Figure 4.5. TRANES of CVL in [bmMim][Tf_2N] at 23°C measured at different delay times. The data represents the Gaussian fit to the area normalized emission data at different delay times. Isoemissive point is identified at 21,670 cm^{-1}.

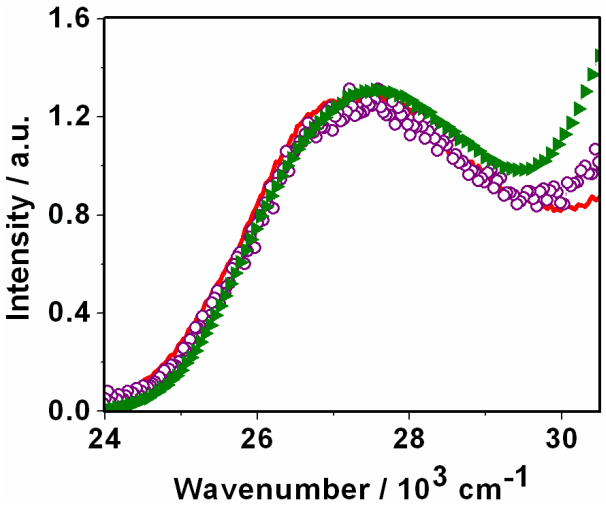

Figure 4.6. Excitation spectra of CVL in [bmMim][Tf_2N]. Solid line represents the excitation spectrum recorded by monitoring emission at 440 nm (corresponding to CT_A band), the spectrum with empty circles represents excitation spectrum recorded by monitoring emission at 575 nm (corresponding to CT_B band). The spectrum with triangles represents absorption spectrum of CVL in [bmMim][Tf_2N].

4.6. Estimation of the solvent relaxation time

Even though the signature of slow solvation of the excited state of CVL is clearly evident from the time-dependent shift of the spectral maxima, the solvation time in [bmMim][Tf_2N] cannot be precisely estimated from these data owing to the short fluorescence lifetime of the system and parallel excited state reaction. This is why we have obtained an estimate of the solvation time in this medium by measuring the time-dependent fluorescence Stokes shift of C153 as a probe molecule. These measurements yielded an average solvation time of 690 ps, a value consistent with the viscosity of the RTIL. Therefore, it is evident that the excited state reaction time and solvation time in [bmMim][Tf_2N] are of the same order of magnitude and comparable. The results therefore confirm that the rate of $CT_A \rightarrow CT_B$ transformation, which consists of electron transfer and solvation of the charge separated state, is essentially controlled by the dynamics of solvent reorganization.

4.7. Excitation wavelength dependence

As RTILs are considered to be microheterogeneous media comprising hydrophobic and hydrophilic domains, it is likely that at any given instant the CVL molecules will experience different molecular environments and may exhibit an excitation wavelength dependent emission behavior.[2,4,9,20,39-41] In fact, the dynamic heterogeneity of some RTILs has been dem-

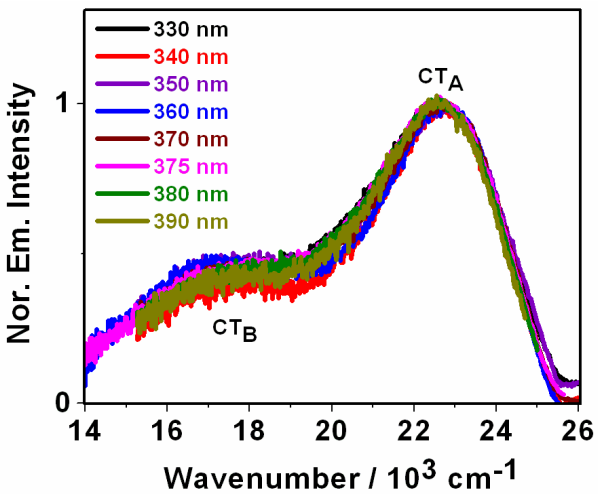

Figure 4.7. Steady state emission spectra of CVL in [bmMim][Tf_2N] at excitation wavelengths of 330, 340, 350, 360, 370, 375, 380 and 390 nm. The emission intensities are normalized to CT_A band to best display the changes in the relative intensities of CT_A and CT_B bands.

onstrated by exploiting the fluorescence response of this system. The emission spectra recorded for different excitation wavelengths are shown in Figure 4.7. Interestingly, we could hardly observe any variation of the spectral position or the relative intensities of the CT_A and CT_B bands on variation of the excitation wavelength in these RTILs. This behavior is, however, not completely unexpected as a large majority of the fluorescent systems do not display any excitation wavelength dependent behavior and whether a system would display excitation wavelength dependence depends on factors such as inhomogeneous broadening of the absorption spectrum due to solute-solvent interaction, and fluorescence lifetime of the solute.[9]

4.8. Conclusion

The fluorescence response of CVL has been investigated in several RTILs. It is shown that the polarity, hydrogen bond donating ability and viscosity of the RTILs can be conveniently exploited for the modulation of the excited state reaction and fluorescence response in these media. The slow solvation dynamics, which is a consequence of the viscous nature of the RTILs, retards the $CT_A \rightarrow CT_B$ transformation significantly making this process viscosity dependent in these viscous media. In fact, it is shown that in highly viscous RTIL such as $[N_{1888}][Tf_2N]$, the $CT_A \rightarrow CT_B$ transformation is completely prevented. The strong influence of the viscosity of the medium is also evident from the fact that even though [bmPr][Tf_2N] and [bmMim][Tf_2N] are more polar than conventional solvent, acetonitrile (wherein CVL exhibits dual emission with more intense CT_B emission), the CT_A fluorescence is more pronounced in these RTILs. The high viscosity coupled with the hydrogen bond donating ability of most 1,3-dialkylimidazolium RTILs make the CT_B fluorescence quite weak in these media. A comparison of the measured solvation time and excited state reaction time suggests that the $CT_A \rightarrow CT_B$ reaction rate in moderately viscous RTILs is primarily dictated by the dynamics of solvation.

REFERENCES

(1) Samanta, A. *J. Phys. Chem. Lett.* **2010**, *1*, 1557.
(2) Samanta, A. *J. Phys. Chem. B* **2006**, *110*, 13704.
(3) Mandal, P. K.; Saha, S.; Karmakar, R.; Samanta, A. *Current Science* **2006**, *90*, 301.
(4) Mandal, P. K.; Paul, A.; Samanta, A. *Journal of Photochemistry and Photobiology, A: Chemistry* **2006**, *182*, 113.
(5) Santhosh, K.; Banerjee, S.; Rangaraj, N.; Samanta, A. *J. Phys. Chem. B* **2010**, *114*, 1967.
(6) Aki, S. N. V. K.; Brennecke, J. F.; Samanta, A. *Chem. Commun.* **2001**, 413.
(7) Karmakar, R.; Samanta, A. *J. Phys. Chem. A* **2002**, *106*, 6670.
(8) Karmakar, R.; Samanta, A. *Chem. Phys. Lett.* **2003**, *376*, 638.
(9) Mandal, P. K.; Sarkar, M.; Samanta, A. *J. Phys. Chem. A* **2004**, *108*, 9048.
(10) Paul, A.; Mandal, P. K.; Samanta, A. *J. Phys. Chem. B* **2005**, *109*, 9148.
(11) Paul, A.; Mandal, P. K.; Samanta, A. *Chem. Phys. Lett.* **2005**, *402*, 373.
(12) Mandal, P. K.; Samanta, A. *J. Phys. Chem. B* **2005**, *109*, 15172.
(13) Paul, A.; Samanta, A. *J. Phys. Chem. B* **2007**, *111*, 4724.
(14) Paul, A.; Samanta, A. *J. Phys. Chem. B* **2007**, *111*, 1957.
(15) Paul, A.; Samanta, A. *J. Phys. Chem. B* **2008**, *112*, 16626.
(16) Bhattacharya, B.; Samanta, A. *J. Phys. Chem. B* **2008**, *112*, 10101.
(17) Khara, D. C.; Paul, A.; Santhosh, K.; Samanta, A. *J. Chem. Sci.* **2009**, *121*, 309.
(18) Saha, S.; Mandal, P. K.; Samanta, A. *Phys. Chem. Chem. Phys.* **2004**, *6*, 3106.
(19) Nagasawa, Y.; Itoh, T.; Yasuda, M.; Ishibashi, Y.; Ito, S.; Miyasaka, H. *J. Phys. Chem. B* **2008**, *112*, 15758.
(20) Jin, H.; Li, X.; Maroncelli, M. *J. Phys. Chem. B* **2007**, *111*, 13473.
(21) Adhikari, A.; Sahu, K.; Dey, S.; Ghosh, S.; Mandal, U.; Bhattacharyya, K. *J. Phys. Chem. B* **2007**, *111*, 12809.
(22) Chakrabarty, D.; Hazra, P.; Chakraborty, A.; Seth, D.; Sarkar, N. *Che. Phys. Lett.* **2003**, *381*, 697.
(23) Fukuda, M.; Terazima, M.; Kimura, Y. *Chem. Phys. Lett.* **2008**, *463*, 364.
(24) Iwata, K.; Kakita, M.; Hamaguchi, H. *J. Phys. Chem. B* **2007**, *111*, 4914.
(25) Mali, K. S.; Dutt, G. B.; Mukherjee, T. *J. Chem. Phys.* **2005**, *123*, 174504.
(26) Mali, K. S.; Dutt, G. B.; Mukherjee, T. *J. Chem. Phys.* **2008**, *128*, 124515.
(27) Jin, H.; Baker, G. A.; Arzhantsev, S.; Dong, J.; Maroncelli, M. *J. Phys. Chem. B* **2007**, *111*, 7291.
(28) Karpiuk, J. *J. Phys. Chem. A* **2004**, *108*, 11183.
(29) Schmidhammer, U.; Megerle, U.; Lochbrunner, S.; Riedle, E.; Karpiuk, J. *J. Phys. Chem. A* **2008**, *112*, 8487.
(30) Margulis, C. J.; Stern, H. A.; Berne, B. J. *J. Phys. Chem. B* **2002**, *106*, 12017.
(31) Reichardt, C. *Green. Chem.* **2005**, *7*, 339.
(32) Chang, H. C.; Jiang, J. C.; Tsai, W. C.; Chen, G. C.; Lin, S. H. *J. Phys. Chem. B* **2006**, *110*, 3302.
(33) Tsuzuki, S.; Tokuda, H.; MIkami, M. *Phys. Chem. Chem. Phys.* **2007**, *9*, 4780.
(34) Thar, J.; Brehm, M.; Seitsonen, A. P.; Kirchner, B. *J. Phys. Chem. B* **2009**, *113*, 15129.
(35) Huddleston, J. G.; Visser, A. E.; Reichert, W. M.; Willauer, H. D.; Broker, G. A.; Rogers, R. D. *Green. Chem.* **2001**, *3*, 156.
(36) Lakowicz, J. R. *Principles of Fluorescence Spectroscopy*, 2nd ed.; Kluwer Academic/Plenum Press: New York, 1999.
(37) Koti, A. S. R.; Periasamy, N. *Res. Chem. Intermed.* **2002**, *28*, 831.

(38) Koti, A. S. R.; Krishna, M. M. G.; Periasamy, N. *J. Phys. Chem. A* **2001**, *105*, 1767.
(39) Lopes, J. N. A. C.; Pauda, A. A. H. *J. Phys. Chem. B* **2006**, *110*, 3330.
(40) Wang, Y.; Voth, G. A. *J. Am. Chem. Soc.* **2005**, *127*, 1219.
(41) Hu, Z.; Margulis, C. J. *Proc. Natl. Acad. Sci. U. S. A* **2006**, *103*, 831.

CHAPTER 5

Specific and Non-Specific Solute-Solvent Interactions of Aminochalcones in RTILs

Unlike most other electron donor-acceptor (EDA) molecules, the aminochalcones exhibit unusual solvent polarity dependent fluorescence behavior. Photophysical behavior of two aminochalcones, namely 4-aminochalcone (AC) and 4-dimethylaminochalcone (DMAC) has been studied in a viscous room temperature ionic liquid, 1-butyl-3-methylimidazolium hexafluorophosphate, [bmim][PF_6], by steady-state and time-resolved fluorescence techniques. The observation of a single emission band in viscous ionic liquid that is similar to the one observed in less viscous polar conventional solvents, suggests no twisting is necessary for the formation of the charge transfer state from which the emission of the aminochalcones originates. The fluorescence decay profiles, solvation dynamics and excitation wavelength dependent emission behavior of AC are found to be quite different from those of DMAC in the ionic liquid. The observed difference is attributed to specific H-bonding interaction between AC and [bmim][PF_6].

5.1. Introduction

Electron donor-acceptor (EDA) molecules have attracted the attention of researchers because of their potential applications in several areas.[1-3] Photoinduced charge separation in EDA molecules is the basis of design and development of systems for the solar energy conversion,[4,5] luminescent systems for sensing environments,[6] nanometer scale wires and logic gates [7-9] and also for making components of molecular electronic devices.[10] The EDA molecules commonly emit from an intramolecular charge transfer (ICT) state, which is most often more polar than the ground state. Several families of EDA molecules have been studied extensively and in most of the cases, a decrease in fluorescence quantum yield and lifetime is observed with increase in solvent polarity.[11,12] In this work, we concentrate on the photophysics of aminochalcones, which contain amino/dimethylamino group as an electron

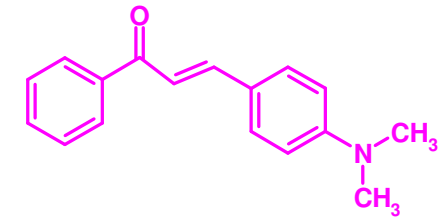

4-dimethylaminochalcone (DMAC)

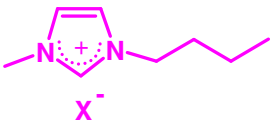

[bmim][PF_6]

(b)

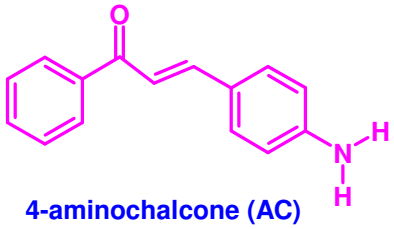

4-aminochalcone (AC)

(a)

Chart 5.1. (a) Structures/Abbreviations of 4-dimethylaminochalcone (DMAC) and 4-aminochalcone (AC) and (b) the [bmim][PF_6] RTIL employed in the present study

donor and a carbonyl group as acceptor (Chart 5.1). These systems exhibit fluorescence behavior which is not common for the EDA systems. The fluorescence quantum yield and lifetimes of the aminochalcones increase with increase in polarity of the medium. Stilbenes,[13] flavones,[14] thioazoloquinoxalines[15] are a few other EDA molecules of this category. It is necessary to consider multiple close-lying excited states to explain the unusual solvent dependence of the fluorescence behavior of such EDA molecules. The number of these excited states varies from system to system. For example, a three-state model in the case of stilbenes[13] and a two-state model in the case of flavone derivatives[14] are proposed.

The excited state mechanism of the aminochalcones was deduced by comparing the photophysical properties of these systems with those of the stilbene derivatives and bridged compounds of chalcones.[16-18] The currently accepted understanding is that the chalcone derivatives are present in their trans (E) form in the ground state. On photoexcitation, the molecule can undergo trans-cis isomerization and/or intramolecular charge transfer from donor (amino moiety) to acceptor (keto group) depending on the nature of the medium. In non polar solvents, these molecules emit weakly from their E* state.[16,17] Competing trans →

cis (E* →Z*) isomerization is believed to be responsible for the weak fluorescence in non polar solvents.[17] In more polar environment, the molecule emits more strongly from the dialkylanilino twisted intramolecular charge transfer (TICT) state, which is commonly termed as A* state.[16,17] Scheme 5.1 illustrates the formation of A* state from the locally excited E* state as a function of the polarity of the medium.

As the fluorescence properties of the chalcones are sensitive to the medium, where both solvent polarity and viscosity play important role, it is interesting to explore whether it is possible to modulate their fluorescence response by the viscous and polar nature of the RTILs. Polarity of the RTIL favors the emission from A* state, whereas the high viscosity of the ionic liquid is likely to slow down the formation of the A* state from the E* state. In order to gain insight into the opposing effects of the viscosity and polarity of the RTILs we have studied photophysical properties of 4-aminochalcone (AC) and 4-dimethylaminochalcone (DMAC) in 1-butyl-3-methylimidazolium hexafluorophosphate, [bmim][[PF_6] RTIL (Chart 5.1). Even though DMAC is studied previously in conventional solvents, to the best of our knowledge, this is the first study involving the photophysics of AC. We have chosen [bmim][PF_6] in this work because of its optical purity, high viscosity and polarity.

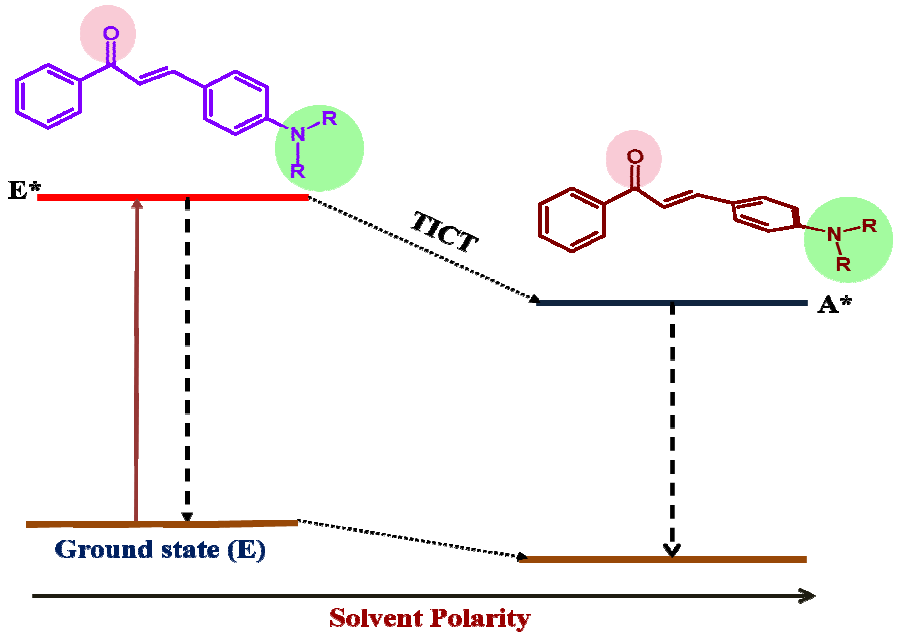

Scheme 5.1.

5.2. Results

The steady-state absorption and emission spectral behavior of DMAC and AC is measured in conventional non-polar and polar solvents, and the spectral data, Φ_f and $\bar{\tau}$ values are collected in Table 5.1. An enhancement of the Φ_f and $\bar{\tau}$ values of these molecules is observed with increase in the solvent polarity. The Φ_f values presented in Table 5.1 indicate that DMAC is more fluorescent than AC. The red shift of the emission maximum with increase in solvent polarity is consistent with the charge transfer nature of the emitting state. The steady-state spectral behavior of the systems in [bmim][PF_6] (shown in Figure 5.1) is compared to that in conventional solvents. The absorption and emission spectral maxima of the compounds in RTIL are redshifted relative to that in conventional solvents, indicating that spectral positions are dependent on the polarity of the medium. This is consistent with the intramolecular charge transfer nature of the excited state of the molecules. That the ICT character of the emission increases with increase in inductive influence of the donor group is

Table 5.1. Comparison of the steady-state spectral data and fluorescence lifetimes of DMAC and AC in conventional solvents and [bmim][PF_6] at 296 K

Solvent/E_T^N	λ_{max}^{abs} / nm		λ_{max}^{em} / nm		Φ_f / 10^{-3}		$\bar{\tau}$ / ps	
	AC	DMAC	AC	DMAC	AC	DMAC	AC	DMAC
Toluene/0.099	368	405	444	465	-	11.0	<50	90
1,4-Dioxane/0.111	370	405	462	480	2.5	30.0	<50	220
$CHCl_3$/0.259	375	410	475	505	4.6	66.0	70	480
DCM/0.309	376	415	485	515	5.3	153.0	100	1120
Acetone/0.355	380	418	500	520	30.0	265.0	270	1550
DMSO/0.444	406	425	527	555	113.0	206.0	450	1140
Acetonitrile/0.460	383	410	506	540	38.0	186.0	290	930
[bmim][PF_6]/0.676	388	420	512	550	100.0	190.0	1200	1400

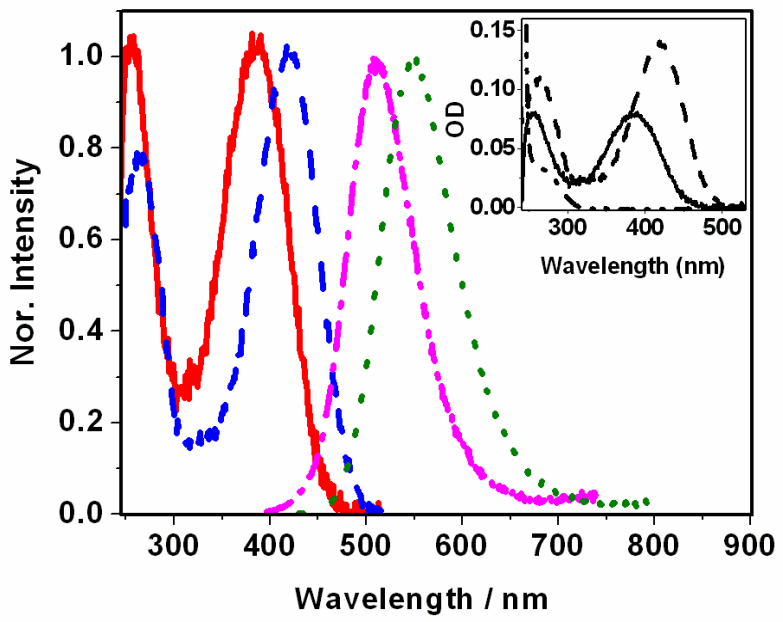

Figure 5.1. Normalized absorption spectra of AC (solid line), DMAC (dashed line) and emission spectra of AC (dash-dot line), DMAC (dotted line) in [bmim][PF_6]. Inset shows the absorption spectrum of the [bmim][PF_6] (dash-dot-dot) along with the absorption spectra of AC and DMAC highlighting the optical transparency of the ionic liquid. All the spectra were recorded with air as reference.

evident from the large red shift of the absorption and emission maxima of DMAC compared to AC in all the solvents.

It was earlier proposed that the charge transfer state is associated with TICT conformation.[16-18] As the aminochalcones have so far been studied only in less viscous conventional solvents, the role of viscosity on the photophysics of these molecules is not yet explored. In highly viscous environment, as the twisting of the dialkylanilino group is expected to be retarded (Scheme 5.1) one can expect emission from the E* state despite the polar nature of the media. However, Figure 5.1 shows a single emission band in highly viscous and polar [bmim][PF_6], which is similar to the reported A* emission in conventional solvents.

Figure 5.2 shows emission wavelength dependent fluorescence decay profiles and normalized time-resolved emission spectra (TRES) of DMAC in [bmim][PF_6] at room tempe-

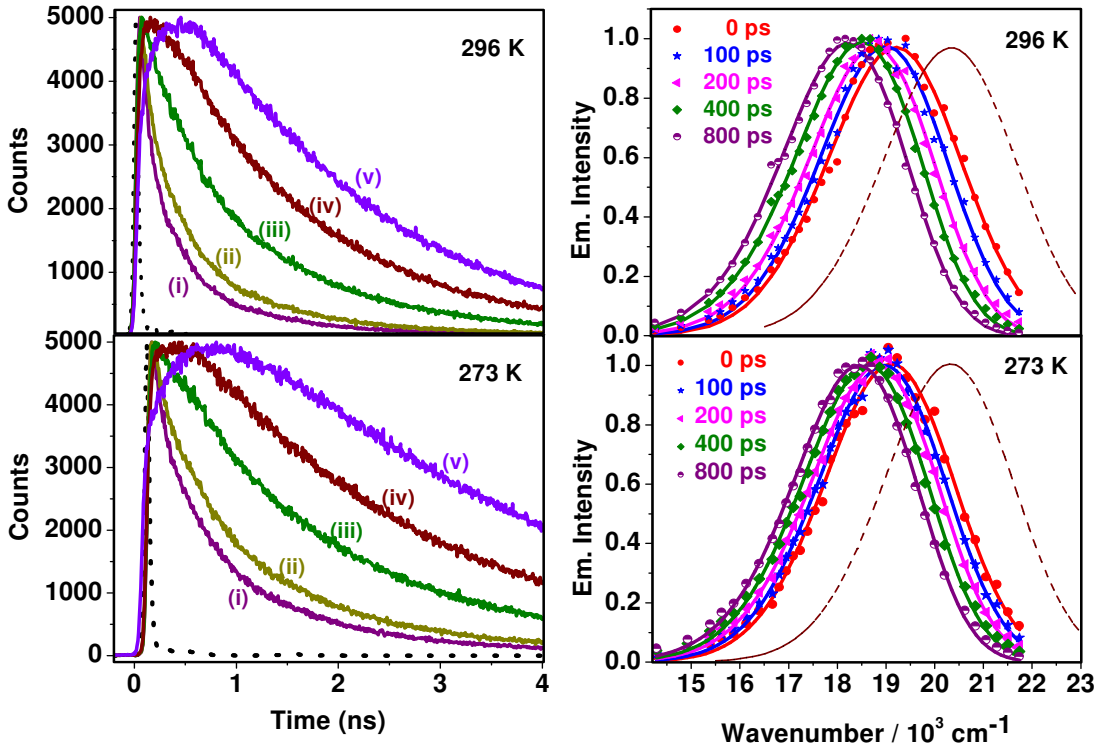

Figure 5.2. Emission wavelength dependent fluorescence decay profiles of DMAC (left panel) in [bmim][PF_6] at 296 K and 273 K. The monitoring wavelengths are (i) 490, (ii) 500, (iii) 525, (iv) 550 and (v) 600 nm. Lamp profile is shown as dotted line. Normalized TRES of DMAC in [bmim][PF_6] at different delay times are shown in the right panel. Spectrum with dotted line represents the estimated time-zero spectrum. λ_{exc} = 405 nm.

rapture (296 K) and 273 K. TRES at both the temperatures represent single emission maxima. The rise of the fluorescence intensity followed by a decay behavior at the longer emitting wavelengths is a manifestation of the slow solvation dynamics of the fluorescent state of the DMAC in [bmim][PF_6]. As shown in Figure 5.3, solvation times are estimated by fitting the data to stretched exponential equation (see chapter 2 for the experimental details). With decrease in temperature an increase in the solvation time is evident from Figure 5.3 and Table 5.2. The spectrum with dotted line (Figure 5.2) represents time zero spectrum estimated following the procedure outlined in the experimental section. The calculated time-zero emission maximum $\bar{\nu}(0)_{calc}$ deviates from the value $(\bar{\nu}(0)_{exp})$ estimated from the experimental data. As shown in Table 5.2, the magnitudes of the shift $(\bar{\nu}(0)_{calc} - \bar{\nu}(0)_{exp})$

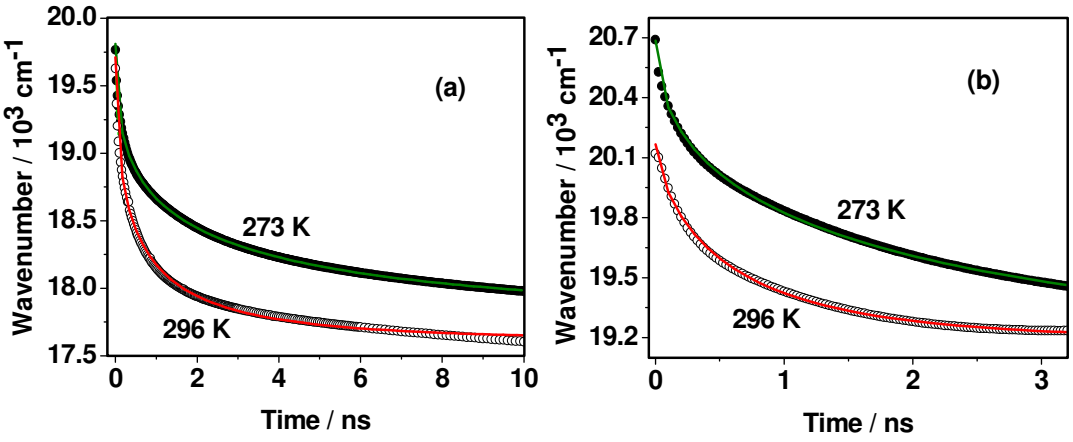

Figure 5.3. Stretched exponential fit to the solvation data in [bmim][PF_6] at 273 and 296 K for DMAC (a) and AC (b).

TABLE 5.2. TRES data of DMAC and AC in [bmim][PF_6] at 296 and 273 K

Temp.	Sample	$\bar{\nu}(0)_{calc} - \bar{\nu}(0)_{exp}$ / cm^{-1}	$\bar{\nu}(0)_{exp} - \bar{\nu}(\infty)$ / cm^{-1}	$\bar{\nu}(0)_{calc} - \bar{\nu}(\infty)$ / cm^{-1}
296 K	DMAC	670	2013	2683
	AC	2810	884	3694
273 K	DMAC	532	2055	2587
	AC	2240	1370	3610

Missing Component	$\bar{\tau}_{solv}$ / ns
25%	1.2
76%	0.6
21%	5.5
62%	1.2

of time-zero emission maxima of DMAC at 296 and 273 K are minimal and the calculated missing components of the solvation dynamics in [bmim][PF_6] are 25 and 21 % at 296 and 273 K, respectively, which are in accordance with the reported missing components of the solvation dynamics in highly viscous RTILs.[19]

Though TRES of AC also characterized with single emission maximum (Figure 5.4), fluorescence decay profiles and TRES data of AC are quite different from those of DMAC. Unlike DMAC, at the two different temperatures (296 and 273 K), no rise for the emission intensity-time profile of AC is noticed at longer emitting wavelengths. The stretched exponential fit to the solvation data of AC is shown in Figure 5.3. From Table 5.2, it is clear that the $\bar{\tau}_{solv}$ values of AC are much less than those of DMAC at both temperatures and values of

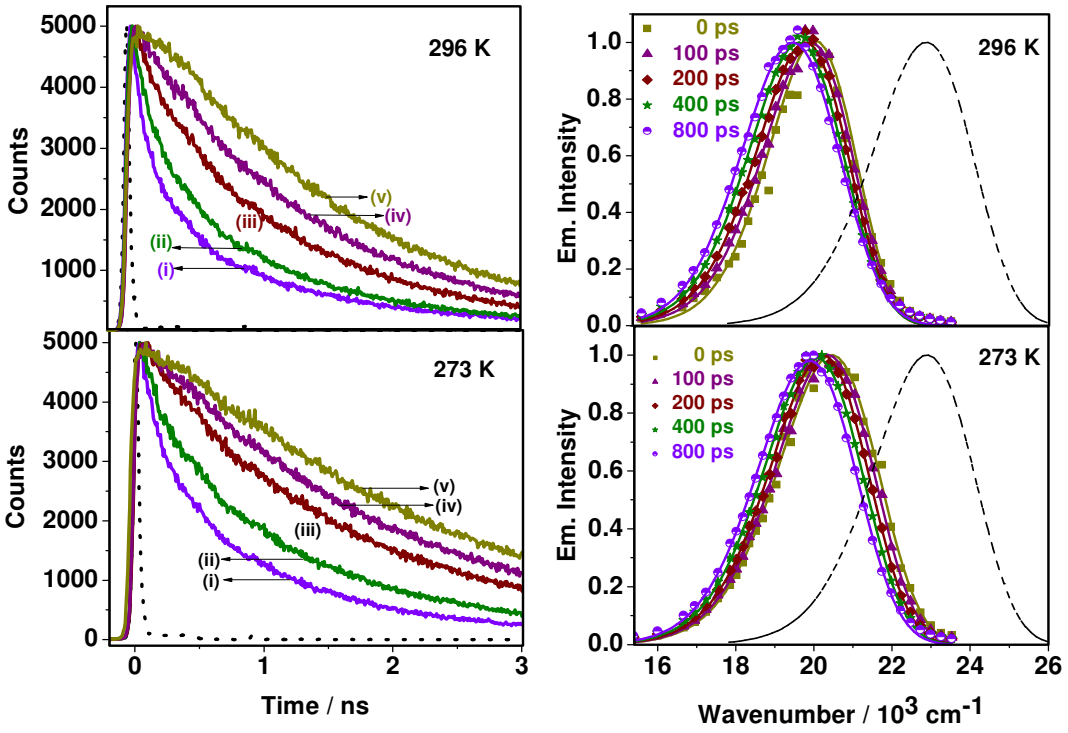

Figure 5.4. Emission wavelength dependent fluorescence decay profiles of AC (left panel) in [bmim][PF_6] at 296 K and 273 K. The monitoring wavelengths are (i) 475, (ii) 490, (iii) 515, (iv) 535 and (v) 580 nm. Lamp profile is shown as dotted line. Normalized TRES of AC in [bmim][PF_6] at different delay times are shown in the right panel. Spectrum with dotted line represents the estimated time-zero spectrum. λ_{exc} = 405 nm.

the shift in time-zero emission maximum $(\bar{\nu}(0)_{calc} - \bar{\nu}(0)_{exp})$ of AC are high compared to DMAC. The missing components estimated using the experimental and calculated time dependent Stokes shift $\left(\bar{\nu}(0) - \bar{\nu}(\infty)\right)$ values are exceptionally high and 76% at 296 K decreases to 62% at 273 K.

Even though in conventional less viscous solvents the chalcone derivatives do not display excitation wavelength dependent emission behavior, both DMAC and AC are found

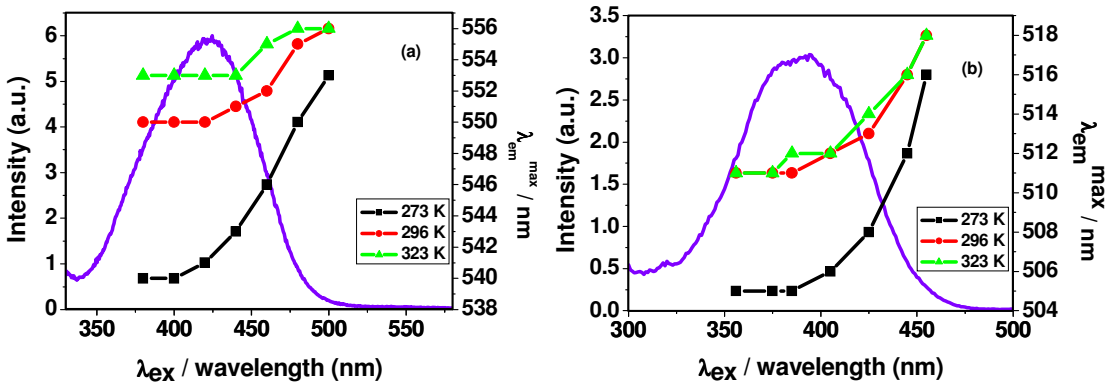

Figure 5.5. λ_{em}^{max} vs λ_{ex} plots of DMAC (a) and AC (b) in [bmim][PF_6] at three different temperatures. Excitation spectra of the compounds at 296 K are also shown.

TABLE 5.3. Excitation wavelength dependent shift of the fluorescence maxima of DMAC and AC in [bmim][PF_6] at different temperatures

Sample	Temp. / K	Shift of the fluorescence maximum / nm	$\bar{\tau}_{solv}$ / ns	$\bar{\tau}$ / ns
DMAC in [bmim][PF_6]	273	12	5.5	2.00
	296	6	1.2	1.40
	323	3	-	0.70
AC in [bmim][PF_6]	273	11	1.2	1.90
	296	7	0.6	1.20
	323	7	-	0.62

to display excitation wavelength dependent emission behavior, when excited at the red side of the absorption spectra in [bmim][PF_6]. Figure 5.5 shows the excitation wavelength dependent shift in the emission maxima of these molecules at different temperatures and their excitation spectra at 296 K. The magnitudes of the λ_{exc} dependent red shift of the spectral maxima of DMAC and AC measured at three different temperatures (273, 296 and 323 K) are compared (Table 5.3). DMAC shows a red shift of 12 nm at 273 K, which decreases gradually to 6 nm at 296 K and 3 nm at 323 K. AC also shows a similar trend in the temperature range of 273 to 296 K (shift from 11 to 7 nm), but behaves quite differently at higher temperature region, 296 to 323 K. Unlike DMAC, the spectral shift exhibited by AC is found independent of the temperature in the entire region from 296 to 323 K (Table 5.3).

5.3. DISCUSSION

5.3.1. Number and nature of the state

The data presented in Table 5.1 and spectral features depicted in Figure 5.1 clearly show that the emission of aminochalcones, DMAC and AC, originates only from a single charge transfer state. The time-resolved fluorescence measurements not only substantiate this but they also provide insights into the nature of this state. Despite high viscosity (285 cP) of [bmim][PF_6] at 296 K, the TRES of DMAC do not show any second emission component at room temperature. Even at a much lower temperature, 273 K, when [bmim][PF_6] is in its semi solid form, one anticipates a further slowdown of the twisting of a large moiety, which is necessary for the formation the A* state, and expects emission largely from the E* state with small or negligible contribution from the A* state. However, this is not the case. Figure 5.2 shows a single emission maximum even at low temperature. The findings are very similar for AC as well. Lack of dual emission in the TRES of the two compounds at room or low temperature unambiguously establishes that these molecules emit only from a single state, which can be either the A* state formed due to ultrafast E* $\rightarrow$ A* transformation (even in highly viscous medium) or the E* state which does not require any twisting.

According to literature, the aminochalcones emit from the E* state in non-polar solvents and from A* state in highly polar solvents.[16,17] However, if this were indeed the case, one would have observed some separation of the two emission bands with change in polarity of

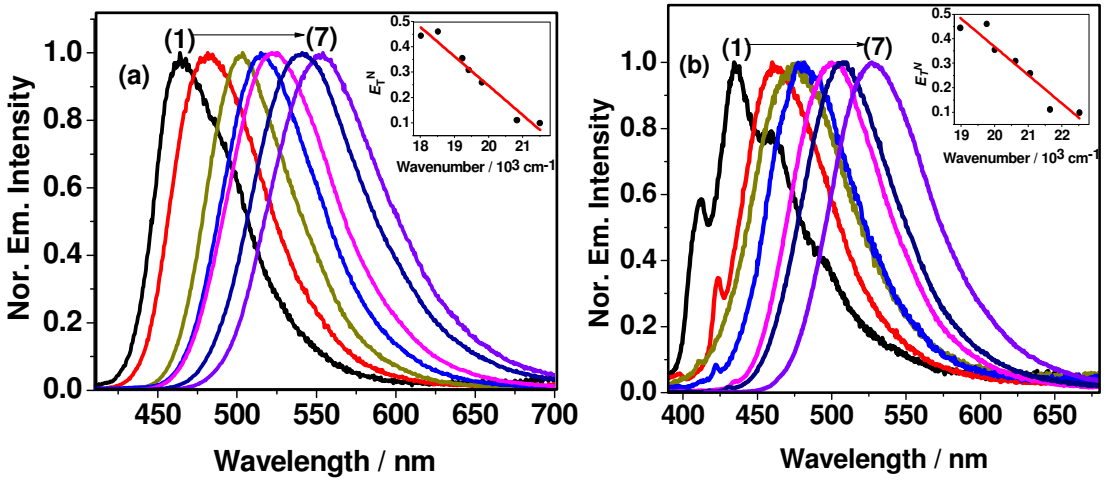

Figure 5.6. Emission spectra of DMAC (a) and AC (b) in different non polar and polar solvents. Solvents from (1) to (7) are toluene, dioxane, $CHCl_3$, DCM, acetone, acetonitrile and DMSO. E_T^N vs emission maximum (in cm^{-1}) plots are shown as insets.

the medium. However, as shown in Figure 5.6, this is not the case. The spectra in conventional solvents represent only one emission, which shows solvatochromic shift. The inset of Figure 5.6 shows the variation of the emission maximum with the polarity (E_T^N) of the medium. Had there been a change in the nature of the emitting state with variation of the polarity of the medium, there would have been a departure from the linear relationship, which is observed here. That the fluorescent state of the molecule is not associated with twisting of the dialkylanilino group is also evident from the change of dipole moment ($\Delta\mu = \mu_E - \mu_G$) on excitation. From the plots of Stokes shift $(\bar{\nu}_a - \bar{\nu}_f)$ vs E_T^N for both DMAC and AC (shown in Figure 5.7), the estimated $\Delta\mu$ values of DMAC and AC are 6.2 and 4.6 D, respectively. The $\Delta\mu$ value of the former, which is known already, is close to the estimated value.[16,17]. This change is too small to be explained in terms of the TICT model, particularly when the large distance of separation of the charge centres are taken into consideration. For example, even for a small molecule like 4-(N,N′-dimethylamino) benzonitrile (DMABN) or crystal violet lactone (CVL), where the TICT mechanism was invoked, the $\Delta\mu$ values (16 and 20 D) [20-22] are much higher than that for the present system. One can also use more line of arguments to come to the same conclusion. Firstly, the linearity of the plots clearly rules out

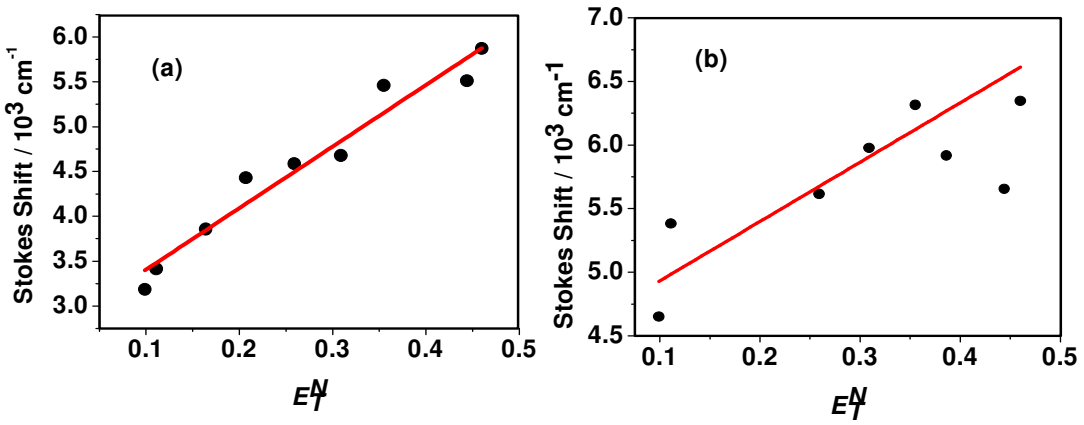

Figure 5.7. Stokes shift vs E_T^N plots of DMAC (a) and AC (b) in different solvents of different polarities.

any possibility of either the change of the nature of the state with polarity or involvement of the multiple states as found in some cases.[12,23] Secondly, had there been any involvement of the multiple fluorescent states, the fluorescence decay profiles would have been multi-exponential in nature. However, the single-exponential nature of the fluorescence decay profiles, as observed for the present systems, clearly point to the involvement of a single emitting state, which is clearly shown to be not the A* state.

5.3.2. Contrasting behavior of AC and DMAC

It is interesting to note the large difference of the fluorescence decay profiles and TRES of two structurally similar aminochalcones. The decay profiles of AC do not show any rise with time as observed in the case of DMAC. The time dependent shift of the emission spectra could be observed more clearly only in the case of DMAC. It is evident from the data that this difference is the result of significantly faster solvent relaxation of the fluorescent state of AC compared to DMAC. This aspect, i.e. a faster solvation of AC, is also evident from the shift of the actually observed time-zero spectrum from the expected time-zero spectrum. The difference in the peak frequencies of these two spectra, which is the result of fast solvation dynamics compared to the time resolution of the setup and is termed as the 'missing component' of the solvent relaxation, is much higher (76% and 62% at 296 and 273 K) in the case of AC compared to DMAC indicating clearly that solvent relaxation of the fluorescence

state of AC is much faster for the former system.

A faster solvation dynamics of AC in [bmim][PF_6] can be understood considering the specific solute-solvent interactions. Maroncelli and coworkers have shown that molecules which are engaged in H-bonding interaction with the solvent are characterized by faster solvation times than those which do not interact with the solvent molecules through specific interactions.[24] As the amino hydrogens of AC can involve in the H-bonding interactions with $[PF_6]^-$ of the RTIL, whereas DMAC cannot, the specific solute-solvent interaction can be considered as the factor responsible for faster solvation of AC in [bmim][PF_6]. This specific H-bonding interaction of AC with [bmim][PF_6] can also be used to understand the difference in the excitation wavelength dependence of the emission behavior of the two compounds in [bmim][PF_6]. At room temperature (296 K), DMAC and AC show an excitation wavelength dependent emission spectral shift of 6 and 7 nm, respectively (Table 5.3 and Figure 5.5).[25] A comparable solvation time and fluorescence lifetime of DMAC at 296 K makes it understandable why it exhibits excitation wavelength dependent emission behavior. However, as solvation time of AC is less than its fluorescence lifetime, the excitation wavelength dependent emission behavior of this system cannot be explained comparing the time scale of solvation time and fluorescence lifetime. To understand the origin of the excitation wavelength dependent emission spectra of AC, experiments have been carried out at lower (273 K) and higher (323 K) temperatures (Figure 5.5). Table 5.3 compares the solvation and fluorescence lifetimes of DMAC and AC at different temperatures. At lower temperature (273K) as the solvation time (5.5 ns) of DMAC is significantly higher than its fluorescence lifetime (2.00 ns), one observes emission from incompletely solvated state giving rise to a greater excitation wavelength dependence. At higher temperature (323K), as the solvation time of DMAC is lower than its fluorescence lifetime, the excitation wavelength dependent spectral shift becomes less pronounced. However, as the solvation times of AC are lower than the fluorescence lifetime at all working temperatures, its excitation wavelength dependence should not be due to the emission from incompletely solvated states. It is well known that hydrogen bonding interaction between the solute and solvent also gives rise to excitation wavelength dependent fluorescence behavior.[26] As AC is involved in the H-bonding interaction with $[PF_6]^-$, it is this factor that contributes to the excitation wavelength dependence of this molecule in [bmim][PF_6].

5.4. Conclusion

The present study reveals an interesting difference of the photophysical behavior of two structurally similar aminochalcones in ionic liquid. The nature of the emitting state in these compounds is also found to be different from the commonly accepted model. It is concluded that the emission in aminochalcones in polar environment (including ionic liquid) originates from a dipolar state which does not require any twisting. The fluorescence decay profiles, solvation dynamics and excitation wavelength dependent emission behavior of DMAC are found to be quite different from those of AC. A faster solvation dynamics and greater excitation wavelength dependence of the emission behavior of AC are attributed to specific H-bonding interactions of this compound with the RTIL.

REFERENCES

(1) Yang, C.-H.; Liao, S.-H.; Sun, Y.-K.; Chuang, Y.-Y.; Wang, T.-L.; Shieh, Y.-T.; Lin, W.-C. *J. Phys. Chem. C* **2010**, *114*, 21786.

(2) Rand, B. P.; Xue, J.; Uchida, S.; Forrest, S. R. *J. Appl. Phys.* **2005**, *98*, 124902/1.

(3) Bard, A.; Fox, M. A. *Acc. Chem. Res.* **1995**, *28*, 141.

(4) Bi, D.; Wu, F.; Qu, Q.; Yue, W.; Cui, Q.; Shen, W.; Chen, R.; Liu, C.; Qiu, Z.; Wang, M. *J. Phys. Chem. C* **2011**, *115*, 3745.

(5) Kawatsu, T.; Coropceanu, V.; Ye, A.; Bredas, J.-L. *J. Phys. Chem. C* **2008**, *112*, 3429.

(6) Huang, J.-H.; Wen, W.-H.; Sun, Y.-Y.; Chou, P.-T.; Fang, J.-M. *J. Org. Chem.* **2005**, *70*, 5827.

(7) Silva, A. P. d.; Leydet, Y.; Lincheneau, C.; McClenaghan, N. D. *J. Physics: Condensed Matter* **2006**, *18*, S1847.

(8) Montenegro, J.-M.; Perez-Inestrosa, E.; Collado, D.; Vida, Y.; Suau, R. *Org. Lett.* **2004**, *6*, 2401.

(9) Andersson, M.; Sinks, L. E.; Hayes, R. T.; Zhao, Y.; Wasielewski, M. R. *Angew. Chem. Int. Ed.* **2003**, *42*, 3139.

(10) Kondratenko, M.; Moiseev, A. G.; Perepichka, D. F. *J. Mater. Chem.* **2011**, *21*, 1470.

(11) Soujanya, T.; Fessenden, R. W.; Samanta, A. *J. Phys. Chem.* **1996**, *100*, 3507.

(12) Saha, S.; Samanta, A. *J. Phys. Chem. A* **2002**, *106*, 4763.

(13) Lapouyade, R.; Czeschka, K.; Majenz, W.; Rettig, W.; Gilabert, E.; Rulliere, C. *J. Phys. Chem.* **1992**, *96*, 9643.

(14) Sarkar, M.; Kanaparthi, R. K.; Bhattacharya, B.; Samanta, A. *J. Phys. Chem. A* **2008**, *112*, 3302.

(15) Shaikh, M.; Mohanty, J.; Singh, P. K.; Bhasikuttan, A. C.; Rajule, R. N.; Satam, V. S.; Bendre, S. R.; Kanetkar, V. R.; Pal, H. *J. Phys. Chem. A* **2010**, *114*, 4507.

(16) Wang, P.; Wu, S. *J. Photochem. and Photobiol. A: Chemistry* **1995**, *86*, 109.

(17) Rurack, K.; Dekhtyar, M. L.; Bricks, J. L.; Resch-Genger, T.; Rettig, W. *J. Phys. Chem. A* **1999**, *103*, 9626.

(18) Jiang, Y.-B.; Wang, X.-J. *J. Photochem. Photobiol. A: Chem.* **1994**, *81*, 205.

(19) Paul, A.; Samanta, A. *J. Phys. Chem. B* **2007**, *111*, 4724.

(20) Schuddeboom, W.; Jonker, S. A.; Warman, J. M.; Leinhos, U.; Kuhnel, W.; Zachariasse, K. A. *J. Phys. Chem.* **1992**, *96*, 10809.

(21) Rappoport, D.; Furche, F. *J. Am. Chem. Soc.* **2004**, *126*, 1277.

(22) Karpiuk, J. *J. Phys. Chem. A* **2004**, *108*, 11183.

(23) Kosower, E. M. *Acc. Chem. Res.* **1982**, *15*, 259.

(24) Chapman, C. F.; Fee, R. S.; Maroncelli, M. *J. Phys. Chem.* **1995**, *99*, 4811.

(25) Mandal, P. K.; Sarkar, M.; Samanta, A. *J. Phys. Chem. A* **2004**, *108*, 9048.

(26) Mandal, P. K.; Paul, A.; Samanta, A. *J. Photochem. and Photobiol. A: Chemistry* **2006**, *182*, 113.

CHAPTER 6

On the Mechanism of Fluorescence Quenching of Quantum Dots by Organic Fluorophores

Fluorescence quenching of CdS quantum dots (QDs) by 4-azetidinyl-7-nitrobenz-2-oxa-1,3-diazole (NBD), where the two quenching partners satisfy the spectral overlap criterion necessary for Förster resonance energy transfer (FRET), is studied by steady state and time-resolved fluorescence techniques. The fluorescence quenching of the QDs is accompanied by an enhancement of the acceptor fluorescence and a reduction of the average fluorescence lifetime of the donor. Even though these observations are suggestive of a dynamic energy transfer process, it is shown that the quenching actually proceeds through a static interaction between the quenching partners and is probably mediated by charge-transfer interactions. The bimolecular quenching rate constant estimated from the Stern–Volmer plot of the fluorescence intensities is found to be exceptionally high and unrealistic for the dynamic quenching process. Hence, a kinetic model is employed for the estimation of actual quencher/QD ratio dependent exciton quenching rate constants of the fluorescence quenching of CdS by NBD. The present results point to the need for a deeper analysis of the experimental quenching data to avoid erroneous conclusions.

6.1. Introduction

The quantum dots (QDs), wherein 3-dimensional quantum confinement of the electrons and holes results in discrete size-dependent interesting optical properties, have attracted tremendous interest because of their potential applications as biological reporters, light harvesting elements in solar energy conversion and tunable emitters in light-emitting diodes (LEDs), etc.[1-10] The intense fluorescence of the QDs is due to recombination of the bound electron (e) and hole (h) pair, known as exciton, produced on electronic excitation. Any process that leads to destruction of the electron or the hole contributes to fluorescence quenching of the QDs. As majority of the applications of the QDs are linked to the exciton quenching dynamics,[11-15] a clear understanding of the mechanism of fluorescence quenching

of the QDs is absolutely essential. Perhaps, this explains why the fluorescence quenching studies of the QDs have received significant attention in recent years.[11,13,14,16-25]

Charge (electron or hole) and energy transfer are the two most commonly encountered exciton quenching mechanisms. While quenching due to energy transfer process is governed by the spectral overlap of the donor emission and acceptor absorption and the donor-acceptor distance, the charge transfer induced quenching is determined by the redox potentials of the donor and acceptor.[17,26-30] The literature suggests that fluorescence quenching of the QDs by organic molecules is attributed to the energy transfer mechanism most often on the basis of the spectral overlap criterion and decrease in average lifetime.[31-35] Exciton dissociation of QDs by Förster resonance energy transfer (FRET) is a dynamic quenching process, whereas the quenching of QD emission by charge transfer (electron and/or hole) can proceed through either dynamic or static quenching mechanism.[28,29,36] There are some cases where both dynamic and static quenching mechanisms contribute to the QD exciton quenching.[37] Quenching process is also found to be dependent on the nature of quencher and the QD.[29,36]

The present work addresses some important issues concerning fluorescence quenching of the QDs by organic molecules, in particular, the static vs dynamics nature of the quenching and the energy transfer vs other mechanisms of quenching by investigating the fluorescence quenching of hexadecylamine capped CdS QDs by a highly fluorescent nitrobenzoxadiazole derivative, 4-azetidinyl-7-nitrobenz-2-oxa-1,3-diazole (NBD, Figure 6.1). The niitrobenzoxa-diazole derivatives belong to the family of electron donor-acceptor (EDA) molecules and are extremely popular candidates as fluorescent probes in biological applications.[38-40] Many NBD derivatives have been used in fluorescence depolarization and energy transfer studies.[41] Effect of the amino functionality on the fluorescence behavior of the NBD derivatives has also been studied.[42] The present couple displays excellent overlap of the emission spectrum of CdS and absorption spectrum of NBD, and exhibits quenching behavior typical of an energy transfer quenching process. However, a deeper study reveals that the quenching process is neither governed by the energy transfer process, nor it is dynamic in nature. We discuss the possible quenching mechanisms and show that CdS fluorescence quenching by NBD proceeds through static interaction between the two. The quenching rate constants are shown to be dependent on the number of NBD molecules adsorbed on the CdS surface and

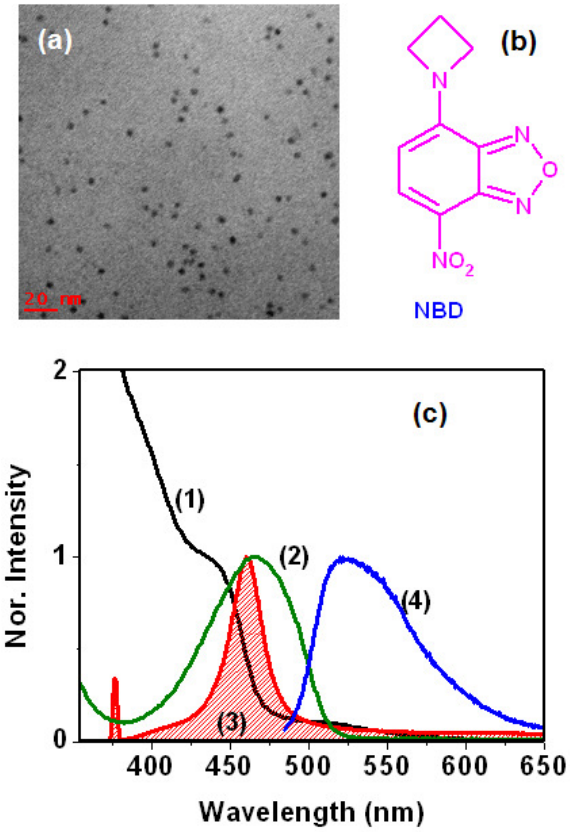

Figure 6.1. (a) TEM images of CdS QDs. (b) Structure of NBD. (c)Absorption spectra of CdS (1), NBD (2) and emission spectra of CdS (3) and NBD (4). Shaded region is the overlap region of CdS emission with NBD absorption.

the values of which have been estimated by employing a model suggested by Lian and co-workers.[22,36,43]

6.2. Steady state and time-resolved experiments

The QDs display typical broad absorption with the first exciton band maximum at ~ 436 nm and a narrow blue emission with maximum at ~ 460 nm (Figure 6.1). The spectral data presented in Figure 6.1, shows a significant overlap between the absorption spectrum of NBD and the emission spectrum of CdS QDs, thus making the present couple ideally suited for FRET interaction. The steady state and time-resolved fluorescence quenching studies have been performed by exciting the solutions at 375 nm, at which the absorbance due to the QDs

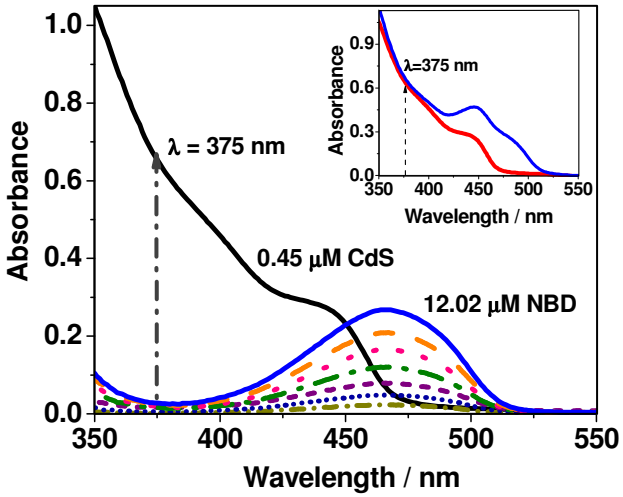

Figure 6.2. Comparison of the absorption spectrum of 0.45 µM CdS solution with those for various concentrations of NBD, highlighting the difference of the OD at the excitation wavelength (375 nm). Inset shows the absorption spectra of CdS (0.45 µM) in the absence and presence of 12.02 µM NBD.

(0.66 for the 0.45 µM solution used in all measurements) is much higher (by a factor of 22) than that due to NBD even for its highest concentration used in this study (0.03 for 12.02 µM solution), a condition ideally suited for a typical energy transfer experiment, which ensures that the excitation light is primarily absorbed by the donor. In order to highlight the OD values at the excitation wavelength, as shown in Figure 6.2, the absorption spectra of CdS and various concentrations of NBD are presented separately. Inset of the Figure 6.2 shows negligible contribution of the NBD towards the OD at 375 nm excitation wavelength. It also shows that the position of the first exciton band maximum of CdS remains constant even in the presence of highest concentration of NBD, thus indicating the stability of CdS QDs in the presence of NBD molecules.

Figure 6.3 shows a progressive decrease of the fluorescence intensity of CdS QDs and an enhancement of the emission of NBD with increase in concentration of the latter. The fluorescence quenching of the QDs leads to changes in the fluorescence decay parameters as well. The fluorescence decay profile of the QDs in the absence of NBD is best represented by a sum of three exponentials, $I(t) = a_1 \exp(-t/\tau_1) + a_2 \exp(-t/\tau_2) + a_3 \exp(-t/\tau_3)$,

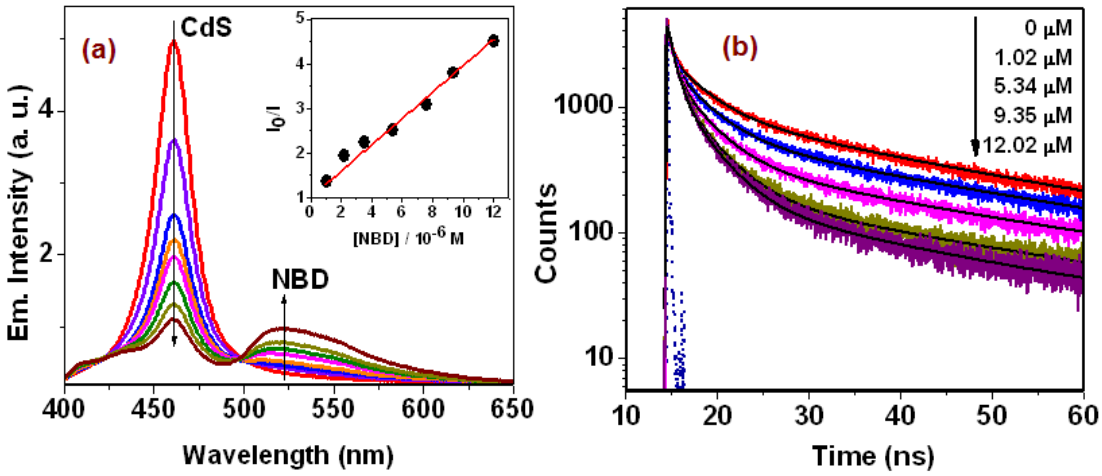

Figure 6.3. (a) Quenching of 0.45 µM CdS QD fluorescence with increasing NBD concentration from 1.02 µM to 12.02 µM. Inset shows the Stern–Volmer plot of the steady state emission intensities. (b) Fluorescence decay profiles of 0.45 µM CdS for different concentrations of NBD.

Table 6.1. Time-resolved fluorescence parameters of CdS (0.45 µM) for various concentrations of the quencher

[NBD] µM	[NBD]/[CdS]	τ_1 (b_1) [a] ns	τ_2 (b_2) [a] ns	τ_3 (b_3) [a] ns	$\langle\tau_{i0}\rangle$ ns	$\langle\tau_{a0}\rangle$ ns
0	CdS alone	3.73 (0.20)	27.80 (0.76)	0.40 (0.04)	21.90	5.44
1.02	2.27	3.67 (0.26)	28.60 (0.68)	0.50 (0.06)	20.43	4.40
2.23	4.98	3.63 (0.29)	28.68 (0.63)	0.50 (0.08)	19.16	3.90
3.56	7.96	3.64 (0.30)	29.22 (0.61)	0.58 (0.09)	18.96	3.83
5.34	11.97	3.52 (0.32)	28.53 (0.57)	0.63 (0.11)	17.46	3.42
7.57	17.00	3.69 (0.34)	30.25 (0.50)	0.71 (0.16)	16.50	3.05
9.35	21.11	3.60 (0.38)	28.30 (0.42)	0.76 (0.20)	13.41	2.60
12.02	27.38	3.40 (0.41)	25.10 (0.36)	0.78 (0.23)	10.61	2.33

(a) $b_i = a_i\tau_i/(a_1\tau_1+a_2\tau_2+a_3\tau_3)$

with the lifetime components of 3.73, 27.8 and 0.4 ns. These imply an intensity averaged lifetime $< \tau_{i0} >$, defined as $< \tau_{i0} > = (a_1\tau_1^2 + a_2\tau_2^2 + a_3\tau_3^2)/(a_1\tau_1 + a_2\tau_2 + a_3\tau_3)$, of 21.9 ns and an amplitude averaged lifetime $< \tau_{a0} >$, defined as $< \tau_{a0} >= (a_1\tau_1 + a_2\tau_2 + a_3\tau_3)/(a_1 + a_2 + a_3)$, of 5.44 ns. The multi-exponential nature of the fluorescence decay profile and the average lifetime of the CdS QD is consistent with the literature.[34] NBD induced changes in the fluorescence decay profile of QDs are depicted in Figure 6.3 and the decay parameters, which are collected in Table 6.1, show that the $< \tau_{i0} >$ and $< \tau_{a0} >$ values decreased to 10.61 and 2.33 ns, respectively in the presence of NBD (12.02 μM). The rate constant of quenching estimated from the Stern-Volmer plot of steady state intensities of the QD (Figure 6.3) using the $< \tau_{i0} >$ and $< \tau_{a0} >$ values are 1.4 x 10^{13} and 5.5 x 10^{13} $M^{-1}s^{-1}$, respectively. These quenching rate constants are several order of magnitude higher than the diffusion-limited value (10^{10} $M^{-1}s^{-1}$) expected from the Smoluchowski equation ($k_{diff} = 8RT/3\eta$) [44] and hence, the unrealistically large quenching constants cannot be understood with the help of Stern-Volmer equation if only the dynamic nature of the quenching process is considered.

6.3. Possible mechanisms of fluorescence quenching

6.3.1. FRET

Considering the excellent spectral overlap of the QD-NBD couple and the results described above if the fluorescence quenching is attributed to FRET interaction, questions may not be raised as increase of fluorescence intensity of the acceptor (NBD) is considered as evidence of FRET. In fact, one can even calculate some of the quenching parameters from the experimental data. For example, the Förster distance (R_0), estimated from the overlap integral and quantum yield of CdS, is 30.4 Å.[45] As a matter of fact, this is a fortuitous case, where the acceptor is also fluorescent. In cases involving the non-fluorescent acceptors, if the donor and acceptor exhibit good spectral overlap, the reduction of the fluorescence intensity and lifetime of the donor are the only experimental parameters used to assign a dynamic quenching mechanism involving FRET.

However, we show that when the experimental results are analyzed more carefully by raising deeper questions, which are most often disregarded, the FRET mechanism of fluores-

cence quenching, which appears rather obvious, actually turns out to be incorrect.

First, we attempt to reexamine whether the fluorescence quenching is indeed a dynamic process, which is apparently indicated by the reduction of <τ> value of the QDs. A close look at the fluorescence decay parameters of the QDs (Table 6.1), however, suggests that the individual lifetimes, which are expected to change in the case of dynamic quenching, do not change with increase in concentration of the acceptor (NBD), what varies are the preexponential factors associated with these components. Therefore, even though the average lifetime of the QD is decreased with increase in quencher concentration, the quenching process is not a dynamic one. As the short lifetime components of the QDs are believed to be due to the core states and the long-lived lifetime component arises from the surface states,[46-50] NBD induced changes of the relative contributions of different components, in particular, the decrease in contribution of the long-lived component, is indicative of destruction of the surface states due to static interaction between the QDs and NBD. As static interaction affects mainly the surface of the QDs, the contribution of the long-lived emission decreases and consequently, the relative contributions of the short and medium lifetime components increase. It is thus evident that a reduction of the <τ> value is not a reflection of the dynamic nature of quenching, but is the result of preferential destruction of the surface states of the QDs by the quencher on formation of the complex. The static quenching mechanism can only explain how the bimolecular rate constant of quenching can be higher than the diffusion controlled rate constant, an observation noted earlier, but was not paid any attention.[18,34]

Next, we analyze the time-dependence of the acceptor fluorescence, which, in the case of an energy transfer process, should show a rise (growth) of intensity with time (with the rise-time equal to the decay time of the donor). However, in our experiment, the fluorescence time profiles of the acceptor (NBD) (Figure 6.4) reveals no rise component (which is characterized by a negative pre-exponential factor), indicating that the emitting state of NBD is not produced due to energy transfer from the QD. One may argue that it may not be possible to observe a rise of the emission intensity of the acceptor when the rise-time is short and comparable to the finite time resolution of the experimental setup. However, the present case does not belong to this category as the QDs are characterized by long fluorescence lifetime and the rise component of the acceptor has in fact been observed in several cases.[18,19,51]

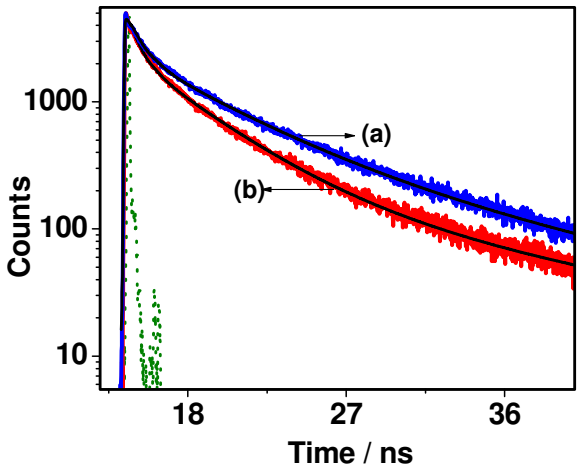

Figure 6.4. Fluorescence decay profiles of a toluene solution of NBD for different [NBD]/[CdS] ratios of 2.27 (a) and 27.38 (b). Lamp profile is shown as a dotted line. λ_{exc} = 375 nm. The fluorescence was monitored at 545 nm.

An acceptor need not be a fluorescence system, but when it is, the energy transfer efficiency (E) can be estimated from the enhancement in the acceptor fluorescence using the following relation,[22]

$$E = \frac{(I_{NBD/CdS} - I_{NBD})/\emptyset_{NBD/CdS}}{I_{CdS}/\emptyset_{CdS}} \qquad (1)$$

where, $I_{NBD/CdS}$ and I_{NBD} are the integrated fluorescence intensities of NBD in the presence and absence of CdS. Subsequently, we show that even enhancement of the steady state emission intensity of the acceptor, which appears as clinching evidence of the FRET mechanism, actually results from direct excitation of the acceptor, even though the quenching experiments have been carried out in best possible conditions (section 6.2). This is evident from the control experiments involving 375 nm excitation of 12.02 μM NBD in the absence and presence of 0.45 μM CdS, which showed that the emission intensity of NBD in the presence of CdS ($I_{NBD/CdS}$) is lower than that in the absence of CdS (I_{NBD}) (Figure 6.5) thus clearly establishing that FRET is not responsible for quenching of CdS QDs.

6.3.2. Depassivation of the QD surface

Depassivation of the surface ligands can also lead to fluorescence quenching. However, El-Sayed and coworkers have shown that replacement of the surface ligand (HDA) is possible only by small, straight chain amines like n-butylamine.[52] As bulky amines such as NBD cannot get through the capping agents easily, depassivation as a mechanism of fluoresc-

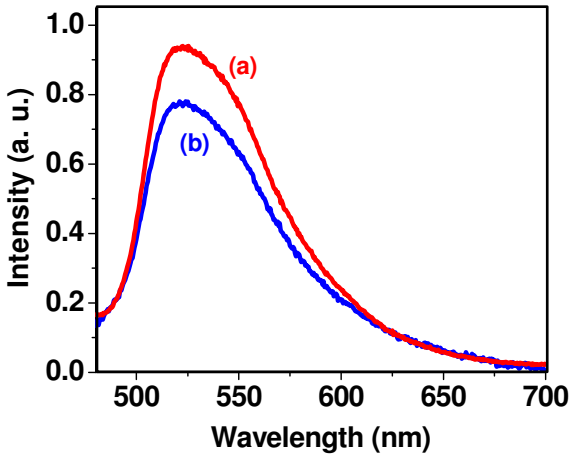

Figure 6.5. Emission spectra of 12.02 µM toluene solution of NBD in the absence (a) and presence (b) of 0.45 µM CdS solution. Both the emission spectra were recorded by exciting the samples at 375 nm.

ence quenching in this case can be ruled out. Replacement of stronger binding hexadecylamine (HDA) ligand by bulky NBD, whose ligating ability is greatly reduced due to the involvement of the lone pair of electrons of the amino group in intramolecular charge transfer with the nitro group, at a molar ratio (NBD:CdS = 2.27-27.38) at which it quenches the CdS emission is extremely unlikely.[53] It is also possible that depassivation of the surface ligands leads to aggregation of the QDs and contribute to the red shift in the first exciton band and fluorescence emission maxima. In our case, the CdS emission maximum and position of the first exciton band maximum remain unchanged throughout the experiment with the addition of NBD. The possibility of fluorescence quenching of the QDs due to the free unbound HDA also does not arise as the surface capped QDs were thoroughly washed with ethanol subsequent to its synthesis to ensure removal of all free/unbound HDA.

6.3.3. Charge transfer

Charge (electron or hole) transfer between the QDs and organic molecular systems, which is primarily governed by the redox potentials of the donor-acceptor couple, can be an alternative mechanism of fluorescence quenching of the QDs. In the present case, considering the redox potentials of CdS and NBD, we find that charge transfer between the two is a distinct possibility.

The redox potentials of the nano semiconductors (QDs) shift from their bulk flat band potentials and the extent of shift depends on the size of the QDs.[54,55] The bulk CB and VB potentials of CdS QDs are -0.7 V and +1.72 V (vs SCE) respectively.[27] The energy of the

lowest exciton band is dependent on the energy of the 1S electron in the conduction band and the 1S hole in the valence band. The energy of the first exciton band is given by equation (2),[27]

$$E_{CdS*}[1S_e, 1S_h] = E_g + \frac{\hbar^2\pi^2}{2R^2m_e^*} + \frac{\hbar^2\pi^2}{2R^2m_h^*} - \frac{1.8e^2}{4\pi\varepsilon_0\varepsilon R} \qquad (2)$$

where E_g is the bulk band gap energy (for CdS E_g= 2.42 eV), R is the radius of the QD (2.25 nm in the present case). m_e^* and m_h^* are the effective masses of the electron and hole. For CdS QDs the effective masses will be $m_e^* = 0.2m_0$ and $m_h^* = 0.8m_0$, where m_0 is the free electron's rest mass. Second and third terms represent the confinement energies of the electron in the conduction band and hole in the valence band respectively. The final term of the equation (2) explains the Coulomb attraction between electron and hole. Following the reported procedures, the estimated excited state oxidation ($CdS^*[1s_e, 1s_h] \rightarrow e + CdS^+[1s_h]$) and reduction ($CdS^*[1s_e, 1s_h] \rightarrow h + CdS^-[1s_e]$) potentials (vs SCE) for the QDs used in this study are -1.04 V and +1.64 V, respectively.[27,54,55] The oxidation and reduction potentials (vs SCE) of NBD are +1.54 V and -0.80 V respectively.[56] Schematic representation of these potentials (Scheme 6.1) clearly indicates that both electron and hole transfer are possible from CdS to NBD. The estimated values of the free energy change, however, suggest that the electron transfer process is thermodynamically more feasible (ΔG = -23.16 kJ/mol) compared to the hole transfer (ΔG = -9.65 kJ/mol).

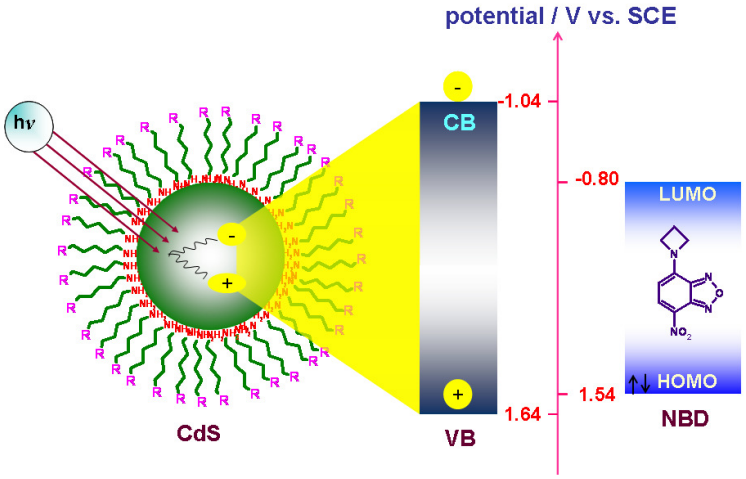

Scheme 6.1.

The charge transfer mechanism, which appears as a distinct possibility in the present case, can explain lack of enhanced emission of the acceptor or rise time associated with its emission time profile. The literature suggests different scenarios arising of fluorescence quenching of the QDs by the organic molecules involving charge transfer mechanism,[36] indicating that it can be a static or a dynamic process. Our case, where the individual lifetime components do not change but their relative contributions vary with change in the quencher concentration is similar to the quenching of CdTe QDs by pyromellitimide derivative (PI-CA),[28] is indicative of a static charge transfer quenching mechanism in accordance with the literature, which clearly suggest that the influence of charge transfer interaction on the lifetime is highly dependent on the nature of the quantum dot and the quencher.

That fluorescence quenching of CdS QD by NBD seems to proceed through a charge transfer mechanism is evident from a study of quenching of the QDs with another amine, p-phenylenediamine (PPD) in place of NBD. The low oxidation potential of PPD (0.016 V vs SCE) makes it an efficient hole scavenger,[17] but its higher excited state energy compared to the first exciton band energy of the QDs, rules out any possibility of the energy transfer process (Figure 6.6). Hence, PPD induced fluorescence quenching of the QDs, if any, must be due to charge (hole) transfer from the QDs to PPD only. Figure 6.7 accounts the quenching of QD fluorescence and lifetime by PPD and the lifetime time data at different quencher concentrations is tabulated in Table 6.2. This control experiment indeed shows effi-

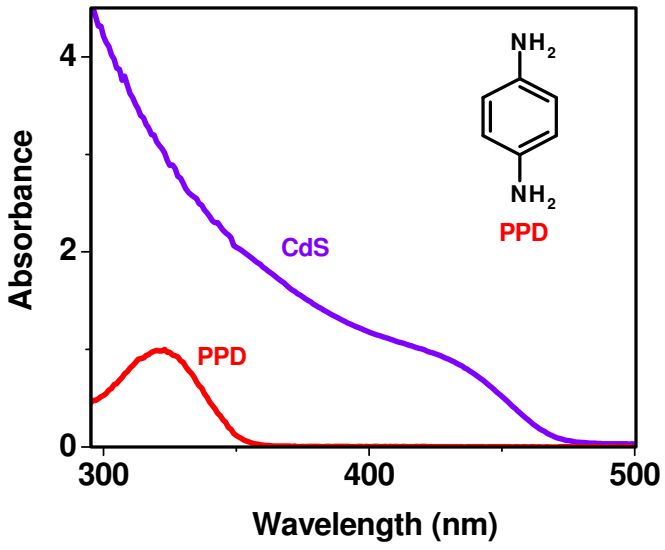

Figure 6.6. Absorption spectra of p-phenylenediamine (PPD) and CdS in toluene. Chemical formula of PPD is shown as inset.

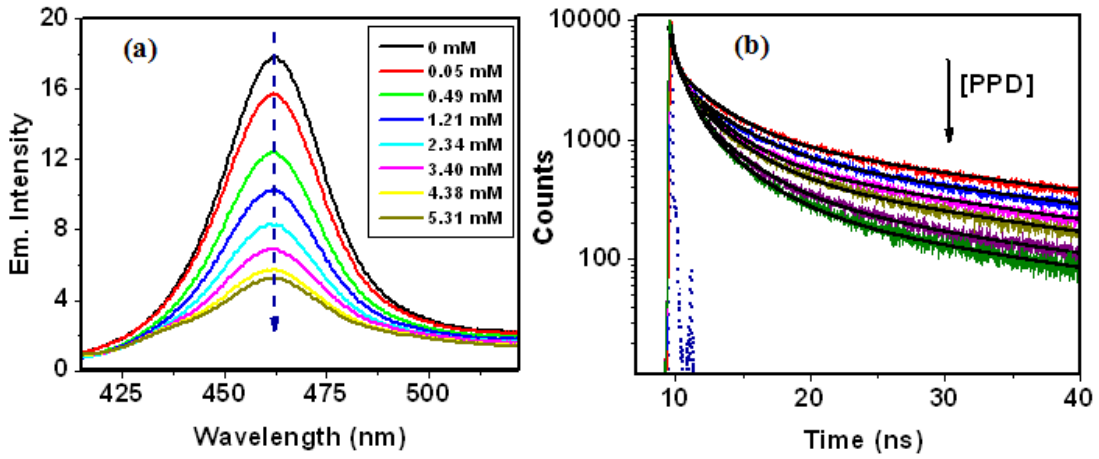

Figure 6.7. Fluorescence emission spectra (a) and fluorescence decay profiles (b) of 0.85 µM CdS in toluene at different concentrations of PPD from 0 to 5.31 mM. λ_{exc} = 405 nm for steady state and time-resolved experiments. Emission decay profiles were recorded by monitoring emission at 460 nm. Lamp profile is shown as dotted line.

Table 6.2. Time-resolved fluorescence parameters of 0.85 µM toluene solution of CdS at different PPD concentrations

[PPD] mM	τ_1 (b_1) [a] ns	τ_2 (b_2) [a] ns	τ_3 (b_3) [a] ns	$<\tau_{i0}>$ ns
CdS alone	3.05 (0.28)	22.5 (0.66)	0.28 (0.06)	15.6
0.12	3.40 (0.30)	21.2 (0.63)	0.50 (0.07)	14.4
1.21	3.15 (0.33)	19.8 (0.50)	0.65 (0.15)	11.0
2.34	2.85 (0.30)	19.2 (0.47)	0.44 (0.20)	10.2
3.40	3.43 (0.36)	19.6 (0.42)	0.89 (0.22)	9.6
5.31	3.24 (0.37)	19.5 (0.33)	0.84 (0.30)	7.9

(a) $b_i = a_i\tau_i/(a_1\tau_1+a_2\tau_2+a_3\tau_3)$

cient fluorescence quenching and reduction of the average fluorescence lifetime of the QDs (with negligible change in the individual lifetimes) in the presence of PPD. As this

observation is similar to that observed in the case of NBD and as PPD can quench the QD fluorescence only by charge transfer interaction, it is evident that NBD interacts with the CdS excitons through a charge transfer mechanism.

6.4. QD fluorescence quenching: The kinetic model

CdS exciton quenching by NBD proceeds in competition with the unimolecular decay process and leads to a decrease in steady state emission intensity and average lifetime of CdS. As stated in section 6.2, the bimolecular quenching rate constant estimated from the Stern-Volmer equation is much higher than the diffusion limited rate constant. This is something that is difficult to comprehend, though such high values have been reported in the literature.[18,34] Even though in the concentration range used herein no deviation from linearity in the Stern-Volmer plot is observed, which is most often indicative of the static nature of the quenching, the variation of lifetime with quencher concentration has unambiguously established the static nature of the quenching, thus making the Stern Volmer equation unsuitable in the present case. The literature reports do indicate that the Stern Volmer equation is not obeyed in some cases of quenchinng of the QD fluorescence by organic molecules and the quenching rate constants are estimated assuming that quenching occurs in the associated complex between QD and the quencher.[17,57] For an associated complex comprising two species, the quenching rate constant is given by equation,[58]

$$k_q = 1/\tau - 1/\tau_0 \qquad (3)$$

where, τ and τ_0 are the decay times of the QD in the presence and absence of the quencher. The present case of CdS quenching by NBD is also the result of preferential destruction of the surface states of the QDs by the quencher on formation of the complex.

The quenching rate constant estimated from equation (3) is dependent on the concentration of NBD and Table 6.3 depicts the variation of these k_q values. The values, as expected, vary considerably, depending on whether intensity averaged ($k_{q(i)}$) or amplitude averaged ($k_{q(a)}$) lifetime is used. As all NBD molecules in the solution may not participate in the quenching process and only those closely associated with the surface of the CdS are effective in quenching of the QDs, the k_q values shown in the 2nd and 3rd columns of Table 6.3 may not represent the correct rate constants for the quencher concentration used.

Therefore, one should have a knowledge of the NBD(adsorbate)/CdS ratio dependent exciton quenching dynamics. For this purpose, we have used a model developed by Lian and coworkers,[22,36] which involves finding out the average number of NBD molecules attached to the surface of each QD.

Table 6.3. Quenching rate constants

[NBD] μM	$k_{q(i)}$ [s^{-1}]	$k_{q(a)}$ [s^{-1}]	[NBD]/[CdS]	m		$k_{q(m)}$ [s^{-1}]
1.02	0.3 x 10^7	0.4 x 10^8	2.27	1.8		4.3 x 10^8
5.34	1.2 x 10^7	1.1 x 10^8	11.97	2.2	$k_{q(1)}$= 2.4 x 10^8 s^{-1}	5.3 x 10^8
9.35	2.9 x 10^7	2.0 x 10^8	21.11	2.8		6.7 x 10^8
12.02	4.9 x 10^7	2.5 x 10^8	27.38	3.0		7.2 x 10^8

Assuming that the adsorption of NBD on the surface of the CdS is random and is not dependent on the number of NBDs already adsorbed on the CdS surface, the number of NBD molecules on the surface of a QD can be obtained from the Poisson distribution, according to which the probability (f_n) of finding QD with n number of NBD molecules adsorbed is given by equation (4),

$$f_n = \sum_n \frac{m^n}{n!} e^{-m} \qquad (4)$$

where m is the average number of NBD molecules adsorbed on each CdS QD.

Assuming that the rate of quenching depends linearly on the number of quencher molecules adsorbed, if $k_{q(1)}$ is the quenching rate in 1:1 NBD/CdS system, then the rate of quenching ($k_{q(n)}$) in n:1 NBD/CdS system is given by

$$k_{q(n)} = nk_{q1} \qquad (5)$$

Thus if $k_{q(1)}$ and m are known, $k_{q(m)}$ can be estimated for different concentrations of the NBD.

According to this model, if $[N_0^*]$ is the initial concentration of the excited CdS QDs having an average of m number of NBD molecules adsorbed on its surface, the concentration

of the excited CdS at a time t is given by[22]

$$\left[N_t^*\right] = \left[N_0^*\right]\left[\sum_j A_j \exp(-m + me^{-k_{1j}t})\right]\left[\sum_i b_i e^{-k_i t}\right] \qquad (6)$$

where, b_i and k_i are the relative amplitude and decay rate constant of the i^{th} component of the fluorescence decay of CdS QDs in the absence of NBD and obtained simply by fitting the decay profile of free CdS QDs to $I(t) = a_1\exp(-t/\tau_1) + a_2\exp(-t/\tau_2) + a_3\exp(-t/\tau_3)$ with $b_i = a_i\tau_i/(a_1\tau_1+a_2\tau_2+a_3\tau_3)$. The other parametrs ($A_j$, k_{1j} and m) of equation (6) are obtained by fitting this equation to the fluorescence decay profiles of the QDs for different NBD concentrations. Using the values of A_i and k_{1j}, the m values for other quencher concentrations were obtained by fitting the respective plots. The quenching rate estimated for the 1:1 NBD/CdS system ($k_{q(1)}$) is 2.4 x 10^8 s^{-1}. The m values for different concentrations of NBD and the corresponding $k_{q(m)}$ values are shown in Table 6.3 and compared with the $k_{q(i)}$ and $k_{q(a)}$ values.

6.5. Conclusion

Fluorescence quenching of CdS QDs by a fluorescent organic molecular system, NBD, was studied. Even though the two interacting species display quenching behavior, which appears typical of a FRET mechanism, careful investigation reveals that the quenching process is neither dynamic nor does it involve the FRET mechanism. It is shown that the quenching actually proceeds through a static interaction between the quenching partners and is probably mediated by a charge transfer process. The quenching behavior is explained assuming that quenching occurs in the associated complex formed between CdS and NBD. The quenching rate constant, which is dependent on the number of NBD molecules adsorbed on the CdS surface, has been evaluated from the kinetic data using a recently developed model. The results show that unless utmost care is taken with the interpretation and analysis of the quenching data, one may end up with an incorrect picture of the mechanism of fluorescence quenching of the QDs and a wrong estimate of the quenching rate constant.

REFERENCES

(1) Kamat, P. V.; Tvrdy, K.; Baker, D. R.; Radich, J. G. *Chem. Rev.* **2010**, *110*, 6664.

(2) Willard, D. M.; Carillo, L. L.; Jung, J.; Orden, A. V. *Nano Lett.* **2001**, *1*, 469.

(3) Bakalova, R.; Zhelev, Z.; Ohba, H.; Baba, Y. *J. Am. Chem. Soc.* **2005**, *127*, 11328.

(4) Nagasaki, Y.; Ishii, T.; Sunaga, Y.; Watanabe, Y.; Otsuka, H.; Kataoka, K. *Langmuir* **2004**, *20*, 6396.

(5) Pons, T.; Medintz, I. L.; Wang, X.; English, D. S.; Mattoussi, H. *J. Am. Chem. Soc.* **2006**, *128*, 15324.

(6) Robel, I.; Subramanian, V.; Kuno, M.; Kamat, P. V. *J. Am. Chem. Soc.* **2006**, *128*, 2385.

(7) Huynh, W. U.; Dittmer, J. J.; Alivisatos, A. P. *Science* **2002**, *295*, 2425.

(8) Tachibana, Y.; Akiyama, H. Y.; Ohtsuka, Y.; Torimoto, T.; Kuwabata, S. *Chem. Lett.* **2007**, *36*, 88.

(9) Coe, S.; Woo, W. K.; Bawendi, M.; Bulovic, V. *Nature* **2002**, *420*, 800.

(10) Zhao, J. L.; Bardecker, J. A.; Munro, A. M.; Liu, M. S.; Niu, Y. H.; Ding, I. K.; Luo, J. D.; Chen, B. Q.; Jen, A. K. Y.; Ginger, D. S. *Nano Lett.* **2006**, *6*, 463.

(11) Medintz, I. L.; Konnert, J. H.; Clapp, A. R.; Stanish, I.; Twigg, M. E.; Mattoussi, H.; Mauro, J. M.; Deschamps, J. R. *Proc. Natl. Acad. Sci. USA* **2004**, *101*, 9612.

(12) Shim, M.; Wang, C.; Guyot-Sionnest, P. *J. Phys. Chem. B* **2001**, *105*, 2369.

(13) Huang, J.; Stockwell, D.; Huang, Z.; Mohler, D. L.; Lian, T. *J. Am. Chem. Soc.* **2008**, *130*, 5632.

(14) Sykora, M.; Petruska, M. A.; Alstrum-Acevedo, J.; Bezel, I.; meyer, T. J.; Klimov, V. I. *J. Am. Chem. Soc.* **2006**, *128*, 9984.

(15) Schaller, R. D.; Sykora, M.; Jeong, S.; Klimov, V. I. *J. Phys. Chem. B* **2006**, *110*, 25332.

(16) Baker, D. R.; Kamat, P. V. *Langmuir* **2010**, *26*, 11272.

(17) Sharma, S. N.; Pillai, Z. S.; Kamat, P. V. *J. Phys. Chem. B* **2003**, *107*, 10088.

(18) Funston, A. M.; Jasieniak, J. J.; Mulvaney, P. *Adv. Mater.* **2008**, *20*, 4274.

(19) Medintz, I. L.; Pons, T.; Susumu, K.; Boeneman, K.; Dennis, A. M.; Farrell, D.; Deschamps, J. R.; Melinger, J. S.; Bao, G.; Mattoussi, H. *J. Phys. Chem. C* **2009**, *113*, 18552.

(20) Lutich, A. A.; Jiang, G.; Susha, A. S.; Rogach, A. L.; Stefani, F. D.; Feldmann, J. *Nano Lett.* **2009**, *9*, 2636.

(21) Noone, K. M.; Anderson, N. C.; Horwitz, N. E.; Munro, A. M.; Kulkarni, A. P.; Ginger, D. S. *ACS Nano* **2009**, *3*, 1345.

(22) Boulesbaa, A.; Huang, Z.; Wu, D.; Lian, T. *J. Phys. Chem. C* **2010**, *114*, 962.

(23) Rawalekar, S.; Kaniyankandy, S.; Verma, S.; Ghosh, H. N. *ChemPhysChem* **2011**, *12*, 1729.

(24) Verma, S.; Gupta, A.; Sainis, J. K.; Ghosh, H. N. *J. Phys. Chem. Lett.* **2011**, *2*, 858.

(25) Rawalekar, S.; Kaniyankandy, S.; Verma, S.; Ghosh, H. N. *J. Phys. Chem. C* **2010**, *114*, 1460.

(26) Tvrdy, K.; Frantsuzov, P. A.; Kamat, P. V. *Proc. Natl. Acad. Sci. USA* **2011**, *108*, 29.

(27) Boulesbaa, A.; Issac, A.; Stockwell, D.; Huang, Z.; Huang, J.; Guo, J.; Lian, T. *J. Am. Chem. Soc.* **2007**, *129*, 15132.

(28) Cui, S.-C.; Tachikawa, T.; Fujitsuka, M.; Majima, T. *J. Phys. Chem. C* **2008**, *112*, 19625.

(29) Vinayakan, R.; Shanmugapriya, T.; Nair, P. V.; Ramamurthy, P.; Thomas, K. G. *J. Phys. Chem. C* **2007**, *111*, 10146.

(30) Zhang, Y.; Jing, P.; Zeng, Q.; Sun, Y.; Su, H.; Wang, Y. A.; Kong, X.; Zhao, J.; Zhang, H. *J. Phys. Chem. C* **2009**, *113*, 1886.

(31) Goldman, E. R.; Medintz, I. L.; Whitley, J. L.; Hayhurst, A.; Clapp, A. R.; Uyeda, H. T.; Deschamps, J. R.; Lassman, M. E.; Mattoussi, H. *J. Am. Chem. Soc.* **2005**, *127*, 6744.

(32) Zhou, D.; Piper, J. D.; Abell, C.; Klenerman, D.; Kang, D.-J.; Ying, L. *Chem. Commun.* **2005**, 4807.

(33) Nikiforov, T. T.; Beechem, J. M. *Analytical Biochemistry* **2006**, *357*, 68.

(34) Sadhu, S.; Patra, A. *ChemPhysChem* **2008**, *9*, 2052.

(35) Sadhu, S.; Tachiya, M.; Patra, A. *J. Phys. Chem. C* **2009**, *113*, 19488.

(36) Huang, J.; Huang, Z.; Jin, S.; Lian, T. *J. Phys. Chem. C* **2008**, *112*, 19734.

(37) Jin, W. J.; Fernandez-Arguelles, M. T.; Costa-Fernandez, J. M.; Pereiro, R.; Sanz-Medel, A. *Chem. Commun.* **2005**, 883.

(38) Chattopadhyay, A. *Chem. Phys. Lipids* **1990**, *53*, 1.

(39) Fager, R. S.; Kutina, C. B.; Abrahamson, E. W. *Analytical Biochemistry* **1973**, *53*, 290.

(40) Ferguson, S. J.; Lloyd, W. J.; Radda, G. K. *Biochem. J.* **1976**, *159*, 347.

(41) Allen, D. J.; Benkovic, S. J. *Biochemistry* **1989**, *28*, 9586.

(42) Saha, S.; Samanta, A. *J. Phys. Chem. A* **1998**, *102*, 7903.

(43) Tachiya, M. *J. Chem. Phys.* **1982**, *76*, 340.

(44) Paul, A.; Samanta, A. *J. Phys. Chem. B* **2007**, *111*, 1957.

(45) Santhosh, K.; Patra, S.; Soumya, S.; Khara, D. C.; Samanta, A. *ChemPhysChem* **2011**, *12*, 2735.

(46) Bawendi, M. G.; Carroll, P. J.; Wilson, W. L.; Brus, L. E. *J. Chem. Phys.* **1992**, *96*, 946.

(47) Wang, X.; Zhang, J.; Nazzal, A.; Darragh, M.; Xiao, M. *Appl. Phys. Lett.* **2002**, *81*, 4829.

(48) Klimov, V. I.; McBranch, D. W.; Leatherdale, C. A.; Bawendi, M. G. *Phys. Rev. B: Condens. Matter Mater. Phys.* **1999**, *60*, 13740.

(49) Wang, X.; Qu, L.; Zhang, J.; Peng, X.; Xiao, M. *Nano Lett.* **2003**, *3*, 1103.

(50) Yang, Z.; Liu, Y.; He, X.; Wen, Y.; Yang, Y. *J. Appl. Phys.* **2010**, *108*, 094309.

(51) Soujon, D.; Becker, K.; Rogach, A. L.; Feldmann, J.; Weller, H.; Talapin, D. V.; Lupton, J. M. *J. Phys. Chem. C* **2007**, *111*, 11511.

(52) Landes, C. F.; Braun, M.; El-Sayed, M. A. *J. Phys. Chem. B* **2001**, *105*, 10554.

(53) McArthur, E. A.; Morris-Cohen, A. J.; Knowles, K. E.; Weiss, E. A. *J. Phys. Chem. B* **2010**, *114*, 14514.

(54) Brus, L. E. *J. Chem. Phys.* **1983**, *79*, 5566.

(55) Brus, L. E. *Chem. Phys.* **1984**, *80*, 4403.

(56) Saha, S. Influence of Amino Functionality and Polarity of the Medium on the Photophysical Behavior of Some Electron Donor-Acceptor Molecules, Ph. D. Thesis, University of Hyderabad, 2002.

(57) Cui, S.-C.; Tachikawa, T.; Fujitsuka, M.; Majima, T. *J. Phys. Chem. C* **2010**, *114*, 1217.

(58) Lakowicz, J. R. *Pronciples of Fluorescence Spectroscopy, 2nd ed.*; Kluwer/Plenum: New York, 1999.

CHAPTER 7

Exploring the CdTe Quantum Dots in RTILs

Poor solubility of the semiconductor quantum dots (QDs) severely restricts studies on these substances in RTILs. It also limits applications, which require both these promising classes of materials. In this work, a simple method employing a task-specific thiol-functionalized imidazolium ionic liquid (**SH-UMIM**) is developed that allows study of luminescent CdTe QDs of different sizes in a large number of RTILs. Luminescence studies based on ensemble and single-particle blinking measurements have been performed to investigate the role of the capping agent and the media (RTILs) on the stability and luminescence properties of the QDs in these media. The results suggest that improved luminescence properties of the CdTe QDs in RTILs is due to the capping agent, **SH-UMIM**, and the enhanced stability of the QDs toward molecular oxygen is provided by the RTILs because of low solubility of oxygen in these viscous media.

7.1. Introduction

QDs and RTILs are two promising classes of materials, which have attracted a great deal of attention in recent years because of their potential in many applications.[1-12] As discussed in the previous chapters, the QDs exhibit interesting size-dependent optical properties due to three-dimensional quantum confinement of the electrons and holes, produced on photoexcitation.[13] Strongly luminescent QDs offer several advantages over the organic dye molecules in many applications as biological reporters, tunable emitters in light emitting diodes (LEDs), photo-detector devices due to their high molar extinction coefficient, thermal stability, long luminescence lifetimes and photostability.[7,14,15] In addition, low cost of these materials, size dependent tunability of the luminescence properties and possibility of multiple exciton generation (MEG) allow QDs to produce high-performing and low-cost QD-based photovoltaic devices.[2,3,16-19]

On the other hand, low volatility, high thermal stability, ability to dissolve many inorganic and organic compounds have made the RTILs as possible alternatives to the

volatile organic solvents in chemical reactions, catalysis and separation processes.[9,20,21] Because of their high ionic conductivity, low reactivity and wide electrochemical window provided by the RTILs, these serve as excellent electrolytes in electrochemical applications such as in lithium-ion batteries, double-layer capacitors, fuel cells and actuators.[22-26] In materials chemistry, RTILs have been used for the synthesis of inorganic nanomaterials, metal oxide nanorods and nanowires.[27,28] Transition-metal nanoparticles synthesized in RTILs have been found to show high stability and good catalytic activity.[29]

The QD-sensitized solar cells (QDSCs) have attracted significant attention in recent years.[2,3,16-19] The sulfide/polysulfide and ferricyanide/ferrocyanide salts in aqueous media or $[\mathrm{Co(o-phen)_3}]^{2+/3+}$ in organic solvents are usually used as electrolytes in these studies.[30-32] However, practical limitations of leakage and evaporation of the solvent is a major impediment to the commercialization and long term use of these devices for applications.[33] RTILs are being considered as viable electrolyte alternative to the electrolyte solutions in aqueous or organic solvents to enhance the durability of the solar cells.[33-35] Grätzel and coworkers have in fact used RTILs as electrolytes in dye sensitized solar cells (DSSCs).[33,35] Recently, an attempt has been made to use sulfide/polysulfide-based RTIL for QDSCs to avoid problems due to the water-based electrolyte solution.[34]

Prior to the employment of the RTILs in QDSCs, it is necessary to study the interaction of the RTILs with the QDs, in particular, the influence of the RTILs on the luminescence properties of the QDs as the efficiency of a solar cell depends on the interactions of the electrolytes with the photosensitizers.[36] However, these studies are severely limited by the solubility issue of the QDs in RTILs. Even though metal and metal oxide nanoparticles have been studied in RTILs,[27,37] very few studies dealing with interactions between QD and RTIL have been made so far.[38-43] Nakashima and Kawai managed to transfer the CdTe QDs into an hydrophobic RTIL by extracting an aqueous solution of cationic thiol derivative-capped QDs with 1-butyl-3-methylimidazolium bis(trifluoromethanesulfonyl)imide.[42] While this was a first successful attempt of transfer of the QDs into a RTIL, one of the major drawbacks, which was recognized by these authors, is that the applicability of this method is restricted only to the hydrophobic RTILs.[43] In fact our attempts to prepare the RTIL-soluble QDs following the procedure of Nakashima et al.[42,43] employing an alkaline solution of 3-

mercaptopropionic acid or aminoethanethiol hydrochloride were unsuccessful despite the ionic nature of the capping agents.

In this work, we deal with the poor solubility of CdTe QDs in RTILs, which makes these two otherwise extremely useful materials almost incompatible, by first designing a simple new task-specific imidazolium ionic liquid (IL) and then integrating it with the QDs in the form a QD-IL hybrid. We demonstrate that this method allows one to work with the CdTe nanocrystals of all sizes in both hydrophilic and hydrophobic RTILs to characterize these hybrids and investigate the role of the RTILs and capping agent by luminescence studies based on ensemble and single particle blinking experiments.

7.2. CdTe/SH-UMIM QD-IL Hybrids

The task specific thiol-functionalized IL, **SH-UMIM**, was first synthesized by reaction between 1-methylimidazole and 11-bromoundecanethiol according to the procedure detailed in chapter 2. A dilute $CHCl_3$ solution of **SH-UMIM** (0.05 M) was slowly added to a solution of hexadecylamine (HDA) capped CdTe nanocrystals in $CHCl_3$ until the particles flocculate out of the solution as a precipitate of the QD-IL hybrid, **CdTe/SH-UMIM**, on replacement of the capping agent, HDA, by **SH-UMIM** (Scheme 7.1). The fluorescent precipitate (QD-IL hybrid) was separated out from $CHCl_3$ by centrifugation and then the solubility of the hybrid was examined in several hydrophilic and hydrophobic RTILs (Chart 1.6), which consisted of both imidazolium and non-imidazolium RTILs. Except for $[N_{1888}][Tf_2N]$, the **SH-UMIM** capped CdTe QDs are found to be soluble in all other RTILs to give a clear solution of the QDs in these media. The hydrophobic pockets formed by the long alkyl chains could be responsible for the insolubility of the polar hybrid in $[N_{1888}][Tf_2N]$ RTIL.[44]

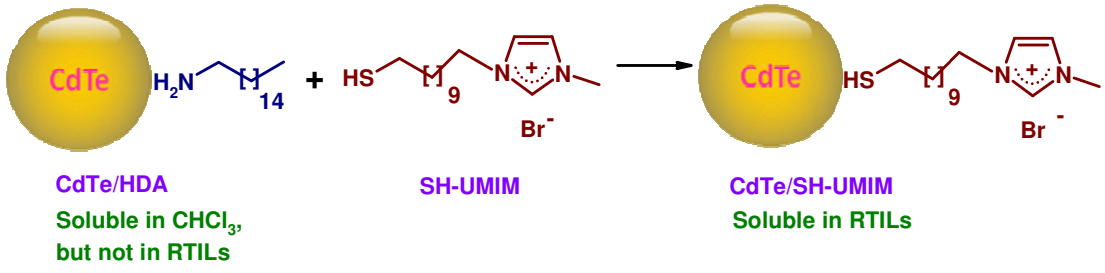

Scheme 7.1. Capping agent replacement

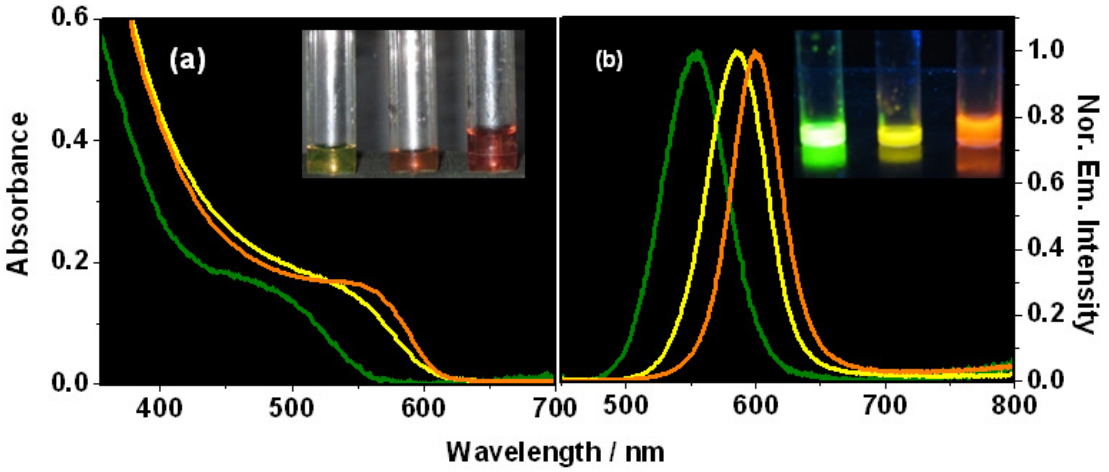

Figure 7.1. Absorption (a) and fluorescence (b) spectra of CdTe/SH-UMIM of three different sizes (2.07, 3.06 and 3.29 nm) in [bmim][BF_4]. λ_{exc} = 440 nm

QD-IL hybrids of three different sizes have been prepared and their absorption and emission spectra in [bmim][BF_4] RTIL are shown in Figure 7.1. Irrespective of the size, all three QD samples are fluorescent in RTIL. As the solubility of the QDs commonly depends on the nature of the capping agent and is independent of the size of the QD, this method works for CdTe nanocrystals of different sizes. Figure 7.2 compares the spectral properties of the HDA-capped QDs in $CHCl_3$ with the **CdTe/SH-UMIM** hybrids in three different RTILs; hydrophilic [bmim][BF_4] and hydrophobic [bmim][PF_6] and [bmim][Tf_2N]. As shown in Figure 7.2 and the data presented in Table 7.1, the QD-IL hybrids exhibit a blue shift of the λ_{max}^{abs} and λ_{max}^{em}values in RTILs relative to the corresponding spectra of CdTe/HDA QDs in $CHCl_3$. This observation is consistent with the literature, which indicates that replacement of an amine capping agent with mercaptopropionic acid or aminoethanethiol hydrochloride gives rise to similar shift.[45] A redistribution of the electronic density and increase in the confinement energy due to a stronger thiol-Cd binding compared to the amine-Cd one perhaps contributes to the observation. Similar blue shift of the CdSe emission was also observed when TOPO was replaced with primary amines.[46] The inset of Figure 7.2 shows a TEM image of the QD-IL hybrid in [bmim][PF_6]. As the size of the QDs in [bmim][PF_6] obtained from the TEM image (3.4 nm) matches reasonably well with the calculated (3.3 nm) value following a reported procedure,[47] the sizes of the remaining QD samples in $CHCl_3$ (3.5

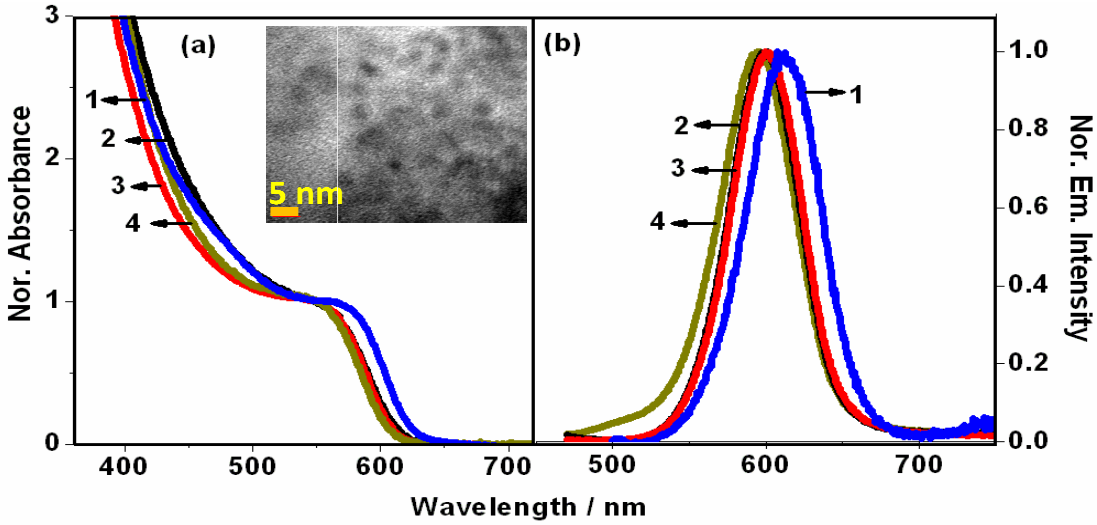

Figure 7.2. Absorption (a) and emission (b) spectra of CdTe/HDA in $CHCl_3$ (1) and CdTe/SH-UMIM in [bmim][PF_6] (2), [bmim][BF_4] (3) and [bmim][Tf_2N] (4). Inset shows the TEM image of the CdTe/SH-UMIM QDs in [bmim][PF_6].

nm), [bmim][BF_4] (3.3 nm) and [bmim][Tf_2N] (3.3 nm) have been estimated following the same method. The error limits of the estimated sizes are within ± 5 – 10 %.[47] The narrow emission width (fwhm ≈ 45 nm) of all the QD samples rules out the possibility of any significant inhomogeneity in the sample. The independence of the emission maximum on the excitation wavelength of each sample also reveals that the QD-IL samples are homogeneous. It is important to note that even though the size of the QD decreases on replacement of the capping agent, HDA by **SH-UMIM**, the size of the QD-IL hybrid, **CdTe/SH-UMIM**, is independent of the nature of the RTIL in which it is dissolved. No deep trap emission is indicated by the luminescence spectrum of **CdTe/SH-UMIM** indicating that **SH-UMIM** effectively protects the QD surface by reducing the number of trap states on the surface. The replacement of HDA by **SH-UMIM** leads to ~2-fold enhancement of the photoluminescence quantum yield (Φ_f) and fluorescence lifetime ($<\tau>$) values of the QDs in RTILs compared to $CHCl_3$ (Table 7.1). Figure 7.3 shows the effect of ligand exchange on the fluorescence decay profiles of the CdTe QDs. The decay profiles are fitted to a tri-exponential function and Table 7.1 collects the individual lifetime components and average lifetime values of the QDs in $CHCl_3$ and different RTILs. Transfer of the QDs from $CHCl_3$ into RTIL enhances the indi-

Table 7.1. Spectral properties, fluorescence quantum yield and decay parameters of the QDs in $CHCl_3$ and few common imidazolium RTILs

Sample	λ_{max}^{abs} / nm	λ_{max}^{em} / nm	Φ_f
CdTe/HDA in $CHCl_3$	575	612	0.12
CdTe/SH-UMIM in [bmim][PF_6]	556	600	0.24
CdTe/SH-UMIM in [bmim][BF_4]	554	600	0.28
CdTe/SH-UMIM in [bmim][Tf_2N]	551	595	0.25

τ_1 (a_1)	τ_2 (a_2)	τ_3 (a_3)	<τ> [a] / ns
2.80 (0.30)	13.50 (0.57)	0.18 (0.13)	8.55
5.98 (0.33)	20.72 (0.60)	0.90 (0.07)	14.46
5.27 (0.30)	20.44 (0.64)	0.52 (0.06)	14.70
5.00 (0.29)	18.74 (0.63)	0.80 (0.08)	13.32

(a) The error associated with <τ> will be within ± 0.15 ns.

vidual lifetime components, but very little variation of the lifetime could be observed in different RTILs.

In order to evaluate the role of the capping agent, **SH-UMIM** and the medium (RTIL) on the luminescence properties of the QDs, single particle blinking experiments have been carried out for three different immobilized samples; CdTe/HDA (**I**), **CdTe/SH-UMIM** (**II**) and **CdTe/SH-UMIM/**[bmim][PF_6] (**III**). Scheme 2.3 of chapter 2 represents QD immobilization for the samples of the single particle blinking studies.

As the single particle blinking behavior is found very similar for **II** and **III**, the fluorescence intensity trajectories, on- and off-time histograms, on- and off-time probability

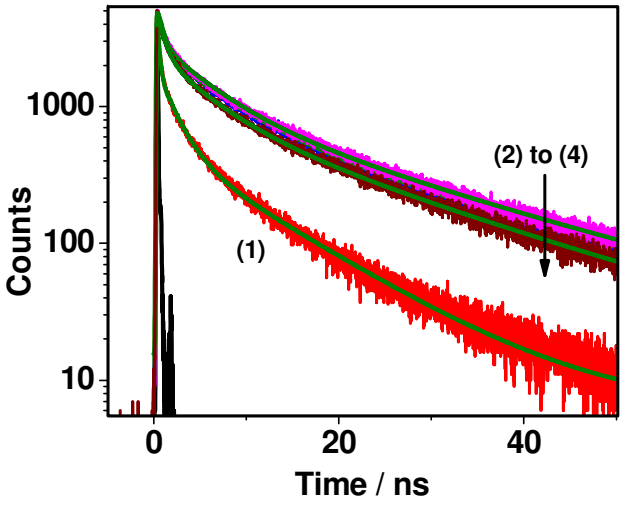

Figure 7.3. Fluorescence decay profiles of CdTe/HDA in $CHCl_3$ (1) and CdTe/SH-UMIM in [bmim][PF_6] (2), [bmim][BF_4] (3) and [bmim][Tf_2N] (4). λ_{exc} = 439 nm.

distributions, and fluorescence lifetime histograms of only **II** are shown in Figure 7.4 along with those of **I**. The average values of the data collected for several single particles are given in Table 7.2. Figure 7.4a highlights the difference in single particle intermittency (blinking or intensity fluctuation) of **I** and **II**, showing an enhancement of the fluorescence intensity and a decrease in the 'off' states in **II** compared to **I**.

Histograms of the on (τ_{on}) and off (τ_{off}) events are shown in Figure 7.4b and the τ_{on} and τ_{off} values are estimated from the single exponential fit to the corresponding histograms. Table 7.2 compares the τ_{on} and τ_{off} values of samples **I-III**. It is evident that the exchange of HDA by **SH-UMIM** significantly enhances the τ_{on} values and decreases the τ_{off} values. Interestingly, these values are very similar for samples **II** and **III**. For each QD, a wide distribution of the τ_{on} and τ_{off} values is observed. To quantify the occurrence of the "on" and "off" times of duration time "t", as shown in Figure 7.4c, the probability densities, $P_i(t)$, of the "on" and "off" times of each QD are calculated as follows.

Fluorescence photons binned over 50 ms were used to construct the fluorescence intensity trajectories as a function of the arrival time. QDs show a distribution of "on" and "off" times with a duration time of t. The probability density $P_i(t)$ of the both "on" and "off" times of duration time t was achieved by following equation[48,49]

$$P_i(t) = \frac{N_i(t)}{N_{total}} \times \frac{1}{\Delta t_{avg}} \qquad (\text{i} = \text{on } or \text{ off}) \qquad (1)$$

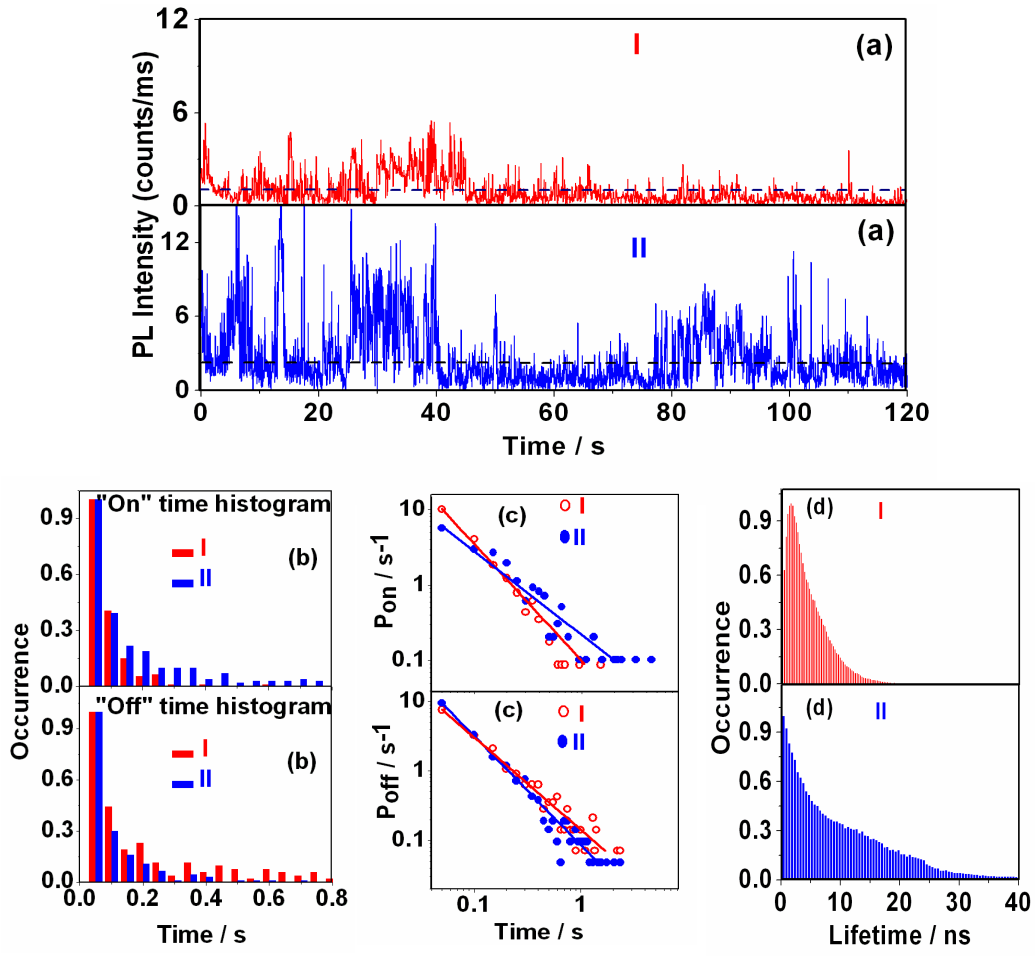

Figure 7.4. Fluorescence intensity trajectories (a), on- and off- time histograms (b), on- and off- time probability distributions (c) and fluorescence lifetime distributions (d) of I and II. The dotted line (a) indicates a threshold; data points above and below which are assigned to the fluorescence on and off times respectively.

where, N(t), N_{total} and Δt_{avg} are the number of "on" or "off" events, total number of "on" or "off" events and the average time between the nearest neighbor event bins respectively. Now the $P_i(t)$ values are fitted to a simple power law equation,

$$P_i(t) = At^{-m_i} \qquad (\text{i = on } or \text{ off}) \qquad (2)$$

where, A is the amplitude and m_i is the power law component that describes the "on" or "off" time distribution.[48,49] The m_i values given in Table 7.2 show noticeable difference between **I**

and those for **II** and **III**. The data suggests a longer on-time events and shorter off-time events for **II** compared to **I**. The lifetime distributions of several single particles of **I** and **II** (Figure 7.4d) account for the improved lifetimes of the CdTe nanoparticles on replacement of HDA with **SH-UMIM**.

These results can be understood considering a stronger binding ability of the thiols compared to the amines to the surface cadmium of the CdTe QDs. The "On" state corresponds to the emission resulting from the recombination of the electron-hole pair, whereas the "off" state of the QDs can be due to many factors such as Auger ionization, trap states on the surface of the QDs, etc.[50-52] A reduction of the processes contributing to the off-states can decrease the τ_{off} value and enhance the τ_{on} values of the QDs. As amine-Cd bonding is relatively weaker, it leaves some trap states on the surfaces of the QDs. Replacement of the amine-based capping agents like HDA by thiol-based ones like **SH-UMIM**, which binds to the surface much stronger and hence, can reduce the number of trap states, decreases the τ_{off} value, increases the τ_{on} value and improves the lifetime distribution. This explanation is in agreement with the enhancement of the luminescence efficiency and lifetime observed in ensemble measurements. The similar τ_{on}, τ_{off}, m_{on} and m_{off} values of **II** and **III** suggest that the media (RTILs) play no role in controlling the trap states. Thus the findings of the single particle study are consistent with those obtained from the ensemble study supporting that it is the capping agent, **SH-UMIM**, which is responsible for the enhancement in the Φ_f and $<\tau>$ values of the QDs in RTILs compared to $CHCl_3$. Thiol induced suppression of the single particle QD blinking and enhancement of the Φ_f and $<\tau>$ values are documented in the literature.[45,53,54]

Table 7.2. Photoblinking parameters[a] of the CdTe QDs

Sample	τ_{on} / s	τ_{off} / s	m_{on}	m_{off}
I	0.098	0.188	1.57	1.21
II	0.130	0.160	1.35	1.37
III	0.137	0.156	1.38	1.35

(a) Error in τ_{on} and τ_{off} values: ± 5 % and in m_{on} and m_{off} values: ± 3 – 5 %

These QD-IL hybrids are characterized by their remarkable stability towards molecular oxygen in RTILs. It is found that the fluorescence of the QDs capped either with the amines or thiols when exposed to air, is quenched due to slow reaction of the QDs with O_2.[55,56] As expected, on exposure to air the CdTe/HDA QDs in $CHCl_3$, a blue shift of the absorption and emission maxima, a decrease in the peak amplitude of the absorption and quenching of the

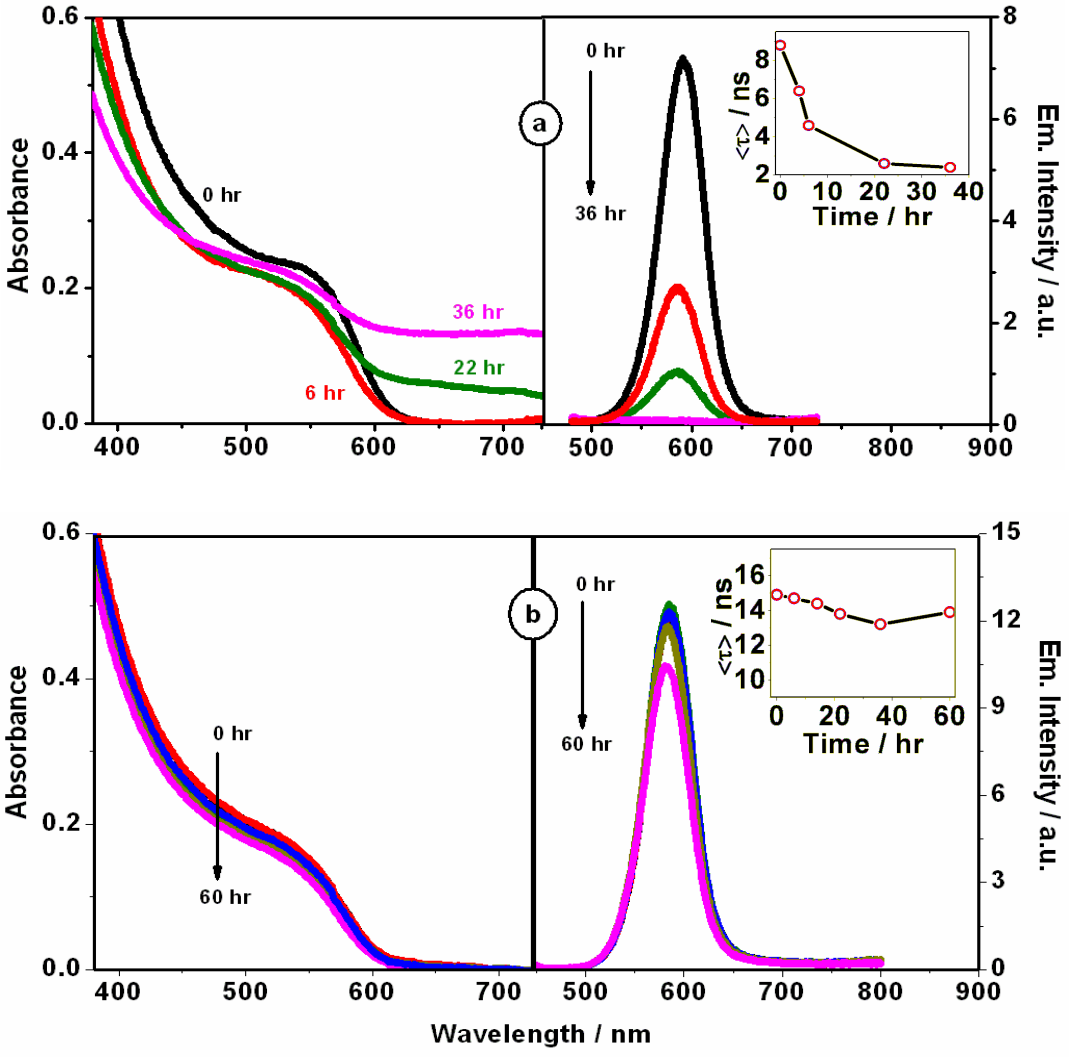

Figure 7.5. A comparison of the effect of exposure to air on the absorption and fluorescence spectral behavior and fluorescence lifetime of the CdTe/HDA QDs in $CHCl_3$ (a) and CdTe/SH-UMIM QDs in [bmim][BF_4] (b).

fluorescence intensity and lifetime are observed (Figure 7.5a) with time. The same experiment, when performed with **CdTe/SH-UMIM** in [bmim][BF_4], reveals (Figure 7.5b) the stability of QD-IL hybrids towards O_2. Unlike in $CHCl_3$, the absorption and emission behavior of the QD-IL hybrids is very little unaffected even after exposure to air for several hours. This remarkable stability of the QDs towards O_2 can be due to the protection offered by the capping agent. Literature suggests that thiol based capping agents may or may not protect the QD surface from oxidation.[56] 3-mercaptopropionic acid, for example, does not provide any protection from O_2, whereas β-mercaptoethanol (BME) due to its antioxidant properties does protect the CdTe QDs from surface oxidation.[56] In $CHCl_3$, O_2 has a very good solubility (9.8 mM)[57] and when the QDs are exposed to air, O_2 molecules can easily diffuse through this solvent and the capping agent to destroy the surface of the QDs leaving the metal ions and chalcogenide oxides in the solution. The non-zero absorption in the 600-700 nm region observed for higher exposure time (Figure 7.5a) is due to the scattering from insoluble metal ions and tellurium oxide in $CHCl_3$.[55,58-61] That in $CHCl_3$, neither the solvent nor the capping agent protects the QDs from surface oxidation is evident from the Figure 7.5a. Thus the remarkable stability of the QDs in RTILs should be attributed to the viscous nature of these liquids and low solubility of O_2. Poor solubility (< 0.2 mM)[62,63] of O_2 in RTILs and its slow diffusion in these viscous media make the interaction between O_2 and QD surface an unimportant event in RTILs. Hence, it is not the capping agent, **SH-UMIM,** but the RTIL that protects the QDs from O_2 and enhances stability of the QD-IL hybrids.

7.3. CdSe/SH-UMIM QD-IL Hybrids

We have also tested this new IL-based capping agent (**SH-UMIM**) on the solubility of the CdSe QDs in RTILs. Figure 7.6 compares the absorption and emission spectral properties of CdSe/**SH-UMIM** in [bmim][BF_4] with those of CdSe/HDA in $CHCl_3$. Even though these **CdSe/SH-UMIM** QDs are soluble in RTILs, the fluorescence of the system is quenched by the capping agent **SH-UMIM**, like most other thiols.[64] As shown in Figure 7.6b, the band edge emission is quenched completely with the evolution of a deep trap emission on transfer of the CdSe QDs from $CHCl_3$ into [bmim][BF_4]. This observation is similar to that observed by Kamat and coworkers, who suggested strong binding between the Cd atom of QDs and S atom of the thiol weakens the Cd-Se bond of QD causing Se vacancies on the QD surface,[65]

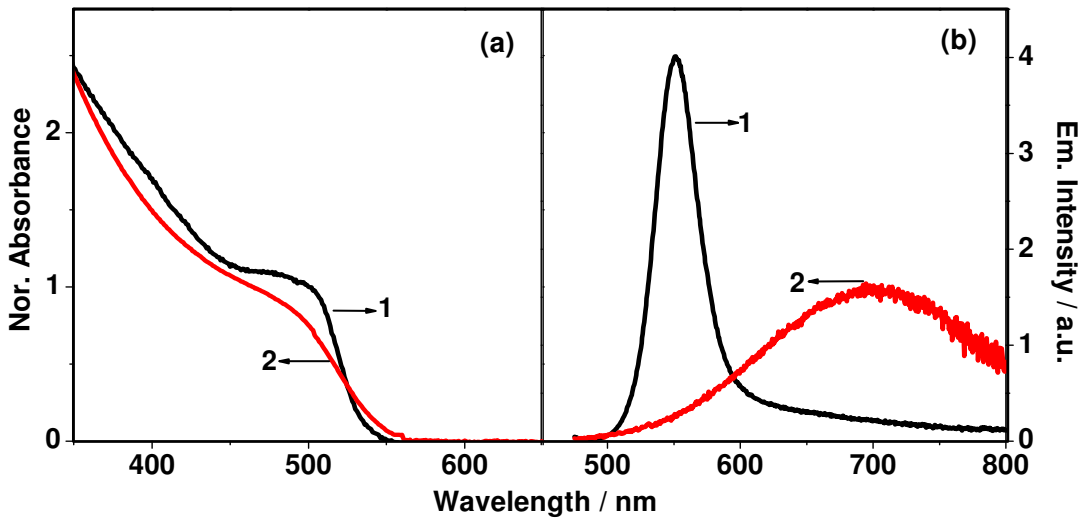

Figure 7.6. Absorption (a) and fluorescence (b) spectra of CdSe/HDA in $CHCl_3$ (1) and CdSe/SH-UMIM in [bmim][BF_4] (2).

which are responsible for the formation of deep trap emission and quenching the band edge emission.[66,67] The thiol can also act as a hole scavenger for the CdSe QDs and quench their fluorescence via a hole transfer mechanism.[64]

7.4. Conclusion

In summary, a simple method for the preparation of luminescent CdTe QD-IL hybrids, which are soluble in both hydrophilic and hydrophobic RTILs, is developed. Investigation of the role of the RTILs and task-specific capping agent, **SH-UMIM**, by luminescence studies based on both ensemble and single particle blinking measurements, reveal that improved emission properties of the QDs in RTILs is due to the protection offered to it by **SH-UMIM** and enhanced stability of the QDs towards O_2 is due to low solubility of O_2 and viscous nature of the RTILs. The present results, which provide the first opportunity to work with the CdTe nanocrystals in almost all RTILs without sacrificing their luminescence properties and stability, are likely to stimulate new investigations, thus raising the possibility of development of a new generation of promising materials.

REFERENCES

(1) Kamat, P. V.; Tvrdy, K.; Baker, D. R.; Radich, J. G. *Chem. Rev.* **2010**, *110*, 6664.
(2) Kamat, P. V. *Acc. Chem. Res.* **2012**, *45*, 1906.
(3) Robel, I.; Subramanian, V.; Kuno, M.; Kamat, P. V. *J. Am. Chem. Soc.* **2006**, *128*, 2385.
(4) Huynh, W. U.; Dittmer, J. J.; Alivisatos, A. P. *Science* **2002**, *295*, 2425.
(5) Pons, T.; Medintz, I. L.; Wang, X.; English, D. S.; Mattoussi, H. *J. Am. Chem. Soc.* **2006**, *128*, 15324.
(6) Coe, S.; Woo, W. K.; Bawendi, M.; Bulovic, V. *Nature* **2002**, *420*, 800.
(7) Bakalova, R.; Zhelev, Z.; Ohba, H.; Baba, Y. *J. Am. Chem. Soc.* **2005**, *127*, 11328.
(8) Willard, D. M.; Carillo, L. L.; Jung, J.; Orden, A. V. *Nano Lett.* **2001**, *1*, 469.
(9) Seddon, K. R. *Ionic Liquids, Industrial Applications for Green Chemistry, American Chemical Society, Washington DC*, 2002.
(10) Plechkova, N. V.; Seddon, K. R. *Chem. Soc. Rev.* **2008**, *37*, 123.
(11) Zhang, Y.; Chen, X.; Lan, J.; You, J.; Chen, L. *Chem. Biol. Drug Des.* **2009**, *74*, 282.
(12) Zhen, Y.; Wubin, P. *Enzyme Microb. Technol.* **2005**, *37*, 19.
(13) Smith, A. M.; Nie, S. *Acc. Chem. Res.* **2010**, *43*, 190.
(14) Hoshino, K.; Gopal, A.; Glaz, M. S.; Bout, D. A. V.; Zhang, X. *Appl. Phys. Lett.* **2012**, *101*, 043118/1.
(15) Vaillancourt, J.; Vasinajindakaw, P.; Lu, X. *Optics and Photonics Lett.* **2011**, *4*, 57.
(16) Etgar, L.; Zhang, W.; Gabriel, S.; Hickey, S. G.; Nazeeruddin, M. K.; Eychmüller, A.; Liu, B.; Grätzel, M. *Adv. Mater.* **2012**, *24*, 2202.
(17) Yang, Z.; Chen, C.-Y.; Roy, P.; Chang, H.-T. *Chem. Commun.* **2011**, *47*, 9561.
(18) Nozik, A. J. *Chem. Phys. Lett.* **2008**, *457*, 3.
(19) Schaller, R. D.; Klimov, V. I. *Phys. Rev. Lett.* **2004**, *92*, 186601/1.
(20) Dubreuil, J. F.; Bourahla, K.; Rahmouni, M.; Bazureau, J. P.; Hamelin, J. *Catal. Commun.* **2002**, *3*, 185.
(21) Hallett, J. P.; Welton, T. *Chem. Rev.* **2011**, *111*, 3508.
(22) Enomoto, T.; Nakamori, Y.; Matsumoto, K.; Hagiwara, R. *J. Phys. Chem. C* **2011**, *115*, 4324.
(23) Ngo, H. L.; LeCompte, K.; Hargens, L.; McEwen, A. *Thermochim. Acta* **2000**, *357*, 97.
(24) Armand, M.; Endres, F.; MacFarlane, D. R.; Ohno, H.; Scrosati, B. *Nat. Mater.* **2009**, *8*, 621.
(25) Lewandowski, A.; Swiderska-Mocek, A. *J. Power Sources* **2009**, *194*, 601.
(26) Ding, J.; Zhou, D.; Spinks, G.; Wallace, G.; Forsyth, S.; Forsyth, M.; MacFarlane, D. *Chem. Mater.* **2003**, *15*, 2392.
(27) Yang, L. X.; Zhu, Y. J.; Wang, W. W.; Tong, H.; Ruan, M. L. *J. Phys. Chem. B* **2006**, *110*, 6609.
(28) Okazaki, K.-i.; Kiyama, T.; Hirahara, K.; Tanaka, N.; Kuwabata, S.; Torimoto, T. *Chem. Commun.* **2008**, 691.
(29) Migowski, P.; Dupont, J. *Chem. Eur. J.* **2007**, *13*, 32.
(30) Kamat, P. V. *J. Phys. Chem. C* **2008**, *112*, 18737.
(31) Lee, H. J.; Yum, J.-H.; Leventis, H. C.; Zakeeruddin, S. M.; Haque, S. A.; Chen, P.; Seok, S. I.; Grätzel, M.; Nazeeruddin, M. K. *J. Phys. Chem. C* **2008**, *112*, 11600.
(32) Tena-Zaera, R.; Katty, A.; Bastide, S.; Levy-Clement, C. *Chem. Mater.* **2007**, *19*, 1626.
(33) Zakeeruddin, S. M.; Grätzel, M. *Adv. Funct. Mater.* **2009**, *19*, 2187.

(34) Jovanovski, V.; Gonzalez-Pedro, V.; Gimenez, S.; Azaceta, E.; Cabanero, G.; Grande, H.; Tena-Zaera, R.; Mora-Sero, I.; Bisquert, J. *J. Am. Chem. Soc.* **2011**, *133*, 20156.
(35) Bai, Y.; Cao, Y.; Zhang, J.; Wang, M.; Li, R.; Wang, P.; Zakeeruddin, S. M.; Grätzel, M. *Nat. Mater.* **2008**, *7*, 626.
(36) Licht, S.; Peramunage, D. *Nature* **1990**, *345*, 330.
(37) Yoo, K.; Choi, H.; Dionysiou, D. D. *Chem. Commun.* **2004**, 2000.
(38) Feng, Q.; Dong, L.; Huang, J.; Li, Q.; Fan, Y.; Xiong, J.; Xiong, C. *Angew. Chem. Int. Ed.* **2010**, *49*, 9943.
(39) Sun, L.; Fang, J.; Reed, J. C.; Estevez, L.; Bartnik, A. C.; Hyun, B.-R.; Wise, F. W.; Malliaras, G. G.; Giannelis, E. P. *Small* **2010**, *6*, 638.
(40) Green, M.; Rahman, P.; Smyth-Boyle, D. *Chem. Commun.* **2007**, 574.
(41) Choi, S. Y.; Shim, J. P.; Kim, D. S.; Kim, T. Y.; Suh, K. S. *J Nanomaterials*, *2012(2012)*, Article ID 519458/1.
(42) Nakashima, T.; Kawai, T. *Chem. Commun.* **2005**, 1643.
(43) Nakashima, T.; Nonoguchi, Y.; Kawai, T. *Polym. Adv. Technol.* **2008**, *19*, 1401.
(44) Lopes, J. N. A. C.; Pádua, A. A. H. *J. Phys. Chem. B* **2006**, *110*, 3330.
(45) Wuister, S. F.; Swart, I.; Driel, F. V.; Hickey, S. G.; Donega, D. D. M. *Nano Lett.* **2003**, *3*, 503.
(46) Bullen, C.; Mulvaney, P. *Langmuir* **2006**, *22*, 3007.
(47) Yu, W. W.; Qu, L.; Guo, W.; Peng, X. *Chem. Mater.* **2003**, *15*, 2854.
(48) Cui, S.-C.; Tachikawa, T.; Fujitsuka, M.; Majima, T. *J. Phys. Chem. C* **2008**, *112*, 19625.
(49) Jin, S.; Hsiang, J.-C.; Zhu, H.; Song, N.; Dickson, R. M.; Lian, T. *Chem. Sci.* **2010**, *1*, 519.
(50) Cragg, G. E.; Efros, A. L. *Nano Lett.* **2010**, *10*, 313.0
(51) Tang, J.; Marcus, R. A. *J. Chem. Phys.* **2005**, *123*, 054704/1.
(52) Kuno, M.; Fromm, D. P.; Hamann, H. F.; Gallagher, A.; Nesbitt, D. J. *J. Chem. Phys.* **2001**, *115*, 1028.
(53) Mandal, A.; Tamai, N. *Appl. Phys. Lett.* **2011**, *99*, 263111/1.
(54) Hohng, S.; Ha, T. *J. Am. Chem. Soc.* **2004**, *126*, 1324.
(55) Derfus, A. M.; Chan, W. C. W.; Bhatia, S. N. *Nano Lett.* **2004**, *4*, 11.
(56) Nadeau, J. L.; Carlini, L.; Suffern, D.; Ivanova, O.; Bradforth, S. E. *J. Phys. Chem. C* **2012**, *116*, 2728.
(57) Monroe, B. M. *Photochem. and Photobiol.* **1982**, *35*, 863.
(58) Katari, J. E. B.; Colvin, V. L.; Alivisatos, A. P. *J. Phys. Chem.* **1994**, *98*, 4109.
(59) Jang, A.; Jun, S.; Chung, Y.; Pu, L. *J. Phys. Chem. B* **2004**, *108*, 4597.
(60) Xu, M.; Deng, G.; Liu, S.; Chen, S.; Cui, D.; Yang, L.; Wang, Q. *Metallomics* **2010**, *2*, 469.
(61) Hines, D. A.; Becker, M. A.; Kamat, P. V. *J. Phys. Chem. C* **2012**, *116*, 13452.
(62) Alvaro, M.; Ferrer, B.; Garcia, H.; Narayana, M. *Chem. Phys. lett.* **2002**, *362*, 435.
(63) Anthony, J. L.; Anderson, J. L.; Maginn, E. J.; Brennecke, J. F. *J. Phys. Chem. B* **2005**, *109*, 6366.
(64) Wuister, S. F.; Donega, C. D. M.; Meijerink, A. *J. Phys. Chem. B* **2004**, *108*, 17393.
(65) Baker, D. R.; Kamat, P. V. *Langmuir* **2010**, *26*, 11272.
(66) Ramsden, J. J.; Grätzel, M. *J. Chem. Soc., Faraday Trans. 1* **1984**, *80*, 919.
(67) Landes, C. F.; Braun, M.; El-Sayed, M. A. *J. Phys. Chem. B* **2001**, *105*, 10554.

CHAPTER 8

Concluding Remarks

This chapter summarizes the results of the findings outlined in this thesis. The scope of further studies based on the present findings and literature reports has also been outlined.

8.1. Overview

This thesis presents work on two classes of promising materials, room temperature ionic liquids (RTILs) and nanocrystalline semiconductor quantum dots (QDs). The main objective is to explore the RTILs as media for photophysical reactions and to study the impact of their properties on the excited state intramolecular electron transfer reactions. For this purpose several electron donor acceptor (EDA) molecules have been employed, where polarity and viscosity of the solvent show opposing effects on the rates of their intramolecular electron transfer reactions and allow one to understand which of these two properties of the RTIL actually control the rate of the reaction. Some EDA molecules, whose fluorescence efficiency depends on solute-solvent specific H-bonding interactions, have been chosen with a view to explore the influence of the H-bonding interactions of the RTILS with the solute molecules. QDs are selected with a two-dimensional objective, firstly, to investigate the mechanisms of fluorescence quenching and secondly, to explore luminescent QDs in RTILs. Several methods and instrumental techniques, which include NMR for compound characterization, TEM for QD morphology identification, cone and plate viscometer for RTIL viscosity measurements, UV-vis spectrophotometer, steady-state and time-resolved fluorescence techniques, multiphoton confocal fluorescence microscope for ensemble photophysical studies and time-resolved confocal fluorescence microscope for fluorescence measurements at single particle level have been employed for carrying out the work presented here. The results of the finding are summarized below.

Though many photophysical studies have been carried out in RTILs to understand their microscopic properties, the influence of the properties of the RTILs on the excited state intramolecular charge transfer (ICT) reactions has remained largely unexplored. To explore

RTILs as a medium for such reactions, dual fluorescent 4-(N,N′-dimethylamino)benzonitrile (DMABN), which undergoes excited state twisted intramolecular charge transfer (TICT) reaction to emit from locally excited (LE) and TICT states, is considered. Interestingly, it is found that DMABN undergoes photobleaching under mild excitation conditions that leads to a time-dependent change of the fluorescence response of the system. Near reversibility of photobleached emission is observed due to high viscosity of the RTILs, which is not the case in conventional less viscous solvents. Multiphoton confocal fluorescence microscopy study of the fluorescence recovery after photobleaching (FRAP) of DMABN has allowed the estimation of the diffusion coefficient of the molecule in 1-butyl-3-methylhexafuorophosphate, [bmim][PF_6], RTIL. The finding reveals that the microviscosity surrounding DMABN is quite different from the bulk viscosity of the medium. Time-resolved emission behavior of DMABN in [bmim][PF_6] reveals that excited state LE →ICT transformation is mainly controlled by polarity of the RTIL, though possible influence of the ultrafast component of the solvation dynamics on the electron-transfer process cannot be ruled out.

Crystal violet lactone (CVL) is a dual fluorescent molecule, which emits from two charge transfer states, CT_A and CT_B. Emission from CT_B state is sensitive to the viscosity and hydrogen bonding interactions of the surrounding solvent. To modulate the excited state intramolecular electron transfer reaction and dual fluorescence of CVL, fluorescence response of CVL has been investigated in six RTILs using steady state and time-resolved fluorescence techniques. It is shown that the excited state CT_A → CT_B transformation and dual fluorescence of CVL can be controlled by appropriate choice of the RTILs. While the second emission from the CT_B state can barely be seen in 1,3-dialkylimidazolium RTILs, dual fluorescence is quite prominent in 1-butyl-2,3-dimethylimidazolium RTIL, [bmMim][Tf_2N]. These contrasting results have been explained taking into account the hydrogen bonding interactions of the 1,3-dialkylimidazolium ions (mediated through the C(2)-hydrogen) with CVL and the viscosity of the RTILs. A comparison of the measured solvation time and excited state reaction time suggests that the CT_A → CT_B reaction rate in moderately viscous RTILs is primarily dictated by the dynamics of solvation.

Aminochalcones are electron donor-acceptor (EDA) molecules, which unlike most other electron donor-acceptor (EDA) molecules exhibit unusual solvent polarity dependent

fluorescence behavior. Though the emission is characterized by a single emission band, commonly accepted model of aminochalcones involves two fluorescent states to explain the unusual fluorescence behavior of these molecules in conventional less viscous solvents. Photophysical behavior of two aminochalcones, namely 4-aminochalcone (AC) and 4-dimethylaminochalcone (DMAC), has been studied in viscous RTIL, [bmim][PF_6], by steady-state and time-resolved fluorescence techniques in an attempt to observe the emission from both the excited states. The experiments reveal that the emitting state in these compounds is different from the one suggested in commonly accepted model. The studies also reveal an interesting difference of the photophysical behavior of two structurally similar amino chalcones in [bmim][PF_6] RTIL. The differences of fluorescence decay profiles, solvation dynamics and excitation wavelength dependent emission behavior of AC from DMAC are attributed to specific H-bonding interactions of the former system with the RTIL.

As majority of the applications of QDs are linked to the exciton quenching dynamics, a clear understanding of the mechanism of fluorescence quenching of the QDs is absolutely essential. We have studied the fluorescence quenching of CdS QDs by 4-azetidinyl-7-nitrobenz-2-oxa-1,3-diazole (NBD), where the two quenching partners satisfy the spectral overlap criterion necessary for Förster resonance energy transfer (FRET), by steady-state and time-resolved fluorescence techniques. Even though the two interacting species display quenching behavior, which appears typical of a FRET mechanism, careful investigation reveals that the quenching process is neither dynamic nor does it involve the FRET mechanism. It is shown that the quenching actually proceeds through a static interaction between the quenching partners and is probably mediated by a charge transfer process. The quenching rate constant, which is dependent on the number of NBD molecules adsorbed on the CdS surface, has been evaluated by employing a kinetic model. The present results point to the need of a deeper analysis of the experimental quenching data to avoid erroneous conclusions.

Low cost of the materials, size dependent tunability of the luminescence properties and possibility of multiple exciton generation (MEG) allow QDs to produce high-performing and low-cost quantum dot sensitized solar cells (QDSCs). The sulfide/polysulfide and ferricyanide/ferrocyanide salts in aqueous media or $[Co(o\text{-}phen)_3]^{2+/3+}$ in organic solvents are usually used as electrolytes in quantum dot based liquid junction solar cells. However,

practical limitations of leakage and evaporation of the solvent is a major impediment to the commercialization and long-term use of these devices for applications. As RTILs are non volatile and thermally stable, they can be a better alternative to the volatile organic solvents. Prior to the employment of the RTILs in QDSCs, it is necessary to study the interaction of the RTILs with the QDs, in particular, their influence on the luminescence properties of the QDs in view of the fact that the efficiency of a solar cell depends on the interactions of the electrolytes with the photosensitizers. To make these studies possible, a task specific ionic liquid (**SH-UMIM**) has been designed and successfully employed to prepare luminescent CdTe/**SH-UMIM** QD-ionic liquid hybrid, which is soluble in most of the hydrophilic and hydrophobic RTILs. Fluorescence studies based on both ensemble and single-particle blinking measurements reveal that improved emission properties of the QDs in RTILs are due to the protection offered to it by **SH-UMIM** and enhanced stability of the QDs toward O_2 is due to low solubility of O_2 and viscous nature of the RTILs.

8.2. Future scope and challenges

Experimental and simulation studies have suggested that RTILs are heterogeneous in nature and the measured microscopic viscosity and polarity can be different from their bulk values. While it is clear that the microscopic polarity, $E_T(30)$, of RTILs is higher than the dielectric constant values representing the bulk polarity, the microscopic viscosity can be higher or lower than that of the bulk viscosity. The microviscosity of [bmim][PF_6] RTIL measured using molecular rotor, 9-(dicyanovinyl)julolidine, is lower compared to its bulk viscosity. However, reverse is the case observed when the microviscosity of [bmim][PF_6] is measured through FRAP experiments. The contradiction in the different experimental results suggests further studies on the microviscosity of different variety of RTILs and their comparison with the bulk viscosity values.

We have studied excited state intramolecular electron transfer reaction of two different EDA molecules, DMABN and CVL in RTILs to understand the influence of the properties of the latter on the rates of the electron transfer reactions. Interestingly different results are observed for the two systems. Excited state electron transfer reaction of DMABN is hardly dependent on the viscosity of the RTIL, whereas the electron transfer reaction of CVL is completely solvation dependent and controlled by the viscosity of the RTIL. While the

excited state populations of two fluorescent states of DMABN are excitation wavelength dependent, the dual emission of CVL is independent of the excitation wavelength. All the experimental results suggest that the excited state electron transfer reaction of DMABN is dependent on the polarity of the RTIL and that of CVL is dependent on the viscosity of the medium. Since these two results do not indicate clearly which of the two properties of RTILs controls the excited state electron transfer reaction, further investigation is needed on additional EDA systems of this kind in RTILs.

Several solvation dynamics studies in RTILs show that solvation of RTILs is a slow process and this has been attributed to high viscosity of the medium. However, none of these studies highlights the effect of specific solute-solvent interactions on the solvation dynamics. The solvation dynamics studies of aminochalcones in [bmim][PF_6] show that due to the H-bonding interactions between solute and the RTIL, the dynamics of solvation becomes faster despite the high viscosity of the medium. Since this study is first of its kind, it needs further investigation and we hope that similar studies on different solute molecules capable of specific interactions with the RTILs will continue to grow in the coming years.

Through fluorescence quenching of CdS QDs by NBD, we have shown that donor-acceptor pairs, which meet the spectral overlap criterion and show decrease in fluorescence lifetime may not always undergo fluorescence quenching through FRET mechanism. It is also shown that quenching due to charge transfer is more efficient than energy transfer, when both quenching mechanisms are possible. While this study improves our understanding of the fluorescence quenching mechanism of QDs by organic molecules, complete studies through identification of transient radical ions are very few. Therefore, further investigations focusing on the characterization of transient species through laser flash photolysis experiments are necessary to differentiate the charge transfer process from the energy transfer quenching mechanism.

Synthesis of QD-ionic liquid hybrids helps exploration of the QDs in RTILs. It allows studies of the influence of RTILs on the optical properties of the QDs. We have demonstrated with the help of ensemble time-resolved fluorescence and single particle blinking experiments that RTIL can be considered as electrolyte in these studies as it does not affect the properties of the QDs and additionally protects them from molecular oxygen in the environment. However, these are a few fundamental studies. For practical applications, real

challenge lies in understanding the effect of RTIL on the rate of electron transfer from the QD (sensitizer) to TiO_2 nanoparicles and hole scavenging in these media. We think that the potential of the RTILs and QDs will be fully realized when these studies are undertaken.